Development of Renewable and System-Supportive Heat Supply Concepts and Infrastructures for Existing Districts

Johannes Röder

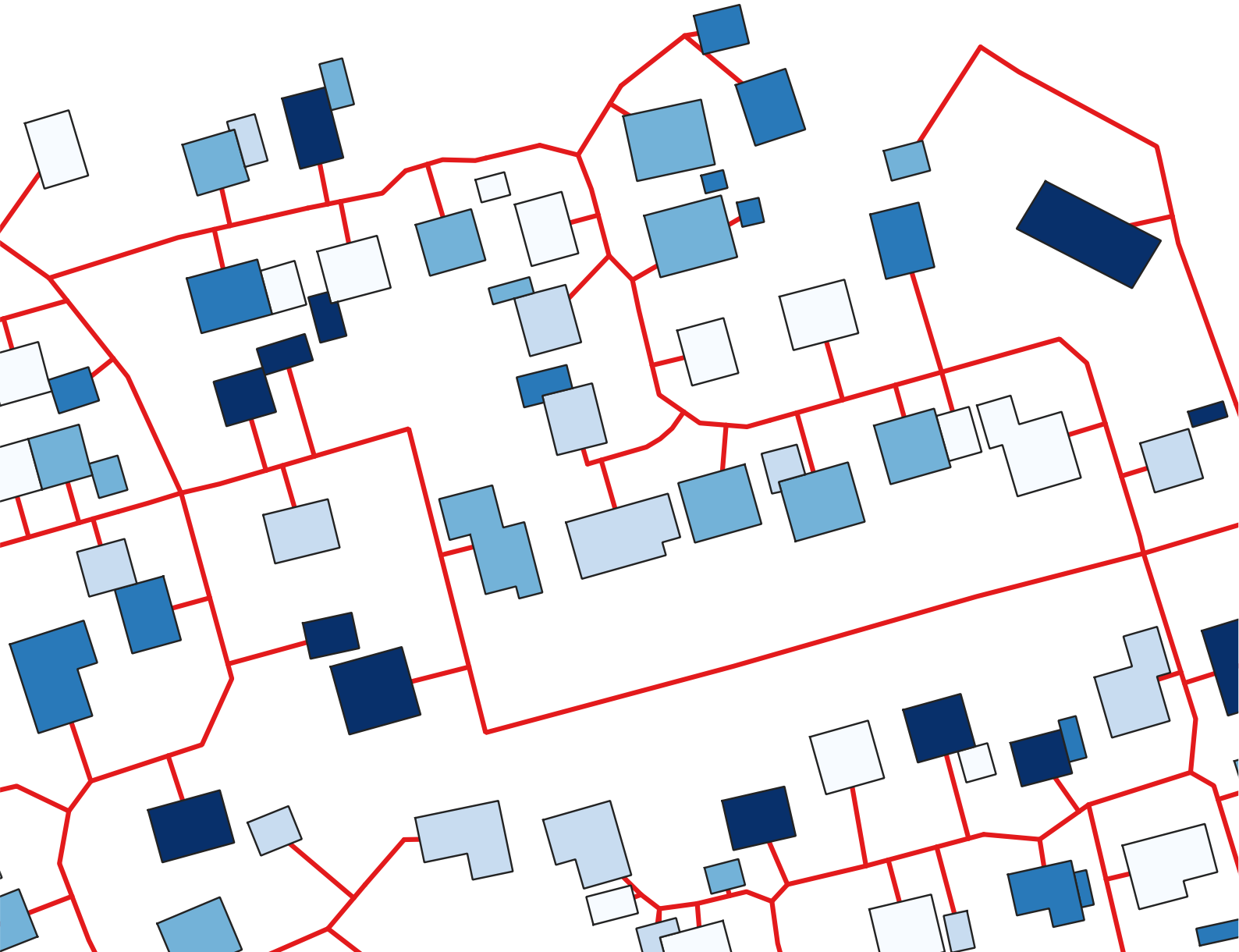

Development of Renewable and System-Supportive Heat Supply Concepts and Infrastructures for Existing Districts

Vom Fachbereich Produktionstechnik

der

UNIVERSITÄT BREMEN

zur Erlangung des Grades

Doktor der Ingenieurwissenschaften (Dr.-Ing.)

genehmigte

Dissertation

von

M. Sc. Johannes Röder

Gutachter: Prof. Dr. ir. Edwin Zondervan, University of Twente (Niederlande)

Gutachter: Prof. Dr. Arnim von Gleich

Tag der mündlichen Prüfung: 22. November 2022

Acknowledgments

At this point I would like to express my sincere thanks to all persons who supported the realization of this thesis. First of all, I would like to thank Prof. Dr. ir. Edwin Zondervan for the supervision and support throughout the last years. I really appreciated the regular exchange and your constructive manner. Many thanks to Prof. Dr. Arnim von Gleich, who was willing to take the role as second assessor. Thank you very much for your valuable comments and suggestions for improvement. Furthermore, I would like to thank all members of the doctoral committee for your time and engagement.

A special thanks go to my colleagues from the department of the Resilient Energy Systems group. Especially Torben Stührman, who kept the group together in the past difficult years. Furthermore, I would like to thank Tino and Benedikt for our fruitful discussions in the project Quarree100. A further big thanks goes to Uwe for the interesting exchange and especially for your support with the development of Python packages. I would like to thank Joris from Steinbeis-Innovationszentrum energieplus very much for providing the energy related data of the Rüsdorfer Kamp. I am very thankful to Jane, Sven, Nina and Vroni for your thorough proofreading. Moreover, I would like to thank all of my colleagues from the Resilient Energy group for the cooperative atmosphere in the group. A big thank you goes to my parents, who always encouraged and supported me. Thank you Vera, for your outstanding moral support.

Abstract

The transformation of the energy system is a crucial task for achieving the climate goals. Therefore, the use of fossil resources needs to be reduced in all energy sectors and replaced by renewable resources. A major challenge is the transformation of the heat supply of the building sector. Especially the existing building stock consumes a large amount of energy due to a lack or a low quality of insulation. Most of the urban built-up districts are supplied by fossil heating systems such as oil or gas boilers. In many districts renewable energy resources are limited, and the heat supply relies on energy imports from the upstream energy infrastructures, especially the gas and electricity grid.

Within the ongoing transformation of the energy system, there are several promising developments and chances for the transformation of the heat supply of the existing building stock. First, energetic refurbishment, the aim of which is to reduce the demand for space heating. Second, sector-coupling and electricity based-heating. However, this demands a system-supportive design as the main resources of renewable electricity are the volatile wind and solar power. A further trend is hydrogen and renewable synthetic gas that could be supplied with the often existing gas infrastructure, even though the share of hydrogen in the gas network is limited without further action. And finally, district heating systems have a great potential for supporting the energy transition towards a renewable energy system. These trends and developments are far-reaching upheavals in the energy system and pose extreme challenges for energy infrastructure planning at a district level. However, infrastructure decisions must be taken in advance due to the high costs and long life time, and investments in infrastructures that are economic today may not be in future.

One of the most far-reaching and cost-intense infrastructure decision made at the municipal and district level is about the implementation of a district heating system. However, there are many districts, where it is unclear whether a district heating system is a “future-proof” investment decisions. The term “future-proof” refers to no-regret investment decisions under different transformation paths of the upstream energy system as well as within the district to obtain a carbon-neutral energy system. Therefore, the objective of this thesis is the development of methods and tools for the design of renewable and system-supportive heat supply concepts and infrastructures, and the application of these tools to answer the following research questions: How should future-proof district heating systems, including the district heating network and the energy converter and storage units of the heat supply sites, be designed? In which cases and under which scenarios is a district heating system a future-proof infrastructure compared to an individual buildings-wise heat supply, with respect to economic and ecological criteria? Is it possible to derive required heat density thresholds for the economic feasibility of district heating in existing districts? And how do these values turn out for different scenarios? The term heat density of a district refers to the heat demand density per district area and is an important indicator for the economic feasibility of district heating compared to individual heat supply.

The methodical approach of this thesis is based on techno-economic optimization models for the different components of district energy systems, including the district heating network,

the design of the heat supply site and the energy supply at the building level. An overall approach is developed and applied that connects these single models and design tasks. In that process, special attention is paid to the aspect of sector-coupling and system-supportiveness with respect to the upstream electricity grid. This includes both, the combined evaluation of the electricity and heat supply at the building level and the consideration of the time-resolved characteristics of the volatility of renewable energies in the electricity grid. Both aspects have not yet been sufficiently considered for a comparison of district heating with individual heat supply and strive to meet the current challenges of an integrated sector-coupled development of district heating systems. For the detailed planning of district heating networks, a new open source library has been developed that provides a flexible optimization tool to determine the topology and the sizing of the pipeline network of potential district heating systems for a fast estimation of the costs for different scenarios.

The upstream infrastructures of the electricity and gas networks are in an ongoing process of transformation into a renewable energy system with uncertain speed and depth. Therefore, a comprehensive scenario analysis is performed that considers different transformation paths of the upstream energy infrastructures with different shares of renewable energies. Additionally, local scenarios are defined that describe the potential developments at district level such as refurbishment measures. The local scenarios are further characterized by different shares of buildings connected to a potential district heating system (connection quota) to investigate the required heat density threshold for the feasibility of a district heating system with respect to economic and ecological criteria. By the in-depth analysis of an existing district with a sparse to moderate heat density, where it is undecided if district heating is a future-proof infrastructure, the impact of the different scenarios on the design and feasibility of district heating compared to individual heat supply options is studied.

The results of the optimization of the heat supply site shows that heat pump capacities in combination with thermal storage are of great importance for a future carbon-neutral heat supply in all considered scenarios. A combined heat and power unit helps to reduce emissions in the short term by the system-supportive feed-in of electricity into the upstream power grid. However, only if the gas network has a high share of renewable energies, this technology will be able to compete with electricity-based heating via heat pumps. The results show that the installation of an electrolysis within the district heat supply, at least in short term, is not a viable option for designing a cost-efficient carbon-neutral district heat supply. Also in the long term, the only scenario in which the electrolysis becomes relevant for a cost-efficient emission reduction is when the generated hydrogen can contribute to a displacement of fossil gas used elsewhere, but not for hydrogen storage and also not for heat and electricity generation within the district.

Within the optimization approach for the design of the district energy system, it could be shown that the applied methodical approach based on a dynamic emission factor leads to a system-supportive electricity exchange with the upstream power grid. Therefore, a reduction of the overall emissions of the district energy system implies an appropriate design of the energy converter and storage units and a system-supportive unit commitment. Although, it is difficult to define absolute values of emission reduction that make a system sufficiently system-supportive, the method enables a comparison of different energy supply strategies

and helps to identify the most cost-efficient emission reduction strategies for a renewable and system-supportive design towards a carbon-neutral energy system.

The comparison of district heating and individual heat generation shows that district heating systems are economically feasible at lower heat densities if a carbon-neutral electricity and heat supply is the goal. The impact of the scenarios of the upstream gas network considering a low or a high share of renewable synthetic gas on the heat density threshold is low. In scenarios with a high availability of renewable gas, district heating is even favored in some scenarios, as the synthetic gas can be more efficiently used at an aggregated level in a district heating facility compared to the building level. The individual characteristics and potentials at building level and refurbishment status have a strong influence on the heat density threshold. For the future decision making on district heating systems, individual factors such as usable roof area for photovoltaic systems, electricity demand, e-mobility, geothermal or other heat potentials and also space for the installation of thermal storage capacities must be taken into account. These factors impact the possibilities to become carbon-neutral at building level and to react to the volatile characteristic of renewable energy generation in the upstream power grid. The analysis of different refurbishment scenarios with different temperature levels and a reduction of the space heating demand clearly shows the benefits of refurbishment to obtain carbon-neutrality. However, in contrast to literature sources, no shift to lower but rather to higher heat demand densities can be observed with increasing refurbishment measures and lower supply temperatures for achieving carbon-neutrality.

The decision making process for energy infrastructure investments becomes increasingly complex in future sector-coupled energy systems. The approach and the tools developed in this thesis support planning and decision making at district level and aim to broaden the conventional planning perspective and methods towards a systemic approach that respect the local energy system as part of an integrated overall system. The tools and findings of this thesis contribute to make sustainable economic and ecological investment decisions in the development of heat supply concepts and infrastructures for a successful energy transition.

Keywords: district heating system, district heating network, optimization models, dimensioning, design, system-supportive, renewable energies, heat density, individual heat supply, sector-coupling, emission factor, hydrogen, scenario analysis, planning approach, decision-making

Kurzfassung

Die Transformation des Energiesystems ist für das Erreichen der Klimaziele essentiell. Damit diese gelingt, muss die Nutzung fossiler Ressourcen in allen Energiesektoren reduziert und durch erneuerbare Energien ersetzt werden. Dabei stellt die Transformation der Wärmeversorgung des Gebäudesektors eine der wesentlichen Herausforderung dar. Vor allem Bestandsgebäude verbrauchen wegen ihres oft niedrigen energetischen Standards und einer schlecht gedämmten Gebäudehülle viel Energie. Die meisten Bestandsquartiere werden mit fossilen Heizsystemen wie Öl- oder Gaskesseln versorgt. Zudem sind in vielen städtischen Quartieren die Potentiale an erneuerbaren Energien begrenzt und die Wärmeversorgung ist auf den Energiebezug aus den vorgelagerten Energieinfrastrukturen, insbesondere dem Gas- und Stromnetz, angewiesen.

Im Rahmen der laufenden Umgestaltung des Energiesystems gibt es mehrere vielversprechende Entwicklungen und Chancen für die Transformation der Wärmeversorgung des Gebäudebestandes. Erstens, die energetische Sanierung, deren Ziel es ist, den Heizwärmebedarf zu senken. Zweitens, die Sektorenkopplung und strombasierte Wärmeerzeugung. Dies erfordert jedoch eine systemdienliche Auslegung und Betrieb der Anlagen, da der Hauptteil der erneuerbaren Stromerzeugung aus der volatilen Erzeugung von Wind- und Solaranalgen kommt. Ein weiterer Trend ist Wasserstoff und erneuerbares synthetisches Gas, das mit der vorhandenen Gasinfrastruktur verteilt werden könnte, auch wenn der Anteil an Wasserstoff im Gasnetz ohne Anpassungsmaßnahmen begrenzt ist. Und schließlich, Wärmenetze. Nah- bzw. Fernwärmesysteme haben ein großes Potenzial zur Unterstützung der Energiewende hin zu einem erneuerbaren Energiesystem. Diese Trends und Entwicklungen sind weitreichende Umwälzungen im Energiesystem und stellen die Energieinfrastrukturplanung auf Quartiersebene vor große Herausforderungen. Infrastrukturentscheidungen müssen jedoch wegen der hohen Investitionskosten und langen Lebensdauer sehr vorausschauend getroffen werden. Denn Investitionen in Infrastrukturen, die im heutigen Energiesystem wirtschaftlich sind, sind es nicht notwendigerweise in Zukunft.

Eine der weitreichendsten und kostenintensivsten Infrastrukturentscheidungen, die auf Quartiers- bzw. kommunaler Ebene getroffen werden, ist die Umsetzung eines Wärmenetzes. Gleichzeitig gibt es viele Quartiere, in denen unklar ist, ob ein Wärmenetz eine “zukunftsfähige” Investitionsentscheidung ist. Der Begriff "zukunftsfähig" bezieht sich auf Investitionsentscheidungen, die sich in Bezug auf mögliche zukünftige Transformationsszenarien des vorgelagerten Energiesystems und innerhalb des Quartiers zur Erreichung eines klimaneutralen Energiesystems als wirtschaftlich und nachhaltig erweisen. Das Ziel dieser Arbeit ist daher die Entwicklung von Methoden und Werkzeugen für die Gestaltung von erneuerbaren und systemdienlichen Wärmeversorgungskonzepten und -infrastrukturen, und die Anwendung dieser Werkzeuge zur Beantwortung folgender Forschungsfragen: Wie sollte ein zukunftsfähiges leitungsgebundenes Wärmeversorgungssystem einschließlich des Wärmenetzes und der Energiewandler und -speicher der Wärmeversorgungszentrale ausgelegt werden? In welchen Fällen und unter welchen Szenarien ist ein Wärmenetz unter ökonomischen und ökologischen Gesichtspunkten die bessere Infrastrukturentscheidung im Vergleich zu einer individuellen Wärmeversorgung auf Gebäudeebene? Lassen sich erforderliche Wärmedichte-Grenzwerte für die wirtschaftliche Machbarkeit von Wärmenetzen in Bestandsquartieren ableiten? Und welchen Einfluss haben

verschiedene Entwicklungsszenarien auf diese Grenzwerte? Der Begriff Wärmedichte eines Quartiers bezieht sich auf die Wärmebedarfsdichte pro Quartiersfläche und ist ein wichtiger Indikator für die wirtschaftliche Machbarkeit von Wärmenetzen im Vergleich zur individuellen Wärmeversorgung.

Der methodische Ansatz dieser Arbeit basiert auf technisch-wirtschaftlichen Optimierungsmodellen für die verschiedenen Bestandteile des Wärmeversorgungssystems. Dies schließt die Dimensionierung des Wärmenetzes, die Gestaltung der Wärmeversorgungszentrale und die Energieversorgung auf Gebäudeebene ein. Im Rahmen der Arbeit wird ein übergeordnetes Vorgehen entwickelt und angewendet, das die einzelnen Modelle und Planungsaufgaben miteinander verbindet. Dabei wird ein besonderes Augenmerk auf den Aspekt der Sektorenkopplung und die Systemdienlichkeit in Bezug auf das vorgelagerte Stromnetz gelegt. Dies beinhaltet die kombinierte Betrachtung der Strom- und Wärmeversorgung auf Gebäudeebene und die Berücksichtigung der zeitlichen Charakteristik des Stromnetzes durch die volatile Einspeisung erneuerbarer Energien. Beide Aspekte sind für einen Vergleich von leitungsgebundener Wärmeversorgung mit individueller Wärmeversorgung noch nicht hinreichend berücksichtigt. Mit dieser Arbeit wird angestrebt den aktuellen Herausforderungen einer integrierten sektorengekoppelten Entwicklung von Wärmeversorgungssystemen gerecht zu werden. Für den Entwurf und die Planung von Wärmenetzen wurde eine neue Open-Source-Bibliothek entwickelt, die ein flexibles Optimierungstool zur Bestimmung der Topologie und der Dimensionierung des Leitungsnetzes bietet und eine schnelle Abschätzung der Kosten von potentiellen Wärmenetzen für verschiedenen Szenarien ermöglicht.

Die vorgelagerten Infrastrukturen der Strom- und Gasnetze befinden sich in einem laufenden Transformationsprozess hin zu einem erneuerbaren Energiesystem allerdings mit ungewisser Geschwindigkeit und Transformationstiefe. Daher wird eine umfassende Szenario-Analyse durchgeführt, die verschiedene Transformationspfade der vorgelagerten Energieinfrastrukturen mit unterschiedlichen Anteilen erneuerbarer Energien berücksichtigt. Zusätzlich werden lokale Szenarien definiert, die mögliche Entwicklungen auf Quartiersebene beschreiben, wie zum Beispiel Sanierungsmaßnahmen. Die lokalen Szenarien sind weiter durch unterschiedliche Anschlussquoten von Gebäuden an das Wärmenetz gekennzeichnet. Die Betrachtung verschiedener Anschlussquoten hat das Ziel, den erforderlichen Wärmedichte-Grenzwert für die Machbarkeit eines Wärmenetzes unter ökonomischen und ökologischen Gesichtspunkten zu untersuchen. Durch die vertiefte Analyse eines bestehenden Quartiers mit geringer bis mittlerer Wärmedichte, welches damit im Grenzbereich der wirtschaftlichen Umsetzbarkeit eines Wärmenetzes liegt, werden die Auswirkungen der verschiedenen Szenarien auf die Auslegung und Machbarkeit eines Wärmenetzes im Vergleich zu Wärmeversorgungsoptionen auf Gebäudeebene untersucht.

Die Ergebnisse der Optimierung der Wärmeversorgungszentrale zeigen, dass Wärmepumpen in Kombination mit einem thermischen Speicher in allen Szenarien von großer Bedeutung für eine zukünftige klimaneutrale Wärmeversorgung sind. Ein Blockheizkraftwerk hilft kurzfristig, Emissionen zu reduzieren durch eine system-dienliche Einspeisung von Strom in das vorgelagerte Stromnetz. Allerdings wird diese Technologie nur dann mit der strombasierten Wärmeversorgung über Wärmepumpen konkurrieren können, wenn das Gasnetz einen hohen Anteil an erneuerbaren Gas aufweist. Die Ergebnisse zeigen, dass die Installation einer Elektrolyse in der Energiezentrale eines Stadtquartiers zumindest kurzfristig keine sinnvolle Option für

eine kosteneffiziente klimaneutrale Wärmeversorgung ist. Und auch langfristig ist das einzige Szenario, in dem die Elektrolyse für eine kosteneffiziente Emissionsminderung relevant wird, der Fall, dass der erzeugte Wasserstoff zur Verdrängung von fossilem Gas an anderer Stelle beitragen kann, allerdings nicht zur Wasserstoffspeicherung und Wärme- und Stromerzeugung im Quartier.

Es konnte gezeigt werden, dass der angewandte methodische Ansatz zur Gestaltung der Wärmeversorgungszentrale auf Basis eines dynamischen Emissionsfaktors zu einem systemdienlichen Stromaustausch mit dem vorgelagerten Stromnetz führt. Eine Reduktion der Gesamtemissionen der Wärmeversorgungszentrale bewirkt eine entsprechende Auslegung der Energiewandler und -speicher sowie einen systemdienlichen Anlageneinsatz. Es ist jedoch schwierig, absolute Werte für die Emissionsreduktion zu definieren, die ein System hinreichend systemdienlich machen. Die Methode ermöglicht jedoch den Vergleich verschiedener Versorgungsoptionen und hilft dabei, die kosteneffizientesten Strategien für eine erneuerbare und systemdienliche Anlagenauslegung hin zu einem klimaneutralen Energiesystem zu ermitteln.

Der Vergleich von Wärmenetzen und individueller Wärmeerzeugung zeigt, dass Wärmenetze bei niedrigeren Wärmedichten wirtschaftlich sind, wenn eine klimaneutrale Strom- und Wärmeversorgung angestrebt wird. Die Auswirkungen der Szenarien des vorgelagerten Gasnetzes, die einen niedrigen und einen hohen Anteil an erneuerbarem synthetischem Gas betrachten, auf die erforderliche Wärmedichte zur wirtschaftlichen Umsetzung von Wärmenetzen sind gering. In den Szenarien mit einem hohen Anteil von erneuerbarem Gas im Gasnetz werden Wärmenetze sogar teilweise begünstigt, da das synthetische Gas auf aggregierter Ebene in der Energiezentrale des Wärmenetzes effizienter verwertet werden kann als auf Gebäudeebene. Die individuellen Eigenschaften und Potenziale auf Gebäudeebene und der Sanierungsstand haben im Gegensatz dazu einen wesentlich stärkeren Einfluss auf den Wärmedichte-Grenzwert. Für zukünftige Entscheidungen über den Bau von Wärmenetzen bedeutet dies, dass gebäudeindividuelle Faktoren wie nutzbare Dachflächen für Photovoltaikanlagen, Strombedarf, E-Mobilität, geothermische oder andere Wärmepotenziale, aber auch Platz für die Installation von thermischen Speicherkapazitäten viel stärker berücksichtigt werden müssen. Diese Faktoren beeinflussen die Möglichkeiten, auf Gebäudeebene klimaneutral zu werden und auf die volatile Charakteristik der erneuerbaren Energieerzeugung im vorgelagerten Stromnetz zu reagieren. Die Analyse verschiedener Sanierungsszenarien mit unterschiedlichen Temperaturniveaus und einer Reduzierung des Raumwärmebedarfs zeigt deutlich die Vorteile einer Sanierung zur Erreichung der Klimaneutralität. Allerdings ist im Gegensatz zu Literaturquellen bei einem niedrigeren Temperaturniveau des Wärmenetzes im Falle eines sanierten Quartiers keine Verschiebung der wirtschaftlichen Machbarkeit zu niedrigeren, sondern zu höheren Wärmebedarfsdichten zu beobachten.

Der Entscheidungsfindungsprozess für Investitionen in die Energieinfrastruktur wird in zukünftigen sektorengekoppelten Energiesystemen zunehmend komplexer. Der Ansatz und die Werkzeuge, die in dieser Arbeit entwickelt wurden, unterstützen die Planung und Entscheidungsfindung auf Quartiersebene und zielen darauf ab, die herkömmliche Planungsperspektive und -methoden hin zu einem systemischen Ansatz zu erweitern, der sich als Teil eines integrierten Gesamtsystems versteht. Die Tools und Erkenntnisse diese Arbeit tragen dazu bei, nachhaltig wirtschaftliche und ökologische Investitionsentscheidungen bei der Entwicklung

von Wärmeversorgungskonzepten und -infrastrukturen zu treffen, und damit der Energiewende zum Erfolg zu verhelfen.

Schlagwörter: Wärmeversorgung, Wärmenetz, Optimierungsmodelle, Dimensionierung, Auslegung, Systemdienlichkeit, erneuerbare Energien, Wärmedichte, dezentrale Wärmeversorgung, Sektorenkopplung, Emissionsfaktor, Wasserstoff, Szenario-Analyse, Planungsansatz, Entscheidungsfindung

Contents

List of Figures

List of Tables

List of Abbreviations

API	application programming interface
BDEW	Bundesverband der Energie- und Wasserwirtschaft e.V. (German Association of Energy and Water Industries)
CHP	combined heat and power plant
CN	carbon-neutrality
CO_2	carbon dioxide
COP	coefficient of performance
DHS	district heating system
DHW	domestic hot water
DN	nominal diameter
DSO	distribution grid operator
EF	emission factor
E-fuels	electro-fuels (gaseous and liquid hydrocarbon fuels synthesized from hydrogen and CO_2)
GEG	Gebäudeenergiegesetz (German Buildings Energy Act)
GIS	geographic information system
GSC	grid support coefficient
H_2	hydrogen
HV	high voltage
KfW	Kreditanstalt für Wiederaufbau (German Reconstruction Loan Corporation)
KSB	Klimaschutzgesetz (German Climate Protection Act)
LOHC	liquid organic hydrogen carrier
LP	linear programming
MFH	multi-family house
MILP	mixed integer linear programming
MV	medium voltage
NRB	non-residential building
PEF	primary energy factor
PEM	polymer electrolyte membrane
PHH	private households

PV	photovoltaic system
RE	renewable energy
RO	research objective
SFH	single-family house
SIZ	Steinbeis-Innovationszentrum energieplus (Braunschweig)
ST	solar thermal
TCS	trade, commerce and service
TSO	transmission system operator
VRE	volatile renewable energy sources

List of Symbols

Latin letters

a_1, a_2	heat loss coefficients of solar thermal collector
C	absolute costs
c	variable costs
c_{invest}	variable investment costs (dependent on capacity)
$c_{investfix}$	fixed investment costs (independent of capacity)
$capex$	capital expenditure
E	absolute emissions
e	emission factor
f_{corr}	correction factor
f_{icing}	efficiency reduction factor for icing
f_{loss}	capacity dependent loss factor
$f_{lossfix}$	fixed loss factor
$f_{n,cap-in}$	maximum charging power (related to storage capacity)
$f_{n,cap-out}$	maximum de-charging power (related to storage capacity)
$f_{sum,max}$	maximum summed flow (maximum full load hours)
$f_{t,fix}$	fixed normed flow
$f_{t,max}$	maximum flow factor
$f_{t,max}$	maximum power factor
f_m	annual maintenance cost factor
G	grid-based reference quantity
GSC_{abs}	absolute grid-support coefficient
I	solar irradiance
N	technical lifetime
P	generic flow variable
P_{invest}	investment flow (variable capacity)
P_{loss}	power loss
$\dot{Q}$	thermal power
q_{carnot}	Carnot quality grade
T	temperature

Δt	time-step width
W_{el}	electrical energy
W_{invest}	investment storage (variable capacity)
$wacc$	weighted average cost of capital
y	binary investment status variable

Greek letters

β	state of charge dependent loss factor
γ	capacity dependent loss factor of storage
δ	absolute loss factor of storage
η	efficiency / conversion factor
η_0	maximum solar thermal collector efficiency
$\eta_{hp,nominal}$	heat pump efficiency at nominal power

Additional indices

(i, o)	flow (from node to node)
C	solar thermal collector
$high$	upper
hp	related to heat pumps
i	from node
$init$	initial (time step)
$invest$	related to an investment (with variable capacity)
$limit$	limitation
$loss$	energy loss
low	lower
max	maximum
min	minimum
n	node / component
$nominal$	related to the nominal capacity
o	to node
t	time-step
$total$	total / sum
var	variable

1 Introduction

> *„Handel so, dass die Wirkungen deiner Handlung verträglich sind mit der Permanenz echten menschlichen Lebens auf Erden.“*
>
> *“Act so that the effects of your action are compatible with the permanence of genuine human life on earth.”*
>
> – Das Prinzip Verantwortung, Hans Jonas (Jonas 1979; Jonas et al. 1985)

1.1 Motivation

It is undoubted and targeted in many political agreements, like the Paris Climate Agreement in 2015, that the carbon dioxide (CO_2) emissions need to be reduced significantly within the coming years to keep the global temperature level well below 2 °C, preferably below 1.5 °C (UNFCCC 2015). An increase in the global average temperature above 2 °C compared to pre-industrial levels will have disastrous ecological effects. Potential tipping points might lead to highly dynamic and irreversible changes in our environment (Umweltbundesamt 2008). The climate goals are clearly formulated, for example, in the EU Green New Deal and imply carbon neutrality by 2050 (European Comission 2019).

The main part of greenhouse gas emissions is caused by carbon dioxide, which is almost exclusively produced by combustion processes (approximately 95 %) (Umweltbundesamt 2022b). Figure 1.1 shows the development of the greenhouse gas emissions in Germany from 1990 to 2020 divided into the energy sectors defined by the German Climate Protection Act (Klimaschutzgesetz, KSG 2021).

Coming from a value of 1242 million tons of carbon dioxide equivalent in 1990, the greenhouse gas emissions were reduced by 35.6 % in 2019 and by more than 40 % in 2020. However, the year 2020 cannot be interpreted as a trend due to the impact of the Corona crisis. Either way, most of the effort still lies ahead. In the same time period in which emissions have been reduced by one-third, in future, emissions must be reduced by a further two-thirds to net-zero emission in the upcoming decades. This means that the emission reduction rate in the upcoming years needs to be drastically increased to achieve the climate goals. Consequently, the measures to reduce greenhouse gas emissions need to be enforced in all sectors as fast as possible. According to the German Climate Protection Act (KSG), the emission should be reduced to 438 mill. tons CO_2-equivalent by 2030, which is a reduction of 65 % compared to 1990. The aim is to achieve net zero emission in 2045 (KSG 2021).

Historically, the energy industry accounts for the largest share of greenhouse gas emissions with about one third of the overall emissions, followed by the industry and transport sector (Figure 1.1). The building sector, that comprises private households and the trade, commerce and services (TCS) sector, accounted in total for 15 % of the greenhouse gas emissions in 2019. According to the underlying accounting method of emissions as shown in Figure 1.1, the emissions are attributed to those sectors where the actual physical emissions take place, for example due to combustion processes (BMU 2021). This means that the indirect emissions, e.g.

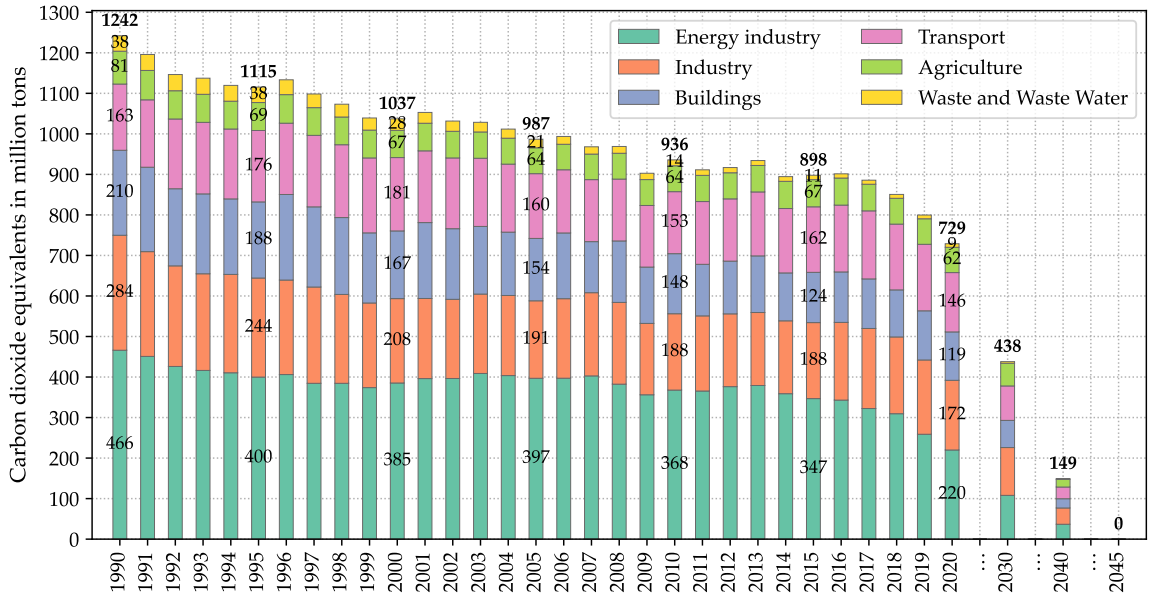

Figure 1.1: Historical sectoral emission of greenhouse gases in Germany covered by the UN Framework Convention on Climate, and emission reduction targets of Germany. Reproduced from (Umweltbundesamt 2022a). Climate goals according to (KSG 2021).

by importing electricity from the power grid, or sourcing heat from a district heating system (DHS), are attributed to the corresponding sector where the emissions are produced. If the indirect emissions were included, the total emissions from the building sector would result in about 30 % of the total emissions in Germany (BMU 2020). Most of the emissions from the building sector are related to energy appliances, especially for the provision of heat for space heating and domestic hot water (see Section 1.2.1). Related to the total energy consumption, space heating and domestic hot water add up to 30 % of the total end-energy consumption in Germany (BMWi 2021).

Therefore, an emission reduction in the building sector is a significant requirement for achieving the overall climate targets. Especially the provision of renewable heat plays a crucial role as shown in the following section. This requires a far-reaching transformation of the current status of the building energy supply and demands for the development of renewable energy supply concepts and corresponding infrastructures. To achieve this, existing infrastructures must be questioned and new supply strategies at district level must be developed that meet the future requirements. Existing districts are a particular challenge, and their transformation is a huge task for municipalities and communities.

1.2 Status quo, trends and developments

The following sections provide detailed background information on the status-quo of the energy supply in the building sector and review the current developments, trends and opportunities that are discussed for the transformation of the existing building stock.

1.2.1 Energy supply of buildings in Germany

From an energy consumption perspective, the economic sectors can be divided into four groups: private households, the TCS sector, transport and industry (BMWi 2021). According the to German Climate Protection Act (KSG 2021), private households and the TCS sector are subsumed in the building sector. The energy consumption of industrial buildings is attributed to the industry sector, as the main part of the energy consumption is determined by the individual product that is manufactured or processed. Figure 1.2 gives an overview of the use of energy (on the left), and the share of secondary (end)-energy commodities sources in the building sector in 2019 (on the right).

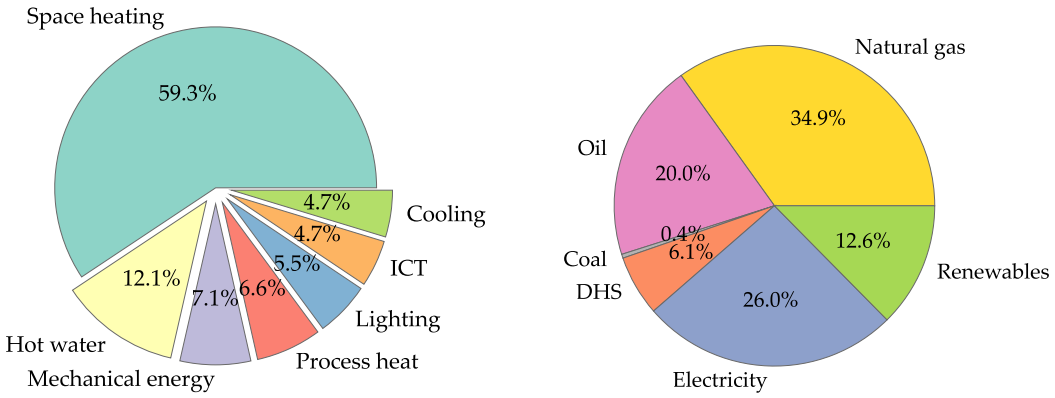

(a) Energy applications (b) End-energy

Figure 1.2: Sources of (a) energy applications and (b) end-energy in the building sector. Reproduced illustration. Data sources: (BMU 2021; BMWi 2021).

In regard to residential and commercial buildings, by far the main part (59 %) of the end-energy is needed for space heating (Figure 1.2(a)). The second largest part of end-energy (12 %) is used for domestic hot water. The remaining part is distributed almost equally among process heat (e.g. cooking), mechanical energy, lighting, electricity for information and communication (e.g. computer, television) and cooling appliances. The largest part of the energy supply is provided by natural gas (37.8 %), followed by electricity, oil and renewable energies (Figure 1.2(b)). District heating currently plays a minor role, and the share of coal in the energy supply of private households and commercial buildings is negligible.

As shown in Figure 1.2, the heat demand for space heating and domestic hot water accounts for about 70 % of the total energy consumption in the building sector in Germany. Figure 1.3 shows a more detailed breakdown of the end-energy commodities for the two heat applications space heating and domestic hot water for the year 2019.

Related specifically to the energy consumption of space heating and domestic hot water, the share of renewable energies lay at 16.5 % for the building sector in 2019 (Figure 1.3(a)). The renewable energies for heat generation are mainly biomass and solar thermal collectors (BMWi 2021). In total, 70 % of the heat demand is covered by the direct combustion of natural gas and oil via boilers in the building, 8 % originates from district heating and 5 % is electricity-based. To provide a complete picture of the energy carrier composition for the heat supply in the

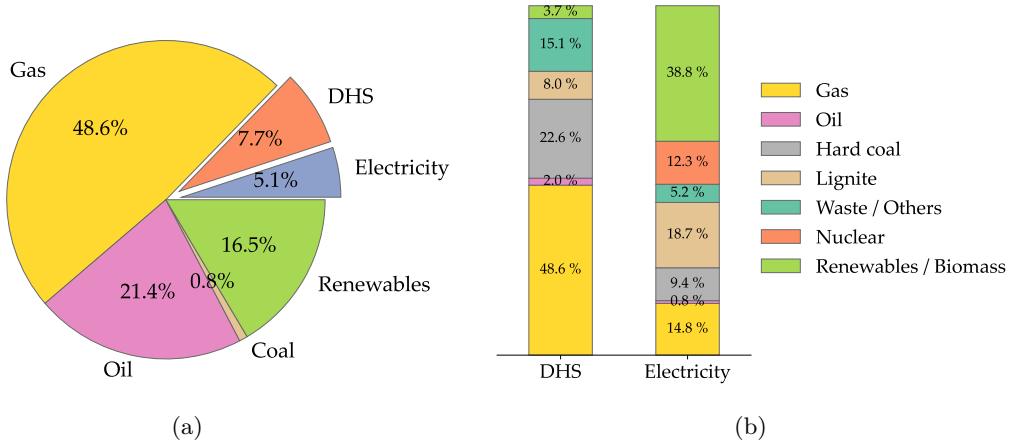

Figure 1.3: Energy commodities for space heating and domestic hot water of Germany in 2019. DHS: district heating system. Own illustration. Date source: (BMWi 2021).

building sector, Figure 1.3(b) shows the composition of the energy carriers of district heating and electricity generation in the year 2019.

In Germany, the energy input of DHS is mainly based on fossil fuels (Figure 1.3(b), left column). The share of natural gas, coal and oil accounted for more than 80 % of the district heat generation in 2019. The share of biomass lay at only 4 %. Due to the expansion of wind and solar power plants in the past decades in Germany, the electricity sector is characterized by the largest share of renewable energies with 39 % of the gross electricity generation in 2019. The fossil share accounts for 43.7 % with a share of more than two thirds on the basis of hard coal and lignite. That means that the overall fossil share of the energy supply for space heating and domestic hot water in the building sector accounted for 79 % if the indirect fossil shares of district heating and electricity are included.

Besides the energy source, the CO_2 emissions in the building sector are determined by the energy-efficiency of the building itself. Ultimately, a building serves, among other purposes, to provide a comfortable warm place that is independent of the weather and provides a shelter against rain and cold. To provide a certain level of indoor air comfort, the energy-efficiency standard of the building is crucial. The energy-efficiency standard of buildings defines certain levels of energy demand, mostly expressed in kilowatt-hours per square meter and year (kWh/(m²a)), and sets requirements to the maximum transmission heat loss. In Germany, the energy-efficiency standards are regulated by the Buildings Energy Act (GEG (2020), formerly defined in the Energy Saving Ordinance (EnEV, “Energieeinsparverordnung”)), and include minimum technical requirements for the construction of buildings, e.g. heat transfer coefficients for the different parts of the building’s envelope. Based on the minimum energy-efficiency standard of the GEG, the German Reconstruction Loan Corporation (Kreditanstalt für Wiederaufbau, KfW) defined energy-efficiency standards, also known as KfW-efficiency-houses, that are relevant for subsidies in the building sector.

A more efficient building that demands less energy for providing the same comfort level causes less CO_2 emission for energy supply. The energetic standard of buildings is affected by the

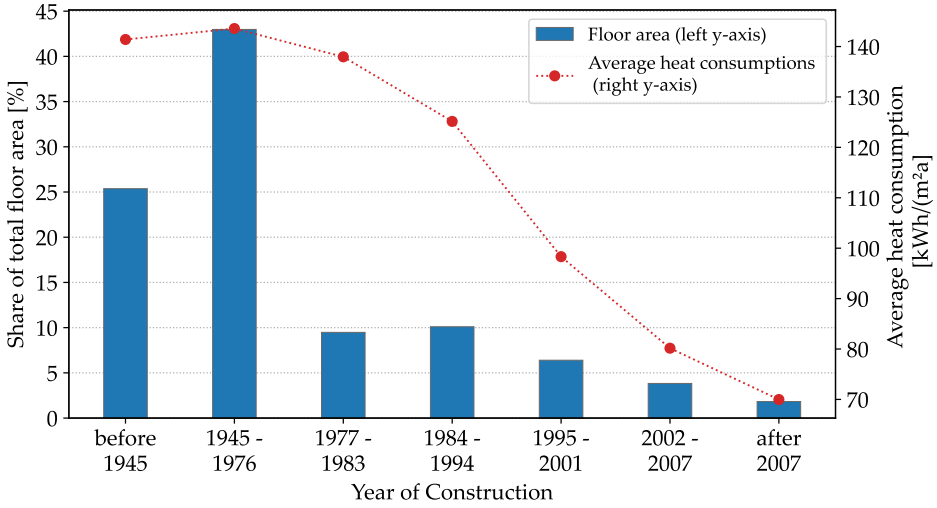

Figure 1.4: Construction years of residential building stock in Germany and average weather-corrected heat consumption of these floor areas (space heating and domestic hot water). Own illustration. Data sources: (co2online 2022; Metzger et al. 2019).

legislation in place in the year of construction. Figure 1.4 shows the distribution of the floor areas of residential buildings by age of construction in Germany. Most buildings originate from the fifties and sixties after the second world war (period from 1945 to 1976). However, before 1977 there was no minimum legal requirement for the energetic standard of buildings (BMU 2019). Thus, the share of buildings with insulation before 1977 is significantly lower than the average building stock (Cischinsky et al. 2018). From 1977 onwards, legislation for a minimum energetic standard for new buildings was defined. In Germany, this started with the first Heat Insulation Ordinance ("Erste Wärmeschutzverordnung") in 1979, followed by the second and third heat insulation ordinances in 1984 and 1995 (IWU 2015). From 2002 onwards, the first EnEV ("Energieeinsparverordnung") entered into force, was further developed in 2009 (IWU 2015) and finally replaced by the Buildings Energy Act in 2020 (GEG 2020). The successive increase of the required energetic level led to an average decrease of demand in end-energy. However, in Germany about two third of all buildings originated before 1977 (Figure 1.4). The share of fossil-based heating systems is significantly higher in the existing building stock than in new buildings of recent years. According to the census data from 2016, the share of oil-based heating systems in buildings before the first Heat Insulation Ordinance lay at 31 % of the residential units; in contrast, the share of heat pumps in new buildings from 2011 to 2015 lay above 40 % (Cischinsky et al. 2018).

The heat demand in buildings is the main origin of CO_2 emissions of the building sector. Especially the existing building stock that was built before the first Heat Insulation Ordinance of 1977 is characterized by a low energetic standard and a high share of fossil heating systems. For these reasons, districts with an existing building stock pose a particular challenge to the energy transition.

1.2.2 Measures, trends and opportunities

In principle, there are two options to tackle the challenge of reducing the emissions of the existing building stock: Firstly, to increase the energy efficiency along the process chain, including the buildings, e.g. insulation, the distribution and generation of heat; and secondly, using renewable energy as a primary heat source (Fraunhofer IWES et al. 2017). In that process, refurbishment measures, sector-coupling, renewable gases and district heating are measures and opportunities of recent years that impact on the transformation of the existing building stock (Figure 1.5). The current discussion of the role of each of these trends is summarized within the next sections.

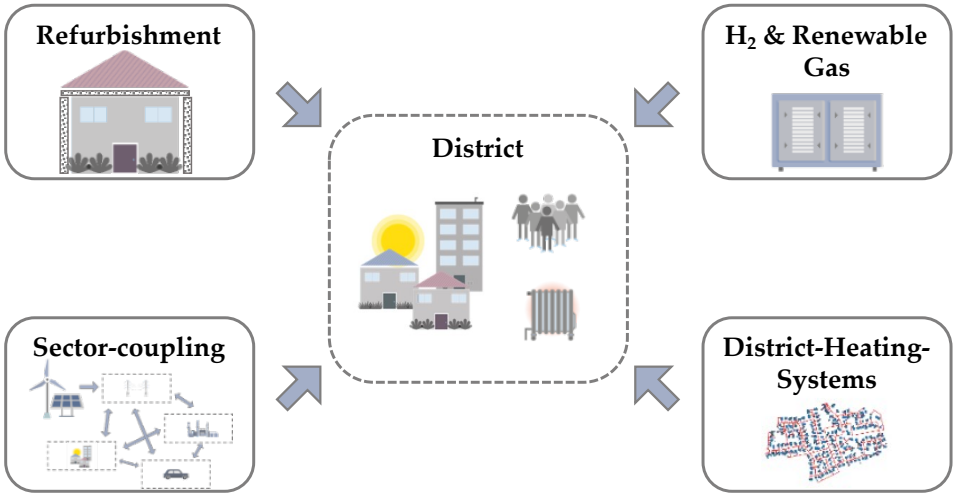

Figure 1.5: Development, trends and opportunities for the transformation of district energy systems regarding the heat supply. Source of footprints of district heating symbol: (OpenStreetMap contributors 2022)

1.2.2.1 Energetic refurbishment

The refurbishment of the existing building stock is an essential part of the emission reduction strategy and crucial for achieving a carbon-neutral building stock (Prognos et al. 2020b; Fraunhofer IWES et al. 2017). A low level of insulation and the often small-sized existing radiators demand high forward temperatures to achieve comfortable indoor temperatures. High forward temperatures worsen the efficiency of the heat generation e.g. in the case of heat pumps (Fraunhofer ISE 2020a) or other renewable energy sources like solar thermal energy. Low temperature heating systems have become a paradigm of modern renewable and efficient heat supply in buildings (Henrik Lund et al. 2014; Hesaraki et al. 2015), and energetic refurbishment is an important measure for achieving those.

More than one third of all residential buildings of the German building stock are energetically un-refurbished (Figure 1.6(a)). About half of the residential buildings are partly-refurbished. The term “partly-refurbished” means that at least one refurbishment measure, such as insulation of the facade, replacement of the windows, insulation of the roof, a cellar ceiling insulation or a renewal of the heating system has been undertaken (Metzger et al. 2019). Only five percent

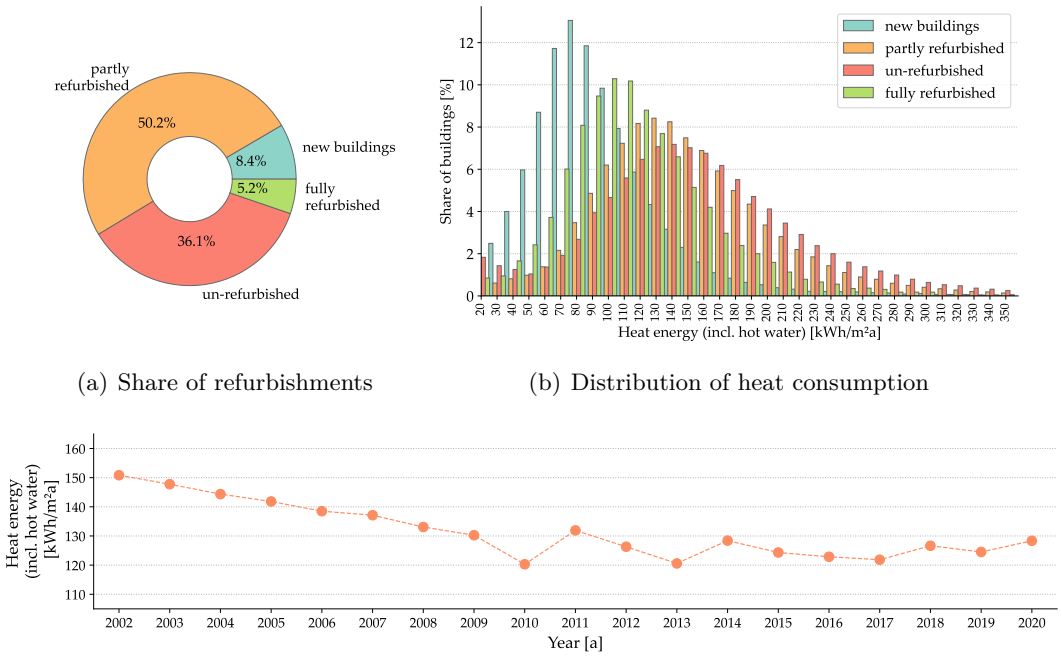

(a) Share of refurbishments

(b) Distribution of heat consumption

(c) Development of specific heat consumption

Figure 1.6: (a) Share of refurbishment categories. (b) Distribution of heat consumption of refurbishment categories. (c) Development of specific weather corrected heat consumption. Data sources: (co2online 2022; Metzger et al. 2019).

of the buildings are fully refurbished, that includes at least four of the above refurbishment measures. Eight percent of the buildings were built from 2002 onward and are categorized as new buildings (Figure 1.6(a)).

In Figure 1.6(b), the distribution of energy consumption for heating is shown for each of the refurbishment categories. There is a broad distribution, especially for the un-refurbished and partly refurbished buildings, that reflects the different building practices influenced by the different legislation as well as the wide range of implemented refurbishment measures in the category partly-refurbished. A clear shift in the distribution of heating energy consumption towards lower values can be observed when a full energetic refurbishment was implemented. However, also in the categories new buildings and fully-refurbished there is still a large share of buildings that are characterized by an energy demand of more than 100 kWh/(m²a). For the future, it is not only important to carry out more refurbishments, but also to achieve the greatest possible depth and quality of refurbishment. Nonetheless, by regulations for new buildings and incentives for refurbishment, it was possible to reduce the floor specific heat consumption over the past years. From 2010 to 2016 the refurbishment rate lay on average at about 1 % per year (Singhal et al. 2019; Cischinsky et al. 2018). The refurbishment rate expresses the share of the building envelope area of all existing buildings that is modernized on average per year (Cischinsky et al. 2018). The specific heating energy consumption per usable floor area (corrected for weather) in residential buildings decreased from 151 kWh/(m²a) in 2002 to 120 kWh/(m²a) in 2010 (see Figure 1.6(c)) (Metzger et al. 2019). However, from 2015 to 2018 this trend reversed and a slight increase can be observed for two-family and

multi-family houses (Singhal et al. 2019). This is also confirmed by the data for the whole residential building stock given in (co2online 2022) that shows a constant level of heat demand from 2010 onward, and a slight increase since 2017 (see Figure 1.6(c)).

There are several obstacles that hinder a fast increase in energetic refurbishment. The decision for refurbishment is highly dependent on the individual situation, and it is difficult to give reasons that are valid in all cases (Renz et al. 2016). According to the interview study of Renz et al. (2016), the most prominent factor is the financial aspect, followed almost equally by ecological considerations and the necessity of restoration (Renz et al. 2016). Thereby, the financial aspect is for all ownership groups (homeowners as well as landlords) the most important factor and plays an even stronger role for landlords (Renz et al. 2016). Typically, confrontation with the topic refurbishment requires a particular reason, such as necessity of restoration or the aim to increase the living comfort, the latter especially in case of homeowners (Renz et al. 2016). With respect to sufficient financial incentive, there is the landlord-tenant dilemma. In Germany, about 52 % of the residential units are rented (dena 2016). The costs of heating are fully apportioned to the tenant. This means that the landlord would not profit from lower heating costs due to the cost-intensive energetic refurbishment measures (Renz et al. 2016). In addition, 5.6 % of the existing buildings that were built before 1979 are listed buildings (Cischinsky et al. 2018), which poses a particular challenge for a deep energetic refurbishment (Dunkelberg et al. 2020).

Altogether, energetic refurbishment is an important element for achieving the climate goals. The refurbishment rate must be increased and the mentioned obstacles that hinder refurbishments need to be resolved. The share of fully refurbished buildings must significantly increase in the next decades to achieve the climate goals in the building sector (Singhal et al. 2019; Cordroch et al. 2022). However, it is unclear how fast refurbishment measures can be rolled out, and how extensive energetic refurbishment measures can be implemented in the individual building, which poses a factor of uncertainty in urban heat planning.

1.2.2.2 Sector-coupling and Smart Energy Systems

Sector-coupled energy systems have a great potential for the development of renewable DHS (Gudmundsson et al. 2018). A sector-coupled energy system in general connects the different energy sectors, which are electricity, heat, mobility and industry, with the aim of increasing the share of renewable energies in all energy sectors. The principle of sector-coupling is defined by the German Association of Energy and Water Industries (BDEW) as

> *"energy engineering and energy economy of the connection of electricity, heat, mobility and industrial processes, as well as their infrastructures, with the aim of decarbonization, while simultaneously increasing the flexibility of energy use in the sectors of industry and commercial/trade, households and transport under the premises of profitability, sustainability and security of supply"*, (BDEW 2017a, p.2) (translation Robinius et al. 2017, p.2f).

To address the integration of volatile renewable energy sources and to properly analyze dependencies and synergies of the different energy sectors in future renewable energy systems, the term *Smart-Energy-System* has become prominent:

> *"A Smart Energy System is defined as an approach in which smart electricity, thermal and gas grids are combined with storage technologies and coordinated to identify synergies between them in order to achieve an optimal solution for each individual sector as well as for the overall energy system."*, (Henrik Lund et al. 2017, p.560) based on (Henrik Lund 2014; David Connolly et al. 2013).

Both concepts have in common that the interconnection of multiple sectors and infrastructures is important for the transformation of the energy systems in the future. Figure 1.7(a) illustrates this principle.

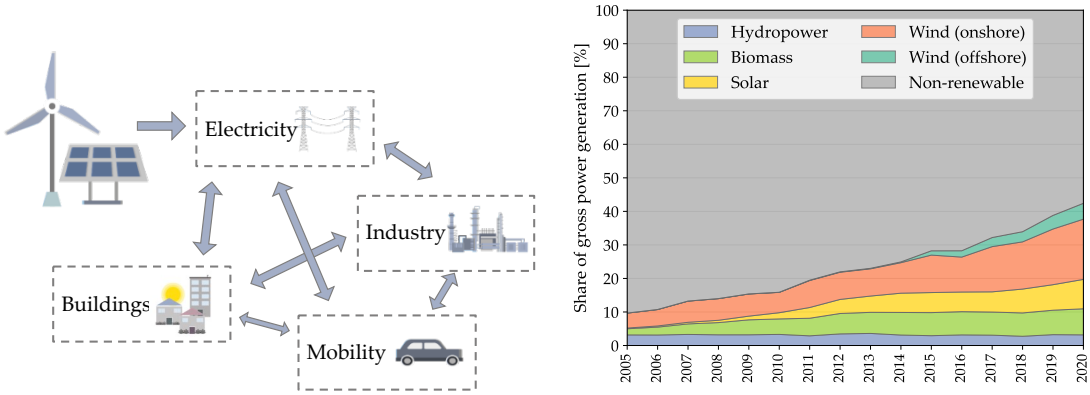

(a) Schema of sector-coupling

(b) Share of renewable energies

Figure 1.7: (a) Schematic overview of the principle of sector-coupling. (b) Share of renewable energies of the gross-electricity generation in Germany. Own illustration. Data-source: (BMWi 2021).

In both concepts of sector-coupling and *Smart-Energy-System*, the electricity sector plays a key role. In Germany the share of renewable energies of the gross electricity generation increased from 9.7 % in 2005 to 42.5 % in 2020 (Figure 1.7(b)). The expansion of volatile wind and solar capacities made the biggest progress in the recent years. The aim is to continue this trend, as the further expansion of wind and solar power plants plays a decisive role for the development of a fossil-free carbon-neutral energy system (Robinius et al. 2017; Prognos et al. 2020b; Fraunhofer ISE 2020b). The shift from controllable large-scale fossil-fuel power plants to distributed volatile renewable energy plants requires adaptations in all sectors. Sector-coupling and *Smart-Energy-Systems* are an opportunity for the reduction of emissions in all sectors, but also challenging as systems become more complex. The different energy sectors must be able to react flexibly to the availability of wind and solar power, the synergies of the different energy sectors must be used and storage capacities must be built. In this thesis, such behavior of an energy sector or an energy subsystem, such as a district energy system, is referred to as system-supportiveness. A system-supportive district energy system supports the integration of fluctuating renewable energies in the upstream electricity system (see also Section 2.1).

Furthermore, hydrogen and *Power-to-Gas* technologies are also important elements of a renewable sector-coupled energy system, which are described below in a separate section.

With respect to the building sector, *Power-to-Heat* technologies, such as heat pumps, are an important element of sector-coupling and *Smart Energy Systems* for the emission reduction in

the building sector (Henrik Lund et al. 2017). However, as a consequence of the interaction with the sector-coupled or *Smart Energy Systems*, the development of future heat supply strategies may require an advanced energy systems analysis (Möller et al. 2019). The traditional planning approaches may not be sufficient any longer, as complex system-interactions with the other sectors need to be taken into account (see Figure 1.7(a)). This demands the development of novel design approaches that achieve a flexible and, with respect to the upstream power grid, a system-supportive design for the integration of fluctuating wind and solar power plants.

1.2.2.3 Hydrogen and E-fuels

Hydrogen generated by electrolysis with renewable electricity is an essential element of a future carbon-neutral energy system (Merten et al. 2020). Electrofuels (E-fuels), which are gaseous or liquid hydrocarbon fuels synthesized from hydrogen and CO_2, could substitute their fossil counterparts without transforming the demand-side to an electricity-ready system (Ueckerdt et al. 2021). The conversion of electrical energy into hydrogen or e-fuels is an important element of a sector-coupled energy system and is also often described as *Power-to-Gas* or *Power-to-Liquid* (Agora Verkehrswende et al. 2018).

In our industrialized economy, there are processes and energy applications that cannot be electrified, that are very difficult to electrify or that need chemical products or gases like hydrogen within the process (Agora Verkehrswende et al. 2018). Examples are the production of steel, fuels for aviation, especially for long-distance flights, maritime transport, heavy transport or high temperature processes (Agora Verkehrswende et al. 2018; Ueckerdt et al. 2021). For some applications, the direct use of biomass, e.g. wood, or the use of biogas (that is based on biomass, such as corn) are an alternative to e-fuels. However, the sustainable use of biomass is limited and *Power-to-Gas* is needed (Henrik Lund et al. 2017; Gatzen et al. 2021). Hydrogen and e-fuels are versatile energy storages, that could support the integration of renewable energies and provide backup capacities at times of low wind and solar generation (Henrik Lund et al. 2016; Nastasi et al. 2016) and are well suited for long-term energy storage (Reuß et al. 2017; Agora Verkehrswende et al. 2018). In the case of hydrogen, however, several challenges need to be met. Hydrogen has with 0.09 kg/m³ a very low density at ambient conditions, which is 0.003 kWh/l (Moradi et al. 2019; Reuß et al. 2017). This means that the energy density needs to be increased, either physically (e.g. compression or liquefaction) or material-based with physical or chemical sorption methods (e.g. liquid organic hydrogen carrier (LOHC)) (Moradi et al. 2019). Despite the problems involved in hydrogen storage, which are, for example, material-related issues such as embrittlement in the case of steel vessels (Moradi et al. 2019), compressed hydrogen storage up to a pressure level of 700 bar is state of the art in the use of carbon fiber composites (Barthelemy et al. 2017; Reuß et al. 2017).

The gas infrastructure is well established in Germany. The total length of the gas distribution network amounted to 555.7 thousand kilometers in 2019 (Bundesnetzagentur 2021). The expansion of the gas network started in the nineteen sixties to diversify the national energy supply and to provide alternatives to coal, oil and nuclear power (Verband kommunaler Unternehmen e.V. 2017). The gas network, with more than 800 TWh per year, delivers more than one and a half times the amount of energy that is supplied by the electricity grid. More than 30 % of private households are directly connected to the gas network. Within the energy

transition, the existing gas network could become a backbone of the future energy infrastructure by transporting renewable gas and hydrogen. (cf. Verband kommunaler Unternehmen e.V. 2017)

For the production of hydrogen and e-fuels, two strategies are possible: the generation within Germany, or the import from countries with a higher availability of renewable energies such as wind and solar power, that may increase full-load hours of the plants to decrease costs. In the latter, case the import from countries like Morocco, Norway and Argentina could be a promising path (Hank et al. 2020; Hampp et al. 2021; Merten et al. 2020). However, it is unclear how fast new gas import routes can be developed, and to what extend imported renewable gases can be expected in the coming decades. Additionally, there is high uncertainty about current and future prices for imported gas (Merten et al. 2020). Furthermore, there is also the question of how sustainable these imports may be. In countries like Morocco, the energy system is based almost entirely on fossil fuels, and it is questionable whether the renewable potential there should be used to produce gas for Europe rather than firstly to decarbonize the energy system in Morocco itself (Merten et al. 2020).

There is common agreement that hydrogen and synthetic gas are important elements in the transformation of certain sectors of the energy system, especially in the industry sector (Prognos et al. 2020b; Fraunhofer ISE 2020b). However, it is controversial if and to what extent hydrogen and e-fuels are future energy carriers in all energy sectors. The usage of hydrogen and e-fuels is, in principle, not as efficient as direct electric applications where they are possible. There are conversion losses in the generation of hydrogen and synthetic gases, and also in the subsequent conversion of gases into the required form of energy such as electricity or heat (Ueckerdt et al. 2021; Agora Verkehrswende et al. 2018). Against this, the Association of the Gas and Water Industries in Germany (DVGW) argues that renewable gases are needed in all energy sectors (Gatzen et al. 2021). In any event, a stronger focus on the electrification of all sectors requires a more extensive reinforcement and expansion of the power grid, which from experience will raise protests by residents living close to the planned transmission capacities (Frontier Economics et al. 2017). By the use of the existing gas infrastructure, the acceptance for energy transition may be improved (Frontier Economics et al. 2017). Also, renewable gases increase the diversification of the energy supply, and could contribute to a more resilient energy supply (Gatzen et al. 2021; Frontier Economics et al. 2017).

With the focus on the heat supply in the building sector, renewable gas is, in principle, also a possible strategy; however, the above stated controversies apply here similarly. The strategy of replacing natural gas for the heating sector with methane or hydrogen from renewable sources and keeping the existing heating systems in buildings is an expensive measure for reducing emissions (Prognos et al. 2020a; Fraunhofer ISE 2020b). However, in many districts there is an existing gas infrastructure that may be used for the distribution of renewable synthetic methane gas. Also, the share of hydrogen in the gas network may be increased. Currently, the maximum share of hydrogen in the gas network amounts to 2 percent by volume, and an increase up to 10 percent by volume is considered to be possible, depending on the customers within the individual distribution grid (Bundesnetzagentur 2020b). A further increase in the share of hydrogen requires an adaption of the infrastructure and especially the adaption of the gas-fueled devices and boilers at the gas consumers possibly even several times (Bundesnetzagentur 2020b).

By blending hydrogen with methane gas in the gas network, hydrogen is no longer available for applications in industry that demand pure hydrogen (Bundesnetzagentur 2020b). Still, increasing the share of renewable gas in the gas network is one option to reduce the emissions, especially in existing un-refurbished building stock that demands for a high supply temperature (Gatzen et al. 2021). Additionally, local hydrogen generation next to cities and urban areas may create synergies by using the excess heat from the electrolysis for the building sector. In other words, hydrogen and renewable gases need to be taken into account in the development of future district energy concepts.

1.2.2.4 District heating systems

District heating refers to a system for distributing heat from one or more centralized plants to the buildings of a district or city that are connected with a network of pipes (Henrik Lund et al. 2014), also called a district heating system (DHS). The size of the area supplied via a DHS can vary greatly, ranging from small neighborhoods with a few buildings to entire metropolitan regions (Dunkelberg et al. 2020). In 2010, Lund et al. concluded that DHS have a great potential for supporting the energy transition towards a renewable energy system in Denmark (H. Lund et al. 2010). Continuing studies for the whole European heating sector have also come to the result that DHS are in many cases an economically feasible option (Persson et al. 2019; Möller et al. 2019).

District heating has the prospect of becoming important within the energy transition in order to utilize and exploit all kinds of punctual heat sources and to distribute the heat to buildings. Examples of such heat sources are excess heat from industrial processes, waste incineration and power plants, deep geothermal energy, large scale solar thermal energy and large scale heat pumps (H. Lund et al. 2010; HIC et al. 2021; Dunkelberg et al. 2020). In the case of large scale heat pumps, sea water, river water or wastewater may be deployed as ambient heat sources. The distribution of heat from these heat sources to buildings requires a DHS. Restricted to the building level, the deployment of this kind of large scale heat source is not feasible. For example, in the case of deep geothermal energy, which could imply a drilling depths of multiple kilometers, this is simply not an option for a single building.

This leads to another advantage of DHS, and that is the economy of scale of heat generation and storage units, also described as efficiency with respect to technical and economic aspects (Rezaie et al. 2012). The economy of scale includes several aspects. Firstly, the specific investment and maintenance costs per kilowatt installed capacity are lower for larger units than for smaller units at building level (compare Danish Energy Agency 2020b; Danish Energy Agency 2021a). Secondly, the energy conversion efficiency of larger units is higher than for smaller units. For instance, in the case of heat pumps, a 1 MW heat pump may achieve a Lorenz-efficiency of 47 %, whereas a 10 MW heat pump may achieve a Lorenz-efficiency[1] of 60 % (Danish Energy Agency 2019). And thirdly, the simultaneity effect of heat consumption, also called concurrency effect, allows for a lower capacity of installed heat generation units. The heat load of a DHS with a large number of customers is lower than the sum of the peak heat loads of each single customer. The ratio of the aggregated heat load of a DHS to the sum of the heat loads of

[1] The Lorenz-efficiency describes the relation of the actual coefficient of performance (COP) to the ideal thermodynamic Lorenz cycle.

the connected buildings is often referred to as the simultaneity factor. This factor depends on the number and kind of customers and can result in values of 50 % or 60 % (Winter et al. 2001). This means that the investment costs for heat generation units can be reduced not only by lower specific costs but also by lower overall heat generation capacities compared to an individual supply scenario. The different aspects of economy of scale also apply to energy storage units. The investment costs as well as the thermal losses of heat storage can be reduced in large scale storage units compared to individual storage units.

The downsides of district heating are the investment costs for the infrastructure and the additional heat losses of the piping system (Persson et al. 2011; Möller et al. 2019). A DHS usually consists of a forward and a return pipeline for transporting the hot water to the consumers and returning the cooled water back to the energy supply site. The civil engineering and construction of the pipeline infrastructure are a decisive cost factor (Persson et al. 2011). The transport of the water itself requires additional electricity for operating grid pumps (Rezaie et al. 2012). Due to the overall distribution costs and heat loss, the economic feasibility of DHS depends highly on the spatial characteristics of the examined area, such as the heat density (Möller et al. 2019; Persson et al. 2011). The term heat density of a district refers to the heat demand density per district area and is an important indicator for the economic feasibility of district heating compared to individual heat supply. To reduce thermal losses of the DHS, the reduction of the supply temperature is essential. Therefore, low temperature DHS are developed, which are described as 4^{th} generation DHS (Henrik Lund et al. 2014). Such DHS are characterized by supply temperatures of 70 °C and below (Henrik Lund et al. 2014). Besides the distribution system, the construction and operation costs of the heat supply represent additional costs compared to individual heat supply that need to be taken into account. The heat supply site also requires room within the district or city. On the other hand, space within buildings may be saved as a DHS only requires a compact substation.

In Germany, the share of DHS in the total heat demand (including industry) lay at 13.7 % in 2016 (BDEW 2017b). The numbers given by BMWi (2021) indicate an even lower share for the building sector (see also Figure 1.3). The share of new buildings supplied via DHS was at 23.8 % in 2016 (BDEW 2017b). In contrast, in Denmark 58 % of residential and service sector buildings were supplied by district heating in 2015 (Persson et al. 2019). In Germany, most of the heat in DHS is generated via combined heat and power plants (CHP) (BDEW 2017b). As shown in Figure 1.3, the main part of the heat generation is based on fossil fuels, while the share of renewable energy lies only at 13.6 % (BDEW 2017b).

According to Möller et al., the economic potential of district heating is in total at 59 % for 14 European countries[2], and for Germany at 66 % in relation to the total net heat demand (Möller et al. 2019). Persson et al. conclude that a share of 50 % of the heat demand for the residential and service sector buildings of the EU28 member states is economically suitable for district heating (Persson et al. 2019). In contrast, scenario based-studies for the development of the overall energy system in Germany until 2050 anticipate lower shares of district heating (as reviewed in HIC et al. 2021). The share of district heating in the total heat demand ranges from 15 % in a conservative scenario with a high persistence and a low acceptance of new

[2] Austria, Belgium, the Czech Republic, Germany, Spain, Finland, France, Hungary, Italy, the Netherlands, Poland, Romania, Sweden and the United Kingdom

technologies and infrastructures throughout the population (Fraunhofer ISE 2020b) to almost 40 %. The trend of the studies considered goes towards a share of 20 to 25 % (HIC et al. 2021).

The basis for potential areas for DHS can be derived from heat density maps (Möller et al. 2014) or analyzed by applying the method for determining suitable areas presented by Knies (Knies 2018). However, not only the heat line density, but also the specific local conditions play a decisive role, and no absolute tipping points for heat line densities to determine the economic feasibility of a DHS can be defined (Knies 2018). This means e.g. that areas with a low and medium heat demand density cannot be excluded from the outset. Since the heating sector needs to be coupled with other energy sectors (Gudmundsson et al. 2018) to establish *Smart Energy Systems* for the integration of fluctuating renewable energies (Henrik Lund et al. 2016), and due to the growing importance of flexibility (Sneum 2020; Sneum et al. 2018), the planning of DHS networks is also becoming increasingly complex. In addition, thermal energy storage will play an important role and needs to be integrated in the planning of DHS (Henrik Lund et al. 2016).

DHS offer promising solutions and might become an important infrastructure within the energetic transformation of existing districts. However, there is a wide range of uncertainty about the future share of DHS from 15 % to more than 60 % of the heat demand, as mentioned above. There are many districts near the threshold range of heat density, where it is not yet decided whether or not a DHS is a feasible infrastructure. In Germany, 9 % of the heat demand is located in areas with a sparse heat density of 20 to 50 MJ/m², and 31 % in areas with a moderate heat density of 50 to 120 MJ/m² (Persson et al. 2019). In both cases, district heating in connected and contiguous areas with such heat densities is in principle possible (Möller et al. 2019). Furthermore, punctual heat sources, like a deep geothermal potential or excess heat sources, the exploitation of which requires a DHS for heat distribution, are not available everywhere. Therefore, the question arises under which circumstances and in which cases a DHS is a cost-efficient infrastructure to reduce emissions, and, especially for districts with a sparse and moderate heat density, to what extent do the different trends and developments summarized in the previous sections impact on the decision to establish a DHS. The planning methods for designing DHS and deciding on the feasibility of DHS must be developed further and additional constraints for developing sector-coupled district energy systems must be taken into account.

1.3 Objective

The trends and developments outlined imply far-reaching upheavals in the energy system and pose extreme challenges for heat- and infrastructure planning, especially at a municipal level. Due to the urgency of the energy transformation, decisions by municipalities and communities on infrastructures need to be made far in advance, although the detailed development paths, the transformation speed and depths are still unknown. To avoid stranded investments in cost-intense infrastructures, future developments must be anticipated. The ongoing coupling of energy sectors makes the planning even more complex, as the development of energy systems at district level needs to be an integrated part of the overall national energy system to unleash

potential synergies between the different energy sectors. Especially the transformation of existing districts poses a particular challenge. In districts with a sparse to moderate heat density, it is often unclear whether DHS are economically feasible solutions.

Therefore, this thesis aims to develop future-proof renewable and system-supportive heat supply concepts and district heating infrastructures for existing districts, as well as software tools and methods for achieving this purpose. This includes an examination of the future role of district heating compared to individual heat supply and an analysis of the factors that impact the economic feasibility of district heating to achieve a carbon-neutral energy supply at building level. The findings aim to support planning and decision making in municipalities and communities. To reach the objective of this thesis, three subordinate research objectives (RO) need to be achieved:

1. Development of methods and tools for the design and techno-economic assessment of renewable and system-supportive heat supply concepts and corresponding infrastructures at district level (RO 1)
2. Development of future-proof renewable and system-supportive district heating systems, including the design of the district heating network and the energy converter and storage units of the heat supply site (RO 2)
3. Analysis of the impact of future developments on the required heat density threshold for the economic feasibility of district heating compared to individual heat supply from a cost-optimal to a carbon-neutral energy supply (RO 3)

For tackling the research objective, the district of the Rüsdorfer Kamp of the city of Heide is examined in detail as a typical existing district. In this thesis the term district refers to a connected and contiguous urban or suburban area of the size of 10 hectares to 50 hectares. The investigated district is characterized by a sparse to moderate heat demand density. This is a heat density range where it is undecided whether the establishment of a DHS is in all cases the best solution (see Section 1.2.2.4). Thus, the selected district is well suited for studying the influencing factors on the feasibility of district heating for future scenarios.

The term future-proof refers to concepts that fit into overall transformation scenarios of the entire energy system and do not result in lock-in effects or stranded investments. Therefore, the outlined trends and developments introduced in Section 1.2.2 are considered in a comprehensive scenario framework for the potential developments at district level and for the transformation of the upstream energy infrastructures. Based on these scenarios, the impact of different developments on a cost-efficient emission reduction of the energy supply is examined in detail for the considered district.

This thesis aims to develop an integrated systemic approach that addresses the current challenges of developing heat supply concepts in an increasingly sector-coupled environment. On the one hand, this includes the consideration of time-resolved characteristics of the volatility of renewable energies in the electricity grid to achieve a system-supportive design. A system-supportive district energy system refers to a system that is capable of supporting the integration of volatile renewable energy sources in the upstream electricity system. And on the other hand, this requires a combined consideration of the heat and electricity sector at building level that might impact the feasibility of district heating in a strongly sector-coupled energy system. Both

aspects strive to meet the future challenges of an integrated sector-coupled development of district energy systems. In doing so, this thesis develops open source tools for supporting the planning of DHS and showcases an overall approach to design future-proof heat supply concepts at local level in connection with a successful energy transition.

1.4 Outline of the thesis

The thesis is structured into four main parts as illustrated in Figure 1.8. Chapter 2 provides the methodical background of the thesis. This includes the introduction of the assessment method for electricity crossing the system-boundary of a district- and local energy system to achieve a renewable and system-supportive design (research objective RO 1). Furthermore, a detailed introduction of the existing district that is used as a reference for the analysis of this thesis is given, as well as the underlying mathematical background to the modeling approach and an overview of the model chain that was developed and applied within the thesis (research objective RO 1).

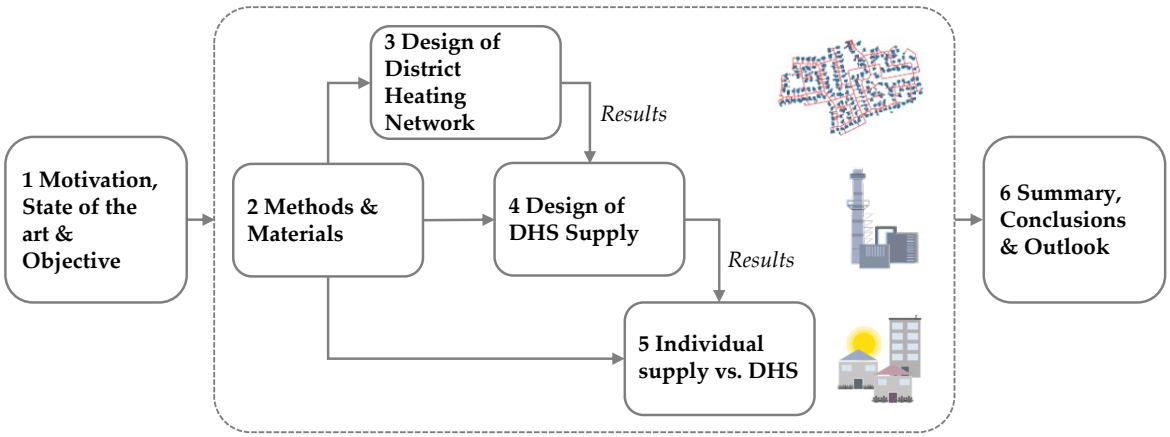

Figure 1.8: Overview and structure of thesis. Source of footprints of district heating symbol: (OpenStreetMap contributors 2022)

The third chapter presents the planning approach for district heating networks that is an essential part of the overall approach for the evaluation of different heat supply concepts (research objective RO 1). The planning tool optimizes the routing and the dimensioning of a district heating piping system and is published as an open source package. With this tool, the investment costs and thermal losses of the district heating network can be estimated in early project stages. In this chapter, the scenarios for the existing building stock (local scenarios) are developed that are investigated in the subsequent parts of the thesis. For each of the scenarios, the district heating network is designed to generate the required parameters for the design of the district heat supply.

Chapter 4 investigates how a future-proof design of the energy converters and storage units of district heat supply systems have to be designed to obtain a renewable and system-supportive heat supply (research objective RO 2). Therefore, a scenario framework for the development path of the upstream energy infrastructures of the power grid and the gas network are defined, and a mixed-integer linear programming model is set up to optimize the energy converter and

storage capacities. The model is applied to the scenarios of the upstream energy infrastructures and to each of the scenarios of the existing building stock of Chapter 3. For each of the scenarios, the trade-off between costs and emissions is analyzed.

Based on the results of Chapter 4, Chapter 5 compares the district heating supply variants for each of the scenarios with an individual heat supply. An analysis is made of the extent to which different transformation paths of the overall national energy system (global scenarios) influence the decision on whether a DHS is economically feasible compared to building-wise heat generation to obtain a zero emission energy supply and to determine cost-efficient emission reduction strategies (research objective RO 3). Therefore, the heat and electricity supply of two reference buildings within the district are optimized for each of the scenarios of the upstream energy systems as well as for the scenarios of the existing building stock. In this analysis, a particular focus lies on a combined consideration of heat and electricity at building level as well as on the time-resolved characteristics of the volatility of renewable energies in the electricity grid. By comparing the results, infrastructure decisions in a sector-coupled energy system for a cost efficient emission reduction are derived (RO 3). Based on the comparison of heat supply with DHS versus individual heat generation, heat density thresholds for the feasibility of a DHS are estimated and the impacts of different scenarios on the feasibility of a DHS are discussed. The existing criteria for DHS are reviewed and potentially new criteria for establishing DHS in the ongoing transition of the energy system are identified.

Finally, the results and conclusions for a future-proof design of a renewable and system-supportive district heat supply are presented in Chapter 6, where the contributions of this thesis to the field are pointed out, and an outlook is given for further research that could follow on from this work.

1.5 Open source as modeling principle

The modeling approach developed and applied in this thesis relies exclusively on open source tools and packages. This implies the usage of existing packages, the improvement and contributions to existing packages, such as *oemof.solph* (Krien et al. 2020), and the publication of tools, that were developed and applied in this thesis. The latter includes a software tool for the flexible design of district heating networks by an optimization of topology and pipeline dimensions, that was published within the *DHNx* package (oemof developer group 2022b), see also Section 3.2), and the developed *oemof.solph* application *q100opt* (Röder et al. 2022a) for the Pareto-optimization of the district heat supply and the energy supply at building level. All tools, that were developed and used in this thesis, are written in Python, which is itself open source (The Python Community 2022). By practicing open source development on the platform GitHub (GitHub, Inc. 2022), the tools can be used and extended by others. This enables a collaborative development and avoids duplicated work in science.

2 Methodical approach

The following chapter introduces the underlying methodical approach and fundamentals of the thesis. This includes the identification and selection of an appropriate assessment and optimization criteria for designing renewable and system-supportive district energy systems (RO 1) and a detailed introduction of the existing district that is investigated in this thesis. Furthermore, the mathematical background of the modeling approach is given, and finally, the overall approach and model chain that is developed in this thesis for investigating the role of district heating for future scenarios is introduced (RO 1).

2.1 Renewable and system-supportive design method

The aim of the modeling and optimization approach in this thesis is to find the most cost-efficient emission reduction concepts and infrastructures for the heat supply in an existing district for future scenarios of the upstream energy system and the local existing building stock. As introduced in Section 1.2.2 the development of sector-coupled district energy systems requires an integrated planning approach. The following sections explain the future requirements of district energy systems, reviews existing assessment parameters and discuss the methodical approach for a prospective design of renewable and system-supportive district energy systems.

2.1.1 Demand for system-supportive design

A district energy system is embedded in and at the same time an essential part of the national (and international) electricity system. As *Power-to-Heat* based heat generation might take a decisive role within the de-carbonization of the heating sector in future sector-coupled energy systems (see also Section 1.2.2), the interaction with the upstream electricity system by importing and exporting electricity is becoming increasingly important. Figure 2.1 illustrates the intersection of both systems.

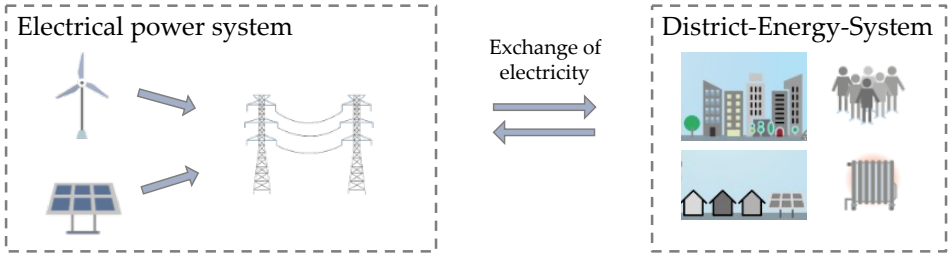

Figure 2.1: Schematic illustration of the intersection of upstream power system and district energy system. Own illustration.

To analyze dependencies and synergies of the different energy sectors in future renewable energy systems, *Smart Energy Systems* approaches, as defined in (Henrik Lund et al. 2017), are needed. Therefore, holistic models containing all parts of the energy system with a focus on the national energy system have been developed. There are many examples of models and analyses that are

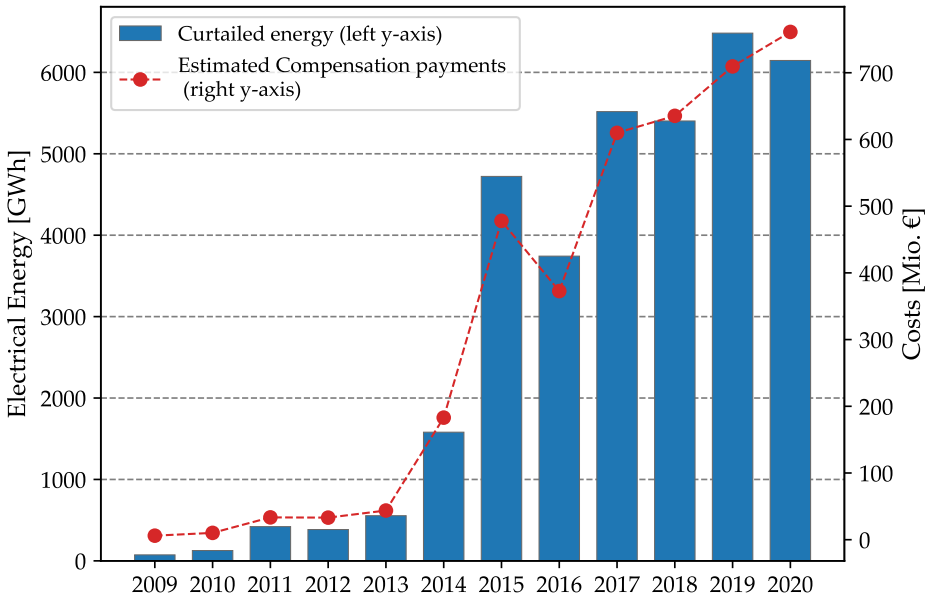

Figure 2.2: Volume and costs of curtailed energy due to feed-in management from 2009 to 2020 in Germany. Own illustration based on (Köppl et al. 2020). Data sources (Bundesnetzagentur 2014; Bundesnetzagentur 2020a; Bundesnetzagentur 2022).

based on integrated energy system models on national (and European) level, e.g. the energy system model EnergyPLAN (Henrik Lund et al. 2017), the open source software *Deflex* (Krien 2019) and many others (Prina et al. 2020; openmod contributors 2021). With such models, optimal solutions for the representation of complex, sector-coupled energy systems considering all synergies can be found and the integration of volatile renewable energies into the power system can be studied (Figure 2.1 - left).

For design decisions on a municipal level, e.g. concerning the selection and dimensioning of energy supply technologies, storage units and infrastructures (e.g. DHS), models with a higher degree of detail for the individual districts are used to both derive individual energy concepts and support the local planning process (Krien 2019; Klemm et al. 2021). In these district energy system models, the national energy system itself cannot be considered anymore in detail, as it means a considerable effort to model the entire energy system for each decision at the district level (Figure 2.1 - right). Therefore, suitable boundary conditions for local energy system models must be defined for the exchange of electricity at the intersection to the upstream energy system (Figure 2.1).

In Germany, as well as in many other countries, the most important renewable power generation plants are – and will be in future – the volatile wind and solar power plants. This is shown by studies based on models of the overall national energy system containing all its sectors, e.g. (Fraunhofer ISE 2020b; Prognos et al. 2020b). This development implies that the number of hours with energy excess will increase, and there will be times with energy shortage (Fraunhofer ISE 2020b). However, already today there are considerable amounts of excess renewable energy at certain times of the year. The historical loss of usable energy due to feed-in management are presented in Figure 2.2.

The expansion of renewable energy sources goes along with an increase in congestion management measures (see Figure 2.2). Congestions in the transmission and distribution power grid occur due to limited transmission capacities and the physical inability of a spatially matching of electricity generation and demand according to the market-based schedule (Fekete 2021). Therefore, the transmission system operators are obligated to resolve congestions in the power grid by feed-in management and redispatch. This means that the electricity generation is increased on one side of the bottleneck and the feed-in is decreased on the other side of the bottleneck (Fekete 2021). In connection with controllable conventional power plants, this is referred to as redispatch. With respect to renewable energy sources such as wind or solar plants, congestion management means a curtailment of the energy sources, also called feed-in management. Both measures are not only a distressing loss of usable energy, but also imply compensation costs, on one side for the subsidized renewable energy plants that are curtailed, and on the other side for the conventional power plants and reserve power plants that are set into operation (the total costs are shown in Figure 2.2) (Köppl et al. 2020). A reinforcement of distribution and transmission capacities could reduce the volume of congestion management in the medium to long term. However, as the expansion of renewable energies must continue strongly to meet the climate goals (Prognos et al. 2020b; Fraunhofer ISE 2020b), and due to a sluggish progress in grid expansion (Fekete 2021), the congestion measures and curtailment of renewable energies are expected to continue strongly (Fekete 2021).

The design of future district energy concepts requires an adequate consideration of the volatile character of renewable power generation in the upstream energy system to support the integration of volatile renewable energies and to avoid congestion management. The integration of renewable energies means the alignment of electricity sourcing according to the volatile renewable energy generation, the avoidance of curtailment of renewable energy generation and an electricity feed-in at times of a low availability of renewable energies. Thus, besides achieving low costs and emissions, the district energy system must be able to contribute to this task.

In this thesis, the term system-supportive refers to the capability of a local energy sub-system to interact with the upstream power grid in such a way that the problems of the integration of volatile renewable energy sources into the overall electricity system are diminished. This implies sourcing electricity from the grid at times of a high availability of volatile renewable energy sources and feeding electricity into the grid at times of a low availability (based on Klein et al. 2016). In this thesis, the term system-supportiveness does not include the technical ability to maintain the frequency and voltage of the electricity grid to avoid a power system failure, but describes the general alignment of the electricity exchange with the upstream power grid according to the volatile renewable energy generation.

Currently, the incentives to design district energy systems as system-supportive with respect to the upcoming extension of wind and solar capacities are low. Sneum extensively investigated the barriers for a flexible operation of district energy systems (with focus on the Scandinavian and Baltic countries) and concluded that the absence of flexibility signals is the most important barrier (Sneum 2020). In Germany, too, the incentives for a grid-supportive operation are low. Reasons may be that the ecological assessment is based on primary energy factors, or that the

volatile share of the electricity price is low due to a high share of fees and taxes, as illustrated in the following section.

Nonetheless, important decisions for the development of future-proof infrastructures at district level must be made already today, even if the detailed design of the future electricity and flexibility markets is still unclear. The development of a system-supportive energy system and infrastructure design must be prospective and needs to be addressed early in advance, as the technical lifetime of facilities and infrastructures lasts for multiple decades. Therefore, a grid-based reference quantity for the assessment of the import and export of electricity into and from a local energy system is necessary for the prospective design of district energy systems.

2.1.2 Review of assessment parameters

The following sections review existing assessment methods for electricity crossing the system-boundary of district- and local energy systems. This includes assessments methods for the ecological aspects of the electricity of the upstream power grid, as well as potential grid-based reference quantities, that address the aspect of system-supportiveness with respect to the upstream power grid of district energy systems. Subsequently, the existing assessment parameters are evaluated in terms of their suitability with regard to the prospective design of district heating systems (DHS) pursued in this thesis. Thereby, the assessment parameter should be well comprehensible and easy to apply, and it must be possible to derive the assessment parameter from energy system models of the upstream energy system, such as *Deflex* (Krien 2019) or *ISAaR* (Böing et al. 2019), to allow their consideration within future scenarios of the upstream energy system.

2.1.2.1 Primary energy factor

The term primary energy factor (PEF) refers to the relation of primary energy consumption per quantity end-energy (Schüwer et al. 2015). The PEF aims to include the energy expenditures from the upstream chains, such as exploitation, processing, conversion, transport and distribution to compare different energy commodities such as oil, gas, coal and electricity (Schüwer et al. 2015). In Germany, the primary energy factor is the mandatory assessment parameter for the evaluation of DHS and the energy supply of buildings according to GEG §22 (GEG 2020). The primary energy factors of electricity imports and exports is defined as listed in Table 2.1.

Table 2.1: Primary energy factors for the sourcing and feed-in of electricity from and into the upstream power grid according to the German Buildings Energy Act (Gebäudeenergiegesetz – GEG). Source: (GEG 2020).

	Primary energy factor (non-renewable)
Electricity – grid-sourced	1.8
Electricity – displacement electricity mix for CHP	2.8

According to Table 2.1, a primary energy factor of 1.8 is attributed to each kilowatt-hour electricity that is imported into the building or district heating facility. For exporting electricity in the electricity grid, that is generated via a CHP, a credit method is applied and a primary energy factor of 2.8 per kilowatt-hour electricity is honored. This method is based on the argumentation that no renewable energies are displaced by the CHP plant but mainly fossil power generation plants (Schüwer et al. 2015).

To design future-proof district energy systems, the primary energy factor as defined in the German regulations is not considered to be an appropriate assessment parameter neither for the ecological assessment nor for the assessment of the system-supportiveness. In the recent years the share of renewable energies (renewable energy generation related to net electricity consumption) in Germany significantly increased from a share of 31.5 % in 2016 to 46.3 % in 2020 especially by the expansion of wind and solar power (Bundesministerium für Wirtschaft und Klimaschutz 2021). The primary energy factor stayed constant throughout this period. Although the primary energy factor for grid-sourced electricity was successively reduced from 3 to 1.8 between 2002 and 2016 (Schüwer et al. 2015), it does not seem reasonable to use an assessment parameter that lags behind reality when it comes to derive future-proof investment decisions. Furthermore, it is not comprehensible that the feed-in of any fossil combined-heat and power plants (CHP) receives a primary energy credit of 2.8 for each kilowatt-hour of electricity feed-in the grid independent of the point in time of feed-in. As stated above, it is argued that the feed-in of electricity displaces large fossil power plants (Schüwer et al. 2015). The displacement value of 2.8 was reviewed and validated for the German electricity system of 2005 (Schüwer et al. 2015; Forschungsgesellschaft für Energiewirtschaft mbH 2007). In this year, the share of renewable energies related to the gross electricity consumption was at 10.3 % in contrast to 2020 with a value of 45.6 % (Bundesministerium für Wirtschaft und Klimaschutz 2021), which strongly questions the timeliness of this value. Pehnt et al. came to similar results regarding the appropriateness of the credit value and recommend the methodical switch from the credit based method to an allocation method for the combined heat and power generation based on the Carnot method (Pehnt et al. 2018). Furthermore, Pehnt et al. recommend to move from primary energy factors to emission factors in CO_2-equivalents in the next years, as this measure relates more to the actual greenhouse gas potential (Pehnt et al. 2018).

Altogether, the current regulations for the ecological assessment in the form of constant primary energy factors in Germany are not suitable for the prospective development of DHS. Furthermore, as it is a constant factor, a system-supportive electricity import and export at times of a high or a low share of renewable energies is not rewarded by this assessment parameter. Thus, the primary energy factor as defined in the GEG is not considered as a suitable assessment parameter for the aim of this thesis.

2.1.2.2 Electricity price

The electricity price is an important element of an economic assessment of different energy supply concepts at district level. Additionally, it is plausible that the consideration of time-resolved electricity prices, e.g. in the form of the day-ahead spot market prices, may also be used to create a system-supporting design of the local energy system, since the price acts as a signal for shortage or excess. As renewable energies like wind and solar operate at almost zero marginal

costs, a very high feed-in of these could displace all other power plants, which might lead to low market prices. With further expansion of renewable energies, this effect will tend to increase. Additional charges for CO_2 emissions throughout the energy system could further increase the volatility of the electricity price and so provoke an incentive for an ecological and system-supportive feed-in and sourcing of electricity into and from the upstream energy system.

However, using solely a volatile electricity price as assessment criteria for the prospective design of district energy systems involves several challenges. First, the main part of the electricity price for district heating utilities as well as for private households consists of fees and taxes. In the year 2020 the volatile part of the electricity price that might reflect an excess of renewable energies or a shortage of electricity was only about one fourth of the total electricity price (Bundesnetzagentur 2021). For private households, it is unclear whether it will be possible that a volatile price can be forwarded to the households by the power supplier at all. The second and even bigger problem is to adequately calculate and forecast electricity prices for future scenarios of the energy system. On the one hand, it is unclear how the taxes and fees, like grid charges or CO_2 charges, will develop and be appointed by policy makers, and on the other hand, the volatility of the future market prices itself is also difficult to predict as the detailed market design itself is subject of discussion and research (Weyer et al. 2020; Risse et al. 2020; Fraunhofer IEE et al. 2021). At the moment, there is just one market zone in Germany, however, different market designs might be possible in future, for instance nodal-pricing (Maurer et al. 2018) or regional flexibility markets (Heilmann et al. 2020). However, the future market design is unknown.

Consequently, for the prospective design of future-proof district energy systems and infrastructures for the next decades, the usage of a volatile electricity market price is not a viable option for the aim of this thesis.

2.1.2.3 Emission factor

The term emission factor refers to the greenhouse gas emissions calculated by equivalents of carbon dioxide (CO_2-equivalents) and attributed to one kilowatt-hour energy. For electricity from the upstream electricity grid, different methodical approaches are common. With respect to the aim of this thesis the most important differentiating characteristics are given and discussed in the following[1] (based on (Hamels et al. 2021; Regett et al. 2018)):

- Temporal resolution: constant or dynamic (time-resolved)
- Market perspective: average or marginal method
- Geographical scope: geographical reference basis
- Assessment boundary: operational perspective or life-cycle perspective

A constant emission factor means a fixed value for the whole observation period, e.g. one year. A dynamic (time-resolved) emission factor implies that individual emission factors are

[1] The same differentiation categories are also applicable to the primary energy factor (see Hamels et al. 2021). However, as the emission factor in CO_2-equivalents relates more to the actual greenhouse gas potential, the usage of emission factors is favored in this thesis.

used for each point in time. For the purpose of this thesis a dynamic method is needed to consider the time-resolved characteristics of renewable energies in the upstream energy system. It is shown that a dynamic assessment of emissions can impact the costs and investment decisions concerning district energy systems and thus stresses the importance of an accurate consideration of the emission from grid-sourced electricity (Röder et al. 2020).

The market perspective can be divided in the average (or mix) method and the marginal method. In the mix method, the emission factor is calculated as average emissions of the electricity generation at a given time. For the marginal method, the emission factor at a specific point in time is the specific emission factor of the marginal power plant in the merit-order of the electricity generation. The aim of the latter approach is to quantify the system effect. If the electrical load is increased or lowered at a certain time, the emission factor of the power plant, that would respond to this change, is taken into account (consequential approach). (Regett et al. 2018; Hamels et al. 2021)

However, there are some challenges involved with the marginal method. They concern the modeling of the marginal power plant, which is a very sensitive issue and difficult to estimate properly. Moreover, the sum of emissions attributed to all consumers does not lead to the sum of emissions produced by the power generation at a certain point in time via the marginal method (Hamels et al. 2021). In addition to Hamels et al., the marginal method could be differentiated further into a pure market based marginal method that is only based on the merit order of the market and a marginal method also considering physical constraints of the power grid. In the first case, however, additional challenges occur, as there are different time scales for the market (Day-ahead, Intra-day, Forward-market) and the merit order of the different markets might deviate. This means that this consideration would need to take into account at which point in time before the event of a reduction or an increase in load the actual decision about the load change takes place. The second approach considering physical constraints of the power grid further includes the consideration of the actual power generation in case that the market-based schedule cannot be kept and curtailment as well as redispatch are needed to balance the power grid. In the cases of a very short term load change, additional control capacities of the power grid (primary-, secondary- and tertiary control capacities) must be considered. Even for a retrospective approach, based on historical data, the marginal emission factors are difficult to obtain and the data availability is low (Pinel et al. 2021; Hamels et al. 2021). For future scenarios of the energy system, this seems to be almost impossible.

Besides the strict differentiation between average- and marginal methods, also mixed methods were developed, in particular the concept of the local emission factor (Röder et al. 2020). The concept is motivated by designing district energy systems for using the excess electricity of renewable energy plant in the case of feed-in management and curtailment: if no curtailment occurs, the average emission factor is the assessment basis of grid sourced electricity. In the case of curtailment in spatial proximity to the district, the emission factor is reduced, as an increase in load avoids the curtailment of renewable energies. Thus, a marginal aspect based on physical constraints is considered. Figure 2.3 illustrates the methodical approach.

A detailed explanation is given in Röder et al. (2020). However, as for the marginal method it is difficult to determine the time and location of curtailment measures for future energy scenarios of the next three decades. Furthermore, a detailed spatial model would be required

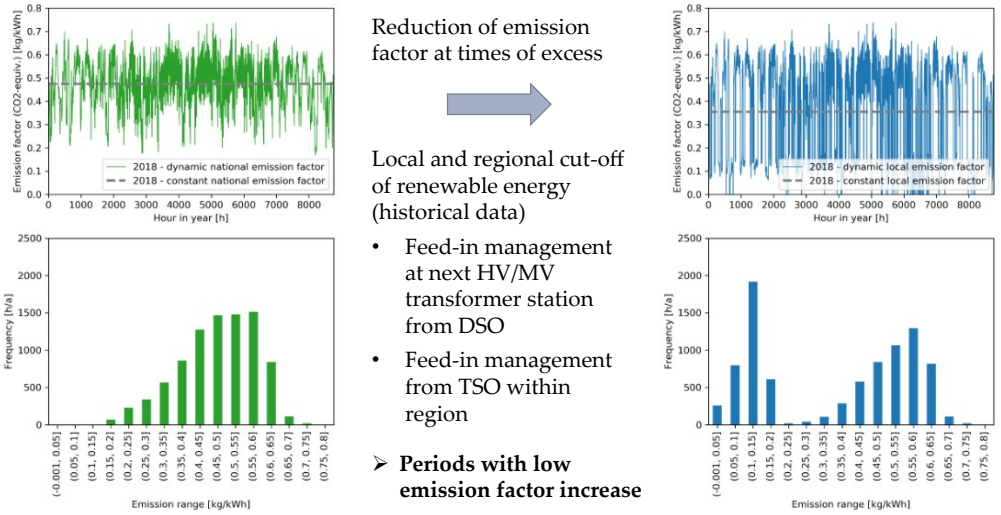

Figure 2.3: Approach and example of the local emission factor. HV: high voltage; MV: medium voltage; DSO: distribution grid operator; TSO: transmission system operator. See also Röder et al. (2020).

to estimate future regional curtailments and the local reinforcement of the power distribution lines would also have to be considered.

Thus, the mix method is used as grid-based reference quantity in the thesis, as it is more suitable to determine the average emission factor with models of the upstream energy system within future scenarios. With respect to the geographical perspective, emission factors for the German electricity system are applied. A further distinction and break-down to a regional level would be desirable, but as for the marginal emission factor, this would demand further detailed assumptions about the distribution of renewable energy sources as well as the grid-expansion for modeling the overall energy system within future scenarios. The emission scenarios deployed in this thesis are characterized by an operational perspective. For the export of electricity into the upstream power grid, a symmetric approach that considers emission credits in the amount of the emission factor at a certain time-step is applied. By this approach, an incentive is set to generate electricity at times of a low share of renewable energies in the upstream power grid and to import electricity at times of a high availability of fluctuating renewable power generation. Further information about the applied scenario framework and the deployed emission scenarios are given in Section 4.2.2.1.

2.1.2.4 Related grid-based reference quantities

In the following related grid-based reference quantities and indicators are presented, that might also be used as signals for shortage or excess of renewable energy generation in the upstream power grid.

The *fraction of fluctuating renewables in the electricity mix* is defined as share of wind and solar generation of the electricity mix. The share of volatile renewable electricity generation anti-correlates with the residual load that is introduced next. (Klein et al. 2016; Klein et al. 2014)

The *residual load* describes the net electricity load profile that is not covered by volatile renewable energies. Thus, the residual load shows very well the load profile that needs to be covered by controllable conventional power plants. (Klein et al. 2016)

The *excess of renewable energies* describes the amount and profile of curtailed renewable energy generation that cannot be integrated into the electricity system. This indicator is mentioned but not explicitly defined in (Regett et al. 2018).

A further grid-based reference quantity is the *non-renewable cumulative energy consumption*. This measure refers to the non-renewable primary energy consumption for the generation of one kilowatt-hour electricity including the primary energy expenses for the construction and dismantling and disposal of the respective power plants. This value can also be calculated as dynamic (time-resolved) grid-based reference quantity. (Klein et al. 2014; Klein et al. 2016)

However, these assessment parameters have not been taken into consideration for this thesis. The *fraction of fluctuating renewables in the electricity mix*, the *residual load* and the *excess of renewable energies* would require an additional assessment of the emissions, if electricity from the upstream power grid is compared to e.g. the use of fossil gas. The *non-renewable cumulative energy consumption* – if considered in a time-resolved manner – is also capable of combining ecological aspects and the provision of a shortage signal. However, as the emission factor in CO_2-equivalents relates more to the actual greenhouse gas potential and the focus of this thesis is on the operational perspective, the emission factor is favored. Nonetheless, they are worth mentioning as they also reflect important characteristics of the upstream electricity system. Therefore, the historical relation of emission factor with the first three mentioned grid-based reference quantities is evaluated in the following section.

2.1.3 A retrospective on the emission factor

As discussed in the previous section, the dynamic average emission factor (in the following emission factor) is selected as assessment parameter for the interface between the district energy system and the upstream electricity system. In the following, a retrospective analysis of the development and relation of the emission factor to other grid-based reference quantities of the electricity grid introduced above is given, based on an analysis of historical data.

Figure 2.4 shows the Pearson correlation of the average emission factor with the reference quantities day-ahead price, share of volatile renewable energies and residual load for the year from 2012 to 2020 for Germany. In this period, the share of renewable energies increased from 24.3 % in 2012 to 46.3 % in 2020.

For the compactness of the illustration, the negative value of the correlation is given for the share of volatile renewable energies, as these quantities anti-correlate. In times of a high share of renewable energies, the average emission factor is low. Both quantities, the emission factor and the share of volatile renewable energies anti-correlated on a very high level independent of the total share of renewable energies.

For the day-ahead price and the residual load, a clear increase of the correlation with the emission factor can be observed with an expansion of renewable energies. The residual load shows a stronger correlation than the day-ahead price independent of the year. For the

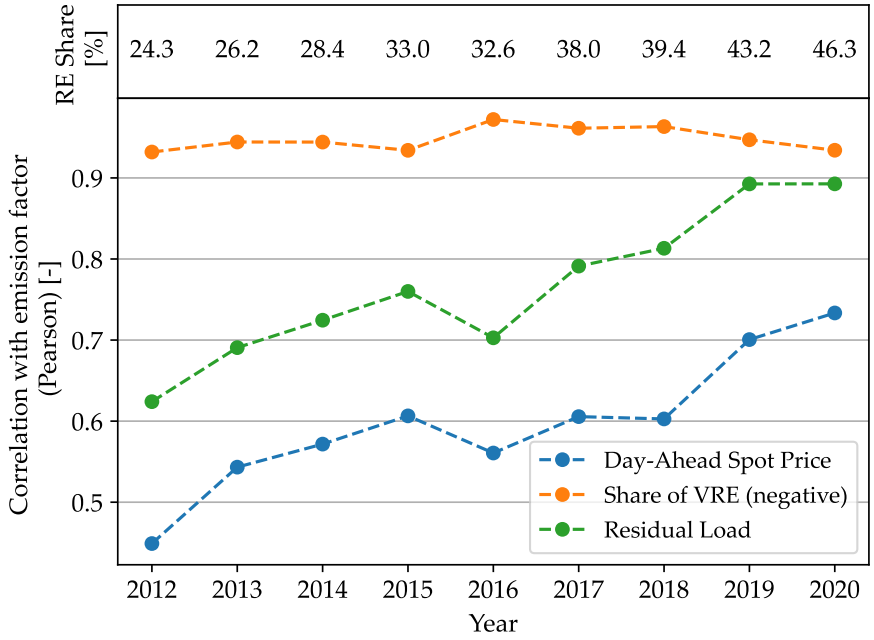

Figure 2.4: Historical correlation of grid-based reference quantities and the emission factor of the electricity mix for Germany. RE: Renewable Energies; VRE: Volatile renewable energy sources (wind and solar). Own illustration. Data source: (Agora Energiewende 2020).

electricity price, the correlation index rises from below 0.5 to above 0.7 within eight years. As the volatile renewable energies have feed-in priority and operate at almost zero marginal costs, the day-ahead price reflects the share of renewable energies more and more with increasing share of renewable energies. For both, the emission factor is a viable indicator, especially as the future market price depends on market design, and the volatile market price is only a fraction of the electricity price of households and district heating facilities (see above).

For the further suitability of the emission factor as grid-supportive measure, the relation of curtailment measures and the emission factor were analyzed (Figure 2.5). In Figure 2.5(a), the frequency distribution of the emission factor is given for the years 2015 to 2019 (blue violin plot). The green line indicates the development of the yearly average of the emission factor. The yearly average emission factor decreased from 2015 to 2019 from 534 g/kWh to 401 g/kWh. The blue horizontal markers show the extrema and the 20 % and 80 % quantile. The red line and markers illustrate the energy-weighted average emission factor of the curtailed renewable energy generation[2]. It can be seen that the average of the energy weighted emission factor is below the 20% quantile interval limit for all considered years.

[2] The curtailment data was collected and published by FfE (2020) and Köppl et al. (2020) and contains the feed-in management data for many – but not all – German distribution system operators. In detail, the following distribution system operators were considered: Avacon, Bayernwerk, EDIS, SH-Netz, Mitnetz, Netze BW (Data only for 2015-2018), Schleswig-Holstein (S-H) Netz, Wemag, Westfalen Weser Netz (Data only for 2015-2017) (FfE 2020). With this data set a large part of the curtailed energy is covered and a spatial distribution over the whole of Germany is given.

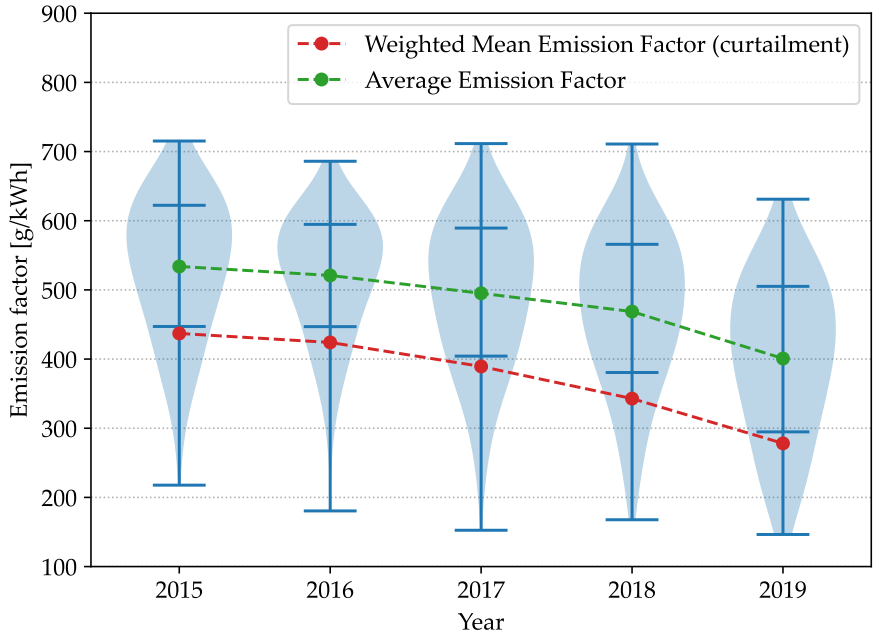

(a) Average emission factor and emission factor of curtailment

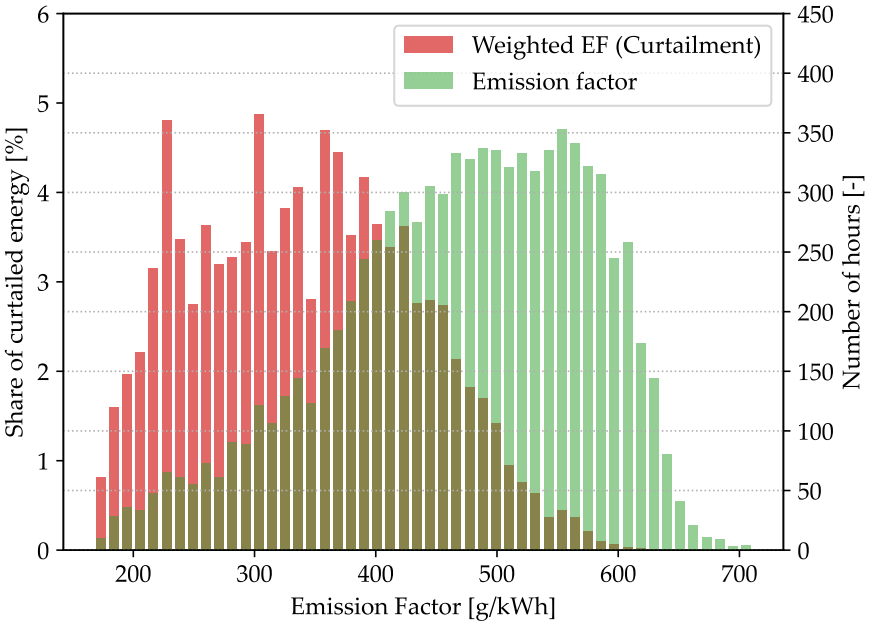

(b) Distribution in 2018

Figure 2.5: Average emission factor and average emission factor of curtailed energy. (a) Historical development for the years 2015 to 2019 for Germany. (b) Detailed frequency distribution of 2018. EF: emission factor. Own illustration. Data sources: Emission factors (Agora Energiewende 2020); curtailed power time-series (FfE 2020; Köppl et al. 2020).

In Figure 2.5(b), this is further illustrated by the year 2018. The occurrence of curtailment dependent on the emission factor (left y-axis) is confronted with the frequency distribution of the emission factor in number of hours per year (right y-axis). On average, curtailment occurs at times of a lower emission factor and thereby at time of a high share of volatile renewable energies. This means that on average a district energy system avoids curtailment of renewable energies if power is sourced from the grid at times of low emission factors. However, it must be noted that this is an analysis on national level, as a detailed regional analysis could not be performed at this point. Nevertheless, this retrospective analysis shows that there is a statistical coincidence of emission factor and curtailment.

The emission factor correlates with other common grid-based reference quantities that address the integration of volatile renewable energies into the electricity system. In addition, the emission factor incorporates an assessment of the greenhouse gas potential of the electricity of the upstream power grid. This allows the comparison of electricity imports with other energy sources of the district energy system, such as natural gas. The application of a dynamic emission factor combines the two objectives of a renewable and system-supportive design of DHS within one parameter. The volatility of the renewable energy generation of the upstream energy system is considered, and modeling and designing the district energy system and infrastructures can be focused. Thus, the dynamic emission factor is selected as assessment criteria for the import and export of electricity from and to the upstream power grid and sets the basis for a prospective renewable and system-supportive design of district energy systems for this thesis.

2.2 Case study: Rüsdorfer Kamp in Heide

The development of future-proof sector-coupled heat supply concepts and infrastructures for existing districts is done by the in-depth analysis of a typical existing district. Therefore, the district Rüsdorfer Kamp of the town Heide in the German state Schleswig Holstein (geographical coordinates 54.1951764 9.1019015) is examined, which is the object of investigation within the research project QUARREE100. The state Schleswig Holstein is characterized by a high number of wind power plants, which need to be curtailed on a regular basis due to congestions in the electricity grid (Schleswig-Holstein Ministerium für Energiewende, Landwirtschaft, Umwelt, Natur und Digitalisierung 2022; Schleswig-Holstein Netz AG 2022; TenneT TSO GmbH 2022). Within the project QUARREE100, an extensive data and knowledge base about the district exists, which facilitates the investigation of this thesis. Figure 2.6 shows a bird's eye view on the neighborhood.

In the following, the building stock of the Rüsdorfer Kamp and the energy-related data basis for the models of this thesis, such as energetic key values and renewable energy potentials, are introduced. It is shown to what extent the building stock of the district can be understood as a representative district, insofar as many aspects of the Rüsdorfer Kamp are characteristic for a typical existing district in Germany.

The data acquisition of the district Rüsdorfer Kamp as well as data verification and processing were not part of this thesis and were carried out by the project partner Steinbeis-Innovationszentrum energieplus (SIZ) in Braunschweig and Fachhochschule Westküste as part of the QUARREE100 project. A previous urban development concept (Dau-Schmidt 2018) was

Figure 2.6: Overview of the analysed district Rüsdorfer Kamp of the town Heide. Source and copyright: Steinbeis-Innovationszentrum energieplus (SIZ).

taken into account as additional data source and validation basis for the stocktaking of existing buildings carried out within the project QUARREE100. The local municipal utility company provided historical data for the gas and electricity consumption at building level. The following sections are based on parts of a not-public project internal report about the energy-related data basis of the Rüsdorfer Kamp that originate from the SIZ. Further, the report of a geothermal response test conducted in the Rüsdorfer Kamp has been considered as source.

2.2.1 Characterization and data basis

The building structure within the district is a diverse mixture of existing building types (see Figure 2.7). It includes single-family houses (SFH), row houses, apartment buildings, commercial properties and industrial buildings. SFH, row houses and semi-attached houses are summarized in the category SFH, in total 108 houses. The number of multi-family houses (MFH) amounts to 41, supplemented by 24 non-residential buildings (NRB) (Figure 2.7(a)). The number of residential units amounts to 251, and in total, about 400 people inhabit the Rüsdorfer Kamp. The overall net floor area of all buildings is 31 thousand square meters, and the total area of the district is about 20 hectares.

The building age is shown in Figure 2.7(b). Most of the buildings originate from the beginning of the 20th century. Many buildings were built in the fifties and sixties, and only a few buildings were constructed after 1978, when the first Heat Insulation Ordinance entered into force. Most of the buildings range from one and a half to 3 full floors.

In many cases, the energetic standard of the buildings is low, and an energy-oriented refurbishment is overdue. This is illustrated in Figure 2.8(a). Only 13 % of the buildings were identified as partly refurbished building. No building of the Rüsdorfer Kamp is identified as a fully refurbished building. Based on the gas consumption in the past the average weather-corrected heat consumption including space heating and hot water per square meter is estimated to 207 kWh/(m²a). The distribution of the specific heat consumption is shown in Figure 2.8(b)

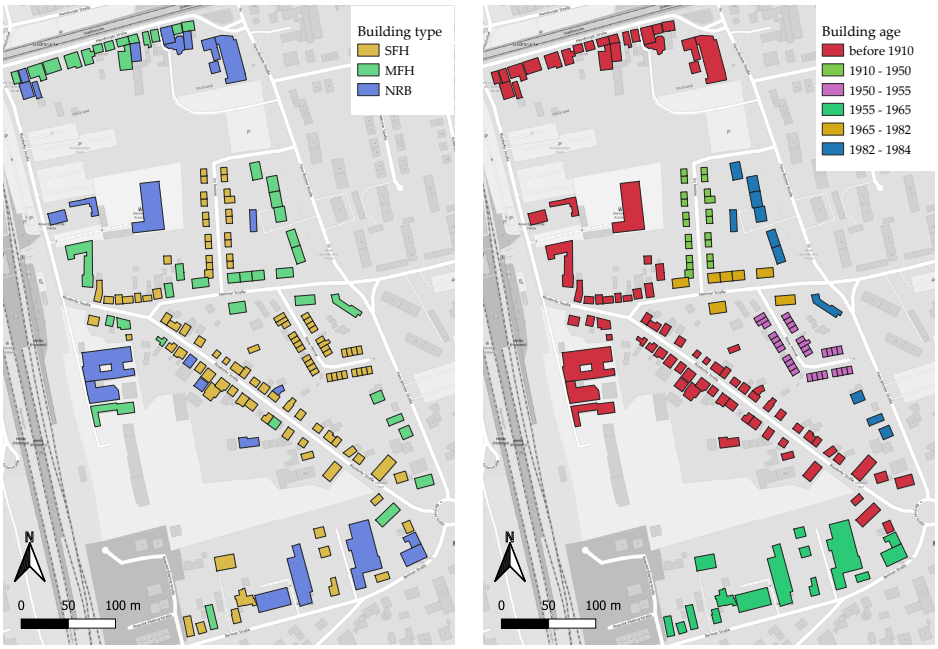

(a) Building type (b) Building age

Figure 2.7: Characteristics of the existing building stock of the Rüsdorfer Kamp. SFH: single-family house; MFH: multi-family house; NRB: non-residential building. Own illustration based on data of the QUARREE100 project. Background map: (OpenStreetMap contributors 2022).

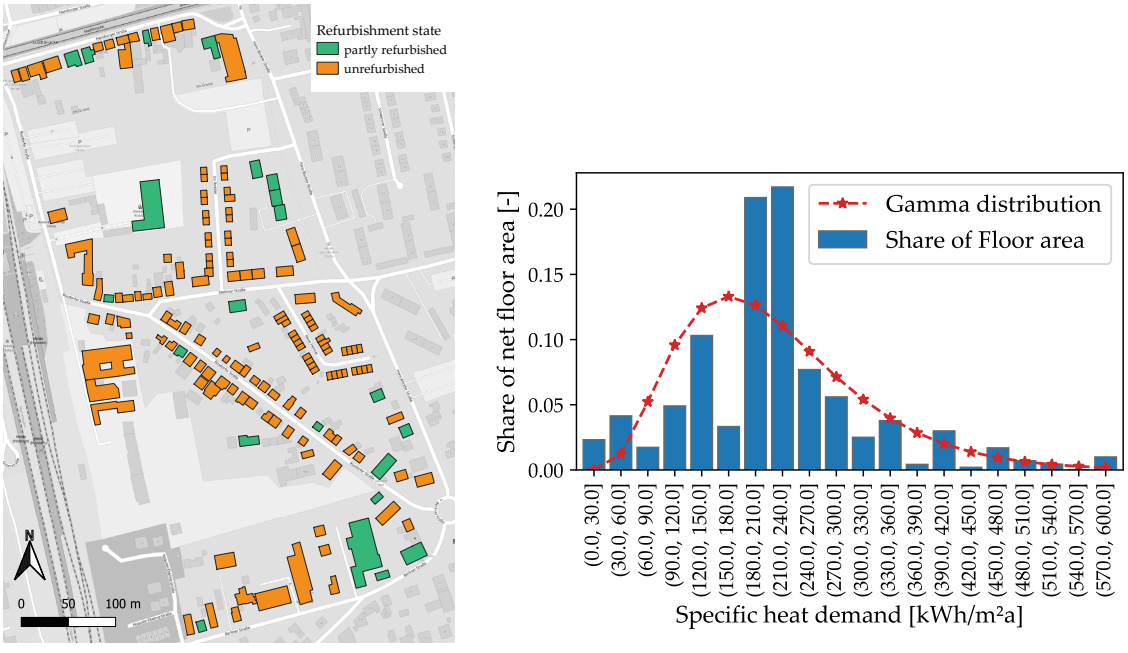

(a) Refurbishment status (b) Distribution of specific heat demand

Figure 2.8: Refurbishment status and heat demand distribution of Rüsdorfer Kamp. Own illustration based on data of the QUARREE100 project. Background map: (OpenStreetMap contributors 2022).

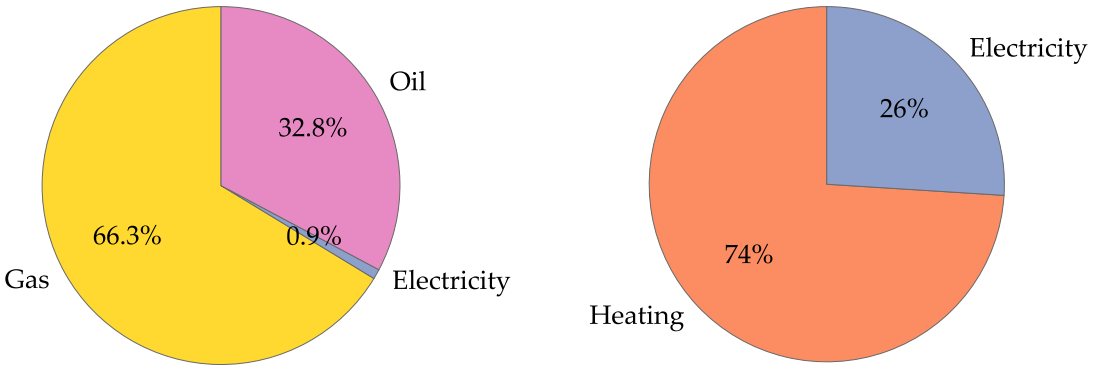

(a) Energy commodities of heat supply

(b) Distribution of energy related emissions

Figure 2.9: (a) Energy commodities of heat supply. (b) Distribution of energy related emissions of the building stock. Own illustration based on data of the QUARREE100 project.

including an approximation via the gamma distribution. Most of the buildings are characterized by a high specific heat consumption of 120 to 270 kWh/(m²a), also several extreme cases occur beyond values of 350 kWh/(m²a). Compared to the average national existing building stock, the distribution of the specific heat consumption is shifted to higher values (compare Figure 1.6).

In most of the cases, the heat supply is provided by individual boilers. About two third of all buildings are supplied via gas boilers, about one third is covered by an oil-based heating system. Even electric night storage heating systems are present in one percent of the buildings (Figure 2.9(a)). The total heat consumption of the building types SFH, MFH and non-residential building is distributed almost equally. The end-energy consumption of heat of the residential buildings accounts with almost 5 GWh/a for 70 % of the total heat consumption.

In total, three quarters of the energy-related emissions of the buildings are caused by the supply of heat. One fourth can be attributed to the electricity consumption in the form of indirect emission of the upstream power system (Figure 2.9(b)).

With respect to the national existing building stock, the Rüsdorfer Kamp can be regarded as a typical existing district. The buildings originate mainly from before the first heat insulation ordinance of 1978 and most of the buildings are characterized by a low energetic standard. Moreover, analogous to the national building stock, most of the buildings in the Rüsdorfer Kamp are supplied with individual gas boilers, and still many oil-based heating systems are present. This corresponds very well to the national existing building stock (see Section 1.2.1).

The heat density related to the total area of the district at the current refurbishment status amounts to 33 kWh/(m²a), which is 118.8 TJ/(km²a), respectively. The Rüsdorfer Kamp is a district with a moderate heat density. In the case of a low connection quota and if energetic refurbishments are pursued, it is undecided whether a DHS is a feasible and energy efficient infrastructure for the heat supply of the buildings (see Section 1.2.2.4). The Rüsdorfer Kamp is a suitable example for studying the impact of different scenarios on the feasibility of DHS to

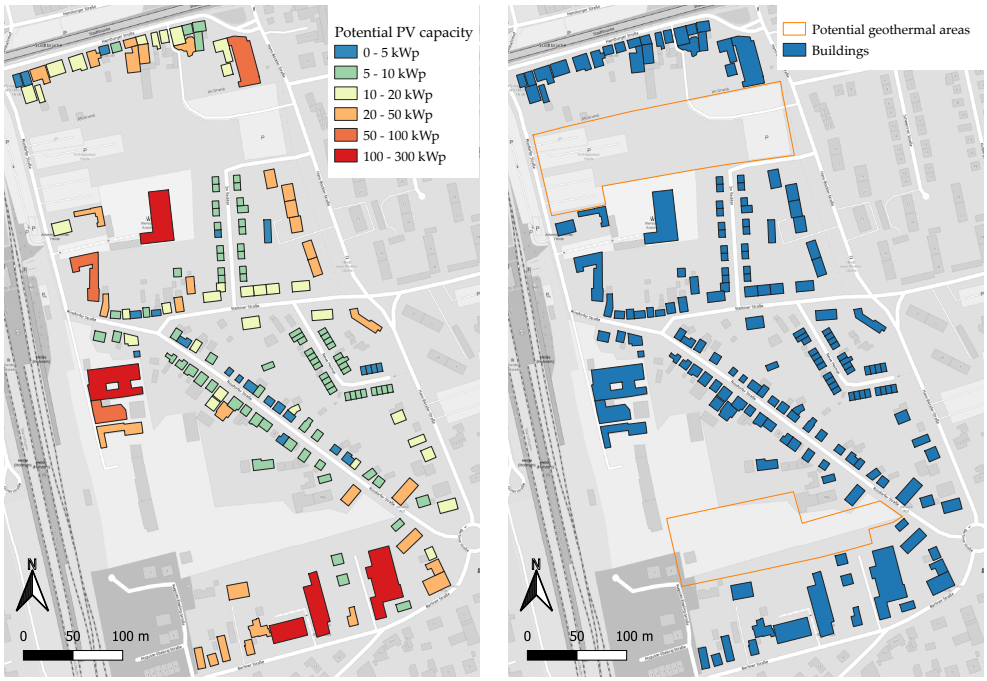

(a) (b)

Figure 2.10: Potential of solar photovoltaic (PV) capacity (a) and open areas for geothermal probes (b). Own illustration based on data of the QUARREE100 project. Background map: (OpenStreetMap contributors 2022).

achieve a carbon neutral heat supply within this thesis. Due to the illustrated similarities with the national existing building stock, the Rüsdorfer Kamp servers well as reference district, and it is expected that the results can also be transferred to other existing districts.

2.2.2 Renewable energy potentials

The main renewable energies potential in many urban and suburban districts such as the Rüsdorfer Kamp are the roof surfaces for solar energy appliances such as photovoltaic systems (PV) and solar thermal collectors. Therefore, a solar register at building level has been established within the stocktaking and data acquisition in the project QUARREE100. The register includes the type of roof, the orientation and the slope. Most of the single- and multi-family houses have a gable roof. The non-residential buildings are often characterized by a flat roof. Based on the roof types and the orientation the usable roof area has been calculated. Here, only roofs were considered that are oriented to the west, south or east. Further correction factors were applied for shading, dormer windows and other limiting factors. In total, the usable roof area for solar appliances of the entire existing building stock of the Rüsdorfer Kamp was estimated to 10 thousand square meter. This corresponds to a potential PV capacity of about 2000 kWp. The solar register and the potential PV capacity of the buildings is shown in Figure 2.10(a). Based on the solar register electricity generation profiles for PV are calculated depending on the slope and orientation individually for each building using the software *TRNSYS* (Thermal Energy System Specialists 2022).

In addition to the roofs for solar energy, there are two undeveloped open areas in Rüsdorfer Kamp that may be used for geothermal energy appliances (Figure 2.10(b)). The area in the northern part of the district is 1.8 hectare and the southern area is 1.2 hectare. A geothermal response tests in the southern area was conducted within the project QUARREE100. The resulting effective thermal conductivity of the underground was determined to 2.65 W/mK which indicates convective ground water flow. The geothermal response test proofs the general suitability of geothermal probes. With a minimum distance of 8 m, a field with geothermal probes in the order of 125 to 150 geothermal probes with a length of 150 meters is possible in the southern area of the district. Depending on the actual available area for the probe field, the detailed arrangement, design and operation of the probes (e.g. the actual operation temperatures and whether or not a regeneration in summer is realized) a total thermal heat extraction rate of 500 to 1000 kW may be possible. The availability of such open areas for geothermal energy is an individual characteristic of each district and the actual quantitative potential varies from district to district. Thus, only the southern area is considered for the analysis of this thesis. It is hypothesized that a certain magnitude of open areas for geothermal probes is also available in other district with a sparse to moderate heat density as in the case of the Rüsdorfer Kamp.

Besides the solar and geothermal potentials, there are no other notable renewable energy sources in the area. There are no large-scale industrial excess heat sources, whose exploitation could feed a DHS, nor any other heat sources, such as sewer or water bodies like rivers. Although this limits the supply options for the conceptualization of the district energy system, it may lead to a broader transferability of the results of this thesis, as individual prerequisites do not largely determine the supply concept. Of course, in general, all form of excess and ambient heat potentials need to be taken into account for the development of renewable heat supply concepts. But there are also many districts such as the Rüsdorfer Kamp without any excess heat potentials, that need to be converted into a carbon-neutral district and therefore more strongly rely on the upstream energy infrastructures.

2.2.3 Energy consumption profiles

The generation of load profiles for heat and electricity as well as the calculation of the generation profiles of PV is not the focus of this thesis. For this thesis, the load and generation time-series developed in the QUARREE100 project by the project partner SIZ were used as data basis. The approach is briefly summarized in the following (see also Röder et al. 2020; Röder et al. 2021).

The heat demand profiles consist of individual profiles for space heating and domestic hot water (DHW). The space heating consumption profiles are obtained with a detailed building simulation of the different building types of the Rüsdorfer Kamp using the software EnergyPlus (NREL 2022; Pacific Northwest National Laboratory 2014). This includes the setup of a 3D building model of each building type including the share of window area, the wall structure and thickness, et cetera. The DHW profiles are based on normalized daily profiles for typical days and are calculated based on the German norm VDI 4655 (VDI - The Association of German Engineers 2008). Then, the load profiles for heating are scaled to the actual annual heating

demand of the corresponding building based on the building type. The actual annual heating demand is based on historical data provided by the local utility company.

Single load profiles are aggregated by taking the simultaneity factor of the demand profiles of multiple buildings into account. This is achieved by applying a time-shift randomly drawn from a normal distribution to each of the profiles, which can be interpreted as one household starting their day earlier or later than the average. By this approach, the usability of heat demand profiles for DHS is improved and the simultaneity effect is already considered within the demand profiles (see also Section 3.2.3 and Röder et al. 2021).

For the electricity consumption profiles the German VDI 4655 (Guideline 4655) is used for SFH, row houses and MFH (VDI - The Association of German Engineers 2008). The electricity profiles of Meier et al. (1999) are used as electricity consumption profiles for the different types of commercial buildings present in the district. Analogous to the heat profiles, a time shift is applied to consider the simultaneity effect within the electricity consumption, and the electricity profiles are scaled to the individual past electricity consumption of each building given by the local utility company (Röder et al. 2020).

2.3 Underlying modeling approach[3]

This section presents the underlying methodical approach for the investment and unit commitment models developed and applied in this thesis. It includes the introduction of the applied optimization method with an overview and classification, the detailed mathematical description of the optimization model and the description of the preliminary and auxiliary calculations of the parameters.

2.3.1 Classification and overview

The aim of the techno-economic optimization is to find trade-off solutions between costs and emissions for designing energy systems at an urban scale. In this work, an energy system model is developed for the heat generation site of a local DHS and for the electricity and heat supply at building level. The optimization models include investment and unit commitment decisions.

The methodical modeling basis of this work is linear programming (LP) and linear mixed-integer programming (MILP). LP and MILP models are widely used and have a long tradition in energy system modeling as Prina et al. and Klemm et Vennemann show (Prina et al. 2020; Klemm et al. 2021). Mathematical programming forms the basis for many energy system models and frameworks, e.g. *Calliope*, *REMix*, *Ficus*, *OSeMOSYS*, *MESSAGE*, *MARKAL/TIMES* and other (Klemm et al. 2021; Prina et al. 2020).

The advantage of LP models is that models can be solved fast (Kuhn 2011) and there are many efficient solvers available, e.g. commercial solver like *Gurobi* (Gurobi Optimization LLC 2022) and open source solvers such as *CBC* (Johnjforrest et al. 2020). The optimal solution using LP models can be attained within reasonable time as the solution space is convex

[3] This section is based on Röder et al. (2020) and Röder et al. (2022b)

(Dorfner 2016). However, the formulation needs to be linear, which means a restriction in the mathematical formulation. MILP models are characterized by at least one decision variable being discrete, e.g. a binary decision variable that is either 0 or 1 (Biegler et al. 2004). Allowing integer variables extends the possibilities of the mathematical formulation and also make the representation of complex interactions possible (Dorfner 2016; Kuhn 2011). However, as the optimization problem becomes non-convex, optimality cannot be guaranteed, and the solving time might increase drastically (Biegler et al. 2004; Dorfner 2016). Non-linear programming and heuristics allow more mathematical flexibility. However, the quality of solution is difficult to assess (Dorfner 2016). In this study, computation time is of particular importance because a bi-objective optimization with costs and emission as optimization criteria is performed for multiple scenarios based on a time period of one year with a hourly resolution. Therefore, the strategy is to use a MILP approach and only use discrete variables when really needed.

The problem statement for this energy system investment and unit commitment optimization can be formulated as follows: Given are different energy demands, which are the heat and electricity demand of an urban district or buildings, energy commodity sources from the upstream infrastructure or local energy generation and energy converters and storage options for the supply of the heat. The technical parameters, such as conversion factors or energy losses and the economic parameters, like capital and operation costs, are known for each energy converter and storage unit. Different energy commodities from the upstream energy infrastructures that are the power grid and the gas network can be imported and also exported. All commodities from the upstream energy system are characterized by energy-specific costs and an emission factor. The optimization problem is concerned with selecting, dimensioning and committing the energy converter and storage units, while minimizing the costs and meeting a given emission limit. The minimum emission limit is calculated via optimization with the total emission as objective function. The mathematical program is characterized by a time-resolution of one hour and an optimization period of one year. The model includes different energy sectors as the energy sectors of electricity, heat and gas, so it is a multi-energy system or a sector-coupled energy system.

The Python open source optimization library *oemof.solph* is selected as modeling basis (oemof developer group 2020a; Krien et al. 2020). *Oemof-solph* is a popular library of the open energy modeling framework (*oemof*), which contains many tools for energy system analysis including different methods for optimization and simulation of energy systems.

2.3.2 Mathematical model description

The *oemof.solph* optimization framework, which is the basis for the developed applications of this work, is a model generator for LP and MILP optimization models in the computing language Python (oemof developer group 2020a; Krien et al. 2020). It is based on a generic graph-based nodes-edges structure and leaves the exact use of the components and variables to the user (Hilpert et al. 2018). In addition, there are several options for different attributes of the components and constraints. Within this thesis, more specific energy system models, such as the *q100opt* package (Röder et al. 2022a) that can be seen as *oemof.solph* application models were developed. Due to the unspecific and generic structure of *oemof.solph*, it is necessary to

define the exact usage of the variables, parameters, as well as the objective function and the constraints of the *oemof.solph* model that is developed and applied in this work.

In the following, the energy system model is introduced. This introduction explains all attributes and constraints from the variety of possibilities of the *oemof.solph* classes that were used in this work to provide a complete mathematical description of the optimization problem. The model is developed with *oemof.solph* version 0.4.1 (oemof developer group 2020a). The mathematical description shown below is based on and derived from the *oemof.solph* documentation that can be found in (oemof developer group 2020b) and follows in its structure Röder et al. (Röder et al. 2020). The designation of the variables is partially adjusted to clarify their use within this thesis.

Objectives and global constraints The applied Pareto-optimization seeks to find the balance between cost- and the ecological system design with respect to the operation related emissions. The emission assessment of the electricity import and export imply a dynamic emission factor for the electricity grid to achieve a system-supportive design (see Section 2.1). Therefore, the two functions of costs and emissions that are minimized are introduced in the following. The cost function considers the sum of all costs C_{total} and is given by the following equation:

$$C_{total} = C_{invest} + C_{var} \tag{2.1}$$

where C_{var} is the sum of all variable costs within the energy system that depend on the actual flow value $P_{(i,o),t}$ of each time-step t:

$$C_{var} = \sum_{(i,o)} \sum_{t} P_{(i,o),t} \cdot \Delta t \cdot c_{(i,o),t} \tag{2.2}$$

The pair of indices (i, o) represents a flow $P_{(i,o),t}$ going from node i to node o. The flows $P_{(i,o),t}$ are decision variables of the energy system model. A flow is considered to be an energy flow of an energy commodity and has the unit of power kW. An energy flow is an electricity flow, a heat flow related to a specific temperature level and temperature spread, a gas or hydrogen flow and is in each case indexed by a time-step t. The applied constraints of the flows are described below. A node is either an instance of the *oemof.solph Bus* class or a component. Since the modeling approach of *oemof.solph* is based on a bipartite graph, *Bus* instances and components alternate. As components, the *oemof.solph* classes *Source*, *Sink*, *Transformer* and *GenericStorage* are deployed in the energy system models of this thesis. The applied attributes and constraints are described in detail below. The time-step width is represented by Δt. The flow-weights $c_{(i,o),t}$ represent variable costs in €/kWh (in terms of energy flow dependent). These are energy prices for the energy commodities that are imported into the district energy system or exported to the upstream energy system, operation-related maintenance costs for energy converter or storage units, or other costs as fees or subsidies, that are related to an energy flow.

The sum of all investment costs C_{invest} of Equation 2.1 is the sum of all investment decisions for all energy flow investments and storage units. It is given by the following equation:

$$C_{invest} = \sum_{(i,o)} (P_{(i,o),invest} \cdot c_{(i,o),invest} + y_{(i,o)} \cdot c_{(i,o),investfix}) \; + \\ \sum_{n} (W_{n,invest} \cdot c_{(n,invest} + y_n \cdot c_{n,investfix}) \tag{2.3}$$

The investment in the capacity of the energy flow $P_{(i,o),invest}$ relates to an investment in an energy converter unit. An energy converter unit consists of a *Transformer* and the connecting in- and outflows. Thus, the investment decision variables $P_{(i,o),invest}$ represent the installed capacity of the energy converter unit the investment flow is related to and has the unit $\mathrm{kW}_{installed}$. For storage units, the investment is considered within the node constraints of the *GenericStorage* class. The storage capacity is represented by the symbol $W_{n,invest}$ with the unit of the energy content in kWh (installed). A detailed description of the applied storage model is given below. The installed capacity of the energy converter units refers to the nominal capacity of the outflow of the energy converter. The specific investment costs $c_{(i,o),invest}$ and $Tc_{(n,invest}$ are the capacity dependent parts of the investment costs and expressed by the units €/kW or €/kWh, respectively. Additionally, for some components, a fixed share of investment costs independent of the capacity is considered by $c_{(i,o),investfix}$ and $c_{n,investfix}$ in €to approximate the actual cost function. In such cases, an additional binary variable y is introduced. The final cost parameter c includes fixed costs for maintenance and operation independent of the unit operation. All investment cost parameter relate to the capital expenses per year. Therefore, all capital costs need to be based on one year. The methodical approach of calculating the annuity is given in Section 2.3.3.

The second objective function is the sum of all emissions E_{total} in $\mathrm{kg}_{CO_2-equivalent}$:

$$E_{total} = \sum_{(i,o)} \sum_{t} P_{(i,o),t} \cdot \Delta t \cdot e_{(i,o),t} \tag{2.4}$$

The energy-specific emission factors are given by $e_{(i,o),t}$ in $\mathrm{kg}_{CO_2-equivalent}$/kWh and are dependent on the time-step t for the emission factor of electricity. First, the cost-optimal and the emission-optimal energy system configuration is identified by performing an optimization for each of the objective functions. This gives the maximum emission value E_{max} for the cost-optimal system and the minimum achievable emission value E_{min}. Then, to calculate the trade-off between costs and emission and to generate the Pareto-Front, multiple cost-optimization runs are performed with a varying emission limit E_{limit}, also known as ε-constraint optimization method:

$$E_{total} \leq E_{limit} \tag{2.5}$$

with

$$E_{min} \leq E_{limit} \leq E_{max} \tag{2.6}$$

Flow constraints As introduced above, an energy flow $P_{(i,o),t}$ is one of the core elements of the energy system model and can be constrained by various options. The constraints applied in this model are described next.

The decision variable for the capacity of a flow $P_{(i,o),invest}$ limits the time-dependent energy flows $P_{(i,o),t}$:

$$0 \leq P_{(i,o),t} \leq f_{(i,o),t,max} \cdot P_{(i,o),invest} \tag{2.7}$$

The additional factor $f_{(i,o),t,max}$ allows for a time-dependent restriction of the maximum energy flow. This becomes important for the modeling of air-source heat pumps, when the maximum thermal power output decreases at low ambient temperatures and a high temperature spread (see also Section 2.3.3).

The investment decision variables $P_{(i,o),invest}$ themselves are restricted by maximum investment values $P_{(i,o),invest,max}$ and can be further constrained by minimum investment values $P_{(i,o),invest,min}$, to apply a minimum investment threshold, if components are not available below a certain size:

$$y_{i,o} \cdot P_{(i,o),invest,min} \leq P_{(i,o),invest} \leq y_{i,o} \cdot P_{(i,o),invest,max} \tag{2.8}$$

In the case of a minimum investment threshold, the binary variable y enables an investment result of zero.

The generation profile of a volatile renewable energy source, like PV, is given as normed time-series relatively to the installed capacity $\mathrm{kW/kW}_{installed}$ and can be multiplied with the installed capacity $P_{(i,o),invest}$ of the outflow a Source object (see below) to get the absolute generation. The normed generation time-series are individually pre-calculated with an external library.

$$P_{(i,o),t} = P_{(i,o),invest} \cdot f_{(i,o),t,fix} \tag{2.9}$$

The energy flows of the heat and electricity demands are modeled in the same way, but the investment variable $P_{(i,o),invest}$ of Equation 2.9 is replaced by the nominal value parameter $P_{(i,o),nominal}$ to give a fixed demand time-series. This energy flow is combined flow with a *Sink* object (see below).

A further limitation to the maximum capacity $P_{(i,o),invest,max}$ is applied to the investment in geothermal heat pumps. To prevent a long-term cool down of the ground, a maximum number of full load hours is set by constraining the sum of the energy flow of the whole optimization period with the maximum factor $f_{(i,o),sum,max}$:

$$\sum_t P_{(i,o),t} \leq P_{(i,o),invest} \cdot f_{(i,o),sum,fix} \tag{2.10}$$

Node constraints The indices n, i and o are used as an index for the instances of a specific node.

The base classes *Source* and *Sink* do not create any additional constraints. Both represent nodes with one outflow or one inflow, respectively. Along with appropriate parameterization of flows, *Sources* represent sources of energy commodities from upstream energy infrastructures of electricity and gas and local sources of renewable energy. *Sinks* are applied to model energy demand and have a fixed flow value.

A *Bus* (node index n) is characterized by a balance equation. At each time step t the sum of inflows is equal to the sum of outflows:

$$\sum_{i \in \text{Inflows}(n)} P_{(i,n),t} = \sum_{o \in \text{Outflows}(n)} P_{(n,o),t} \qquad \forall\ t \tag{2.11}$$

The core of an energy converter unit is the base class *Transformer*, that relates the in- and outflows of the energy converter by conversion factors η:

$$\begin{aligned} &P_{(i,n),t} \cdot \eta_{(n,o),t} = P_{(n,o),t} \cdot \eta_{(i,n),t} \\ &\forall\ i \in \text{Inflows}(n), \qquad \forall\ o \in \text{Outflows(n)}, \qquad \forall\ t \end{aligned} \tag{2.12}$$

The remaining constraints used to describe an energy converter unit are defined at the *Flows* (see above).

An energy storage unit is modeled by the *GenericStorage* and described by the following constraints:

$$\begin{aligned} W_{n,t} \;=\; & W_{n,t-1} \cdot (1 - \beta_{n,t}) \\ & - \gamma_{n,t} \cdot W_{n,invest} - \delta_{n,t} \\ & - \frac{P_{(n,o),t}}{\eta_{(n,o),t}} \cdot \Delta t + P_{(i,n),t} \cdot \eta_{(n,i),t} \cdot \Delta t \end{aligned} \tag{2.13}$$

with $\beta_{n,t}$ as loss factor, which depends on the state of charge, $\gamma_{n,t}$ as loss factor depending on the size of the storage and $\delta_{n,t}$ as absolute loss factor. $P_{(i,n),t}$ and $P_{(n,o),t}$ are the energy flows going in and out of the storage and are multiplied by charging and de-charging efficiencies $\eta_{(n,i),t}$ and $\eta_{(n,o),t}$. Depending on the type of storage, the loss factors are used to meet the different storage characteristics. For thermal storage units, the loss factors are pre-calculated depending on the temperature level and temperature spread of the storage. Equation 2.13 is also set up for relating the initial storage state of charge W_{init} with the state of charge of the first time-step. The initial storage level is set equal to the storage content of the last time-step to comply with conservation of energy:

$$W_{n,init} = W_{n,t_{last}} \tag{2.14}$$

The storage level $W_{n,t}$ and the initial storage level $W_{n,init}$ are restricted by the investment capacity of the storage $W_{n,invest}$:

$$0 \leq W_{n,t} \leq W_{n,invest} \tag{2.15}$$

$$0 \leq W_{n,init} \leq W_{n,invest} \tag{2.16}$$

and the investment capacity is in turn restricted by the minimum and maximum investment limit in analogy to Equation 2.8:

$$y_n \cdot W_{n,invest,min} \leq W_{n,invest} \leq y_n \cdot W_{n,invest,max} \tag{2.17}$$

The in- and outflows $P_{(i,n),t}$ and $P_{(o,n),t}$ are bounded by the in- and outflow capacities $P_{(i,n),nominal}$ and $P_{(o,n),nominal}$:

$$0 \leq P_{(i,n),t} \leq P_{(i,n),nominal} \tag{2.18}$$

$$0 \leq P_{(n,o),t} \leq P_{(n,o),nominal} \tag{2.19}$$

For restricting the charging and de-charging power, the in- and outflow capacities $P_{(i,n),nominal}$ and $P_{(n,o),nominal}$ are related to the size of the storage capacity W_{invest} with the factors $f_{n,cap-in}$ and $f_{n,cap-out}$, also known as C-rates:

$$P_{(i,n),nominal} = W_{invest} \cdot f_{n,cap-in} \tag{2.20}$$

$$P_{(n,o),nominal} = W_{invest} \cdot f_{n,cap-out} \tag{2.21}$$

2.3.3 Preliminary and auxiliary calculations

The cost parameter c_{invest} (Equation 2.3) relates to the annual costs of the investment including maintenance and service costs of a specific energy converter or storage unit as follows ((based on oemof developer group 2020c):

$$c_{invest} = capex \cdot \frac{(wacc \cdot (1 + wacc)^N)}{((1 + wacc)^N - 1)} + f_m \cdot capex \tag{2.22}$$

The calculation follows a static investment assessment with *capex* as capital expenditure, *wacc* as weighted average cost of capital, N as technical lifetime and the factor f_m as fraction of the investment costs for maintenance and service costs per year. The calculation of the capacity-independent part of investment costs $c_{investfix}$ (Equation 2.3) is identical. This formula can be interpreted as static version of the German norm VDI 2067 (Guideline 2067) without considering price changes or price increase factors. In this study, this is covered by different price scenarios.

The *oemof.thermal* library was applied to calculate the parameters of the thermal components of the energy system model (Jnnr et al. 2020a). The conversion factor η_{hp} of the heat pumps, or coefficient of performance (COP), is calculated individually for each time-step depending on the temperature of the heat source T_{low} and the temperature of the heat sink T_{high} of the heat

pump. The calculation is based on the quality grade q_{Carnot} of heat pumps, that relates the performance of the heat pumps to the thermodynamic ideal Carnot cycle and is calculated as follows (Jnnr et al. 2020a):

$$\eta_{hp} = q_{Carnot} \cdot f_{icing} \cdot \frac{T_{high}}{T_{high} - T_{low}} \tag{2.23}$$

The factor f_{icing} is only applied in the case of air-source heat pumps and additionally considers that the efficiency further decreases in the case of low outside temperatures due to the energy that must be applied to de-ice the evaporator. In the case of air-source heat pumps, the nominal power decreases if the outside temperature drops and the temperature lift from the source temperature to the sink temperature increases. This is considered by the factor $f_{hp,t,max}$, which is calculated by the relation of the efficiency at a certain time-step $\eta_{hp,t}$ to the nominal efficiency $\eta_{hp,nominal}$ multiplied by a correction factor f_{corr} (Jnnr et al. 2020a):

$$f_{hp,t,max} = f_{corr} \cdot \frac{\eta_{hp,t}}{\eta_{hp,nominal}} \tag{2.24}$$

The solar thermal heat generation of solar thermal flat plate collectors is calculated with the *oemof.thermal* package and is based on the efficiency characteristic curve of the solar thermal collectors (see Jnnr et al. 2020a; Stiebel Eltron 2017):

$$\eta_C = \eta_0 - a_1 \cdot \frac{\Delta T}{I_C} - a_2 \cdot \frac{\Delta T^2}{I_C} \tag{2.25}$$

The collector efficiency η_C results from the maximum efficiency η_0, when there is no temperature difference between the collector and the environment, the two heat loss coefficients a_1 and a_2, the total solar irradiance I_C on the (tilted) collector and the mean temperature difference ΔT between the collector and the environment. For the calculation of the total solar irradiance on the titled surface, *oemof.thermal* uses the open source package *pvlib* (F. Holmgren et al. 2018). The temperature difference ΔT is affected by the temperature level of the heating system and the outside temperature. The total heat output $\dot{Q}_C$ of the thermal flat plate collector is given by (Jnnr et al. 2020a):

$$\dot{Q}_C = I_C \cdot \eta_C \tag{2.26}$$

2.4 Overview of model chain and data flow

The methodical approach to answer the research objectives presented in Section 1.3 consists of the development and application of techno-economic optimization models for the different parts of the district energy system based on the methodical approach introduced in Section 2.3. With these models different transformation paths are investigated to derive future-proof energy supply concepts. By this analysis the parameters are determined that influence the economic feasibility of district heating compared to individual heat supply for different levels of emission reduction to a carbon-neutral supply in future sector-coupled district energy systems.

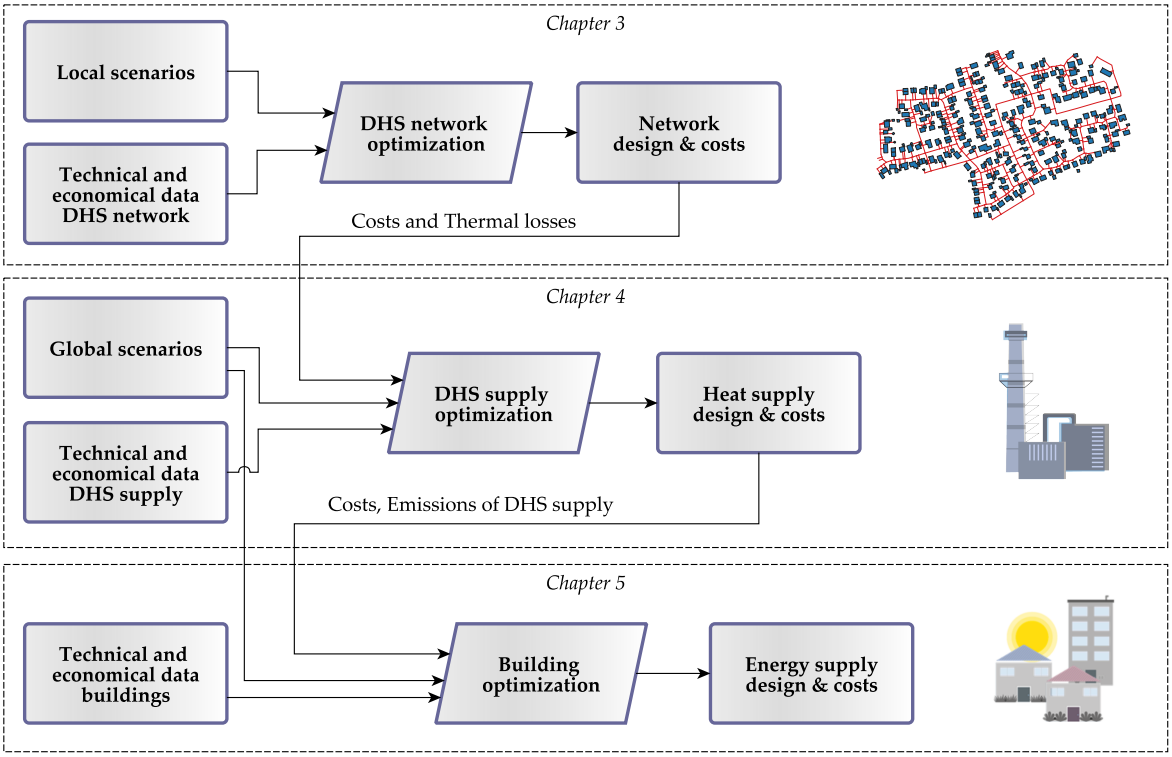

Figure 2.11: Overview of the overall modeling approach and the in- and output data of the single models for the design of future-proof district energy systems. Source of footprints of district heating symbol: (OpenStreetMap contributors 2022)

The following paragraphs provide an overview of the applied modeling steps, including the data flow within the modeling steps that are presented in the following chapters. Figure 2.11 provides an overview of the overall approach.

The first part of the modeling approach is the design of the district heating network (Chapter 3). The *Local Scenarios* consist of refurbishment scenarios and connection scenarios for the existing building stock. The different refurbishment scenarios assume different levels of energetic refurbishment that lead to different demands for space heating and different temperature levels in the buildings. The connection scenarios consider different shares of buildings connected to the DHS. The connection scenarios thereby simulate different heat densities. One single local scenario consists of a set of buildings characterized by heat demand time-series for one year with a certain temperature level. By the application of the planning and optimization tool for district heating networks, that was developed within this thesis and is published within the package *DHNx* (oemof developer group 2022b), the optimal routing and dimensioning of the DHS piping system is calculated for each combination of refurbishment and connection scenario. The results are then used as input parameter for the optimal design of the district heat supply. From the results of the network optimization, the thermal losses are required to determine the total heat demand at the district heat supply site and the costs of the district heating network to calculate the overall heat supply costs.

The next modeling step is the optimization of the district heat supply for each of the local scenarios (Chapter 4). Based on current studies about the overall energy system in Germany,

scenarios are defined for the upstream energy infrastructures of power grid and gas network, respectively. Different shares of renewable energy in the upstream energy infrastructure are assumed for the consideration of different transformation paths of the overall energy system. The aim of this approach is to systematically investigate the impact of possible developments in upstream infrastructures on investment decisions at the local level. The input parameters given by the global scenarios are characterized by price and emission values. In addition to the global scenarios and the results of the district heating network optimization, the technical and economic parameters for the installation of the energy converter and storage units and the construction of the district heat supply facility are required for the model. An investment and unit commitment model of the district heat supply is developed based on a linear mixed-integer programming model. Therefore, the model builder *q100opt* for setting up *oemof.solph* energy systems models with focus on districts and buildings was developed and published on the platform GitHub (Röder et al. 2022a). With this model builder, the trade-offs between a cost-optimal and an emission-optimal design are calculated and illustrated in the form of Pareto-Fronts. In addition to the total costs and emissions, the investment decisions as well as the commitment of the energy converter and storage units are the results of the model. The model is applied for all considered combinations of global and local scenarios.

In the last modeling step (Chapter 5), an investment and unit commitment model for the heat and electricity supply at building level is set up for comparing the individual heat generation with a heat generation via DHS. The model builder for the energy models at building level is also published within *q100opt* (Röder et al. 2022a). In that process, the results of Chapter 4 of the costs and emission for DHS supply are taken as input parameter in the building model. Additional to the previous input data, the technical and economic data for the energy converter and storage units at building level are required for determining the best investment options on individual level. The trade-off between costs and emission in the form of a Pareto-Front is calculated analogous to Chapter 4 for a reference SFH and MFH. Based on the comparison of the results between an individual heat supply and district heating, it is analyzed to what extent different transformation paths of the overall national energy system (global scenarios) influence the decision on whether a DHS is economically feasible compared to a building-wise heat generation as described above.

The three introduced modeling and optimization steps for the design of district energy systems and infrastructures in Figure 2.11 are formulated as optimization problems. The modeling background of the district heating network optimization approach, that is published as stand-alone open source software in the library *DHNx* (Röder et al. 2021; Jnnr et al. 2021), is given in Section 3.2. The second modeling step for the design of the DHS heat supply and the third modeling step for the energy supply at building level are both investment and unit commitment models as introduced in Section 2.3.

3 Design of district heating networks[1]

The first part of the approach of this thesis for the development of district heating systems (DHS) is the design of the district heating networks. The drafting and planning of district heating networks are very important tasks within the development of DHS as the costs and thermal losses of district heating networks decisively impact on the economic feasibility of district heating. Therefore, the topology and dimensioning of prospective district heating networks need to be calculated. The resulting costs and thermal losses of the district heating network are required for the subsequent planning of the DHS supply site for the different scenarios in Chapter 4.

To design district heating networks, a modular and flexible optimization framework, originally published in (Röder et al. 2021), was developed within the scope of this thesis. The development of this tool is an essential contribution to research objective RO 1. The novelty of the approach is a flexible mixed-integer linear problem (MILP) formulation based on existing open source libraries that allows the option to consider further complex optimization tasks, e.g. the consideration of distributed thermal energy storages within the district heating network optimization (presented in Röder et al. 2021). Also, a new method for the consideration of the heat demand simultaneity based on individual load profiles is introduced. The framework is published within the Python open source library *DHNx* (oemof developer group 2022b; Jnnr et al. 2020b), which permits the use and further development by the scientific community. This optimization framework provides the basis for further complex planning tasks of district heating networks in the context of integrated energy systems which goes beyond the application focus of this thesis.

This chapter is divided into the following sections: In the first section the literature is reviewed with respect to existing district heating network planning tools, and the development of a new optimization framework is motivated. Subsequently, the methodical background of the district heating network optimization approach that is published within the open source software package *DHNx* (oemof developer group 2022b) is introduced. The optimization framework is applied for the subject of this thesis and an analysis of different scenarios for Rüsdorfer Kamp in Heide is performed. Therefore, the local scenario framework that includes different demand scenarios, depending on the share of buildings connected to a DHS and the state of energetic refurbishment of the buildings, are introduced, followed by the illustration of the optimization parameters. Finally, the results are presented and discussed, and the conclusions of this chapter are summarized.

3.1 Literature review: District heating networks

This section gives an overview of existing planning methods for designing district heating networks. It is checked if there is already a flexible approach for designing the DHS with a high level of detail, which is published as open source tools and can be used for further development.

[1] Parts of this chapter are published in (Röder et al. 2021).

The THERMOS project provides an open and free-to-use web-based DHS planning tool (THERMOS project 2020). It is based on a high level of detail using a building-wise representation of the heat demand. The tool also includes a bottom-up method for estimating the heat demand of the buildings. The main feature of the THERMOS-tool is the district heating network design. This includes the selection of the heat supply site, the cost-efficient connection of buildings and the routing and dimension of the piping network. Two different objectives are implemented, which represent two different perspectives on the planning problem: the maximization of the net present value for the network operator and the maximization of the whole-system net present value. The modeling background of the THERMOS-tool is based on Kuriyan and Shah (Kuriyan et al. 2019). The THERMOS-tool is a very powerful and practical planning tool. In the meanwhile, in 2021, the source code has been made public (Hinton et al. 2022). However, the software seems to be indented as stand-alone application, which is not practical for a flexible integration in a Python-based workflow. Furthermore, it is licensed under the Reciprocal Public License (Hinton et al. 2022). This makes it impossible to integrate this tool in other software tools that should be published under a free software license. Altogether, a community based development does not seem to be indented.

Weinand et al. developed a combinatorial optimization approach to design district heating networks based on deep geothermal energy (Weinand et al. 2019). Here, the cost-optimal location of a geothermal plant is determined, taking into account the location and characteristics of several settlements, a specification of the heat coverage by the district heating network and restrictions due to geographical conditions like forests. An optimization approach is compared with a heuristic method. The authors conclude that the heuristic method outmatches the optimization approach by a significantly shorter computing time with a deviation of the investment costs of less than 5 percent (Weinand et al. 2019). Though, this approach does not include a detailed representation of the district heating network within the settlements themselves.

Bording et al. also presented a linear integer approach including the piecewise linear approximation of the relation between mass flow and pressure drop (Bordin et al. 2016). This publication also focuses on the connection of new customers to an existing district heating network and therefore maximizes the overall net profit. The stationary peak load case is considered and the global – i.e. a same factor for all consumers – simultaneity factor is applied. However, the approach is limited to networks having a tree configuration with a single plant, and the network itself is an input for the optimization process and not a result based on a larger network with all potential routing options. (Bordin et al. 2016)

Lambert et al. present a multi-stage stochastic programming formulation for the optimal phasing of district heating networks to minimize the investment risk (Lambert et al. 2016). The term phasing refers to the expansion decisions when a district heating network is developed from a ‘seed’ network and evolves over time (Lambert et al. 2016), which is a very important aspect for the planning of future DHS. The authors also state that the approach could be used to show local authorities and planners how their district heating network might expand over the investment period.

Li and Svendsen propose a district heating network design approach using a mixed-integer non-linear optimization (MINLP) formulation and a genetic algorithm for solving (Li et al.

2013). This includes a detailed representation of the thermal and hydraulic relations. Similar to Weinand et al., the location of the district heating plant is optimized on a discrete grid (compare Weinand et al. 2019). A mathematical formulation using the design peak heating load as basis and eight time steps representing the different load states during the year is performed. The approach considers a tree-shaped structure without isolated loops. (Li et al. 2013)

Also using genetic algorithm technique, Razani and Weidlich published a modeling approach for analyzing different DHS layouts including thermal storage units (Razani et al. 2016). A small virtual district heating network supplied by a CHP is analyzed with three different storage configurations: a central storage, semi decentral storages and full decentral storages (Razani et al. 2016). To the knowledge of the authors, this is the only modeling approach that considers thermal energy storages within the network planning. However, the approach can be neither used nor extended by others as it is not published as open source package. Furthermore, it is based on a single heat supply.

For the task of designing and sizing district heating networks, Dorfner presented in his PhD Thesis the open source models DHMIN, originally published in 2014 (Dorfner et al. 2014), *dhmin (seasonal)* and *rivus* (Dorfner 2016). This could be identified as the only fully open source planning tools. The main feature of *dhmin (seasonal)* is the consideration of redundancy of multiple heat generation sites by using multiple time steps. As the title of the 2014's publication already indicates, the *dhmin* family focuses on large scale districts. Therefore, the spatial resolution follows a street-wise aggregation by mapping the buildings to the graph edges. The simultaneity factor (concurrence effects) is considered via a global factor by downscaling the cumulated peak power at each source node. (Dorfner et al. 2014; Dorfner 2016) Although the code is open, there is a lack of modularity for reasonably expanding the model. In addition, the spatial resolution of this model follows a different design concept with a street-wise aggregation. Therefore, this model was not considered for further development.

The literature research shows that there are numerous published modeling approaches for the design and planning of district heating networks. It also shows that most of the models are proprietary and the source code is not published. Certainly, most articles about proprietary models provide important information on the methodical approach, but in most cases it is neither possible to use the model nor to extend it. However, this aspect is crucial for scientific progress.

Hence, a new optimization tool for the design of district heating networks was developed. The software is published within the open source Python software package *DHNx* (Jnnr et al. 2020b), which is part of an existing scientific community. By practicing open source development on the platform GitHub (oemof developer group 2022b), the connectivity is granted and the expandability facilitated. This enables a collaborative development and avoids duplicated work in science.

3.2 DHNx optimization tool

The aim of the techno-economic optimization approach developed in this thesis is to find the most cost-efficient district heating network with a high level of detail at building level and the

option of considering different complex boundary conditions, like distributed thermal energy storages (presented in Röder et al. 2021), multiple heat sources and the possibility of an easy expansion. The optimization process includes the optimal network routing and the sizing of the district heating pipelines based on the design criteria of a maximum specific pressure drop per meter. The general description of the model can be formulated as follows: Given are the heat demand of each consumer of an urban district, a cost-function for the heat distribution pipes and further individual boundary conditions. The heat demand can be given by individual load profiles. Scalar values for the heat load at design condition are also possible. The optimization problem is concerned with deciding on where to build the pipeline system and how to dimension it while minimizing the overall costs. Additionally, the district heating network optimization approach is capable of considering the case of complete redundancy of multiple supply options and can be extended by additional components at the consumers and producers. The modeling approach is implemented in Python as open source tool within the package *DHNx* (Jnnr et al. 2020b; oemof developer group 2022b). For building up the optimization model, the library *DHNx* itself makes use of the open source package *oemof.solph* (Krien et al. 2020; Hilpert et al. 2018), which uses pyomo (Hart et al. 2017) for creating the MILP model. By using *oemof.solph* as optimization basis (see also Section 2.3.2), the coupling of the district heating network optimization with any other *oemof.solph* model is also possible.

The following section provides a detailed description of the underlying topological model and the mathematical background of the model's core elements. Furthermore, a new method for considering the simultaneity of heat demand is introduced, and the workflow and usage of the *DHNx* optimization tool are explained.

3.2.1 Topological input data

The base of this design approach consists of two georeferenced data layers: a line layer containing all potential routing options for DHS, which can be derived e.g. from OpenStreetMap (OpenStreetMap contributors 2022), and a polygon or point layer containing all buildings, which are supplied by the DHS. Figure 3.1(a) illustrates the starting basis.

Based on the given geometry, a consistent nodes-edges structure is generated. This means that the distribution lines are prepared for the optimization model builder, and the connections to the buildings are created. This implies splitting and merging the distribution lines, adding nodes at the ends of all edges and categorizing the nodes according to their representation: consumer, supply and fork. Figure 3.1(b) shows the result of the geometry processing and illustrates the detailed representation of the district heating grid. Each building is connected to the distribution network.

After processing the geometry (see Figure 3.1(b)), an *oemof.solph* energy system is created (oemof developer group 2020a). For all edges, a DHS pipeline component named *HeatPipeline* was developed and will be explained in detail in Section 3.2.2. Besides, the following classes from the *oemof.solph* library are used in the energy system model: *Bus*, *Source*, *Sink* and *Flow*. For all nodes of the district heating network graph an *oemof.solph Bus* is generated. A *Bus* creates an energy balance. The heat demand is given by an individual time-series of the coldest period of the year for each building and is modeled by a *Sink*. At each DHS supply plant,

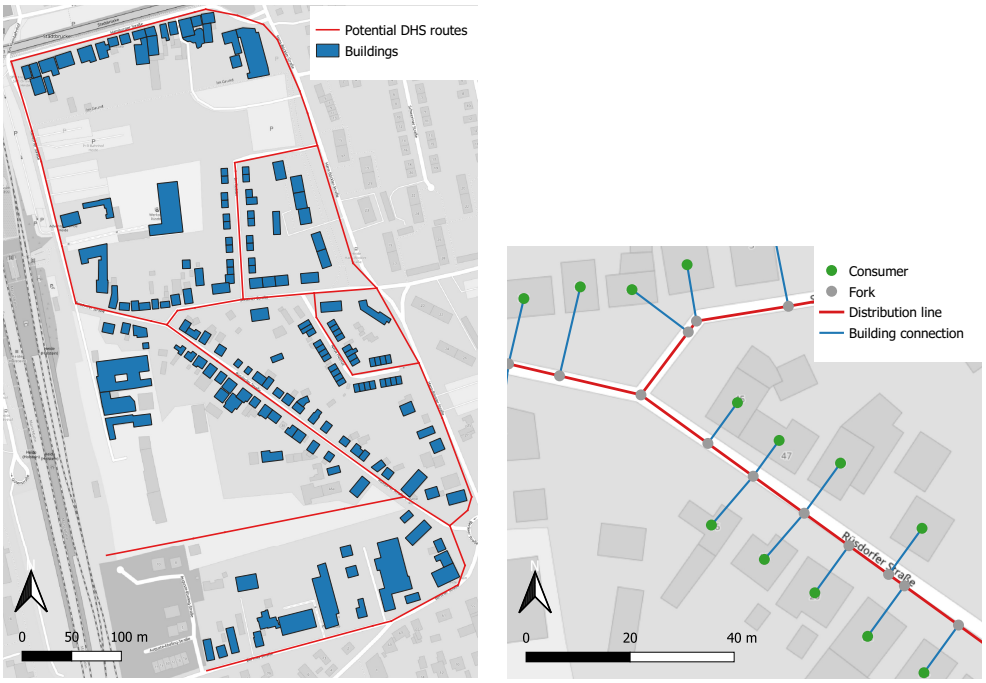

(a) Before geometry processing (b) After geometry processing

Figure 3.1: (a) Geometry input of the district planning and optimization approach. Red: possible district heating routes; blue: considered buildings. (b) Result of the geometry processing and input for the optimization model. Source background map: (OpenStreetMap contributors 2022).

a *Source* represents the heat generation units and ensures the heat feed-in to cover the heat demand of the DHS. The detailed mathematical background of the *oemof.solph* components is given in Section 2.3.2. Further information can be found in the documentation of *oemof.solph* (oemof developer group 2020a). In the following, the *HeatPipeline* component for modeling the district heating piping system is explained in detail.

3.2.2 Model of district heating pipelines

For the DHS pipelines, a MILP model called *HeatPipeline* was developed and is published within the *DHNx* library (Jnnr et al. 2020b). The mathematical formulation is based on (Dorfner et al. 2014). However, this model differs in the level of detail and the way how the heat demand is considered. The forward and return pipes are not modeled separately, but are represented by one component. All edges of the district heating network (see Figure 3.1(b)) are modeled by a *HeatPipeline* component. Figure 3.2 outlines the concept:

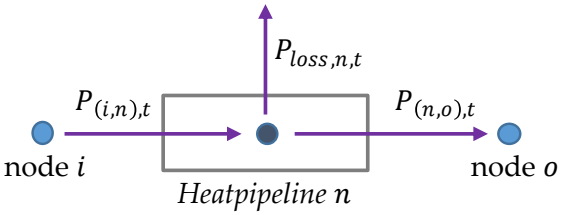

Figure 3.2: Schema of the district heating pipeline model.

The following equations describe the constraints of the *HeatPipeline* component, which represents a single element of the pipeline network:

$$C_n = P_{(n,o),invest} \cdot c_{invest} + y_{(n,o)} \cdot c_{investfix} \tag{3.1}$$

$$P_{loss,n,t} = P_{(n,o),invest} \cdot f_{loss,t} + y_{(n,o)} \cdot f_{lossfix,t} \tag{3.2}$$

$$P_{(n,o),t} = P_{(i,n),t} - P_{loss,n,t} \tag{3.3}$$

$$P_{(i,n),invest} = P_{(n,o),invest} \tag{3.4}$$

$$P_{(n,o),investmin} \cdot y_{(n,o)} \leq P_{(n,o),invest} \leq P_{(n,o),investmax} \cdot y_{(n,o)} \tag{3.5}$$

$$-P_{(i,n),invest} \leq P_{(i,n),t} \leq P_{(i,n),invest} \tag{3.6}$$

$$-P_{(n,o),invest} \leq P_{(n,o),t} \leq P_{(n,o),invest} \tag{3.7}$$

$$y_{(n,o)} \in \{0,1\} \tag{3.8}$$

with the following decision variables:

C_n	Investment costs of DHS pipe n [€]
$P_{(n,o),invest}$	Heat transport capacity of DHS pipe n [kW]
$P_{(n,o),t}$	Heat flow from the DHS pipe n at time step t [kW]
$P_{(i,n),t}$	Heat flow into the DHS pipe n at time step t [kW]
$P_{loss,n,t}$	Thermal loss of DHS pipe n at time step t [kW]
$y_{(n,o)}$	Investment decision variable of DHS pipe n [-]

and the following parameters:

c_{invest}	Capacity dependent investment costs [€/kW$_{transport}$]
$c_{investfix}$	Fix investment costs [€]
f_{loss}	Capacity dependent loss factor [kW$_{loss}$/kW$_{transport}$]
$f_{lossfix}$	Fix loss [kW$_{loss}$]
$P_{(n,o),investmin}$	Minimum pipe capacity [kW$_{transport}$]
$P_{(n,o),investmax}$	Maximum pipe capacity [kW$_{transport}$]

The binary variable $y_{(n,o)}$ is used to create an y-offset in the linear function of the investment costs and thermal losses (see Equations 3.1, 3.2 and 3.8) to better approximate the real costs and thermal losses of the DHS pipelines. Hereby, an investment of zero is possible as well by Equation 3.5. The time dependent actual heat outflow $P_{(n,o),t}$ of a single district heating pipeline element results from the inflow $P_{(i,n),t}$ minus the thermal loss $P_{loss,n,t}$ (see Equation 3.3 and Figure 3.2). The investment capacities of the in- and outflow are set equal 3.4 to generate a symmetry within the component independently of the physical mass flow. Thus, the flow direction does not affect the invested pipe capacity, and bidirectional heat flow values can be allowed (Equations 3.6 and 3.7). For all connection lines to the consumers, only directed *HeatPipeline* components are used, so that in the case of distributed thermal storage units, no heat feed-in from a consumer is possible.

For the parametrization of the DHS pipe component, preliminary calculations are performed to transfer the hydraulic design criteria of a maximum pressure drop per meter into capacity dependent parameters for the optimization model. The scheme given in Figure 3.3 clarifies the approach.

The starting point is a maximum length-specific pressure drop, which is a common criteria for designing DHS pipelines (Thalmann et al. 2018). Furthermore, the roughness of the pipelines' inner surface and the temperature level the DHS is operated at need to be given. By using an iterative calculation approach, the maximum flow velocity is calculated for each DN number

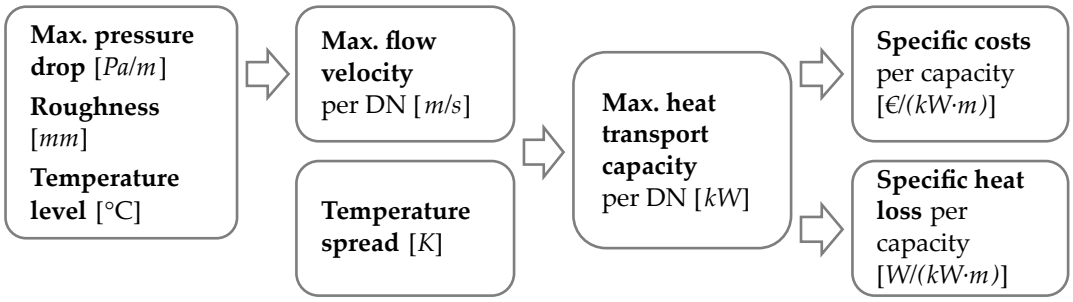

Figure 3.3: Derivation of capacity dependent optimization parameters from hydraulic design guidelines; DN: nominal diameter.

(nominal diameter). Within this iterative approach, the empirical formulas of Blasius, Prandtl, Colebrook and Kármán are used to calculate the pressure drop according to the usual state of the art depending on the flow type and on whether a smooth or rough flow regime is present in the case of a turbulent flow regime. The applied formulas for the calculation of the maximum flow velocity are published in the *DHNx* repository on GitHub (oemof developer group 2022b) (see also Böswirth et al. 2014; Shashi Menon 2015). The maximum heat transport capacity of each DN number results from the forward and return temperature the DHS is operated at. The maximum heat transport capacity thus determines the magnitude to which the costs and the thermal losses are referred to for the optimization model. Section 3.3.2 provides the parameters applied in the case study.

3.2.3 Simultaneity of heat demand

In planning and dimensioning district heating networks, the consideration of the simultaneity of demand plays an important role. In many district heating network optimization models, the simultaneity is taken into account by downscaling the maximum winter heating load of the consumers globally with a fix factor, often called the simultaneity factor (Winter et al. 2001). Since the simultaneity factor depends on the kind and number of heat consumers, the sizing of distribution lines with few customers might be inappropriate by using a global simultaneity factor. For example, in the case of a simultaneity factor of 0.6 for 200 customers of a district, where a specific distribution line supplies five customers with a simultaneity factor of 0.9, a global down-scaling of the consumers' loads with 0.6 may lead to an underestimation of the actual heat load in this specific distribution line.

Therefore, the *DHNx* optimization tool is capable of applying a multi time step approach using individual load profiles of the period around the peak load, e.g. the coldest three days of a year. The idea is that the simultaneity effect is already included in individual load profiles to imitate a real diversified load. Consequently, within the optimization approach for dimensioning the piping network itself no additional effort must be made for considering the simultaneity effect. The particular load profiles can be achieved by individual modeling of the buildings' heat loads or by applying a normal distributed time shift to load profiles types, which is the methodical approach used for the load profiles of this work. The following Figure 3.4 illustrates the principal approach based on three exemplary normed load profiles. The peaks of the load

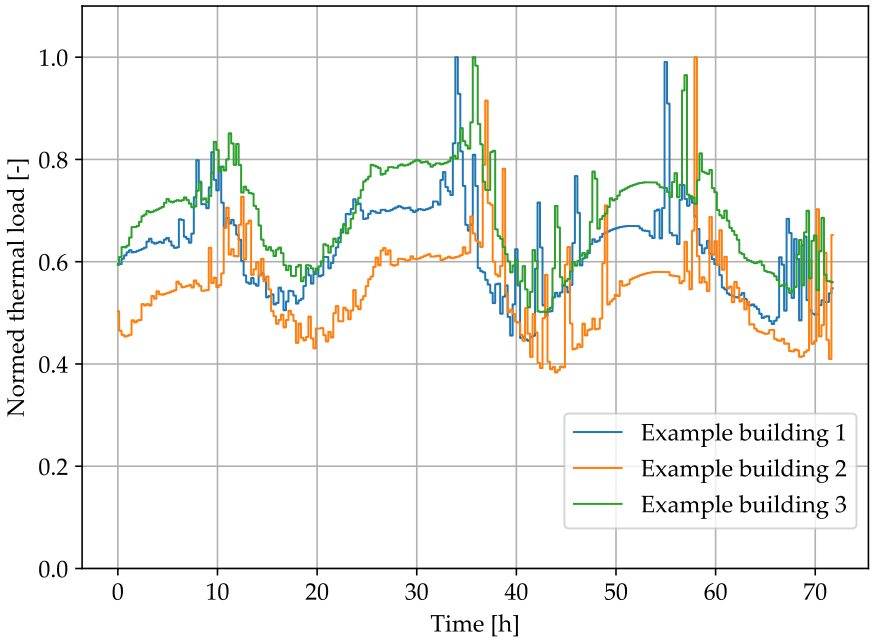

Figure 3.4: Exemplary heat load of three buildings showing the shift in heat load peak, which imitates the simultaneity effect.

profiles occur on different time steps. In the optimization process, theses load profiles of the design period can be used for dimensioning the district heating piping system.

3.2.4 Usage and workflow of the DHNx optimization tool

In the following, an overview of the workflow and usage of the *DHNx* optimization tool is given. The detailed application programming interface (API) is documented in the online documentation of *DHNx* (oemof developer group 2022a).

Figure 3.5 summarizes the different steps in the workflow of the district heating network optimization process, which are the processing of geometry, the pre-calculation of design parameters, the actual optimization of the pipeline network and the post-processing. These different functional units are kept modular to increase the usage for application with different input data. This means that geometry processing or pre-calculation of design parameters may be used also separately if other tools for the pipeline optimization are favored. Alternatively, the optimization process is deployed with other preliminary methods. The actual input data for the district heating network optimization do not need to be georeferenced at all as long as the tabular input data format satisfies the requirements explained in the documentation (oemof developer group 2022a).

The starting point of the overall design process is a georeferenced layer, e.g. a point or a polygon layer, with the buildings that are considered for the district heating network. As the geometry processing module is based on *geopandas* (GeoPandas community 2022), several geographic information system (GIS) formats that can be imported by *geopandas* are possible. Furthermore, the potential routes of the district heating pipelines need to be given. For that purpose, a georeferenced line layer is required. This can be downloaded for example from

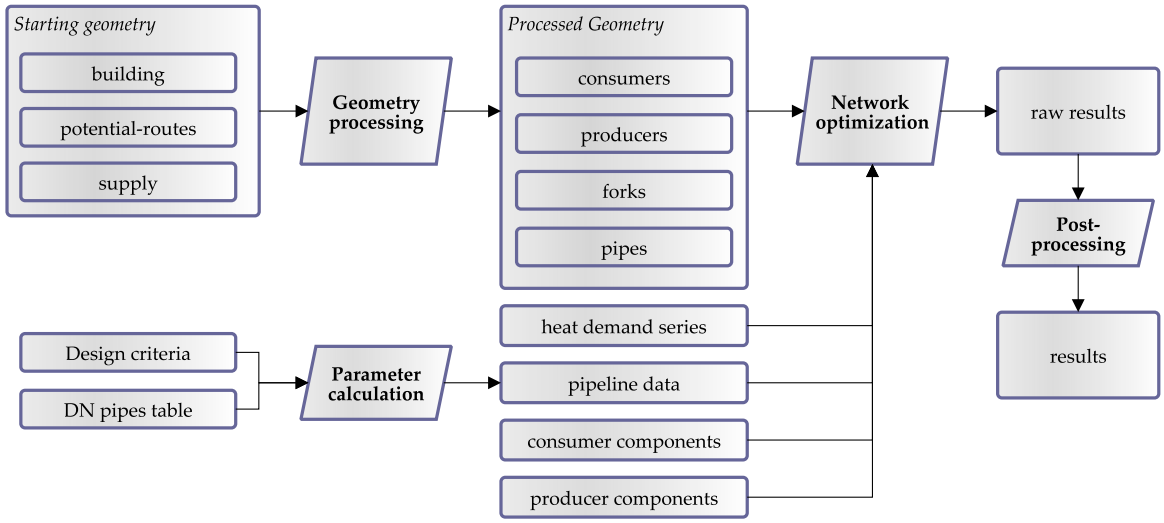

Figure 3.5: Workflow and usage of the *DHNx* optimization tool.

projects such as OpenStreetMaps (OpenStreetMap contributors 2022), e.g. by using the Python library *osmnx* (Boeing 2017), manually drawn with any GIS software or a combination of both. A third polygon or point layer is required that includes the options for potential district heat supply sites. The geometry processing module then prepares the spatial input into a consistent node-edges structure as described in Section 3.2.1. The results are four georeferenced tables as instances of the class *geopandas.GeoDataFrame*, three tables with point geometry (consumers, producers and forks) and the pipes table with line geometries. The pipes table contains the information about the length of the single edges of the graph. Thus, from that point on, also instances of *pandas.DataFrames* (The pandas development team 2021), so tables without georeference, may be used in the subsequent network optimization.

The second preliminary process is the calculation of the parametrization of the *HeatPipelines*. Therefore, a table including the considered DN numbers with technical and economic specifications such as diameter, roughness, costs per meter and the expected operation temperatures must be given. With the design criteria of a maximum pressure drop per meter, the specific costs and thermal losses related to the heat transport capacity are calculated according to Figure 3.3. The so-calculated discrete parameter of each DN number can be linearized in one or more segments. The coefficients of the linear or piecewise linear segments are the input parameter of the optimization model and need to be given to the network optimization in tabular format as a *pandas.DataFrame*. It is also possible to use a parameter table with discrete DN numbers for the optimization. However, as for each linear segment, an additional *HeatPipeline* component is generated in the network optimization, which becomes computationally more complex and the calculation time increases.

In addition to the pipeline data, the heat demand of the individual buildings is required. There are two options: The heat demand can be given as time-series to allow an individual consideration of simultaneity, as introduced in Section 3.2.3, or in the form of a maximum heat load as scalar value. In the latter case, the heat load can already be given within the consumers table, and no additional heat demand table with heat demand time-series is required.

In this case, a global simultaneity factor can be applied for an accurate dimensioning of the distribution pipelines.

Optionally, additional *oemof.solph* components can be created at the producers and consumers with tabular input tables. This allows for example the consideration of storages or energy converter units for more complex network optimization tasks.

Based on the given input data, the network optimization method of the *DHNx ThermalNetwork* class creates and solves an *oemof.solph* model. In the post-processing, the results of the *oemof.solph* model are read out and transferred to the pipes table that contains the georeferenced location of each edge. The linear results of the investment decisions can then be further reckoned back to discrete DN numbers as the user demands, e.g. by rounding-up to the next feasible DN number.

3.3 Data and parameters

The introduced district heating network optimization tool is applied to different local scenarios – or heat demand scenarios – of the district Rüsdorfer Kamp in Heide. Therefore, the heat demand scenarios are explained, followed by the presentation of the district heating network parameters.

3.3.1 Local scenario framework

The local scenarios are the basis of the district heating network design and also serve as input parameter for the analysis of supply strategies in Chapters 4 and 5. The term *local* refers to potential developments at district level. This includes two developments that are of importance for the DHS: the refurbishment state of the existing building stock and the connection quota. The basis of the heat demand scenarios for dimensioning the district heating network are thermal load profiles of the individual buildings, which are comprised of domestic hot water (DHW) demand and heating-energy demand (see Section 2.2.3).

For the energetic refurbishment, three different scenarios are studied: the current status of the existing buildings, a conservative refurbishment scenario and an ambitious scenario considering a deep refurbishment of all buildings. Table 3.1 provides an overview of the three refurbishment scenarios considered and the contemplated parameters. This includes the supply and return temperatures for the design of the DHS, the operation temperatures of the DHS, the secondary side of the substations at the buildings and the reduction of space heating demand relatively to the current status-quo.

The *Status-quo* scenario reflects the current building status of the district. It is characterized by high supply temperatures up to a forward temperature of 80 °C at the secondary side of some buildings. This requires a forward temperature of 85 °C at the heat supply at peak demand. It is assumed that in summer the supply temperature of the DHS can be decreased to 70 °C. Altogether, the temperature level in this DHS supply scenario is sufficient to supply existing domestic hot water systems like hot water puffer storages that need to be operated at

Table 3.1: Overview of the parameters of refurbishment scenarios.

Scenario name	Design temperatures DHS forward / return [°C]	Operation temperatures DHS forward / return [°C]	Operation temperatures at the buildings (secondary) [°C]	Reduction of space heating demand in [%]
Status-quo	80 / 55	70–85 / 55	65–80 / 50	0
Refurb-1	65 / 45	65 / 45	60 / 40	25
Refurb-2	50 / 35	47 / 32	47 / 32	50

least at 60 °C due to the legionella problematic. The temperature spread at the design point is assumed to be 25 K.

In the scenario *Refurb-1* the retrofitting measures are oriented to the reference building defined by the German Buildings Energy Act (GEG), which is also known as Efficiency house 100 (KfW-Effizienzhaus 100/115) (GEG 2020; KfW 2022). This does not mean that all buildings achieve this building standard, some may perform better some worse. It is assumed that the retrofitting measures lead to a lower space heating demand of 25 % on average and to lower supply temperatures for space heating of 60 °C on the secondary side of the DHS substation. In this scenario, the return temperature can also be reduced to 45 °C, which results in a temperature spread of the DHS of 20 K for the primary side. To achieve these improvements, moderate refurbishment measures are required. These are for example an additional insulation of the exterior facade with a thermal insulation composite system with a thickness of 12 cm, an inter-rafter insulation of the roof, an exchange of the windows with a two- or three-pane thermal insulation glazing and an additional insulation of the basement ceiling of 8 to 10 cm. Additionally, very old radiators might be exchanged. The temperature of the DHS is still high enough that existing domestic hot water systems, such as central buffer tanks, can be used.

The scenario *Refurb-2* represents a very ambitious refurbishment scenario that leads to a reduction of space heating demand by 50 %. Therefore, the energetic standard of the building envelope needs to be in the range of Efficiency house 55 (KfW-Effizienzhaus 55) to Efficiency house 70 (KfW-Effizienzhaus 70) (GEG 2020; KfW 2022). It is characterized by significantly higher insulation thickness of the outer facade, the roof and the basement ceiling. Tree-pane thermal insulation glazing is inevitable, and the existing space heating system needs to be upgraded to a low temperature heating system such as a floor heating system or extensive low temperature radiators so that supply temperatures of 45 to 50 °C are sufficient to ensure the supply of the heat demand. For domestic hot water, in many cases, new equipment needs to be installed. This could be the installation of domestic hot water substations in each flat that guarantee a limited volume of three liters on the secondary side of the substation or the application of ultra-filtration technique based on a microporous membrane filter to prevent legionella in the case of central domestic hot water puffer tanks with circulation.

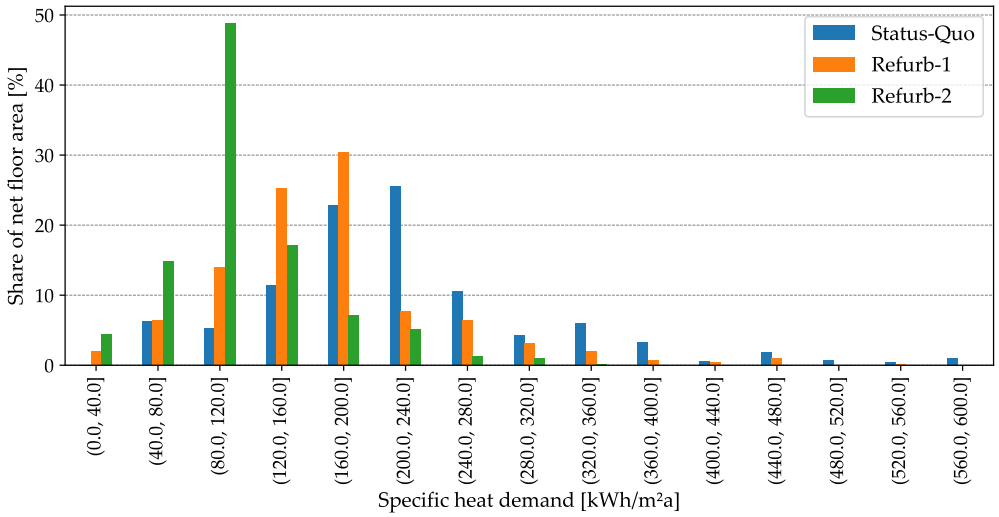

Figure 3.6: Accumulated share of total net floor area of the district for the specific heat demand for the three buildings scenarios *Status-Quo*, *Refurb-1* and *Refurb-2*.

In reality, the implemented refurbishment measures and the respective energy standards achieved vary from building to building. This also means that if e.g. 80 % of the buildings achieve an ambitious energetic standard according to scenario *Refurb-2*, and still 20 % of the buildings remain at *Status-quo*, it is not possible to operate the DHS with forward temperatures of 50 °C without additional measures at the buildings, for instance a decentral temperature booster like a heat pump or a heating rod. In this sense, the refurbishment scenarios introduced stand for exemplary developments for the purpose of studying the differences and impacts on the design of the DHS and for the comparison with individual heat supply concepts.

Figure 3.6 summarizes the heat demand scenarios and shows the accumulated floor area per specific heat demand including space heating and hot water. In the *Status-Quo* scenario, most of the buildings of the Rüsdorfer Kamp are characterized by a specific heat demand of 200 kWh/(m²a) and higher, as illustrated in Figure 3.6. This corresponds to the worse half of the un-refurbished building stock in Germany (compare Figure 1.6). In the refurbishment scenarios, the share of floor area with a heat demand higher than 200 kWh/(m²a) decreases due to the assumed reduction of space heating demand. In the very ambitious scenario *Refurb-2*, more than 60 % of the total net floor area demands 120 kWh/(m²a) or less. This matches well the distribution of fully refurbished buildings according to Figure 1.6.

The second parameter that is investigated in relation to the establishment of a DHS is the connection quota. Figure 3.7 shows one possible connection scenario for the 30 %, 50 %, 70 % and 100 % scenario. The percentage value refers to the number of buildings out of the total number of buildings of the existing building stock that are connected to the DHS. In each connection scenario, the buildings are selected randomly. A high number of buildings that are connected to the DHS is essential for achieving a cost-efficient DHS. To study the tipping point of the economic feasibility of a DHS in contrast to a decentral building-wise generation of heat, different connection quota from 30 to 100 % are taken into consideration. In this analysis, the construction of new buildings and the densification of the district has not been taken into account as the focus lies on the transformation of existing districts. Furthermore, the amount

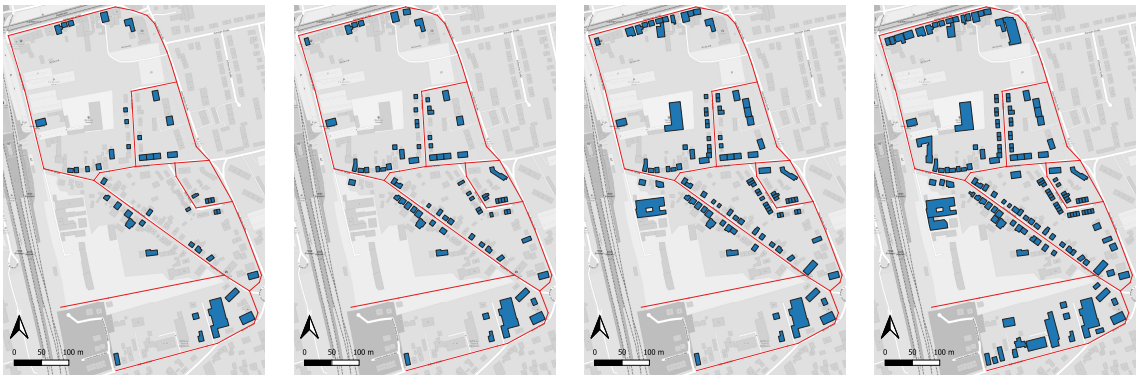

(a) 30 % (b) 50 % (c) 70 % (d) 100 %

Figure 3.7: Example of connection scenarios ranging from 30 to 100 % of the buildings. (a) 30 %, (b) 50 %, (c) 70 %, (d) 100 %. In the 100 % scenario all existing buildings are connected to the district heating network.

of scenarios would increase unmanageably. Of course, the connection quota as well as the refurbishment rate can only be influenced externally to a limited extent. However, the variation of both parameters can serve well as simulating different scenarios for decision making, which represent different heat demand densities. Based on the latter, it is possible to determine heat density thresholds for the feasibility of a DHS. The results can then be transferred to other districts, and the comparison of the findings with results of other studies is possible.

The process of randomly selecting buildings has been repeated several times. Figure 3.8 displays the district dependent scenarios, the specific heat demand density in kWh/(m²a) and the heat line density in kWh/(m a) for the three refurbishment scenarios dependent on the share of total floor area that is connected to the DHS. The building scenarios that are investigated range from 4 kWh/(m²a) in the lowest scenario with a connection quota of 30 % and an ambitious refurbishment of all buildings (refurbishment scenario *Refurb-2*) to 32 kWh/(m²a) in the 100 % *Status-Quo* scenario.

Compared to the threshold values proposed in literature that are reviewed in detail in Section 5.1 the heat densities of the connection scenarios range from heat densities that are at the lower end of heat densities that might be feasible for DHS with values below 20 TJ/(km²a) (equal 5.54 kWh/(m²a)) to heat demand densities that are classified with a moderate to dense heat density with values about 120 MJ/(m²a) (equal to 33.2 kWh/(m²a)) (Persson et al. 2019; Möller et al. 2019). The local scenarios cover a wide range of heat density values from districts with a sparse to medium heat density. Thus, the connection and refurbishment scenarios are suitable for the analysis and review of existing threshold values for establishing a DHS in the context of energy transition and studying the impact of future scenarios of the upstream energy system on the feasibility of DHS.

3.3.2 Parameters of the district heating network

Only discrete pipe diameters are commercially available. Hence, the discrete parameters of individual costs for each pipe with a specific nominal diameter are linearized to obtain a

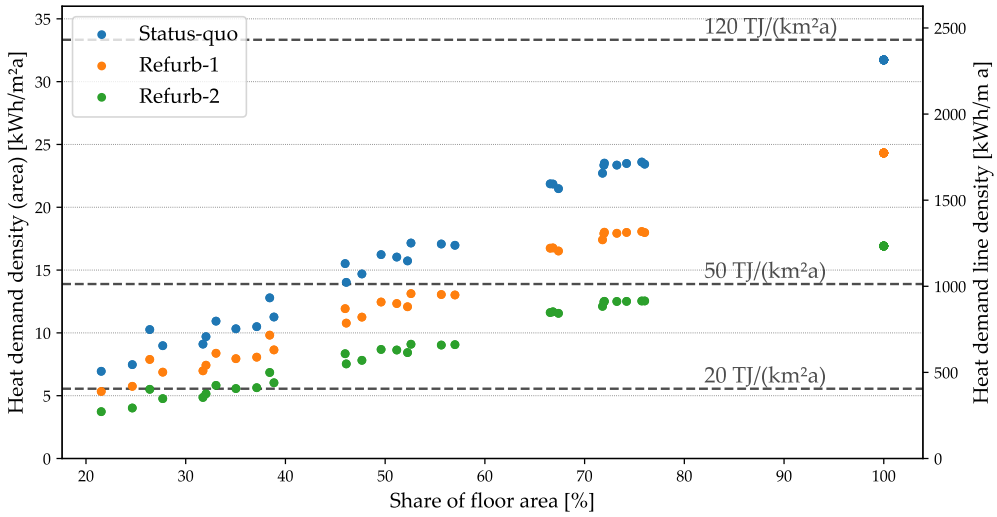

Figure 3.8: Specific heat demand densities of the refurbishment scenarios dependent on the connected floor area. Left y-axis: area dependent heat demand density in kWh/(m²a); right y-axis: heat demand line density in kWh/(m a).

mathematical problem that can be calculated in a reasonable computing time. For each nominal diameter, the maximum heat transport capacity is calculated as described in Section 3.2.2.

According to Best et al., recommendations for the specific pressure drop per meter pipe length range from 70 to 350 Pa/m (Best et al. 2018). Best et al. provides an analysis of the impact of using different design guidelines on the investment costs of transportation pipes and on the total heat distribution costs (Best et al. 2018). Two case studies show that the saving of investment costs can be up to 8 % by using 300 Pa/m instead of 70-100 Pa/m as design guideline (Best et al. 2018). Thus, for this analysis, a value of 200 Pa/m is used as design guideline. The roughness of the inner pipe surface amounts to 0.01 mm, which is the upper bound for new polyethylene (PE) and polyvinylchloride (PVC) pipes (see Vismann 2021, p.1407). The forward and return temperatures that determine the temperature spread in the design point depend on the corresponding refurbishment scenario (see Table 3.1). A ground temperature of 10 °C is assumed for the calculation of thermal losses. The investment costs for district heating pipes depend on many individual factors, and the data given in literature vary depending on the country and the year of publication (compare Nussbaumer et al. 2016; Möller et al. 2016). For this analysis, the project internal cost data and manufacturer data was compared with cost assumption made in literature and other projects (see e.g. THERMOS project 2020). The following costs for the DHS piping network include installation and the costs for civil engineering. The heat losses are based on public technical data sheets of the manufacturer Enerpipe (ENERPIPE GmbH 2022). Figure 3.9 provides the data for the piping network and illustrates the results of the linearization of investment costs and thermal losses.

In both, costs and thermal losses, the linearization leads to slightly higher values for the small pipe diameters, whereas the values for the nominal diameter of DN 75 to DN 125 result in lower values (Figure 3.9).

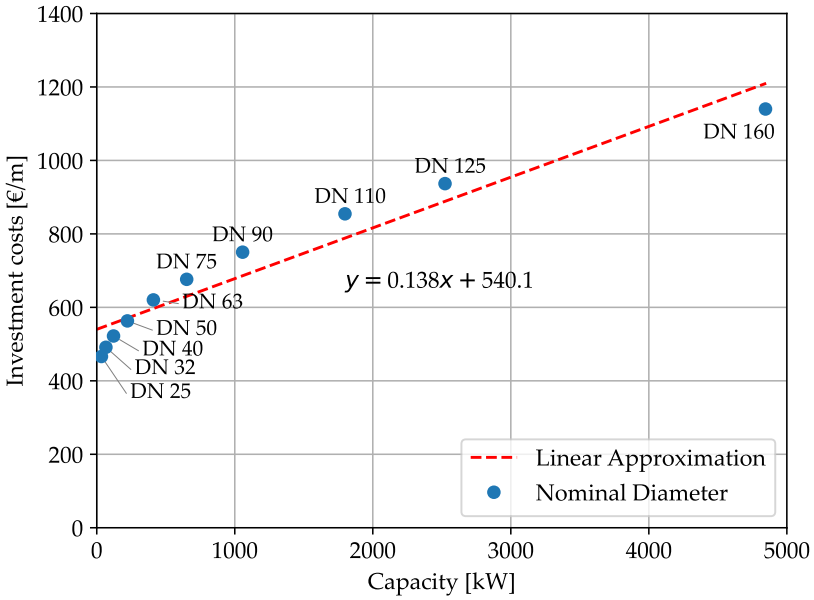

(a) Investment costs

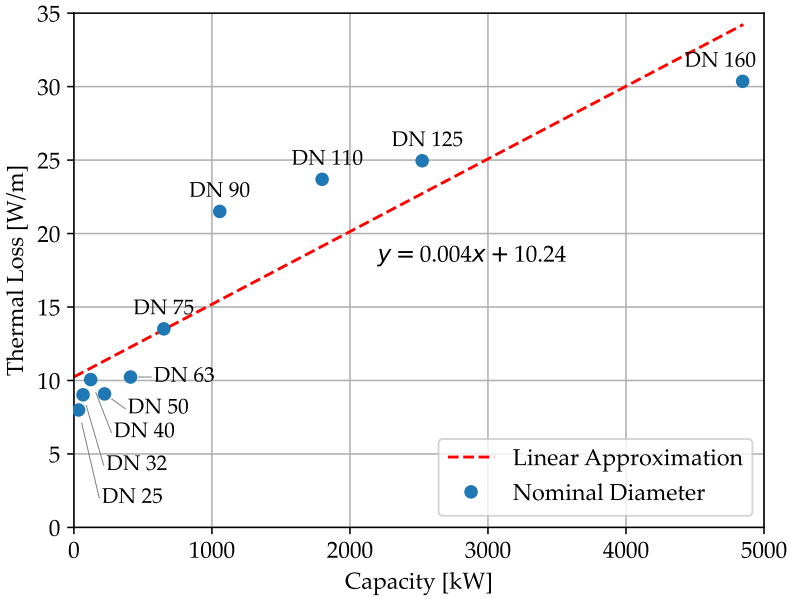

(b) Thermal losses

Figure 3.9: Optimization parameters of the district heating pipelines. Transport capacity and thermal loss depends on the temperature level of the individual scenario. Here, the parameters of scenario *Status-quo* with 80–55 °C are shown. (a) Costs of the district heating pipes per trench length, own assumptions based on (THERMOS project 2020). (b) Thermal losses of the district heating pipes based on (ENERPIPE GmbH 2022).

3.4 Results

The following figures show the results of the optimization of the district heating piping system for the three refurbishment scenarios *Status-Quo*, *Refurb-1* and *Refurb-2* as well as for different connection quota. Here, the selection of buildings for the connection scenarios has been repeated several times (see also Figure 3.8). First, the overall costs and thermal losses of the DHS distribution network are presented both in absolute values (Figure 3.10) and related to the heat demand density of the individual connection scenario (Figure 3.13). Second, the costs and thermal losses of the DHS for the distribution piping system are illustrated.

The comparison of the scenarios illustrates the impact of connection quota and temperature level on the costs and losses of the DHS for the existing district Rüsdorfer Kamp. As Figure 3.10(a) shows, the total costs of the distribution piping system increase with the connected buildings area. However, in the scenarios with a low connection quota there is already a high share of fix costs, e.g. in the scenario with 20 % floor area connected to the DHS the costs of the distribution grid are around 1.2 mill. € due to the fix share of civil engineering costs. The costs for the district heating piping system supplying 30 % of the floor area cause already 75 % of the costs if 100 % of the buildings were connected. The marginal costs for connecting additional buildings to the DHS decrease with an increasing share of buildings.

With respect to the refurbishment scenarios, the costs of the DHS distribution system do not decrease if the houses are retrofitted and the heat demand decreases (Figure 3.10(a)). This results from the assumed decrease in temperature spread in the scenario *Refurb-1* and *Refurb-2* compared to scenario *Status-quo* from a temperature spread of 25 K to 20 K in scenario *Refurb-1* and to 15 K in scenario *Refurb-2*. Thus, the resulting mass flow is in each case almost similar. In scenario *Refurb-2*, the costs for the DHS are even slightly higher compared to *Status-Quo* and *Refurb-1* scenario (see Figure 3.10(a)).

Figure 3.10(b) shows the thermal loss power of the distribution at the design point for the different scenarios. For a given refurbishment scenario or temperature level respectably, the losses behave qualitatively similar to the costs: low connection quota already lead to relatively high thermal losses and a densification of house connections does only moderately increase thermal losses, so that 70 to 90 % of the losses are caused already in the connection scenario of 30 %. In contrast to the costs, the refurbishment scenarios impact the thermal losses of the DHS system. As the temperature difference is the main driver of the thermal network's losses, the temperature level has an extensive impact on the total thermal losses. Decreasing the supply temperature from 80 °C / 50 °C to 50 °C / 35 °C (forward / return) reduces thermal losses by about 40 %.

Figure 3.11 illustrates the results of the accumulated length of each pipe dimension in detail for the distribution lines of the 100 % connection scenario for the three refurbishment scenarios. The scenarios *Refurb-1* and *Status-Quo* show only minor differences and come to the same accumulated length at many DN numbers. Only the scenario *Refurb-2* shows more considerable differences: the DN number 125 is chosen more often and the number 110 less often. The same applies to the DN numbers 63 and 50. Only the DN number 32 is used less often in scenario *Status-Quo* and *Refurb-1* and is replaced by DN number 25 in scenario *Refurb-2*. Overall, this

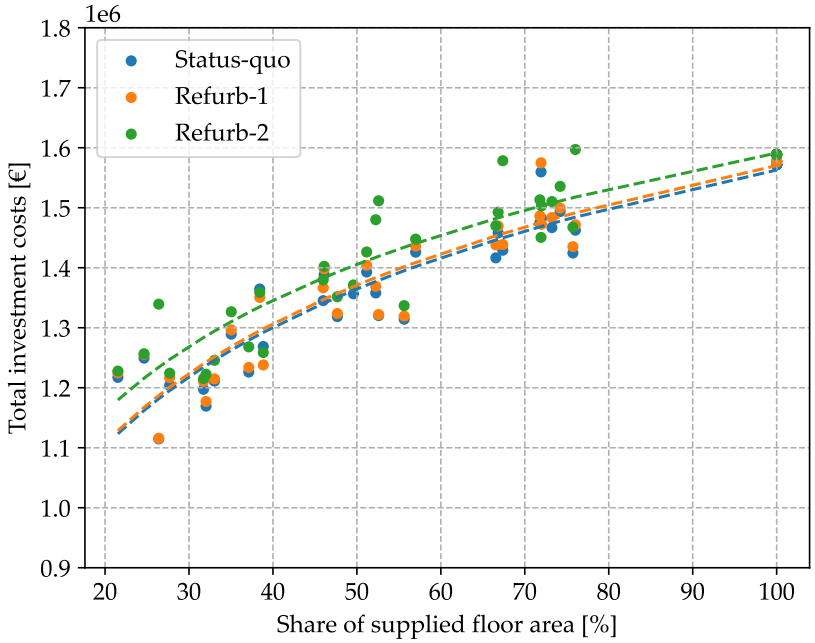

(a) Investment costs

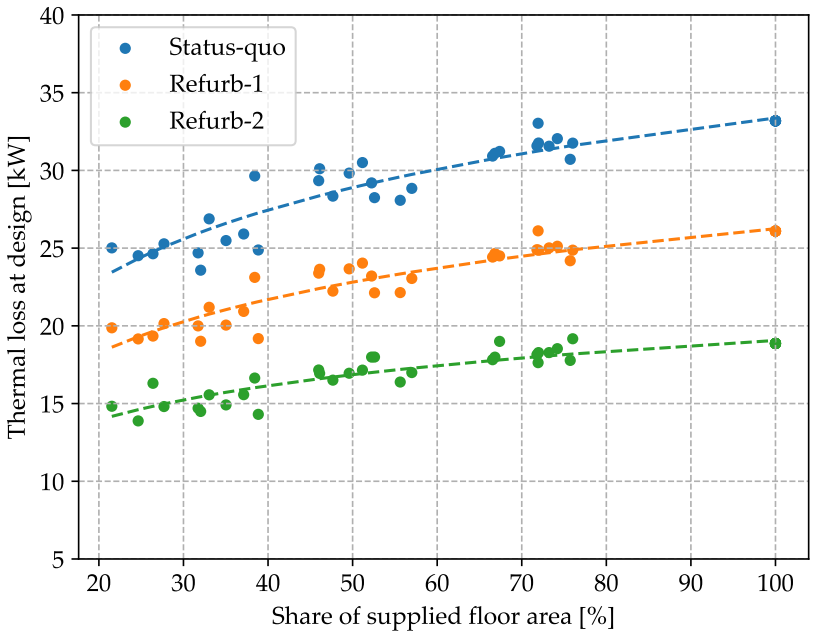

(b) Thermal losses

Figure 3.10: Costs and thermal losses of the DHS distribution piping system of different local scenarios dependent on the share of connected floor area. Dotted lines show the fitting of each scenario $\sim a * log(x) + b$.

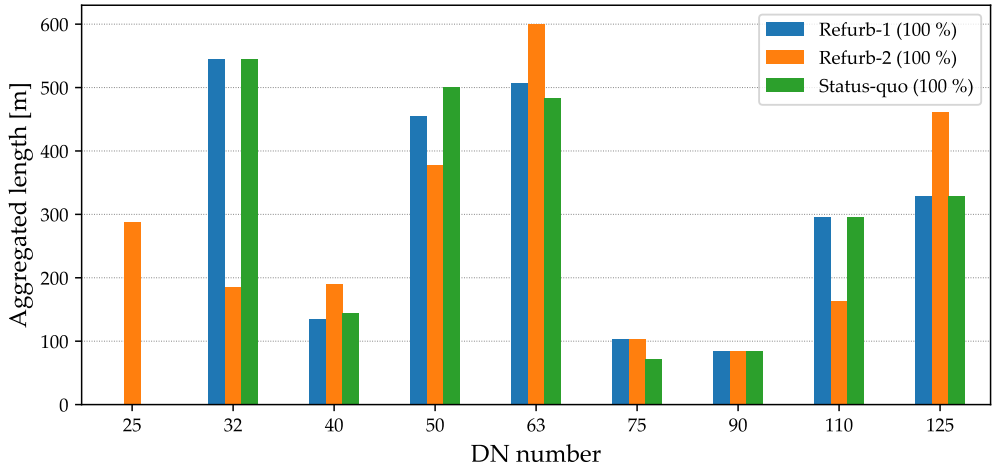

Figure 3.11: Accumulated length of each DN number of the 100 % connection scenario dependent on the refurbishment scenario.

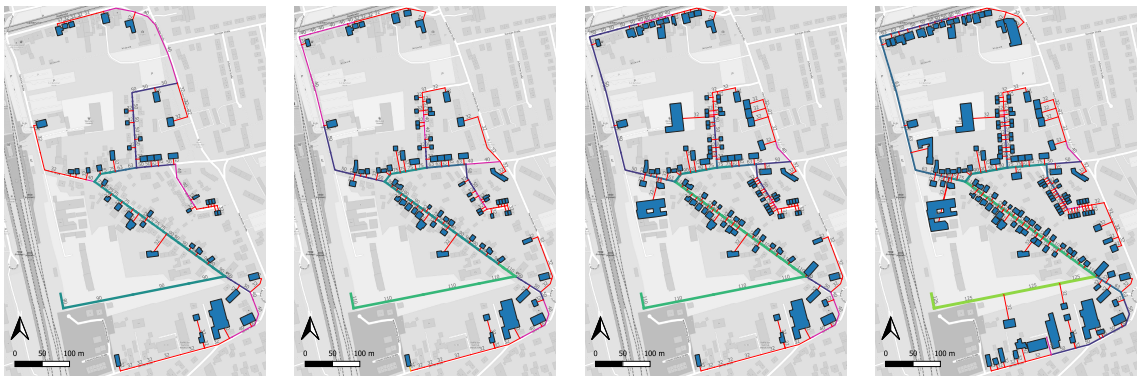

(a) 30 % (b) 50 % (c) 70 % (d) 100 %

Figure 3.12: Results for a single district heating expansion scenario. The optimal routing differs in the 30 % scenario from the scenarios with a higher connection quota.

results in slightly higher costs for the distribution piping system in scenario *Refurb-2* (compare Figure 3.10(a)).

Figure 3.12 shows the results of the different connection scenarios for the retrofitting scenario *Refurb-1*. In the case of a low connection quota, the optimal routing differs as compared to scenarios with a high connection quota. In the 30 % scenario (see Figure 3.12), the northern buildings are connected via the eastern Hans-Böckler-Straße, but in scenarios with a higher connection quota, the western path via Rüsdorfer Straße is chosen as cost-optimal. This underscores the need to think and plan district heating networks from the final expansion stage.

Figure 3.13(a) shows the results of the district heating network optimization by relating the relative costs and losses per delivered end-energy to the characteristic heat line density of the corresponding scenario and derives a mathematical relationship.

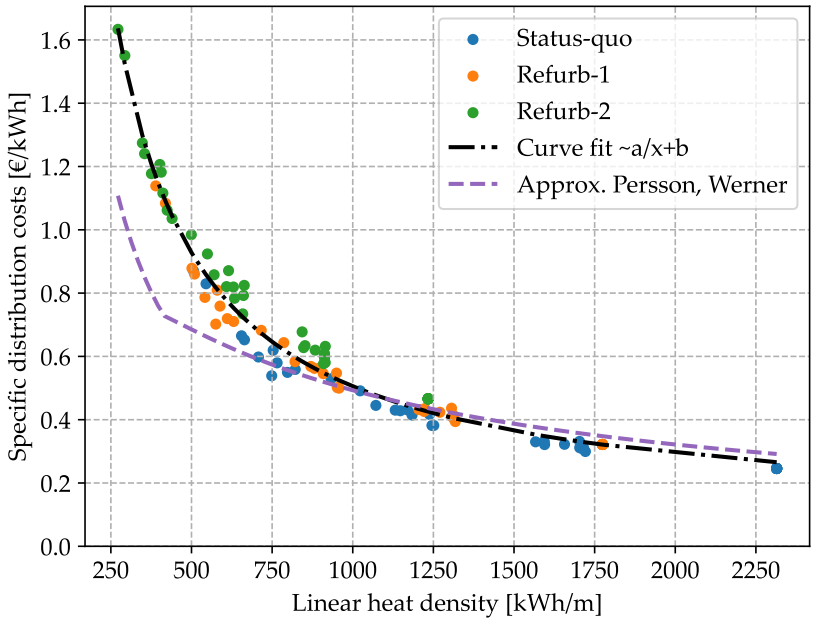

(a) Investment costs

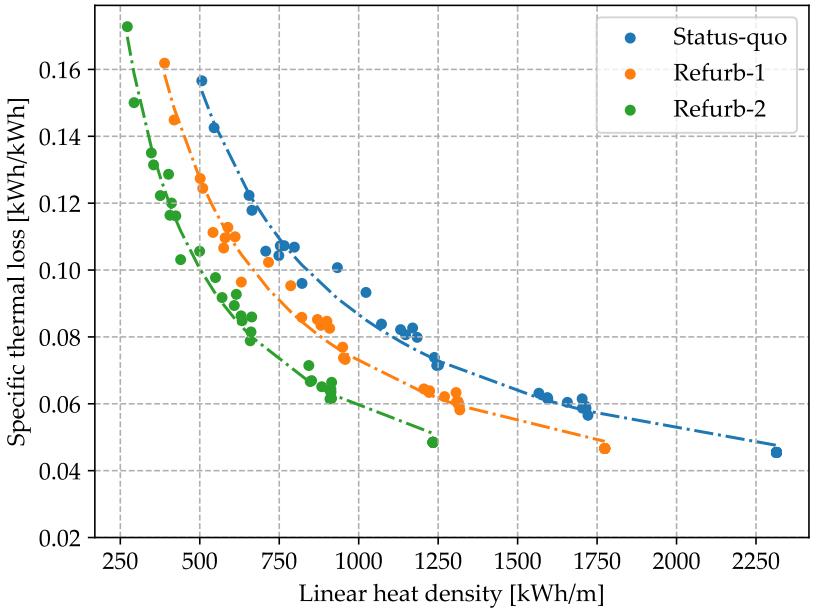

(b) Thermal losses

Figure 3.13: Investment costs (a) and thermal losses (b) of the DHS distribution piping system of the different local scenarios dependent on the linear heat density. Dash-dot lines show the fitting of each scenario $\sim a + b/x$.

Given the specific costs per pipeline trench meter for each DN number and the characteristics of the existing district of this study, the costs per kilowatt-hour heat accounts for all refurbishment scenarios can be approximated with a reciprocal relation to (Figure 3.13(a): black dashed line):

$$c_{q_l} = 0.083 \frac{€}{kWh} + \frac{422.5 \frac{1}{m}}{q_l} \tag{3.9}$$

with q_l as heat line density in kWh/(m a) an c_{q_l} as costs per kilowatt-hour end-energy heat in €/kWh. The higher the connection quota, the better is the economic viability of DHS. Equation 3.9 presents a suggestion for a simple estimation of the distribution costs of DHS for similar projects.

The purple dashed line of Figure 3.13(a) compares the results with an existing district heating distribution costs estimation published by Persson (Persson et al. 2011; Persson et al. 2019), that is given by:

$$c_{q_l} = \frac{C_1 + C_2 \cdot d_a}{q_l} \tag{3.10}$$

with

$$q_l = 0.0486 \cdot \ln q_l + 0.0007 \tag{3.11}$$

C_1 and C_2 are constants describing the construction costs of a district heating piping systems. In (Persson et al. 2019) a value of 212 €/m is applied for C_1 and a value of 4464 €/m² for C_2. The symbol d_a describes the average pipe diameter of a DHS that itself depends on the linear heat density of a given district. As described in (Persson et al. 2019) a minimum average pipe diameter of 0.02 m is applied for low heat densities. The annuity factor of the original formula of (Persson et al. 2011) is omitted in Equation 3.11. Equations 3.10 and 3.11 require the linear heat density in GJ/m. For the comparison, the results are transferred to kWh/m as shown in Figure 3.13(a). It can be seen that the estimation of Persson et al. and the results calculated with the developed optimization method of the *DHNx* tool with the parameter given in Section 3.3.2 match well above linear heat densities of 750 kWh/m. Below heat densities of 750 kWh/m, the detailed modeling of the district heating network pursued in this thesis leads to higher specific heat distribution costs (compare purple dashed line with black dash-dot line). Still, the detailed modeling approach of this work affirms the cost estimation of Persson for the investigated district of this thesis, and the plausibility of the results of this modeling approach is validated respectively.

The thermal loss power of the DHS depends on the temperature level (Figure 3.13(b)). In this case, it is not possible to provide a single equation for all scenarios. With regard to the connection quota, the same applies for thermal loss: a high connection quota (or a high heat demand density) reduces the specific thermal losses for the distribution pipeline system from about 16 % of the supplied heat in the lowest connection scenario to below 5 % in the highest connection scenario. Reducing the temperature level is crucial for lowering thermal losses. However, related to the connected floor area, the specific thermal loss related to the delivered

end-energy heat does not decrease in the given refurbishment scenarios (see Figure 3.13(b)). Or the other way around, despite the lowering of the temperature level, the specific thermal losses per end-energy heat increase at low connection quota or heat densities respectively. This can be shown by the lowest and highest connection quota represented by the lowest and highest heat density values in Figure 3.13(b): the scenario *Refurb-2* shows the highest specific thermal losses above 0.16 $\text{kWh}_{loss}/\text{kWh}_{heatdemand}$ in the lowest connection scenario.

Of course, it is not surprising that the absolute value of thermal loss decreases when the temperature level is lowered. However, relatively to the supplied heat, this might not be necessarily the case. The quantification of the impact of these parameters is necessary for the quantification of the overall benefits of the DHS as the costs of the piping system are only one part of the DHS. Therefore, these results will serve as input for the overall assessment within the trade-off of costs in emission in future energy scenarios that are discussed in Chapter 4.

3.5 Discussion

An integrated optimization approach for the design of district heating networks has been introduced and applied to different scenarios of a typical existing district. However, there are limits within the approach. The results have uncertainties and the tool does not aim to replace a detailed thermo-hydraulic simulation. Nonetheless, the introduced approach is an adequate proceeding in the planning process of hydraulic systems, and it is useful for comparing the effect of different concepts on the pipeline system. By means of the introduced tool, a fast estimation of the costs and thermal losses of district heating networks is possible. It is based on recommendations for dimensioning DHS especially in conceptual stages (Nussbaumer et al. 2016; Best et al. 2018). For this purpose, the design criterion of a maximum pressure drop for all DHS pipelines is applied. Depending on the general conditions the maximum pressure drop of the pipes should be within 100 to 300 Pa/m (Thalmann et al. 2018; Best et al. 2018). The routing and dimensioning results of this optimization method can then be used in the second step as input for a detailed thermo-hydraulic simulation. The results give a detailed estimation of investment costs and thermal losses of the DHS that build the base of an overall cost calculation for DHS.

In the optimization approach, the costs of the DHS pipelines are proportional to the heat transport capacity. Hence, the costs of large pipes are underestimated while the costs of small pipes are overestimated (see Figure 3.9). In most cases this will not affect the optimal routing as the costs per trench meter of district heating network are characterized by a high share of fixed costs. Nevertheless, to get a more exact result, various options for improvement are possible. For example, the linearization could be improved by a piecewise-linear or even discrete representation of the pipelines' cost function. This is already possible and implemented in the published *DHNx* package (oemof developer group 2022b). Alternatively, an iterative approach could be applied: After each iteration, the pipeline segments receive the weighed mean of the specific investment costs of their two neighboring DN numbers. Then, the optimization is executed again considering these new and more accurate cost parameters. However, both methods would be more time-consuming as the complexity of the MILP problem increases if piece-wise linear segments or an iterative approach are used.

Also, rounding up to the next higher DN number leads to an additional inaccuracy. For the subsequent planning process, a mandatory review of the raw optimization results of the transport capacity of the pipelines would reveal these errors. Alternatively, rounding to the next (either smaller) DN number could also be an appropriate proceeding, since the rounding-up causes a systematic additional safety factor, which might not be necessary.

3.6 Conclusion

A flexible open source optimization approach for district heating networks has been introduced that allows the consideration of additional components within the design and planning process that includes a novel method to consider simultaneity. The optimization framework fills the gap of a flexible open source tool for district heating network optimizations and is published within the open source Python library *DHNx* (oemof developer group 2022b; Jnnr et al. 2021). The package hereby sets the basis for further complex DHS optimization models with the option of adding further additional energy converter and storage units at the heat generation site and at the buildings. The presented open source tool is an essential contribution to the development of tools and methods for the design of future heat supply systems (research objective RO 1). The case study successfully showcases the optimization tool, which is capable of performing district heating network optimization for complex future energy system configuration, as also demonstrated in (Röder et al. 2021) by investigating the effect on the presence of distributed thermal energy storages on the investment costs of the piping system.

Within this thesis, the optimization approach has been applied in a scenario analysis for the development of district heating networks under different refurbishment and connection scenarios. The results quantify the required infrastructure costs and thermal losses of the district heating piping system, which are the basis for the subsequent design and analysis of the energy converter and storage units of the heat supply in Chapter 4 and for the comparison of heat supply via DHS versus individual heat supply for future transformation paths for the upstream energy system in Chapter 5. It is shown how the heat density that is modeled with different connection quota impacts the specific infrastructure costs. The results stress the importance of a high connection quota or high heat densities respectively, which is further investigated in this thesis.

4 Design of district heat supply[1]

The following chapter investigates the design of energy converter and storage units for a renewable and system-supportive design of the district heat supply site for addressing research objective RO 2 (see Section 1.3). Therefore, the costs and thermal losses of the district heating network that were calculated in the previous Chapter 3 for the local scenarios given in Section 3.3.1 are the basis for the subsequent development of district heating systems (DHS) following in this chapter.

As introduced in Section 1.2.2, the following measures and opportunities are promising prospects for the transformation of urban districts: Firstly, energetic refurbishment measures are urgently needed for the reduction of space heating demand. Secondly, sector-coupling and *Smart Energy Concepts* are important in the future energy system, which means that energy sectors like electricity, gas, heat and mobility cannot be considered solely but must be coordinated with each other to enable the integration of renewable energy sources (Gudmundsson et al. 2018; Robinius et al. 2017). And thirdly, hydrogen and synthetic methane gas from renewable energy sources are possibilities for a de-carbonization of the energy system and could also be options for the heating sector (Prognos et al. 2020b; Fraunhofer ISE 2020b). Currently there are several projects in Germany that investigate and implement hydrogen generation technologies in urban districts, for example the research project Es_West_P2G2P, ENaQ and QUARREE100 (VDI Technologiezentrum 2019). Finally, DHS are an important infrastructure option for the transformations of existing districts (H. Lund et al. 2010; Möller et al. 2019; D. Connolly et al. 2014).

So far, in Germany the heat sources of DHS are mainly based on fossil fuels dominated by gas-based combined heat and power (CHP) plants (AGFW 2021a). Thus, in the future, new heat supply concepts must be developed that address the current challenges of designing renewable, flexible and sector-coupled DHS. The heat supply concepts must be synchronized with the transformation scenarios of the overall energy system, and hence, anticipate future developments to derive future-proof heat supply concepts.

For this purpose, this chapter presents a scenario-based design approach for the heat supply of DHS for a typical existing district. The design method relies on open source libraries and applies a bi-objective linear optimization approach with costs and emissions as objectives to select and dimension the energy converter and storage technologies of the district heat supply. For creating the *oemof.solph* optimization models, the package *q100opt* was developed and applied (see Röder et al. 2022a). The mathematical modeling background is given in Section 2.3. The special focus of this work lies on the analysis of different scenarios for the upstream energy system up to the year 2050 with the aim of deriving robust and future-proof decisions for the local energy system in the context of the ongoing energy transition. The approach includes an adequate representation of the emissions of grid-sourced electricity by the use of time-resolved emission factors as introduced in Section 2.1 for deriving renewable and system-supportive district energy systems (see also Röder et al. 2020) and a consideration of hydrogen technology options within the district energy system. These two aspects, designing the local energy system

[1] This chapter is in parts published in (Röder et al. 2022b).

dependent on future development paths for the overall energy system and the feasibility of hydrogen based solutions are not sufficiently considered in recent studies concerning the design of DHS as a literature review shows (see Section 4.1). The prospective aspect of this analysis is particularly important, precisely because the design of DHS are linked to very long-term investment decisions in the energy infrastructure.

This chapter is divided into the following sections: The next section gives a short review on recent and – for the subject of this chapter – relevant contributions in literature. Subsequently, the structure and components of the urban energy system and the technology options are introduced and the parameters of the energy converter and storage optimization model are given. Then, the investigated scenario framework is explained, followed by the presentation of the results in Section 4.3 and the discussion of the approach in Section 4.4. Finally, the conclusions are summarized.

4.1 Literature review: Design of district heat supply

The following literature review gives an overview of recent articles about the design of urban heat supply systems for the future energy transition of existing districts. As there is a huge amount of projects and studies in the context of the development of district energy systems (see also Saletti et al. 2020), this chapter only presents a compact selection to showcase the different aspects that have been covered in developing future-proof district heating supply concepts so far. A comprehensive overview of modeling approaches of district heating and district energy systems can be found in Talebi et al. (2016) and Mancarella (2014).

Kersten et al. present a design approach for a district heat supply with respect to 4^{th}-Generation DHS (Kersten et al. 2021). The approach focuses on the implementation of funding and subsidy measures and compares a static versus a time-dependent design approach (Kersten et al. 2021). It considers a scenario framework which implies implies a constant emission factor for electricity of the current power system, however, no statement can be made about the future viability of the resulting energy concepts. Also, hydrogen as a technological option is not considered in this analysis (Kersten et al. 2021).

Dorotic et al. developed a multi-objective optimization approach for the supply technologies of a DHS with costs, emissions and exergy destruction as optimization objectives (Dorotić et al. 2019). The approach is demonstrated using the example of the DHS of the town Velika Gorica in Croatia. Two price scenarios for electricity costs were considered and a phase-out of natural gas technologies is concluded. The authors also acknowledge that the analysis of a single reference year could lead to lock-in effects as the energy system is designed for the next 20 to 30 years although the emission factor of the power sector is expected to decrease in the next years (Dorotić et al. 2019).

Schmeling et al. introduce a decision-supporting framework for distributed energy systems including stakeholder participation and different simulation and optimization tools as well as a risk assessment based on Monte Carlo Simulation (Schmeling et al. 2020). The approach is very comprehensive and addresses all stages of the decision making process for new building quarters (Schmeling et al. 2020). As the focus of this article is on the introduction of the methodical

approach for decision-making, a detailed presentation of the results and implications and recommendations for the design of future-proof energy concepts for districts is unfortunately not provided.

Focusing on the modeling of uncertainty in the case of limited information, Gabrielli et al. developed a framework for the robust design of energy systems (Gabrielli et al. 2019). The optimization is also concerned with minimizing costs and emissions. The uncertain parameters investigated in this analysis are weather data and the heat and electricity demands. The parameters of the upstream energy system, such as the commodity prices and the emission factors, were not investigated. (Gabrielli et al. 2019)

Aunedi et al. present an approach for designing DHS considering the interaction with the electricity infrastructures on national-level (Aunedi et al. 2020). The optimization is concerned with minimizing the overall costs taking constraints for the emissions and the local power network into account. The authors stress that an appropriate design of the district energy system leads to a significant whole-system value by providing flexibility to the electricity grid. Among other aspects, two scenarios for the electricity grid are assumed, representing a low and a high share of renewable energies. Although the article contains very relevant approaches, there is no further consideration of possible future upstream energy systems, since a possible transformation of the gas network as well as hydrogen technologies were not considered (Aunedi et al. 2020).

Altogether, there are many (case) studies regarding the design of district energy systems by applying different objectives and each of them has an individual focus. However, most of them assume that the upstream infrastructures of the power system and gas network are constant and set the focus on designing the district energy system for the *here-and-now* considering the current regulatory fees and subsidies and are based on the current market regulations. There is a lack of evaluating the district energy system relative to the upstream energy system. The development of future-proof concepts must take into account that the concepts fit into the overall energy system transformation scenarios in order to avoid *lock-in* effects and stranded investments. Thus, the current work contributes to the development of future-proof district energy concepts by performing a scenario-analysis including possible transformation paths of the overall energy system.

4.2 Model and parameters

4.2.1 Structure and parameters of district heat supply

The following sections introduce the structure and components of the district energy system and the techno-economic parameters of the energy converter and storage options. Background information on the investigated existing district are given in Section 2.2.

4.2.1.1 Structure of the district heat supply

Figure 4.1 gives an overview of the energy converter and storage units of the district heat supply investigated in this analysis. The considered plants and energy storages represent a generic

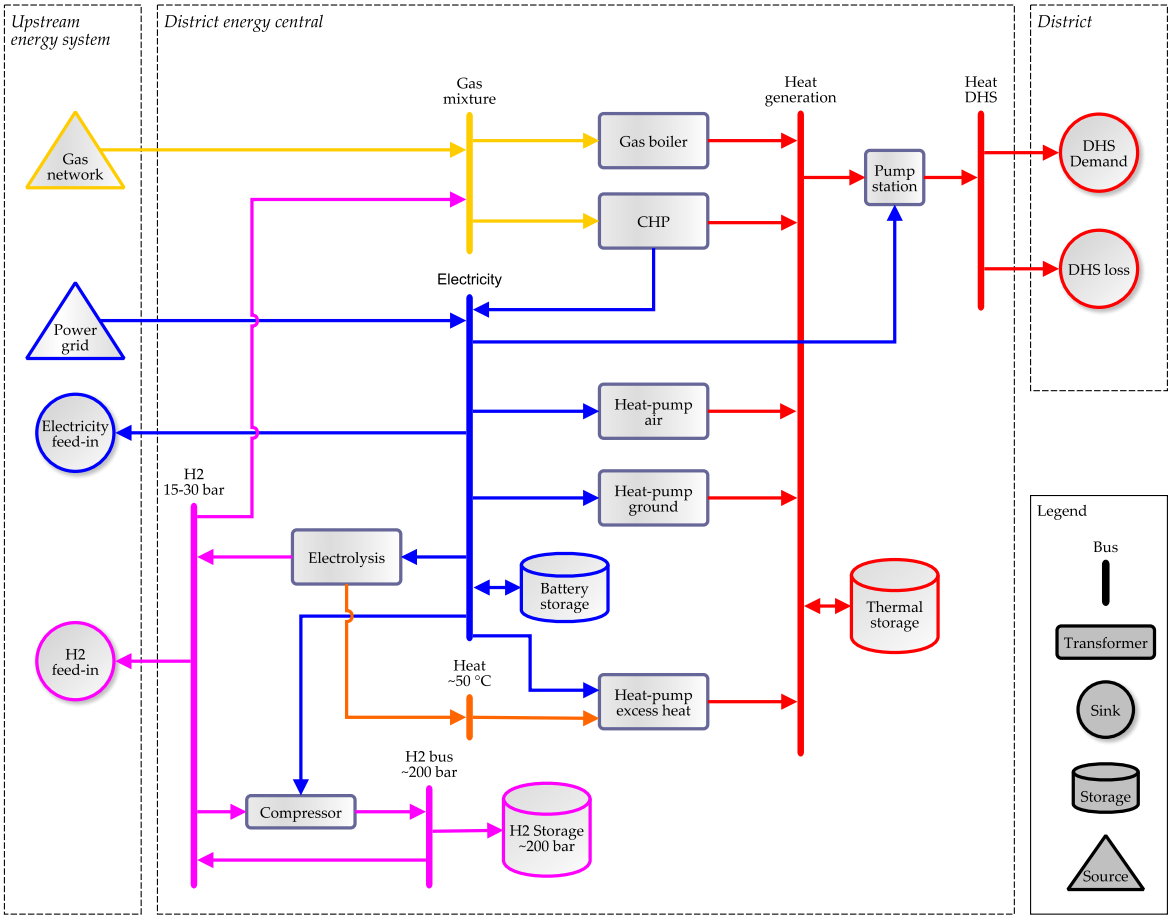

Figure 4.1: Energy converter and storage units of district heat supply. Blue: electricity flows; red: heat flows; orange: low-temperature heat; yellow: gas mixtures; pink: hydrogen flows.

district heat supply, that are based on the Rüsdorfer Kamp introduced in Section 2.2. Based on this structure an energy system model with the open source library *oemof.solph* (oemof developer group 2020a) has been developed. The mathematical background of the attributes and constraints applied in this study is explained in detail in Section 2.3.2.

The energy system is divided into three parts (Figure 4.1): on the left, the connection to the upstream energy infrastructures, in the middle, the energy converter- and storage units of the district heat supply and on the right the connection to the infrastructures and buildings of the districts. The different colors of the energy flows indicate the different energy carriers with blue for electricity, red for heat for the DHS, orange for excess heat at a lower temperature level, depending on the scenario, yellow for gas mixture and pink for hydrogen. The temperature level of heat feed-in the DHS depends on the local scenario that is considered (see Section 3.3.1).

The left part, that constitutes the connection to the upstream energy system, is implemented by energy sources and energy sinks. These components reflect the import and export of energy commodities, that include the purchase of electricity from the power grid, the purchase of gas from the upstream gas network, as well as the feed-in of electricity into the power grid and the

feed-in of hydrogen into the gas network. The parameters of these components are defined by the global scenarios and presented in Section 4.2.2.

The right part of Figure 4.1 connects the district heat supply to the district and represents the buildings of the district as well as the energy infrastructures. In this part, two heat sinks model the connection point of the district heating network to the district heat supply, one sink for the heat demand in the buildings connected to the DHS and the other considering the thermal losses of the DHS.

In the center of Figure 4.1, the energy converter and storage units of the district heat supply are shown. The heat generation technologies for the DHS are a gas boiler, a gas-based combined heat and power plant (CHP). Both can be operated with mixtures of methane and hydrogen, complemented by an air-source heat pump, a ground-source heat pump and the usage of the excess heat from the electrolysis. It is assumed that geothermal probes for ground-source heat pumps can be integrated in parks and green areas in many districts, however, the capacity is limited (see Section 4.2.1.2). In the current debate on the transformation of the energy system, hydrogen could be a relevant energy carrier of the future and is also a potential technology for the transformation of urban energy systems. Hydrogen production in the district energy system could lead to synergies by using the excess heat of the electrolysis. The storage of hydrogen may contribute to the flexibility of heat supply, even though hydrogen may be used as the least viable option for heat and electricity generation due to the efficiency losses at each step of the process chain from generation to application (see also Section 1.2.2.3). Therefore, in this analysis the future viability of combining hydrogen based-technologies and district heat supply is one of the research subjects of this analysis. In the energy system model, a polymer electrolyte membrane (PEM) electrolysis is one of the technology options. The hydrogen can either be fed directly into the gas network as the outlet pressure of the electrolysis is assumed to be sufficient, or fuel the CHP. Furthermore, the hydrogen can be stored in a pressure tank. In this case, an electrical compressor is needed to compress the hydrogen to the appropriate pressure level of the storage tank (see Figure 4.1). Further energy storage options are a hot water storage for heat and a lithium-ion-battery for electricity.

Solar thermal heat generation is not considered in this analysis as open spaces and park areas are a sacred good in many urban areas and also very limited. In addition, biomass fired boilers and CHP are not considered as heat supply options in this analysis, as wood-based heating is not a transferable solution to all urban areas due to limited regional resources. Wood-based biomass also competes with different other applications (Le Truong et al. 2015). Biomass needs to be used especially for high temperature application in industry to achieve a renewable energy system in all sectors (Prognos et al. 2020b). Furthermore, industrial and other waste heat sources are not considered here. In general, these heat sources should definitely be unlocked for urban heat supply in the future. However, these excess heat sources are not available everywhere as this is the case in this exemplary district. Such solutions cannot be generalized to any other district. Thus, the structure of the study remains more generic and the results are more easily transferable to other districts with and without excess heat potential. The renewable energy potentials at building level, such as PV and solar thermal collectors, are considered in Chapter 5, which compares individual heat generation in contrast to district heating.

4.2.1.2 Technical and economic parameters

The following tables present the technical- and economic parameters of the energy converter and storage units for setting up the heat supply site illustrated in Figure 4.1. The cost parameters from different databases and studies were reviewed and compared to project internal data based on price requests from manufacturers that were undertaken for the implementation of a DHS in the research project QUARREE100. Based on that, the assumptions listed in the following section were made. For the future energy scenario, no cost development paths for single technologies were defined. Keeping the technology costs constant makes the results more comprehensible for the investigation of the actual influence of the different scenarios on the design of the district energy system and independent of assumption-related price developments. This concept is also known as *ceteris paribus* proceeding.

Table 4.1 shows the technical parameters of the energy converter units. The efficiencies (coefficient of performance – COP) of the heat pumps are calculated in advance with the library *oemof.thermal* individually for each time step (see Section 2.3.3). The COP values depend on the forward temperature of the DHS as well as the ambient temperature in the case of the air-source heat pump. The test reference year of Heide published by the German weather service (Deutscher Wetter Dienst – DWD) is used as weather data set. A constant temperature of 10 °C is assumed for the ground-source heat pumps with geothermal probes. The assumed Carnot quality grade of 0.5 is based on project-internal technical data sheets of heat pumps with a thermal power in the order of 1 MW provided by manufacturers, that were requested within the research project QUARREE100.

The maximum values of the energy converter units correspond to the local conditions and size of the district and are set in such a way that the energy converter and storage units can be accommodated at the district heat supply. E.g. the capacity of the geothermal heat pump is limited by the number of geothermal probes that can be installed in green areas of the district. Furthermore, the economic parameters of Table 4.3 and Table 4.4 are only valid within a certain capacity range.

Table 4.2 lists the technical parameters of the energy storage units. The efficiency of the battery storage is modeled by using an inflow and an outflow efficiency. The resulting overall system efficiency of the battery is 90 %, which is in the range of system efficiencies of Lithium-Ion batteries (Bürger et al. 2017; C.A.R.M.E.N. e.V. 2021). The maximum inflow and outflow power of 55 % of the capacity corresponds to usual C-rates of Lithium-Ion batteries (C.A.R.M.E.N. e.V. 2021; Danish Energy Agency 2020a).

The thermal storage considered in this analysis is an insulated concrete storage tank filled with water that can be integrated in park areas outside the district heating plant. The maximum capacity is assumed to be 70 MWh, which relates to a volume of about 2000 m^3 at a temperature spread of 30 K. The storage is modeled via two loss terms: The first loss term refers to the thermal loss depending on the state of charge, that is the temperature of the water in fully charged condition in the case of a hot water storage tank. The second loss term represents the fixed thermal losses independent of the state of charge due to the temperature difference of the de-charged storage and the ambient.

Table 4.1: Technical parameter of the energy converter units. Own assumptions based on (Danish Energy Agency 2019; Röder et al. 2020; Kersten et al. 2021; Danish Energy Agency 2021b). The index n refers to the *Transformer* related to the energy converter unit.

	Thermal Efficiency	Electrical Efficiency	H_2 Efficiency	Maximum Full Load Hours (per year)	Maximum power	Maximum Investment Capacity
Symbol	$\eta_{(n,heat)}$	$\eta_{(n,elec)}$	$\eta_{(n,H2)}$	$f_{sum,max}$	$f_{t,max}$	$P_{invest,max}$
Unit	-	-	-	H	-	kW
Gas boiler	0.95	-	-	-	-	3000
CHP	0.55	0.38	-	-	-	2000
Heat pump air	*time-series (0.5 [1])	-	-	-	*time-series	2000
Heat pump ground	*time-series (0.5 [1])	-	-	2500	-	1000
Heat pump electrolysis	*time-series (0.5 [1])	-	-	-	-	1000
Electrolysis	0.18	-	0.62	-	-	1000
H_2 storage compressor	-	0.12 [2]	-	-	-	-
DHS pumps	-	0.015 [2]	-	-	-	-

[1] The value refers to the Carnot quality grade of the heat pump. The resulting efficiencies of the heat pumps depend on the refurbishment scenario and on the outside temperature in the case of air-source heat pumps.
[2] The value refers to the electrical energy consumption per kWh.

Table 4.2: Technical parameter of the energy storage units. Own assumptions partly based on (Röder et al. 2020; Danish Energy Agency 2020a).

	Loss rate per energy content	Loss rate per installed capacity	Inflow efficiency	Outflow efficiency	Relation of inflow capacity to installed capacity	Relation of outflow capacity to installed capacity	Maximum installable capacity
Symbol	β	γ	η_{in}	η_{out}	f_{cap-in}	$f_{cap-out}$	$W_{invest,max}$
Unit	-	-	-	-	kW_{in} / $kWh_{install}$	kW_{out} / $kWh_{install}$	kWh
Battery storage	0	0	0.95	0.95	0.55	0.55	10000
Thermal storage	0.0001	0.0002	0.999	0.999	0.2	0.2	70000
Hydrogen storage	0	0	0.995	0.995	-	-	60000

As hydrogen storage, a stationary compressed gas storage is considered. The inflow capacity depends on the capacity of the compressor that is modeled separately (see Table 4.1). The maximum capacity of the hydrogen storage is determined by the pressure level and the potential sizes of hydrogen storages. Here, a maximum capacity of 60 MWh is assumed, which corresponds to a volume of about 105 m³at a pressure level of 200 bar. At this pressure level, the storage tanks of Type I, that are fully metallic pressure vessels of seamless steel or aluminum, can be used as hydrogen storages (Moradi et al. 2019; Danish Energy Agency 2020a). The hydrogen storage itself can be realized via multiple modular pressure tanks (Danish Energy Agency 2020a).

The economic parameters of the energy converter and storage units are shown in the following Table 4.3 and Table 4.4. The annual investment costs are calculated from the annuity of the investment costs according to Equation 2.22 with the technical lifetime as reference period and a weighted average cost of capital of 2 % per year. The maintenance and operation costs are given as shares of the investment costs of the energy converter units and added to the annualized capital expenses.

In addition to the costs of the energy converters and storage units, the construction of the district heating plant itself needs to be taken into account. This includes the civil engineering costs for the heat supply facility including the chimney and exhaust system, the fuel supply, the electrical plant engineering and the overall planning services. Altogether, based on calculations in the context of the implementation of a DHS of this magnitude in the research project QUARREE100, the total expenditures for the district heating facility are estimated to 1.5 mill. Euro. These costs are valid for a small size district heating plant to supply a district of the

Table 4.3: Economic parameter of the energy converter units. Own assumptions based on (Danish Energy Agency 2021b; Danish Energy Agency 2020b; Fraunhofer ISE 2020c; Dunkelberg et al. 2020; Prognos et al. 2020b).

	Investment Costs	M/O Costs (of *capex*)	Technical Lifetime
Symbol	*capex*	f_m	N
Unit	€/kW$_{heat/electricity/H2}$	% / a	a
Gas boiler (€/kW$_{heat}$)	75	2.5	20
CHP (€/kW$_{electricity}$)	1000	3.5	15
Heat pump air-source (€/kW$_{heat}$)	715	2.5	18
Heat pump ground-source (€/kW$_{heat}$)	1450	3.0	30
Heat pump electrolysis (€/kW$_{heat}$)	450	2.5	25
Electrolysis (€/kW$_{H2}$)	2000	2.5	20
H2 storage compressor (€/kW$_{H2}$)	160	2.5	30

Table 4.4: Economic parameter of the energy storage units. Own assumptions based on (Danish Energy Agency 2020a).

	Investment Costs	M/O Costs (of *capex*)	Technical Lifetime
Symbol	*capex*	f_m	N
Unit	€/kWh	% / a	a
Battery storage	500	1.0	12.5
Thermal storage	14.3	1.0	40
Hydrogen storage	12	2.5	30

size of the generic district of this analysis. Therefore, the costs are absolute and do not depend on the dimension of the single energy converter and storage units, which is included in the optimization model. Furthermore, some of the energy converter and storage units can be located outside the district heating facility building, which means that the building's size itself is more or less independent of the sizing e.g. of the thermal storage.

4.2.2 Global scenario framework

In this section the global scenario framework for the in-depth analysis of a typical existing district is introduced. In the context of this study, the term *global scenario* refers to the upstream energy systems, that are the German national electricity and gas infrastructures. The global scenario framework describes the potential future of the overall energy system during the transformation of the energy system. With respect to the district energy system, the global scenarios define all energy commodities that are available for the district (local) energy system and make assumptions for the costs and emission factors of these commodities.

The scenario framework of this thesis consists of two major pathways for the overall energy system: the *syn-gas-low* path and the *syn-gas-high* path. The development of the global pathways for the district is based on recent well-recognized studies analyzing transformations pathways for the overall energy system in Germany (Prognos et al. 2020b; Fraunhofer ISE 2020b; dena 2018).

The *syn-gas-low* scenario is characterized by a high share of renewable electricity that covers most of the energy services. Synthetic gas like renewable hydrogen or renewable methane is not available in large quantities at reasonable prices. In contrast, the *syn-gas-high* scenario shows a high availability of synthetic gas that is supplied via imports from countries of the Middle East and North Africa as well as by national hydrogen and methane production capacities mainly driven by renewable energy sources like wind and solar power plants.

It must be noted that this work does not make any statements about the probability of occurrence of specific scenarios paths. The scenarios of this thesis need to interpreted as possible futures of the upstream energy system to investigate the impact of these scenarios on the design of the district energy system. The aim of this study is not to evaluate whether a high share of renewable synthetic gases is good or bad, or whether synthetic gases should be used for power and heat generation at all, as the valuable synthetic gases might rather be used in energy applications where no other energy carrier is possible (see Section 1.2.2.3). Instead, the goal of this study is to evaluate the best design decisions at district level for a cost-efficient emission reduction depending on potential developments of the upstream infrastructures.

Figure 4.2 gives an overview of the global scenario framework of this analysis. The figure illustrates the potential developments for both upstream energy infrastructures the district is connected to, i.e. the electricity grid and the gas grid.

Altogether, five scenarios are analyzed that represent the upcoming developments from today to 2050. Here, the years 2030 and 2050 should not be understood strictly as future years, but rather interpreted as short and long term timelines of scenarios for the upstream power system with a lower or higher share of renewable energies. This means that depending on the expansion rate of renewable energies, as it is currently politically discussed, the scenarios

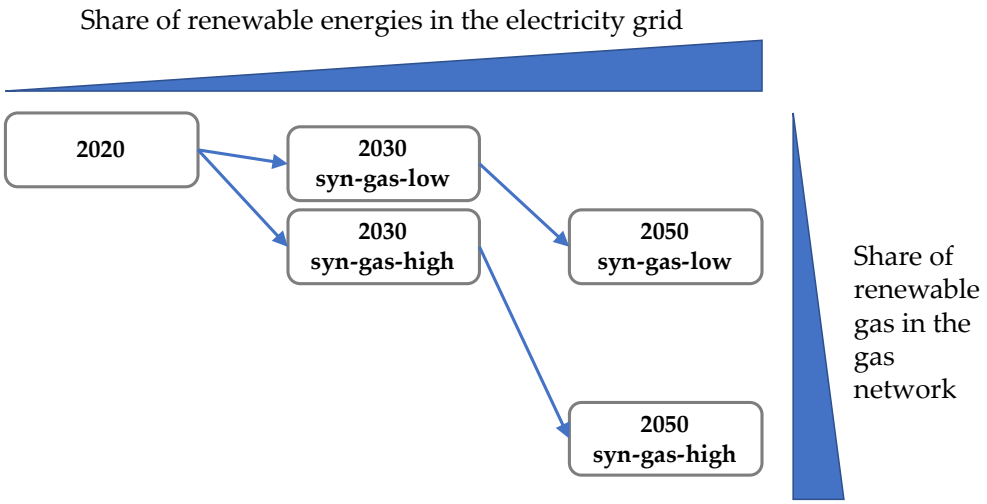

Figure 4.2: Overview of scenario framework of the upstream energy system. For the availability of renewable gas two paths are investigated, one with a low share (*syn-gas-low*) and one with a high share (*syn-gas-high*) of renewable gas.

labeled with 2050 could also be interpreted as scenarios for the year 2040. In all scenarios the share of renewable energy in the national electricity generation increases from the current status (scenario *2020*) to a mainly renewable electricity system in 2050. For the years 2030 and 2050 the *syn-gas-low* path is implemented in such way that the share of renewable gas in the gas grid stays at a low level. In this scenario, a low availability of renewable gas is assumed, and the share of renewable gas is supposed to be 5 % in 2030 and 20 % in 2050. The *syn-gas-high* path reflects a higher share of synthetic renewable gas. Here, the share of renewable gas of average gas mix is 20 % in 2030 and 80 % in 2050 (based on Müller-Syring et al. 2018). From today's perspective the scenario *2050-syn-gas-high* represents the most extreme scenario. For this scenario to occur, it is necessary that large quantities of renewable gas are available and that the existing gas infrastructure as well as the end devices are capable of handling a gas mix with a potentially significantly higher share of hydrogen, unless the majority of the gas mixture consists of methane. However, if the proportion of hydrogen exceeds about 10 percent by volume, the existing infrastructure and especially all end-user devices must be upgraded (Bundesnetzagentur 2020b). With these scenarios it is aimed to represent the expected lower and upper boundaries of the potential developments. Thereby, a broad scenario range is covered for studying the impact of different developments on the optimal – with respect to costs and emissions – design of the heat supply site of a prospective DHS of this chapter and the comparison with individual heat supply strategies in Chapter 5. Both energy carriers, electricity and gas, are characterized by an emission factor and costs, that are given in the following sections.

4.2.2.1 Emission factors

The emission factor indicates the greenhouse gas potential in CO_2-equivalents attributed to one kilowatt-hour of energy imported into the district energy system. For electricity, the emission factor depends on time, since the electricity generation from renewable energy sources like wind

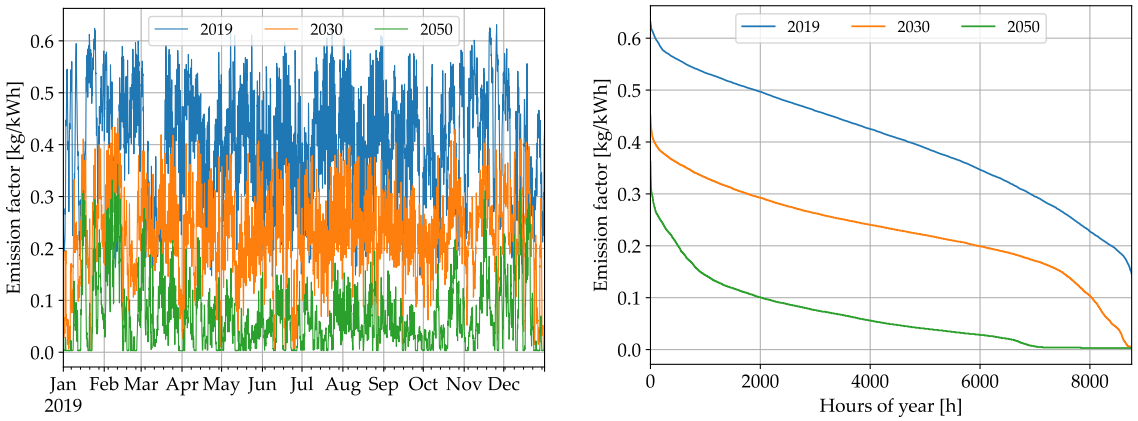

(a) Emission factor time-series

(b) Ordered annual duration curve

Figure 4.3: Emission factor time-series of the different scenarios for the electricity system. (a) time-resolved curve. (b) Ordered annual duration curve. Data source: (Agora Energiewende 2020; Böing et al. 2019).

and solar power is fluctuating. Through the application of time-resolved emission factors, a more accurate assessment of emissions caused by electricity imports and exports is achieved. In contrast to the current assessment methods given by law for DHS in Germany, that are based on a static assessment method by using a constant primary energy factor (AGFW 2021b), here, an incentive is set to source electricity at the "right" time from the grid when there is a high share of renewable energies. This method aims to achieve a system-supportive design and operation of the district energy system if emissions are minimized (see also Röder et al. 2020). The time-resolved representation of the emission factor is particularly important to assess the benefits of energy storage for a cost-efficient transformation into a carbon-neutral energy system. In this analysis, the time-resolved average national emission factor is used as an assessment criterion for the emission of the imported and exported electricity (see Section 2.1). Figure 4.3(a) shows the underlying emission time-series of this analysis. On the left, the time-resolved profile of the emission factors is illustrated, and on the right, the ordered annual curve of each scenario is shown.

The scenario for the status-quo of the electricity system is based on historical data on the power generation in Germany of the year 2019 provided by (Agora Energiewende 2020), since the data from 2020 does not reflect the current state of the energy system due to the effects that were induced by the Corona-crisis. Nevertheless, the status-quo scenario is called *2020* in this work. This emission scenario is characterized by an emission factor of 401 g_{CO_2}/kWh_{el} on average with a maximum of 631 g_{CO_2}/kWh_{el} and a minimum of 146 g_{CO_2}/kWh_{el}. Periods with a high emission factor are characterized by a low feed-in of renewable energies, and periods with a low emission factor result from a high share of renewable energies. The future energy scenarios are based on the results of a model of the German energy system in the years 2030 and 2050 with a medium and a high share of renewable energies by (Böing et al. 2019). The emission factor in 2030 reduces to an average value of 230 g_{CO_2}/kWh_{el} and to 67 g_{CO_2}/kWh_{el} in 2050. In scenario *2050*, there are only 2000 hours with a value above 100 g_{CO_2}/kWh_{el} and about 1000 hours with an emission factor of zero (Figure 4.3(b)). Altogether, the scenarios of

Table 4.5: Emission factors of the gas mix of the upstream gas infrastructure. Own assumptions. Emission factor of natural gas based on (Juhrich 2016).

Share of renewable gas in the gas network	Emission factor of natural gas in [g_{CO_2}/kWh]	Emission factor of renewable gas in [g_{CO_2}/kWh]	Emission factor of gas mix in [g_{CO_2}/kWh]
0 %	202	0	202
5 %	202	0	192
20 %	202	0	162
80 %	202	0	40

Böing and Regett (Böing et al. 2019) are more conservative than the scenarios of Fraunhofer ISE presented in (Fraunhofer ISE 2020b) and from Agora Energiewende (Prognos et al. 2020b). Depending on the detailed scenario, in (Fraunhofer ISE 2020b) the average emission factor results in 147 to 200 g_{CO_2}/kWh$_{el}$ for the year 2030 and in 3 to 9 g_{CO_2}/kWh$_{el}$ for the scenarios of 2050 (Fraunhofer ISE 2020b, p.25). The renewable share of the electricity generation in the scenario presented by Böing and Regett is related to the electricity generation within Germany (without imports and exports) 59.7 % in 2030 and 80.6 % in 2050 (Böing et al. 2019, based on p.11, Figure 4). In comparison, the renewable share of electricity generation of the Agora study ranges depending on the scenario from 68.5 % to 70.8 % in 2030 and from 90.4 to 90.8 % in 2050 (Prognos et al. 2020b, p.54 (Abbildung 22) and p.138 (Abbildung 79)). However, as the detailed results of Fraunhofer ISE and Prognos et al. are not published, the results of the emission factor time-series of Böing and Regett are used in this study for representing an upstream electricity system with a medium and a high share of renewable energies.

For exporting electricity of the district energy system, e.g. by a combined heat and power unit (CHP), or by discharging an electric storage, the negative value of the average emission factor is credited to the district energy system. This sets an incentive to feed electricity into the grid at times of high emission factors and thus low availability of renewable power generation.

The derivation of the assumptions for the emission factor of gas from the gas grid is shown in Table 4.5.

In this study, it is assumed that the emission factor of the current composition of the fossil gas in the gas network is 202 g/kWh (Juhrich 2016) and 0 g/kWh for renewable gas constant for all scenarios. The optimistic assumption of attributing zero emissions to synthetic gas means that the synthetic gas is generated exclusively via renewable energy sources and also the transport is based on renewable energies. The emission factor of the average gas mix in each scenario results from the share of renewable gas and fossil gas within the gas grid. As the gas network itself has the capability of storing gas and as there are further possibilities of storing gas deployed in the German gas infrastructure, e.g. in caverns (Amanpour et al. 2018), it is assumed that the emission factor does not depend on time and so it is assumed to be constant for each scenario. Analogous to the export of electricity, the feed-in of hydrogen into the gas network is rewarded by emission credits for the district energy system in the same amount as sourcing gas, and thereby, the emission credit depends on the scenario.

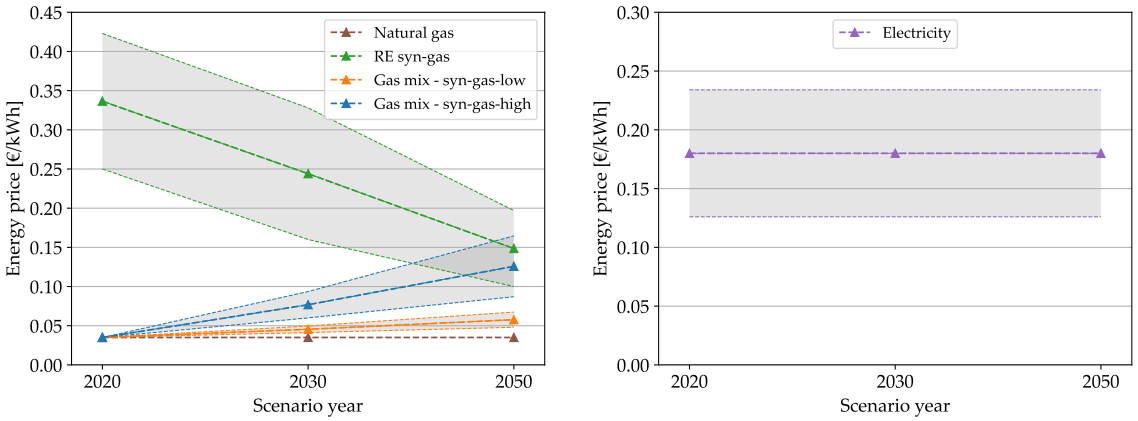

(a) Gas (b) Electricity

Figure 4.4: Commodity price assumptions for the district heating facility. (a) Natural and synthetic gas prices and resulting prices of gas mix from the gas network of the two scenarios *syn-gas-low* and *syn-gas-high*. RE syn-gas: synthetic gas from renewable energy sources. (b) Price range of electricity for district heat supply. Own assumptions based on (Fraunhofer ISE 2020d; Kersten et al. 2021; Hank et al. 2020; Prognos et al. 2020b; Fraunhofer ISE 2020b).

4.2.2.2 Commodity prices

The future prices of the energy commodity sources are difficult to estimate and influenced by many factors, like politics, market developments and many more. In addition, the prices vary depending on the market design, purchase strategy, the total amount available renewable energies and the amount of energy consumed. A forecast of future commodity prices is cumbersome and falls outside the scope of this study. The scenario analysis uses cost assumptions that cover a wide range of potential price developments without considering the unneeded complexity of special incentives and pricing systems. Therefore, the influence of the commodity costs on the results is investigated by assuming a price range with a minimum and a maximum value for the commodity prices starting from the current status quo and considering future developments based on existing literature. In this analysis, the gas and electricity the price refers to the price per energy. A capacity price is not considered in this analysis. This method of energy pricing makes it easier to understand the connections and dependencies of the results of this scenario analysis according to the *ceteris paribus* principle.

Figure 4.4 illustrates the assumption of the commodity prices for a district heating facility applied in this analysis. The prices of electricity are based on the current prices for district heating facilities. All prices are net prices without value-added tax, but take into account all in 2020 applicable provisions on taxes and apportionments of gas and electricity, that are grid charges, concession fees, gas or electricity tax respectively and other apportionments according to the regulatory framework in 2020.

Figure 4.4(a) illustrates the assumption of the costs of gas from the gas network for each scenario year. The natural gas (brown line) is assumed to be constant throughout all scenarios based on the gas price in 2020 for an industrial customer (Kersten et al. 2021; Bundesnetzagentur 2021).

For the renewable synthetic gas, the cost projections of (Fraunhofer ISE 2020d; Hank et al. 2020; Prognos et al. 2020a) are used as basis for defining a low and high cost path (compare Figure 4.4(a) green corridor, RE syn-gas). Based on these cost assumptions, the costs for one kilowatt-hour gas-mix from the gas network are calculated for the individual scenarios for each share of renewable gas shown in Table 4.5. This leads to two different cost developments for each of the two scenarios *syn-gas-low* and *syn-gas-high*: The highest gas prices result at the scenario *syn-gas-high* (see Figure 4.4(a) blue corridor), that is characterized by a high share of renewable gas of 80 % in 2050, that drives the overall gas price. The lowest gas prices occur at the scenario *syn-gas-low*. In this scenario the share of renewable gas is low, that implies lower costs of the gas mix due to the low natural gas price.

In the current market, it is possible to order specific types of gas, e.g. *Biogas*, or renewable synthetic gas in the future. In this study this is not considered and only fixed gas mixtures with a fixed emission factor according to Table 4.5 are used as a commodity source for the district energy system. This is because the share of renewable gas within the gas network should reflect the availability of renewable gas. By considering fixed gas mixtures, the transferability of the concepts to other districts is granted.

Figure 4.4(b) shows the electricity prices of the different scenario years. As stated above, the cost development is very uncertain, also because of more than 70 % of the electricity price in Germany in 2020 is set by taxes and apportionments (Bundesnetzagentur 2021). Thus, two price scenarios are defined for the electricity costs, a high price scenario (upper line of purple corridor) and a low price scenario (lower line) with the same value for all scenario years.

Exporting energy into the upstream energy system is honored by revenues. The income for exporting electricity into the electricity grid is based on the average day-ahead price of the electricity stock exchange for the scenario year 2020. A value of 0.038 €/kWh is assumed for all scenarios. For the feed-in of hydrogen into the gas network, a price of 50 % of the gas price of the respective gas scenario is applied, as the price components that are influenced by the supplier are historically about 50 % for gas (Bundesnetzagentur 2021). Other sales and distribution options for hydrogen that might possibly achieve higher sales revenues are not regarded in this analysis. On the one hand, the scale of the districts and the quantity of hydrogen produced might not be relevant for industrial hydrogen supply. On the other hand, the focus of this study is the heat and electricity supply of existing districts in context of the upstream energy infrastructures of gas and electricity.

4.3 Results

The optimization of the district heat supply is performed for all combinations of global scenarios of the upstream energy infrastructures (see Section 4.2.2) and local scenarios of the existing building stock, that consider different levels of energetic refurbishment and different shares of buildings connected to the DHS (see Section 3.3.1). Figure 4.5 summarizes the investigated scenarios.

The results of this chapter are structured as follows: A detailed analysis of the impact of the global scenarios on the design of the district energy system is given, which is performed

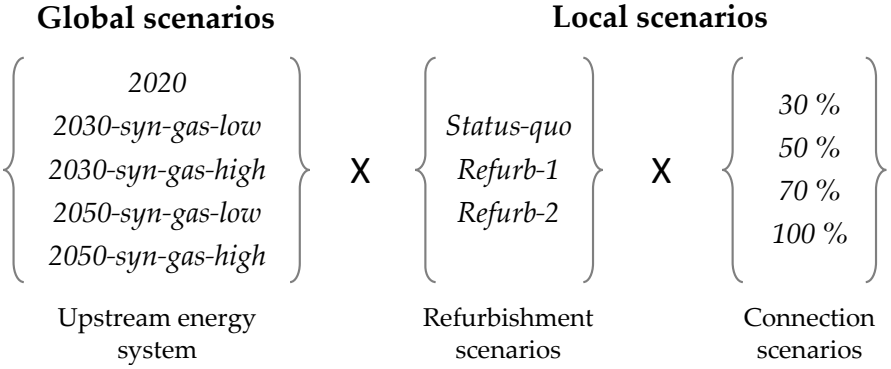

Figure 4.5: Overview of the investigated scenario framework.

based on the moderate refurbishment scenario *Refurb-1*. This includes the presentation of the results of the objectives of costs and emissions, which are shown by the Pareto-fronts, and the detailed investment decisions that are cost-optimal for the reduction of the emissions in each scenario (Section 4.3.1). The following section shows the energy balances and energy flows in the form of Sankey diagrams for each carbon-neutral system configuration and illustrates the unit commitment based on exemplary weeks (Section 4.3.2). Then it is evaluated to what extent the optimization approach also leads to a system-supportive design and electricity exchange with the upstream power grid (Section 4.3.3). The results of the refurbishment scenarios *Status-quo* and *Refurb-2* are discussed and analyzed in Section 4.3.4. The results of this chapter are based on the 100 % connection scenario. The results of the local scenarios with lower connection quota are used in Chapter 5 for the comparison of district heating with individual heat generation at building level. Additionally, the prices of gas and electricity were varied for each global scenario based on the price ranges given in Figure 4.4.

4.3.1 Objectives and investment decisions

Figure 4.6 shows the results of the Pareto-optimization with cost and emission as objectives for the five scenarios about different developments of the share of renewable energies in the upstream infrastructures power grid and gas network (see Figure 4.2). Each point on the Pareto-front corresponds to an optimization for one year with 8760 time steps. By applying different emission limits, the trade-off between costs and emissions is calculated until the emission-optimal configuration is achieved. The results are related to the average costs and average emission per floor area (m^2) and year (a). Relating the results to the supplied floor area allows the comparison of the different refurbishment scenarios, as the total heat demand differs in these scenarios. For each of the scenarios, the medium price development path is shown. The error bars indicate the optimization result by applying the different price ranges for the energy commodities that are introduced in Section 4.2.2.2. The annotations indicate the relative emission reduction compared to the cost-optimal solution of each scenario. That means that the point “1.00” shows the cost-optimal result of each scenario, and the point “0.00” refers to the emission-optimal result. The optimization results with an emission balance of zero

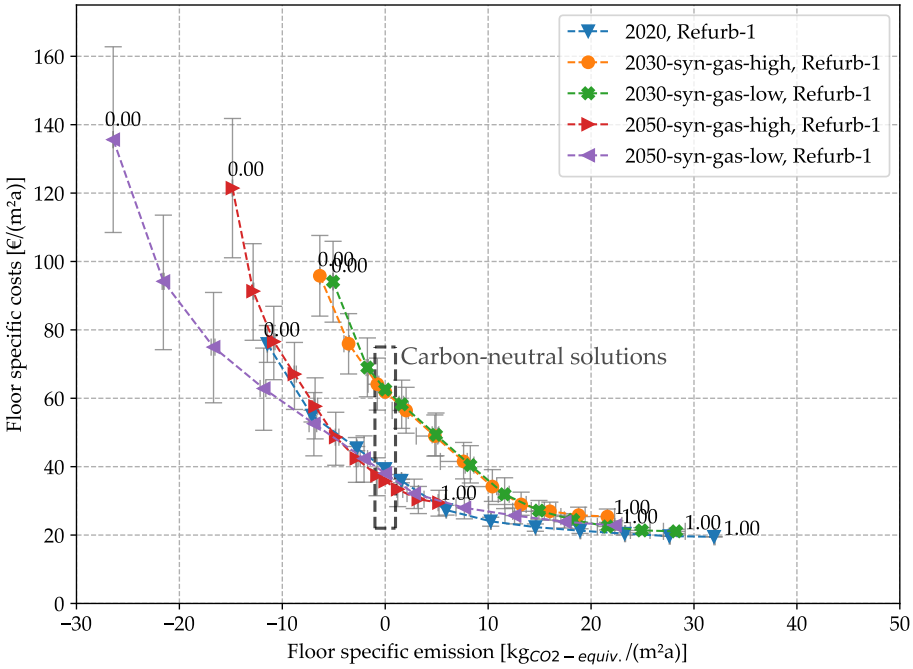

Figure 4.6: Results of the Pareto-optimization of refurbishment scenario *Refurb-1*. Error bars indicate the variation of the commodity prices.

are referred to as carbon-neutral solutions, where the x-axis value of the floor-specific emission equals zero.

In Figure 4.6 starting from the right – the cost-optimal solutions – to the left (emission-optimal solutions), the emissions can be reduced by a moderate increase of costs in all scenarios. The cost-optimal solutions ("1.00") of the scenarios differ in such a way that the scenario *2020* reaches the lowest costs but at the highest emission value. The future scenarios attain slightly lower emission values in the cost-optimal case as the share of renewable energies in the upstream infrastructures increase, however the costs also rise up to 29 €/(m²a) in the scenario *2050-syn-gas-high*. In this scenario, the share of renewable gas in the gas network is assumed to be 80 % which also implies higher cost compared to the fossil-based gas network e.g. in 2020 (see also Section 4.2.2.2).

In all scenarios of Figure 4.6, a greenhouse gas-neutral energy system can be achieved, so that the net specific emission values amount to zero. These solutions are also called carbon-neutral solutions in the following (see Figure 4.6). In these cases, in scenario *2050-syn-gas-high* the specific costs amount lowest with a value of 36 €/(m²a), closely followed by scenarios *2050-syn-gas-low* and *2020*. In the scenarios of the year 2030 carbon neutrality can only be achieved at almost double costs.

Negative total emission values can be achieved by emission credits from energy exports. However, this mechanism is limited, as the emission factor of gas and electricity decreases in the global scenarios of 2030 and 2050 due to the higher share of renewable energies in the upstream energy infrastructures. Furthermore, the energy converter and storage capacities are limited by the plant sizes that can be realized within the heat supply site of the district (see Section 4.2.1.1).

These system configurations would probably be out of question for implementation due to such high costs. However, these results show which technologies lead to a further emission reduction. The points of the emission-optimal system configuration show the theoretical extreme values. According to that, in the scenario *2050-syn-gas-low* the lowest emission value can be achieved followed by the scenario *2050-syn-gas-high*. Also, the deviation in costs of the emission-optimal results for the different price scenarios indicated in Figure 4.6 by the error bar, shows the widest range in the emission-optimal scenarios as the amount of energy flows of imports and exports increases significantly in these scenarios, which will be shown in Figure 4.8 to Figure 4.14 below.

Altogether, in the scenario of 2020, the emission of the district heat supply can be decreased at almost equal costs as in the scenarios of 2050, although the share of renewable energies in the upstream electricity and gas infrastructure in 2020 is much lower than in 2050. In 2020, the emission factor of the upstream power system is still very high. Thus, a combined heat and power generation based on natural gas and the export of the generated electricity can improve the emission balance of the district energy system (see also Figure 4.8). In the scenarios of 2030, this strategy is not possible anymore as the emission factor of the electricity system is lower and the emission credits for electricity export decrease.

Figure 4.7 illustrates the investment decision of the energy converter and storage units for all scenarios in detail. It is shown how the capacities of the energy storage and converters develop depending on the emission value with the specific emission value on the x-axis similar to Figure 4.6. That means that the results of the emission-optimal case are on the left and the results of the cost-optimal case are on the right side of each plot. For each energy converter and storage technology, the shift of the capacity from a cost-optimal to an emission-optimal configuration is shown (from right to left).

The capacity of the gas boiler drops to zero in all scenarios if the emissions are decreased. This shows that burning gas is not a cost-efficient way for an emission reduction of the district heat supply. In contrast, the CHP becomes important when lower emissions are realized in all scenarios – except scenario *2050-syn-gas-low*. Here, the capacity of the CHP drops to zero when emissions are lowered, and in emission-optimality, the maximum CHP capacity is installed. At the carbon-neutral point, the CHP capacity is extended to the full capacity in 2020, which is related to the need of the CHP for improving the emission balance by exporting electricity. In the scenarios *syn-gas-high* of 2030 and 2050, a capacity of 300 to 700 kW is installed to achieve a carbon neutral district energy system. In the *syn-gas-low* scenarios, the CHP is not installed to obtain carbon-neutrality. As the gas has a high emission factor in these scenarios, electricity-based heat supply options with electricity from the upstream power grid are preferred.

The air-source heat pump is part of the cost-optimal system in all scenarios. When emissions are reduced, the capacity of the air-source heat pump is increased up to the maximum possible capacity in all scenarios. The ground-source heat pump, on the other hand, is not present in the cost-optimal energy system in any of the scenarios except in scenario *2050-syn-gas-high*. In scenario *2020*, the ground-source heat pump is only installed in the emission-optimal system.

The implementation of hydrogen electrolysis is in all scenarios the least probable choice of energy converter for the reducing the emissions of the local energy system. In all scenarios

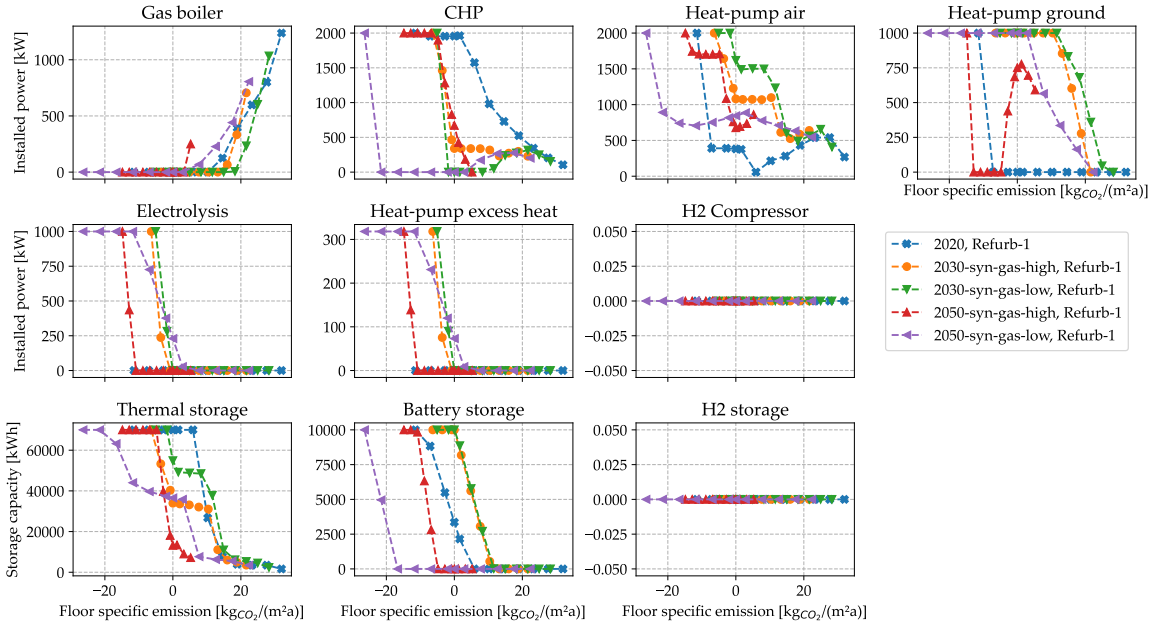

Figure 4.7: Investment decisions of energy converter and storage units of refurbishment scenario *Refurb-1* depending on the specific emissions.

except *2050-syn-gas-low*, electrolysis is only installed in the emission-optimal case and not cost-efficient to obtain carbon-neutrality. In scenario *2020*, the electrolysis does not help to reduce emissions at all. If the electrolysis is installed, the heat pump for the utilization of the excess heat of the electrolysis is used as well.

The thermal energy storage is the most cost-efficient storage option for emission-reduction. A small thermal storage is already included in the cost-optimal energy system. To reduce emissions, first the thermal storage is expanded for all scenarios. The battery storage is not used in the cost-optimal system in all scenarios and extended to the maximum capacity in all scenarios. The role of the battery storage for a cost-efficient emission reduction depends on the scenario: In scenario *2050-syn-gas-low*, the battery storage is only installed at emission-optimality, and in both scenarios of 2030, storing electricity has a higher priority. There is no investment in the hydrogen storage for any of the scenarios.

4.3.2 Energy balances and unit commitment

In the following section, the energy balances of the carbon-neutral system configurations in the form of Sankey-Diagrams and the resulting unit commitment of the energy converter and storage units, based on an exemplary time period, are presented for each of the global scenarios. In the carbon-neutral solutions the emission balances, which result from importing energy from the gas and electricity grid (positive emission values) and emission credits for exporting energy into the upstream infrastructures (negative emission values), amount to zero. For the analysis of the commitment of the energy converter and storage units, the Appendix in Section B.1 provides supplementary material in addition to the main results presented in the following section.

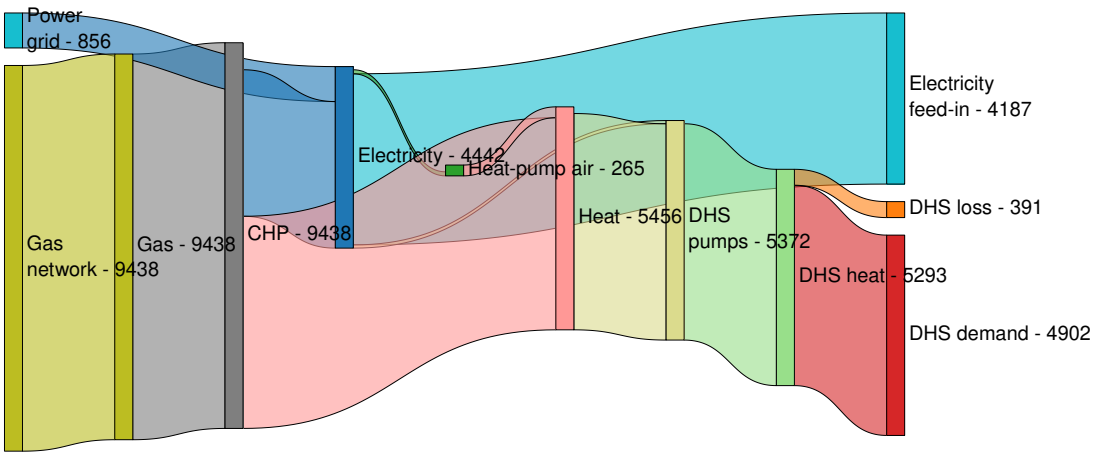

Figure 4.8: Sankey diagram of the carbon neutral result of scenario *2020* for the refurbishment scenario *Refurb-1*. All numbers refer to the energy flow per year in MWh/a; the storages are not shown for the sake of clearness.

4.3.2.1 Scenario 2020

Figure 4.8 shows the Sankey-Diagram of the carbon-neutral solution of scenario *2020*. The bars of the Sankey-Diagrams indicate the nodes of the energy system, that refer to a Bus or a Transformer of the *oemof.solph* energy system (see Figure 4.1). Each energy flow in the Sankey-Diagrams is the annual sum of the energy flow between two nodes in MWh/a. Energy flows that result in zero are not shown. The colors used serve to distinguish the different energy flows at the different nodes of the energy system model and do not refer to specific energy carriers. Also, energy losses are not illustrated except the thermal losses of the district heating piping network. In addition, energy storages and the in- and outflow of energy are not illustrated either.

In the energy system of 2020 and based on the emission assessment introduced above, the most cost-efficient way to reach a carbon-neutral district energy system is by mainly importing gas and deploying a CHP (see Figure 4.8) in combination with a thermal storage (see also Figure 4.7 and Figure 4.9). The main part (95 %) of the heat for the DHS is generated by the CHP. The remaining part is produced by an air-source heat pump. The emissions of the gas are compensated with electricity exports. Additionally, a battery storage helps to shift the electricity from times with a high emission factor in the power grid to times of a low emission intensity, which is illustrated within the supplementary material in the Appendix in Figure B.2.

Figure 4.9 shows the time resolved unit commitment for three weeks in February for illustrating the operation strategy of heat generation to achieve a carbon-neutral heat supply in the upstream scenario *2020*.

The upper diagram of Figure 4.9 shows the emission factor of the electricity grid and the outside temperature. The lower diagram illustrates the operation of the heat generation and the charging and discharging of the thermal storage. The CHP is operated at times of a

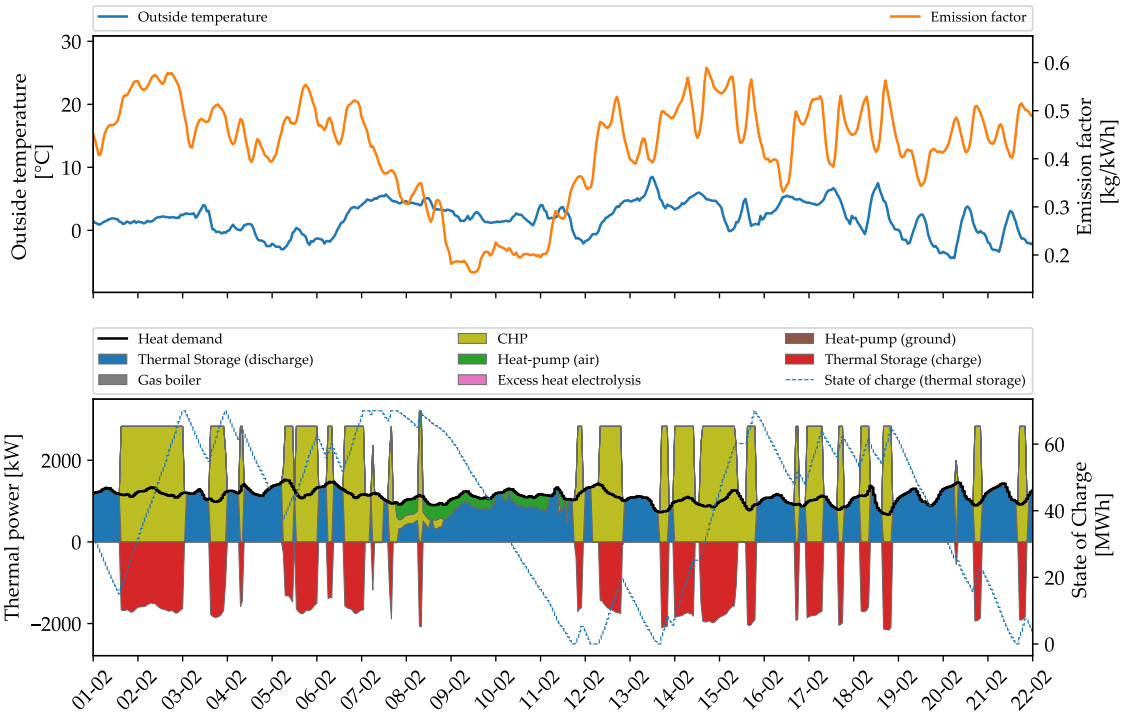

Figure 4.9: Time resolved heat generation of the carbon-neutral solution of scenario *2020* exemplary for three weeks in February. Upper diagram: emission factor of the electricity grid and outside temperature; lower diagram: commitment of heat generation and storage units.

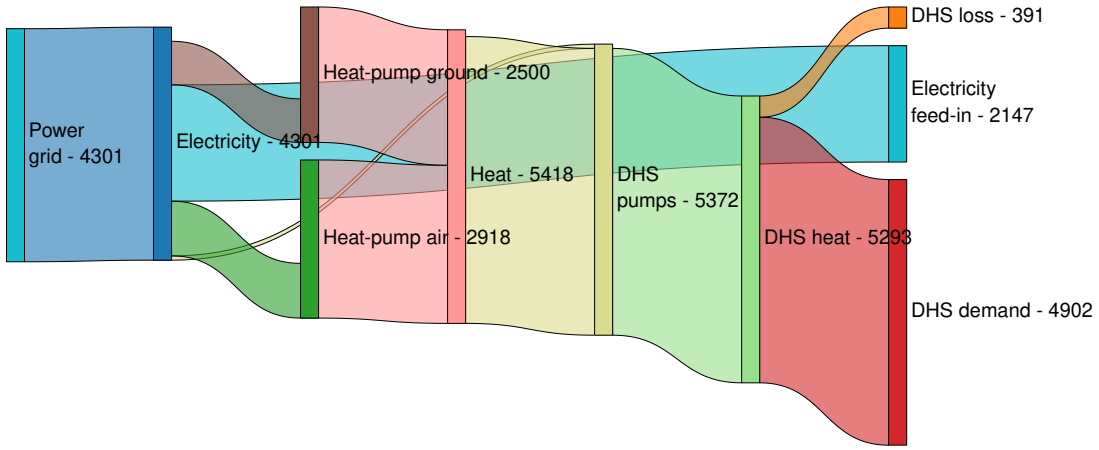

Figure 4.10: Sankey diagram of the carbon neutral result of scenario *2030-syn-gas-low* for the refurbishment scenario *Refurb-1*. All numbers refer to the energy flow per year in MWh/a; the storages are not shown for the sake of clearness.

high emission factor with maximum power, and the generated electricity is exported into the electricity grid. The thermal energy output of the CHP exceeds the heat demand and is used for charging the thermal storage (dashed line). At times of a low emission factor the heat demand is covered by the thermal storage and the air-source heat pump (see Figure 4.9 e.g. from 08-02 to 12-02). The CHP is operated mainly at times of a high emission factor. Figure B.2 and B.3 of the appendix further illustrate this relationship by an analysis of the time-resolved unit commitment dependent on the emission factor of the upstream power grid for the whole optimization period of one year. Thus, the operation strategy follows a – with respect to the emission factor of the electricity grid – system-supportive behavior. The operation of the CHP supports the electricity grid at times of a low emission factor, which corresponds to a low availability of renewable electricity generation in the upstream power grid. A further analysis of the electricity exchange with the upstream power system and an evaluation of the system-supportiveness is provided in Section 4.3.3.

4.3.2.2 Scenarios of 2030

The Sankey-Diagrams of the carbon-neutral solutions of the scenarios of 2030 are given in Figure 4.10 (*2030-syn-gas-low*) and Figure 4.11 (*2030-syn-gas-high*).

In scenario *2030-syn-gas-low* (Figure 4.10), a CHP is not part of the energy converter assets. The strategy of operation the CHP at times of a high emission factor in the upstream power grid and exporting the electricity is not option anymore to improve the emission balance of the district heat supply site, as the emission factor of the power grid is on a lower level in the scenarios of 2030 and the gas mix is still mainly fossil. Instead, the total heat is generated via an air-source and ground-source heat pump. Through this combination, the advantages of both heat pump technologies come into play: the geothermal heat pump is characterized by a higher COP in winter at low outside temperatures compared to the air-source heat pump. The air-source heat pump is cheaper and achieves a better COP at high outside temperatures.

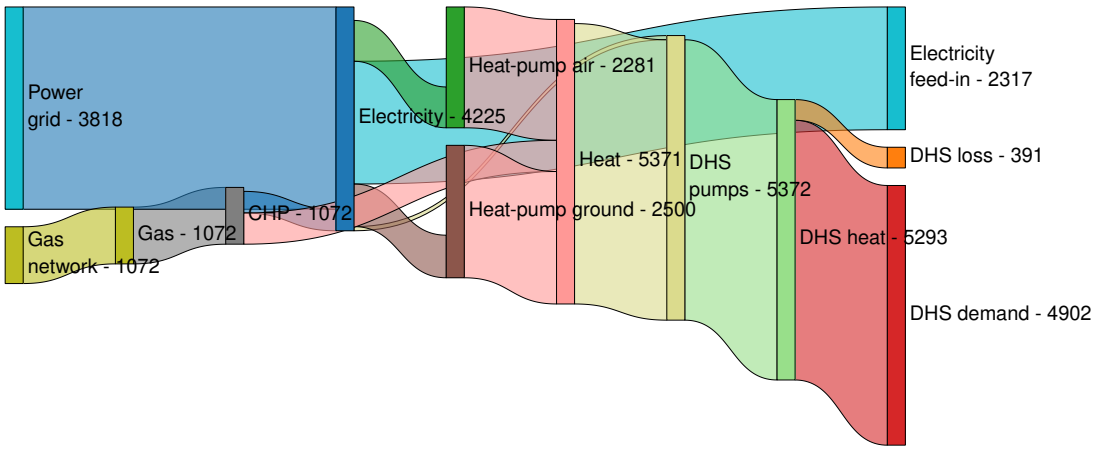

Figure 4.11: Sankey diagram of the carbon neutral result of scenario *2030-syn-gas-high* for the refurbishment scenario *Refurb-1*. All numbers refer to the energy flow per year in MWh/a; the storages are not shown for the sake of clearness.

Thus, the ground-source heat pump is mainly operated at low outside temperatures, and the air-source heat pump is operated when the outside temperature tends to be higher (see Appendix Figure B.4). However, if the emission factor of the upstream power grid is low (which corresponds to a high availability of volatile renewable energy sources), the parallel operation of both heat pumps makes sense (see Figure 4.12 middle diagram and Figure B.5). In combination with a thermal and by the additional installation of an electrical storage, carbon-neutrality can be achieved, however, at very high costs compared to the scenario *2020* and the scenarios of 2050 (see Figure 4.6). This is due to the battery storage, which becomes necessary to further improve the emission balance of the district heat supply site. The scenario *2030-syn-gas-low* is characterized by a high level of electricity imports, almost half of which are fed back into the power grid (2147 MWh/a). Electricity is imported at times of a low emission factor and exported at times of a high emission factor (this relation is further illustrated in the Appendix in Figure B.6).

Figure 4.12 (middle diagram) provides a detailed insight into the unit commitment of the scenario *2030-syn-gas-low*, exemplary for three weeks in February. If the emission factor is low, electricity is imported and the air-source as well as ground-source heat pump are operated and the thermal storage is charged (Figure 4.12 in the middle, e.g. at the 15-02 and 19-02). For the air-source heat pump the outside temperature becomes additionally important. The ground-source heat pump is mainly operated at low outside temperatures in winter, and the air-source heat pump is operated at higher outside temperatures due to a higher COP (see also Appendix Figure B.4).

In scenario *2030-syn-gas-high* the battery storage becomes also important to achieve a carbon-neutral heat supply (Figure 4.11). Analogous to the previous scenarios, a high amount of electricity is exported (2317 MWh/a) with the difference to the *syn-gas-low* scenario that a part of the electricity is generated by a CHP. As the emission factor of gas is lower in this scenario, operating a CHP is emission-efficient at times of a high emission factor in the power

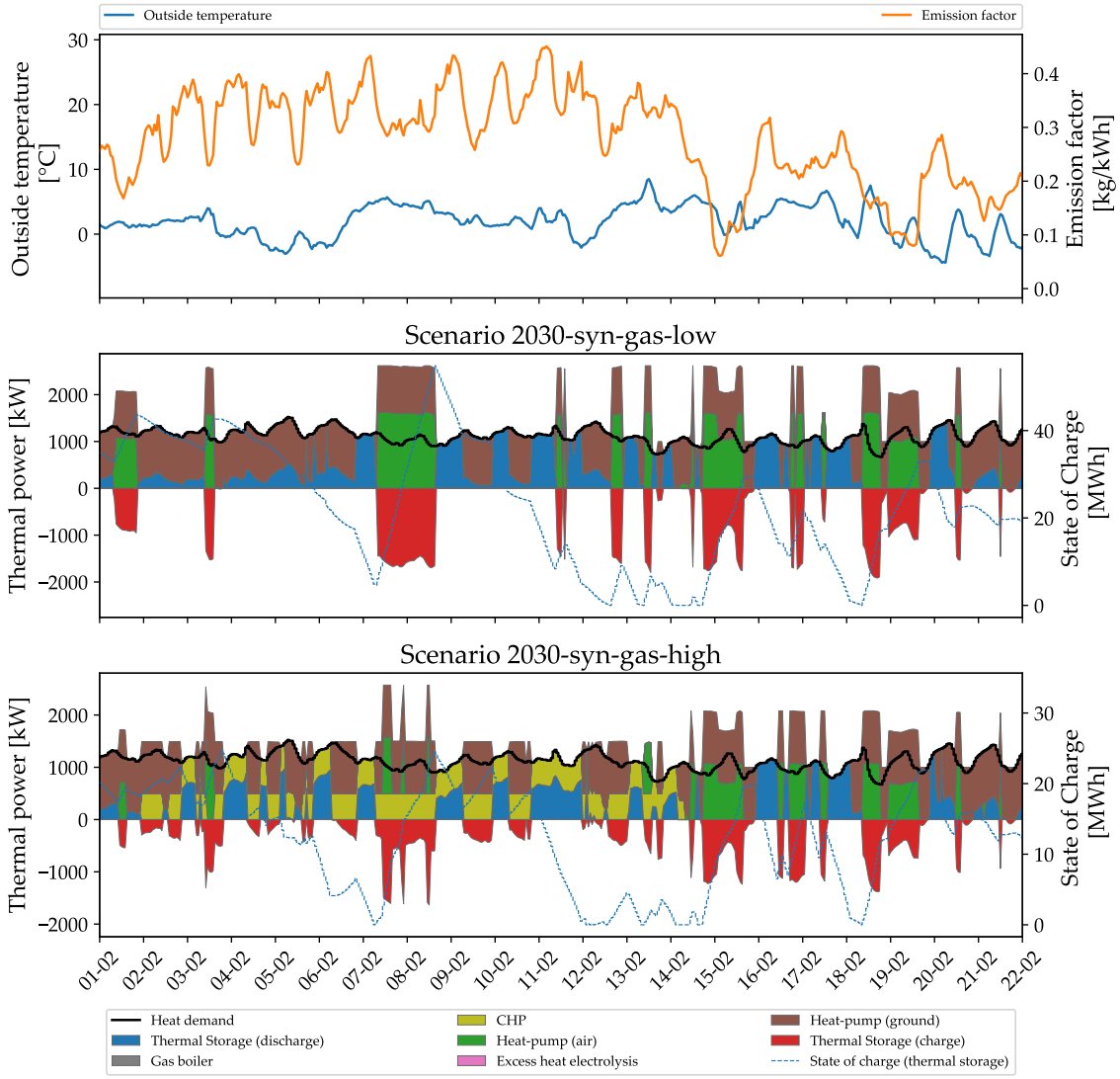

Figure 4.12: Time resolved heat generation of the carbon-neutral solutions of the scenarios for 2030 exemplary for three weeks in February. Upper diagram: emission factor of the electricity grid and outside temperature; middle diagram: scenario *2030-syn-gas-low*; lower diagram: scenario *2030-syn-gas-high*.

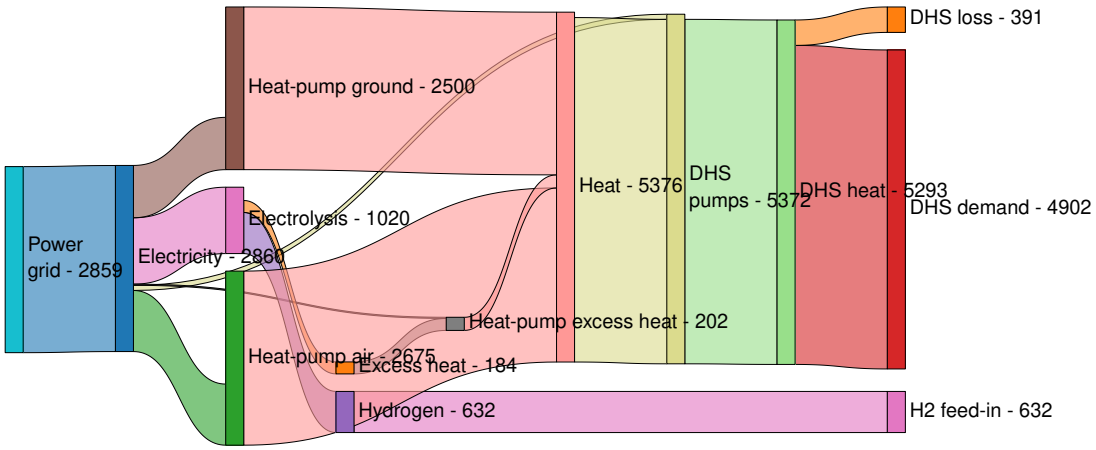

Figure 4.13: Sankey diagram of the carbon neutral result of scenario *2050-syn-gas-low* for the refurbishment scenario *Refurb-1*. All numbers refer to the energy flow per year in MWh/a; the storages are not shown for the sake of clearness.

grid. This is shown by the detailed analysis of the unit commitment given the lower diagram of Figure 4.12 for three weeks in February and by the supplementary material (see Appendix Figure B.7, B.8 and B.9). The strategy for achieving a carbon-neutral heat supply follows the same principle as in scenario *2020*. At times of a high emission factor, the CHP is operated, and the battery is discharged to obtain emission credits for the electricity export (see also Appendix Figure B.9). This also becomes clear in the exemplary period shown in Figure 4.12. In the first two weeks of February (Figure 4.12 lower diagram, from 01-02 to 14-02), the emission factor of the power grid is on a high level. During this period the CHP is operated and temporarily also the ground-source heat pump. The thermal storage is charged at times of a low emission factor in the upstream power grid (see also Appendix Figure B.9). In the third week (Figure 4.12 lower diagram, from 15-02 to 22-02), both heat pumps provide the heat analogous to scenario *2030-syn-gas-low*. Due to the CHP and the lower emission factor of gas assumed in this scenario, it is possible to reduce the thermal storage capacity in comparison to the *syn-gas-low* scenario (see Figure 4.7). Regarding the total costs for carbon-neutrality, both scenarios of 2030 lead to very high levelized costs of energy of about 60 €/(m²a) (see Figure 4.6).

4.3.2.3 Scenarios of 2050

Figure 4.13 and 4.14 provide the energy balances of the carbon-neutral solutions of the scenarios of 2050 in the form of Sankey-Diagrams. Figure 4.15 illustrates the heat generation for three exemplary weeks in February to illustrate the operation strategy to achieve climate neutrality. Analogous to the previous scenarios, the appendix provides a supplementary analysis of the heat generation and the electricity consumption dependent on the outside temperature and the emission factor (see Appendix Section B.1, Figures B.10 to B.15).

Scenario *2050-syn-gas-low* is the only scenario in which an electrolysis is cost-effective for achieving climate neutrality (Figure 4.13). The heat is provided mainly via an air- and ground-source heat pump and all the electricity is imported from the power grid. The strategy

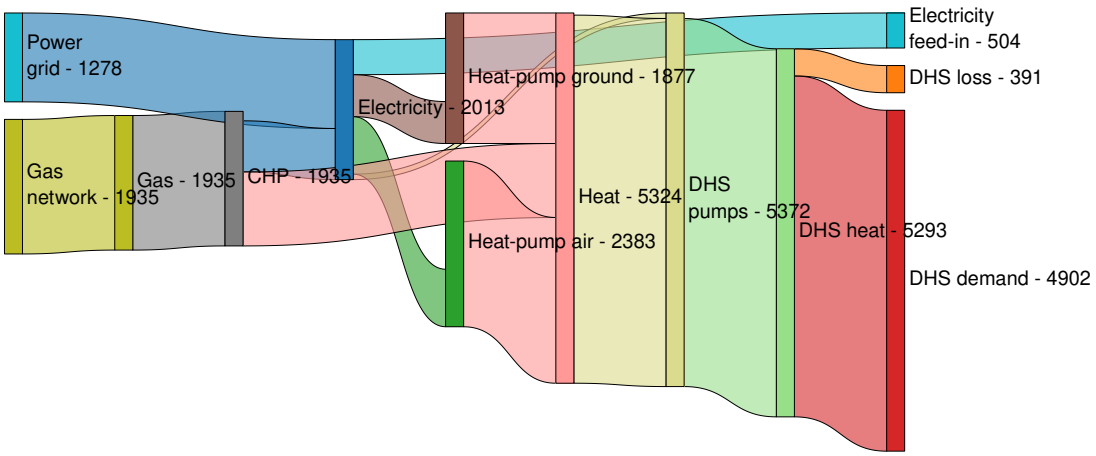

Figure 4.14: Sankey diagram of the carbon neutral result of scenario *2050-syn-gas-high* for the refurbishment scenario *Refurb-1*. All numbers refer to the energy flow per year in MWh/a; the storages are not shown for the sake of clearness.

of deploying an electrolysis is to feed the hydrogen into the gas network. The system earns emission credits through a displacement mechanism as the emission factor of the gas network is much higher in this scenario (160 g/kWh) as the power grid with an average emission factor of 60 g/kWh. This can be observed in detail in Figure 4.15 and is shown in the Appendix in Figure B.11 and B.12. At times of a very low emission factor of below 50 $g_{CO_2-equiv.}$/kWh (e.g. in the case of zero), the electrolysis is operated and contributes to the heat generation through the utilization of the excess heat via a heat pump; even though the overall contribution to the heat supply with 202 MWh/a is low (see Figure 4.13 Heat pump excess heat and Figure 4.15 middle diagram). Similar to scenario *2030-syn-gas-low*, both heat pumps are operated in parallel if the emission factor of the upstream electricity grid is low (see e.g. Figure 4.15 in the middle at 08-02 and 15-02), even though the air-source heat pump tends to be operated at higher outside temperatures (see also Appendix Figure B.10). The thermal storage helps to operate the heat pumps as well as the electrolysis flexibly at times of a low emission factor of the power grid. The thermal storage is charged at times of a low emission factor and discharged at times of a high emission factor (Appendix Figure B.11). A battery storage is not deployed in this scenario for achieving carbon-neutrality (see Figure 4.7).

Figure 4.14 shows the energy flows of scenario *2050-syn-gas-high* that is characterized by a high share of renewable gas within the gas network. This makes the CHP an interesting technology for reducing the emissions again. In this scenario, the main part of heat (about 40 %) is supplied by the air-source heat pump, the other part is provided almost equally by the ground-source and the CHP. The electricity for operating the heat pumps is delivered by two-third from the power grid and one third by the CHP. Analogous to scenario *2030-syn-gas-high*, the CHP is operated at times of a high emission factor (Figure 4.15 lower diagram, from 01-02 to 15-02, and Appendix Figure B.14). Depending on the emission factor of the electricity grid, the power output of the CHP is used to operate the heat pumps or exported into the upstream power grid at times of a high emission factor (see also Appendix Figure B.15). Thus, the upstream electricity is supported at times of a low availability of volatile renewable energy

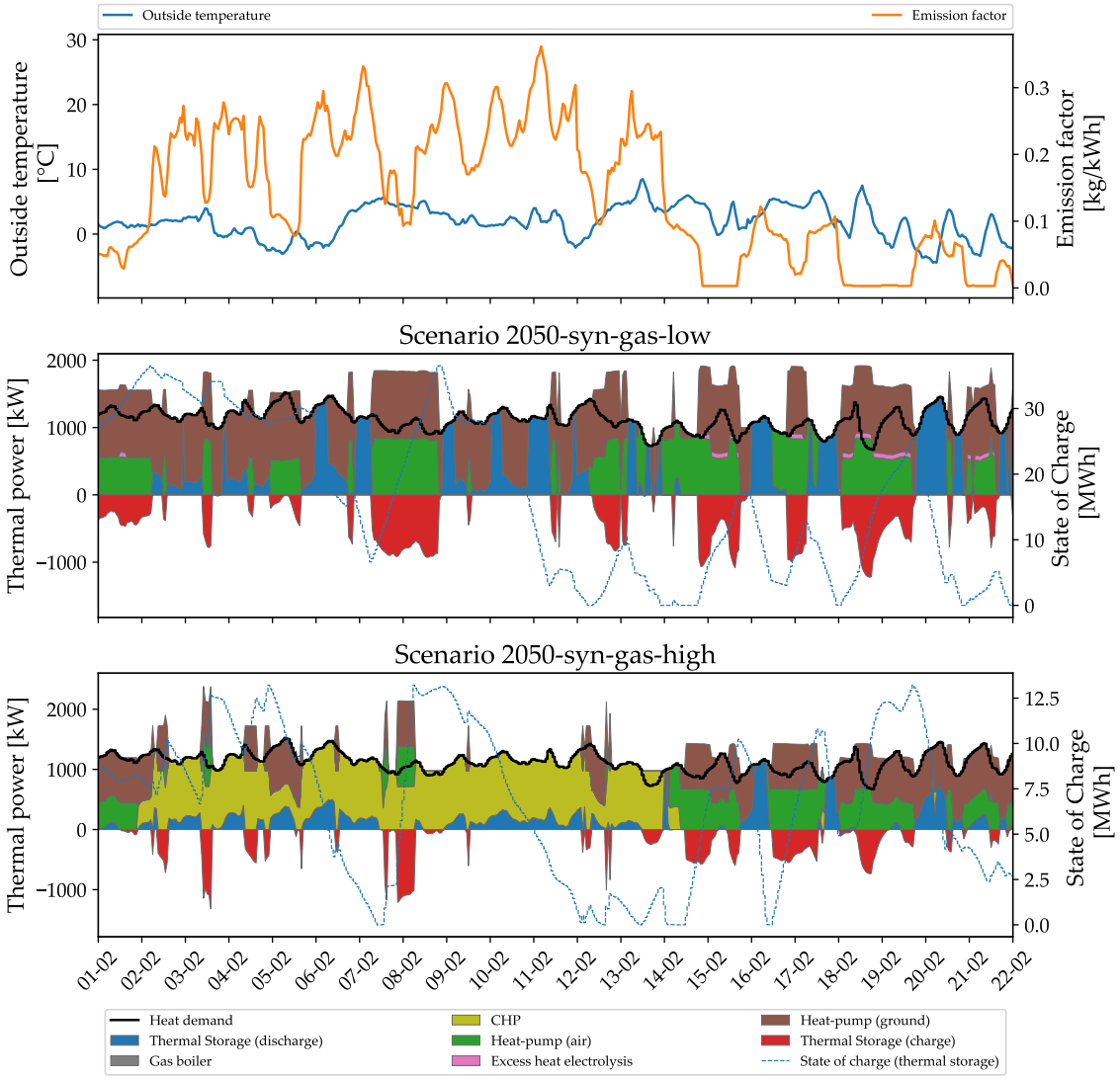

Figure 4.15: Time resolved heat generation of the carbon-neutral solutions of the scenarios for 2050 exemplary for three weeks in February. Upper diagram: emission factor of the electricity grid and outside temperature; middle diagram: scenario *2050-syn-gas-low*; lower diagram: scenario *2050-syn-gas-high*.

sources. This way, the valuable renewable synthetic gas assumed in this scenario is deployed exactly at times of a low emission factor, that corresponds to a low availability of volatile renewable electricity generation in the upstream power grid. Among all carbon-neutral energy systems of refurbishment scenario *Refurb-1*, the size of the thermal storage is the smallest in scenario *2050-syn-gas-high*, and a battery storage is not required for achieving carbon-neutrality. Despite the low emission factor of the upstream power grid, an electrolysis is not a cost-efficient emission reduction option. As the emission factor of the gas network is assumed to be very low in this extreme scenario, the generation and feed-in of hydrogen in the gas network does not improve the emission balance of the local energy system.

The results of the energy balances and an especially the detailed insight and analysis of the time-resolved energy flows for the carbon-neutral solutions of the five scenarios for the upstream gas and electricity grid clearly show that the optimization approach carried out in this thesis leads to a – with respect to the emission factor – system supportive design and unit commitment. The next section further quantifies and compares the system-supportiveness of all solutions of the Pareto-Front for the different scenarios.

4.3.3 Evaluation of the system-supportiveness

The following section analyses to what extent the minimization of the emissions within the Pareto-optimization performed in this analysis and the deployment of the dynamic emission factor for imported and exported electricity lead to a system-supportive district energy system. Therefore, the electricity exchange with the upstream power system of each scenario is summarized and the system-supportiveness of each scenario is evaluated by the use of a quantitative indicator.

Therefore, the absolute grid-support coefficient (GSC) according to Klein et al. is used as a basis for an evaluation of the system-supportiveness (Klein et al. 2016). It is defined as follows (based on Klein et al. 2016):

$$GSC_{abs} = \frac{\sum_{t=1}^{n} W_{el}^{t} \cdot G^{t}}{W_{el} \cdot \overline{G}} \tag{4.1}$$

G refers to a time-resolved reference quantity with G^t representing the value of the reference quantity at time-step t. In this thesis the emission factor is selected as time-resolved reference quantity (see Section 2.1). W_{el}^{t} is the electricity import or export at a single time-step, and W_{el} is the total amount of energy that is imported from the upstream power grid or exported into the upstream power grid in the observation period. The observation period is in the following one year with 8760 time-steps, which is the optimization period of a single energy system optimization. The symbol $\overline{G}$ is the arithmetic mean value of the time-resolved reference quantity (see Klein et al. 2016). The absolute GSC_{abs} represents the weighted and normalized sum of imported or exported electricity. With respect to the emission factor, the value can be interpreted as average emission intensity of the imported or exported electricity (see also Section 2.1.2.3). For the import of electricity into the local energy system GSC_{abs} values greater than one indicate grid-adverse unit commitment while values lower than one indicate grid-supportive behavior (Klein et al. 2016). The opposite is valid for the export of electricity:

Values greater than one indicate grid-supportive behavior while values lower than one indicate grid adverse electricity export (see Klein et al. (2016) for more details).

The upper diagram of Figure 4.16 shows the yearly electricity import and export of the Pareto-optimization of scenario *2020*. The x-axis refers to the single points of the Pareto-front ranging from the point "0.00", which represent the emission optimum, to the point "1.00", which indicates the cost-optimal solution (see Figure 4.6). The abbreviation CN refers to the solution, where carbon-neutrality is achieved.

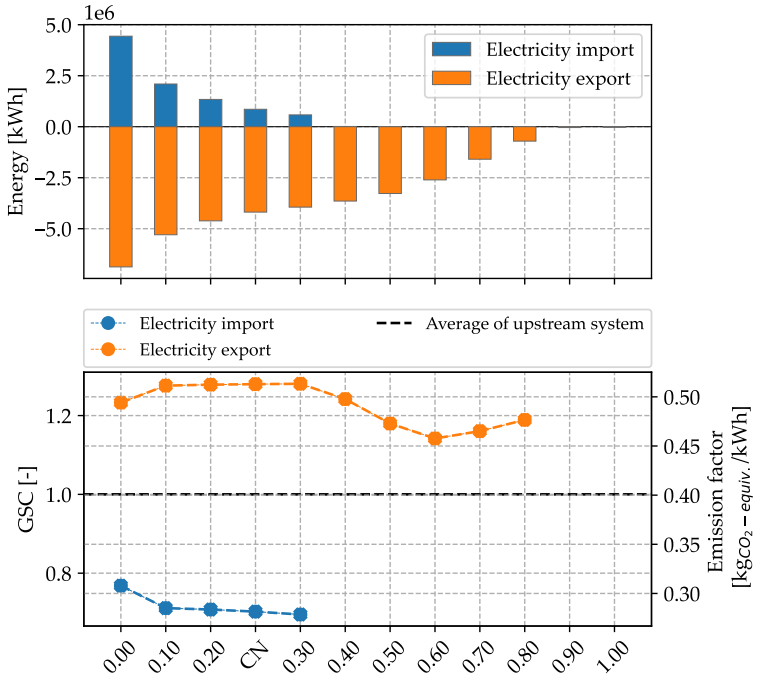

Figure 4.16: Analysis and grid support coefficient of the electricity import and export of scenario *2020*. Upper diagram: electricity import and export; lower diagram: grid-support coefficient and corresponding average emission factor; CN: carbon-neutral solution.

The lower diagram of Figure 4.16 illustrates the absolute GSC (left y-axis) and the corresponding average emission factor of the imported and exported electricity (right y-axis). The dashed line indicates the average emission factor of the upstream electricity grid, which corresponds to a GSC_{abs} value of one and has a value of 401 g/kWh in the scenario *2020* (see Section 4.2.2.1).

In the cost-optimal solution ("1.00"), no electricity exchange with the upstream power grid takes place, as the heat generation is based on gas with a CHP and a gas boiler (see Figure 4.7). If the emissions are reduced (from right to left), electricity from the CHP is exported into the upstream power grid. The absolute GSC results in values significantly above one with a value of about 1.2 (Figure 4.16 lower diagram). If emissions are further reduced (points "0.60." to "0.30" from right to left), the absolute amount of energy exported increases and also the GSC values increase. That means that e.g. at the point "0.40" on average electricity is exported at an emission intensity of the power grid with a value of 0.5 $kg_{CO_2-equiv.}$/kWh. If emissions are reduced further towards emission-optimality, the electricity exports further increase and also electricity imports occur for operating the air-source heat pump and charging and discharging

the battery storage (see also Figure 4.7, 4.8 and B.3). The average emission factor for importing electricity is about 0.3 $kg_{CO_2-equiv.}$/kWh (Figure4.16 lower diagram). While the absolute sums of electricity, that is imported or exported, increase towards the emission-optimal system configuration, the absolute GSC slightly worsens. As the time-steps (or number of hours) with low emission values are limited, that means that the power of importing and exporting electricity needs to increase in order to maintain a certain level of GSC.

Figure 4.17 provides the energy import and export balances as well as the resulting values for the absolute GSC values of the scenarios of 2030 that correspond to the results of the Pareto-optimization presented in Figure 4.6. In contrast to the scenario *2020*, the results of the year 2030 are characterized by higher electricity imports for reducing the system emissions. Both scenarios of 2030 (Figures 4.17(a) and 4.17(b)) show a good performance of the GSC of values about 0.5, when only little electricity is imported (see Figures 4.17(a) and 4.17(b) blue graphs of lower diagrams, points 0.80" and "0.90"). In this cases the system imports the electricity at times of the lowest emission factor of the power grid. When electricity imports are further increased (to reduce the emissions of the local system, in Figure 4.17 from right to left), then points in time with worse emission factors must also be chosen, and the average emission factor (the GSC respectively) of the electricity import increases (e.g. Figure 4.17(a), points "0.80", "0.70", "0.60"). A similar tendency can be observed at the electricity exports. When only little electricity is exported, the GSC of the export achieves high values (e.g. Figure 4.17(b), point "0.60" with above 1.5), which indicates a very grid-supportive electricity export. With increasing electricity exports, the GSC decreases (Figure 4.17(b) lower diagram, orange plot).

The energy balances of the electricity import and export of the scenarios of 2050 are given in Figure 4.18. In scenario *2050-syn-gas-low* the electricity imports reach the highest values of all presented scenarios in this section (Figure 4.18(a), upper diagram). This results from the electricity-based generation of hydrogen for improving the emission balance of the local district energy system. In contrast, this scenario shows the lowest electricity exports in the emission-optimal solution (Figure 4.18(a) upper diagram, orange bars). The GSC values of the electricity import range well below one in the grid-supportive area. At the points "0.60" and "0.70" a maximum occurs. This can be explained by the electrolysis that comes into play for improving the emission balance of the district energy system. Towards the emission-optimal system configuration ("1.00"), the GSC values increase, as observed in the previous scenarios.

In scenario *2050-syn-gas-high* (Figure 4.18(b)), significant amounts of electricity are already imported in the cost-optimal solution (point "1.00"). At this point, the GSC results in a value slightly above one, as the system is not constrainted with any emission limit in the cost-optimal case. Thus, there is no incentive to source electricity at times of a low emission factor. From that point on the GSC of the electricity import improves towards a grid-supportive behavior. In this scenario a CHP is deployed to reduce the emissions of the district energy system due to the low emission factor of the gas network. The export of electricity takes place at times with a very high emission factor, which results in GSC values of above three in the point "0.80". This means that the CHP, which is fueled by a gas mix with a high share of renewable synthetic gas, is operated exactly at the times of a very high emission factor in the upstream power grid (see also Appendix Figures B.14 and B.15), that reflects a low availability of volatile renewable

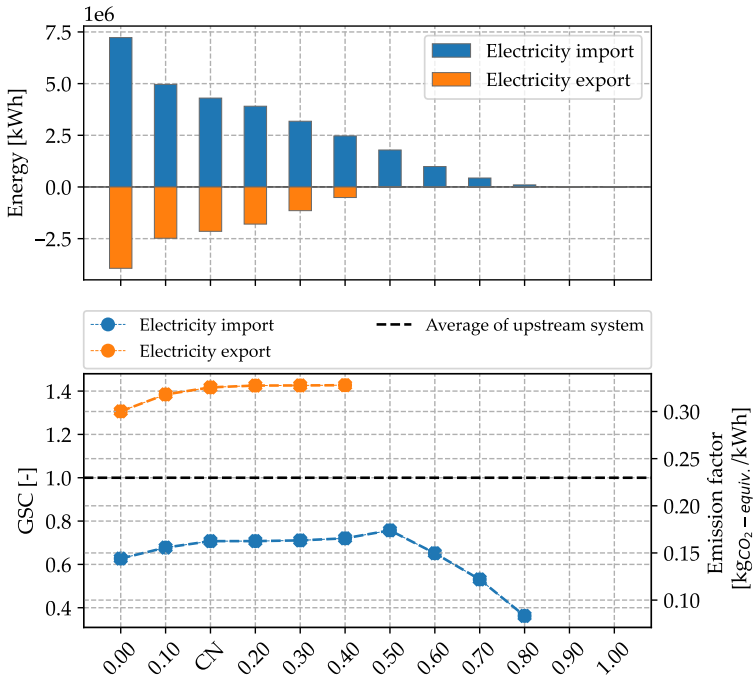

(a) Scenario *2030-syn-gas-low*

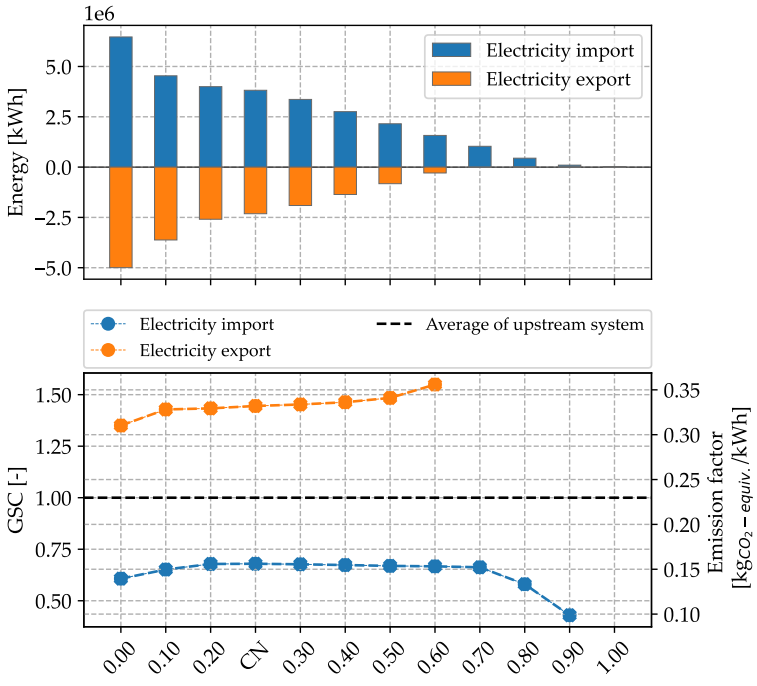

(b) Scenario *2030-syn-gas-high*

Figure 4.17: Analysis and grid support coefficient of the electricity import and export of the scenarios of 2030. Upper diagrams: electricity import and export; lower diagrams: grid-support coefficient and corresponding average emission factor; CN: carbon-neutral solution.

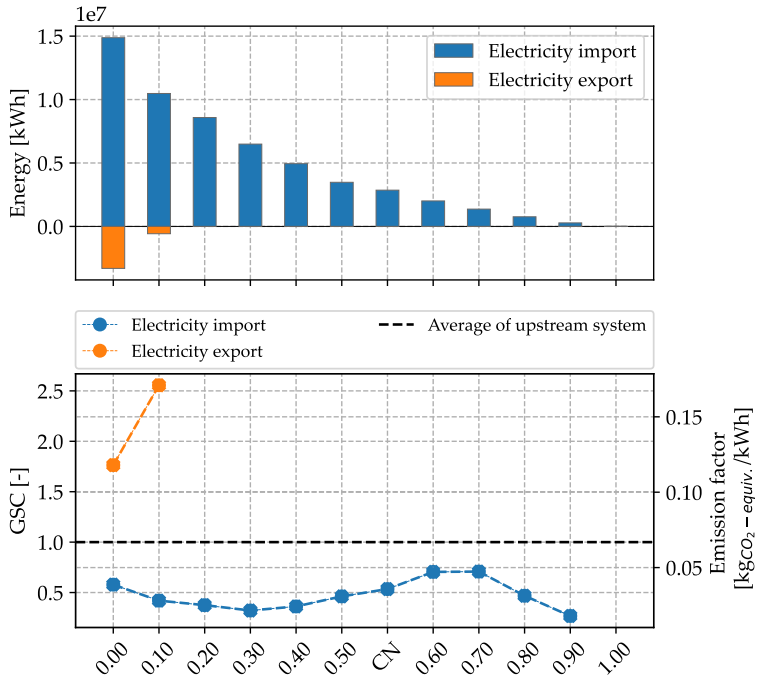

(a) Scenario *2050-syn-gas-low*

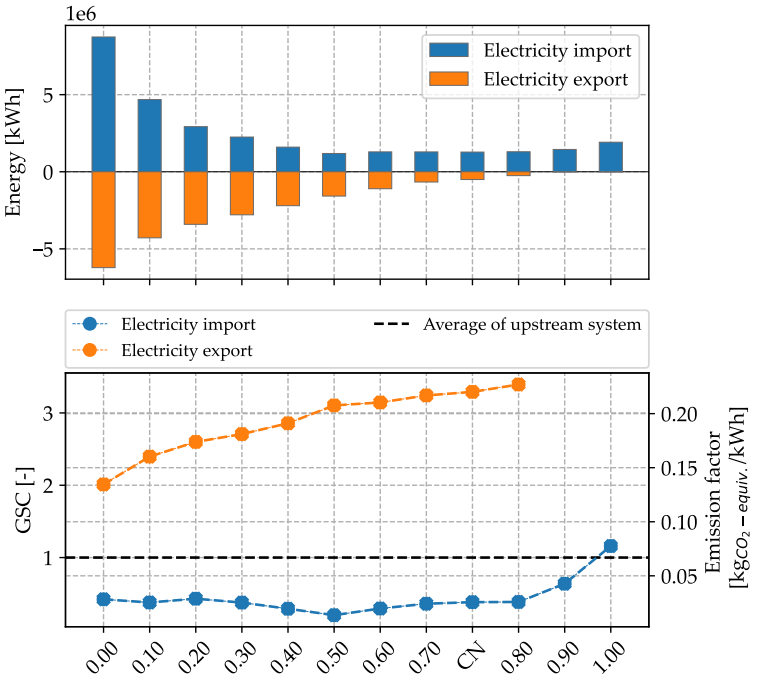

(b) Scenario *2050-syn-gas-high*

Figure 4.18: Analysis and grid support coefficient of the electricity import and export of the scenarios of 2050. Upper diagrams: electricity import and export; lower diagrams: grid-support coefficient and corresponding average emission factor; CN: carbon-neutral solution.

energies. When the emissions are reduced towards the point "0.00", the volume of exports increases, and the GSC of the electricity exports decreases, but still remains above two.

The ex post analysis of the electricity exchange with the upstream power grid demonstrates that the usage of a dynamic emission factor in combination with constraining and optimizing the emission of the district heat supply results in a system-supportive electricity import and export. The dynamic emission factor is capable of combining an assessment of the ecology (in the form of CO_2-equiv.) and providing an incentive for a system-supportive design. If emission limit constraints are set, the GSC values result in values lower than one for the electricity import and values above one for the feed-in of electricity into the upstream power grid. Both indicate grid-supportive behavior. However, the absolute GSC values differ depending on the applied emission limit and for the different scenarios of the upstream electricity system, which imply different input time-series of the emission factor (see Section 4.2.2.1). Section 4.4 further discusses the applicability and limits of the emission factor.

4.3.4 Impact of refurbishment scenarios

Figure 4.19 compares the optimization results of the refurbishment scenarios *Status-quo* and *Refurb-2*. Due to the refurbishment the total heat demand is reduced and the temperature level lowered (see Table 3.1). The costs of the refurbishments themselves are not included as the focus of this analysis is the design of the heat supply.

The refurbishment leads to an overall shift of the Pareto-fronts to the left-lower corner (see Figure 4.19). As the energy demand decreases, the emissions per square meter and year are reduced over-proportionally to the reduce in heat demand. In the scenario *2020* the cost-optimal point ('1.00') moves from about 45 $kg_{CO_2}/(m^2a)$ below 20 $kg_{CO_2}/(m^2a)$. Due to the lower temperature level in the refurbishment scenarios, the efficiencies of the heat pumps improve and the thermal losses of the district heating network decrease. However, the costs do not reduce in the same amount. The point '1.00' of scenario 2020 moves from slightly more than 20 €/(m²a) to slightly below 20 €/(m²a). The same can be observed for the other scenarios for each cost-optimal solution. The high fixed costs of the district heating network and the construction of the heat supply plant explain this shift. In addition, the reduction of heating demand does not mean an equal reduction of the capital expenses of the energy converter and storage units as the overall heat power demand does not decrease proportionally.

However, this changes significantly when emissions are reduced. In the carbon neutral system configuration (see Figures 4.19(a) and 4.19(b) at net zero emission), the cost difference between the *Status-quo* scenario and the *Refurb-2* scenario deviates drastically. In the scenario of 2020 and 2050, the carbon neutral solutions achieve cost values of 25 to 30 €/(m²a) in the refurbishment scenario, whereas the *Status-quo* scenario amounts to almost double the costs of 45 to 50 €/(m²a). In the *syn-gas-high* scenario of 2030, the costs for carbon neutrality are more than double, if the building stock remains un-refurbished and when applying the *syn-gas-low* scenario of 2030, carbon neutrality cannot be achieved at all.

For the transformation paths *syn-gas-high* and *syn-gas-low* of the upstream energy infrastructures, the solutions of both scenarios are closer to each other in the scenarios of 2030 in the

scenario *Status-quo* and show a greater deviation in the scenario *Refurb-2* in the scenarios of 2050.

The results of the investment decisions of the refurbishment scenarios *Status-quo* and *Refurb-2* (Figures 4.20 and 4.21) reveal qualitatively no substantial differences compared to scenario *Refurb-1* presented in Section 4.3.1. The hydrogen storage and the compressor unit are not deployed in any of the scenarios. The electrolysis is the least preferred and most expensive option for an improvement of the emission balance in the scenarios of 2030 and 2050 except in scenario *syn-gas-low* of 2050. Here, the electrolysis is already part of the cost-optimal system for achieving carbon-neutrality. In the scenario of 2020, the electrolysis is not deployed at all. The air-source heat pump is part of the district heat supply in all scenarios of the upstream energy system as well as in the refurbishment scenarios. The ground-source heat pump is deployed to the maximum capacity in the scenarios of 2030 for achieving carbon-neutrality and also in the scenario *syn-gas-low* of 2050. In the scenario *2050-syn-gas-high*, the ground-source heat pump is installed in the cost-optimal case, similar to the scenario *Refurb-1*. In the scenarios of 2050 in the carbon-neutral system configurations, the CHP is only used in the *syn-gas-high* scenarios and not cost-efficient in the *syn-gas-low* scenario (Figures 4.20 and 4.21). Figures 4.20 and 4.21 show that the storage capacities for achieving carbon-neutrality are higher in the scenarios *Status-quo* compared to *Refurb-2*. A battery storage is not needed in the scenarios of 2050 to become carbon-neutral, and the thermal storage is only extended to the maximum for the scenario of 2020 in the refurbishment scenarios *Refurb-2*.

Figure 4.22 gives a detailed overview of the composition of costs of each scenario. The capital expenditures for setting up the district heat supply are equal for each scenario as described in Section 4.2.1.2. The costs of the district heating pipeline network do not show remarkable differences because the design of the piping system results in similar dimensions - independent of the refurbishment scenario. As for both, the temperature spread as well as the heat demand decrease (compare Table 3.1), the pipeline dimensions of the scenario *Status-quo* are sufficient in supplying the building stock of the refurbishment scenarios.

The battery storage is one of the main cost drivers of the energy converter and storage units and is needed in all scenarios of 2020 and 2030 to achieve carbon-neutrality. In the scenarios of 2050 the emission factor of the upstream infrastructure makes lower investments in energy converter and storage units possible. In contrast, the share of costs of the thermal storage is much lower even though the storage capacity is higher.

The energy procurement costs of electricity and gas range from about one third to half of the overall costs. To achieve a carbon-neutral building stock in the medium term, the cost of electricity is a significant factor and determines the total heat production costs to a large extent. For all upstream energy system scenarios, refurbishment results in a lower share of energy costs relative to the total costs. Consequently, refurbishment measures also decrease the risk of various energy price developments especially when the energy procurement costs rise in future.

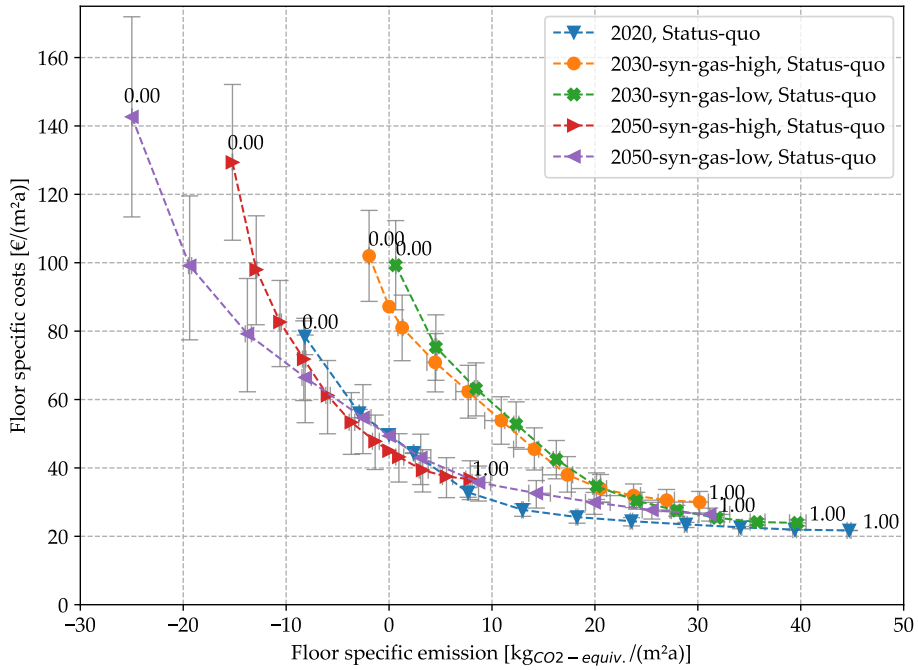

(a) Scenario *Status-quo* (un-refurbished building stock)

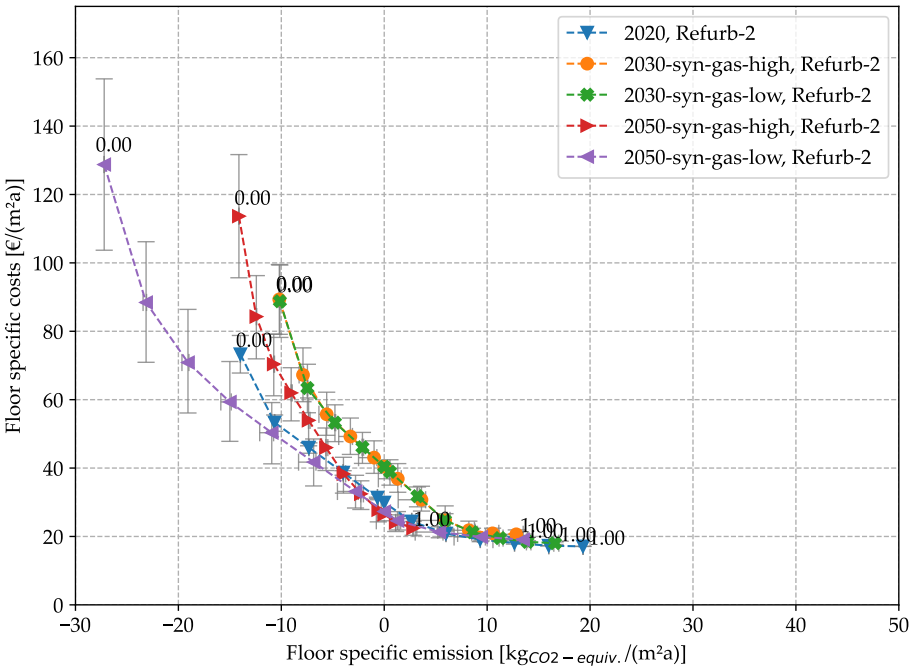

(b) Scenario *Refurb-2* (very ambitious refurbished scenario)

Figure 4.19: Results of the Pareto-optimization of the refurbishment scenarios (a) *Status-quo* and (b) *Refurb-2*. Error bars indicate the variation of the commodity prices.

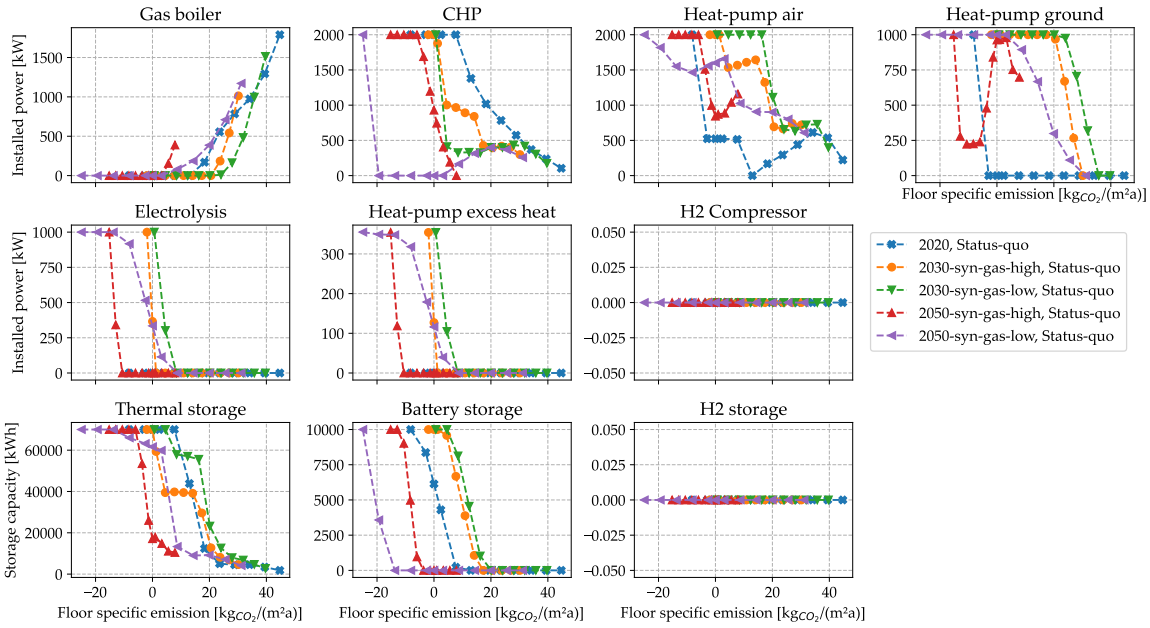

Figure 4.20: Investment decisions of energy converter and storage units depending on the specific emissions of refurbishment scenario *Status-quo*.

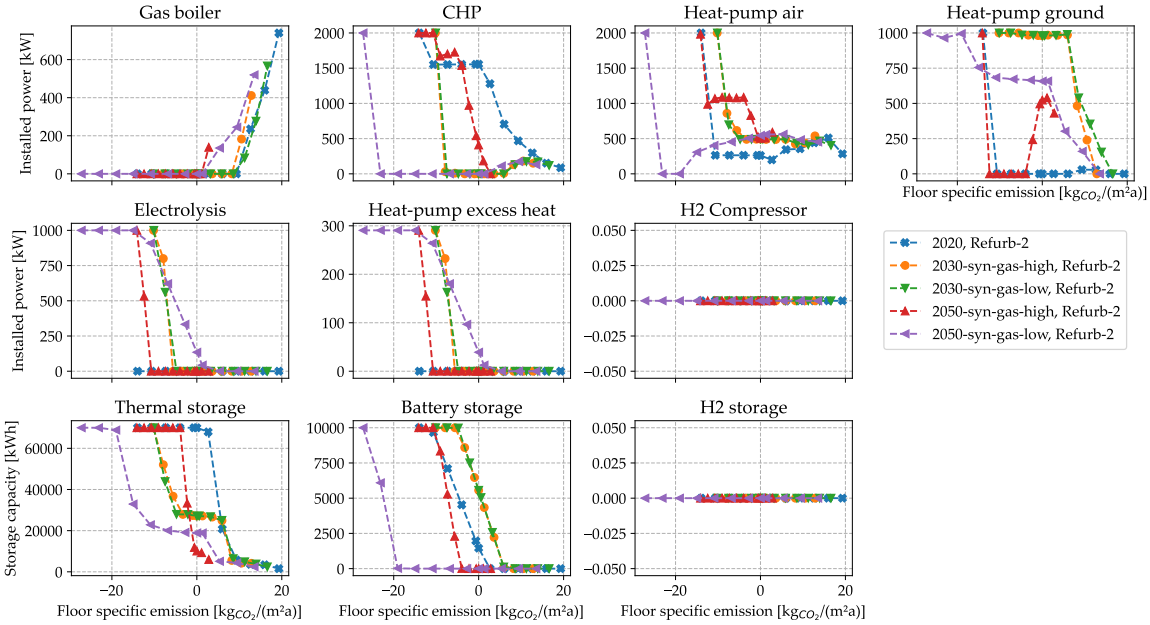

Figure 4.21: Investment decisions of energy converter and storage units depending on the specific emissions of refurbishment scenario *Refurb-2*.

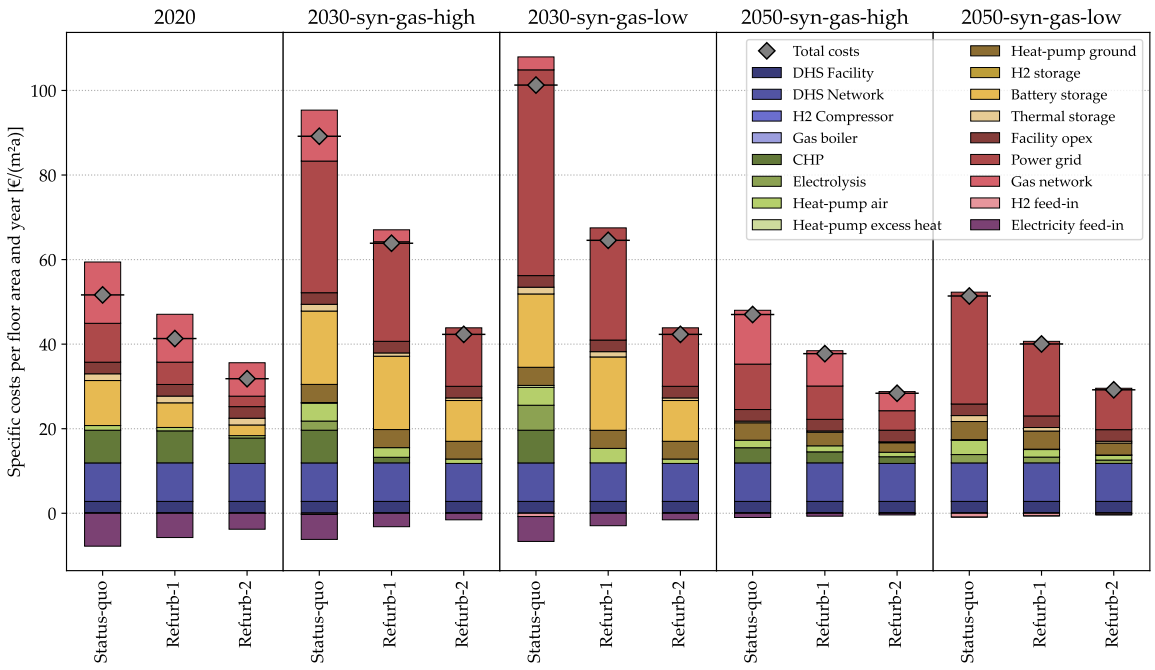

Figure 4.22: Detailed cost summary of carbon-neutral system configurations based on the medium price path. In scenario *2030-syn-gas-low*, the costs of the emission-optimal result are shown as carbon-neutrality cannot be achieved in this scenario.

4.4 Discussion

The methodical approach for the assessment of emissions of electricity export into the upstream power grid and electricity import of electricity from the upstream power grid is based on the dynamic (time-resolved) average emission factor. By adhering to this approach, it is indented to establish a system-supportive design of the district energy system. The usage of the dynamic emission factor is motivated by the correlation between the emission factor, the share of renewable energy generation in the power system and the historically observed congestions and feed-in management measures (see Section 2.1). The emission factor further provides a combined assessment of the actual emissions of grid-sourced electricity (in CO_2-equivalent) for the comparison of electricity imports with other energy sources and, at the same time, provides an incentive for creating system-supportive district energy systems.

The resulting investment decisions show that the heat generation units are expanded to partly oversized capacities and appropriate storage capacities built in order to provide a flexible system that can react on the signal of the emission factor of the upstream power grid (e.g. see Figure 4.7). The presented ex post analysis illustrates that the mechanism of designing of a system-supportive district energy system though the application of a dynamic emission factors works and quantifies the level of grid-supportiveness that is achieved in each scenario on the basis of the absolute GSC (see Section 4.3.3). The resulting GSC values range well below one for the electricity import even if higher amounts of electricity are imported. For the electricity export, the GSC values are well above one for all scenarios also in the cases of a high electricity export.

However, the question now arises whether a larger volume of electricity imports and exports with a slightly worse GSC is preferable for the integration of volatile renewable energies compared to lower volume of electricity exchange with the upstream power grid with a better GSC. In addition, one has to ask which level of GSC is sufficient for a district energy system. Or expressed with respect to the emission factor, the question is which level of emission reduction makes the district energy system sufficiently system-supportive. E.g. the carbon-neutral result of the scenarios of 2050 can be achieved with moderate storage capacities compared to the scenarios of 2020 and 2030 as the emission factor is already on a very low level. However, it could be that higher storage capacities are required in these scenarios. These questions cannot be answered within this thesis and maybe there is no ultimate answer to them. Every district energy is individual and equipped with different potentials and capabilities to become carbon-neutral or even better. Thus, by calculating the marginal costs for the emission reduction in the form of a Pareto-Front, different energy systems can be compared in becoming carbon-neutral, and the measures that can reduce the emissions (and flexibility) at least costs can be implemented first. Thus, the usage of a dynamic emission factor can support the planning of district energy systems to design renewable and system-supportive energy systems based on future scenarios for the upstream energy system without the need to know the future energy market design that would set scarcity signals via monetary incentives. Although no absolute recommendation about the required GSC values can be made, different systems can be compared with each other, as will be done in Chapter 5 through the comparison of individual heat supply solutions with district heating. The consideration of the volatile characteristics of the power grid becomes important in all electricity-based energy applications, which is also the case in the heating sector due to the increasing role of heat pumps.

However, the methodical approach for a system-supportive design based on the emission factor is limited when it comes to a 100 percent renewable upstream electricity system. In the scenarios of 2050, there are already several hours where the emission factor amounts to zero (Figure 4.3). Here, the emission factor is still well differentiated with several hours of high emission values, however, on a lower absolute level compared to the scenarios of 2020 and 2030. However, if the share of renewable energies further increases, and the remaining fossil power generation is replaced by renewable hydrogen or synthetic gas, the emission factor of the upstream power grid would result in zero for all time-steps. In this case, there is no differentiation of the emission factor anymore, and the local system has no information about when it is really urgent to source electricity, e.g. in the case of a massive oversupply of renewable energies. For this case the methodical approach needs to be developed further. During the ongoing energy transition until the completely renewable electricity system, the introduced method based on the emission factor helps to identify inter-sectoral cost-efficient emission reduction strategies. In the scenarios of this thesis, the applied methodology based on time-resolved emission factors is an appropriate measure that addresses both a renewable and system-beneficial design.

The assessment method of the emissions considering a displacement mechanism for the energy exports leads to the effect that the district energy system can improve the emission balance, if the upstream infrastructures have a low share of renewable energies, which corresponds to a high emission factor. This mechanism is intended as it aims to create also a system-supportive export of electricity into the upstream power system. This effect can be observed in the scenario of 2020, in which the natural gas based CHP can achieve a carbon neutral energy system and

also in scenario of *2050-syn-gas-low*, in which the district energy system profits from hydrogen export into a mainly fossil based gas network to improve the emission balance. By the analysis of future scenarios, it could be shown that the concept of improving the emission balance via electricity exports from the CHP does not work anymore in the scenarios of 2030 and 2050 as the emission factor of the power grid decreases. This must be kept in mind if only single scenario years based on the current energy system are reviewed and future development are not anticipated. Therefore, the presented analysis illustrates the importance of designing local energy systems relative to the upstream energy infrastructures.

Undoubtedly, every scenario analysis is limited to the assumptions and scenarios that are investigated. In this context, as stated above, this study does not aim to predict future developments and does not assess the probability of the different scenarios. The aim of this work is to show the interdependencies and impacts of different developments on the optimal design of district heat supply systems for a cost-efficient emission reduction.

4.5 Conclusion

A prospective scenario-based design approach for the selection and dimensioning of energy converter and storage technologies of district heat supply systems has been introduced and applied to a typical existing district for identifying the cost-efficient emission reduction options. Five scenarios for the development of the upstream infrastructures of electricity and gas with different shares of renewable energies were investigated. Additionally, three refurbishment scenarios for the existing building stock were considered. The aim of this chapter was to develop future-proof renewable and system-supportive district heat supply concepts in a strongly sector-coupled energy system in the context of potential upheavals in the upstream energy infrastructure during the ongoing energy transition (RO 2).

For the task of a prospective design of the district heat supply, the installation of heat pumps and a thermal storage in combination with a CHP is a future-proof concept independent of the future energy scenarios. This system configuration provides flexibility regarding the energy source (gas or electricity). Heat pumps are the main heat generation technology in all future scenarios also in the extreme scenario *2050-syn-gas-high* with a high availability and share of renewable synthetic gas in the upstream gas network. The heat pump capacities should be built up modular and easy to extent, as an increase of installed power contributes to flexible district heat supply. In addition to heat pumps, a thermal storage plays an important role in all scenarios, as it is a very cost-effective way of storing energy for operating the heat pumps at times of a low emission factor in the upstream power grid, or – if synthetic renewable gas is available as in the *syn-gas-high* scenarios – operating the CHP at times of a high emission factor. In the sector-coupled energy system shifting energy from times with a high share of renewable energies in the power grid to times with a low share of renewable energies, which is represented in this analysis by a time-resolved emission factor, is an important task. Furthermore, the design and operation of the district energy systems can support the emission reduction of the upstream energy infrastructures. Therefore, the installation of a CHP makes sense in the current state of the energy system in 2020 and in scenarios with a high share of renewable gas in the gas network. If the share of renewable gas does not increase substantially, a CHP

is not part of an carbon-neutral district heat supply as the scenarios *2030-syn-gas-low* and *2050-syn-gas-low* show. However, if renewable gas is available, the deployment of a CHP can provide flexibility and efficiently supply heat and electricity at times of a low emission factor power grid. This also means that future CHP units need to be ready for a high share of renewable gas that might also imply a high share of hydrogen in the gas network.

An electrolysis with the purpose of hydrogen generation for the district heat supply is not part of any cost-efficient emission reduction concept. With respect to the feed-in of hydrogen into the gas network an electrolysis can contribute to an emission reduction only if the share of fossil gas in the gas network is very high and the share of renewable energies in the electricity grid is low (scenario *2050-syn-gas-low*). However, if the share of renewable gas within the gas network increases, the benefit for the emission balance of the district disappears. The utilization of excess heat of the electrolysis is only of minor importance for the district heat generation. Thus, small scale hydrogen production capacities of urban districts compete with other locations, as there is no hydrogen demand in most of the urban districts, and the only synergy to the district is the use of the excess heat. Urban districts already represent an energy sink and it is questionable if these are the right locations for additional electricity consumers such as hydrogen electrolysis from the power grid's point of view. Hence, the decision on where to put electrolysis capacities is more a matter of matching hydrogen demand, existing and potential extensions of the power grid and renewable energy resources at a national level, but not a decision at district level.

5 District heating versus individual heat supply

District heating systems (DHS) are a promising infrastructure for the transformation of the energy system (see Section 1.2.2.4). Following up on the optimal design of the energy converter and storage units of heat supply in the previous chapter, this chapter tackles research objective RO 3: In which cases is a DHS a future-proof infrastructure decision compared to an individual building-wise heat supply, and which future developments impact on the heat density threshold for the feasibility of DHS? The future developments include scenarios for the upstream energy infrastructure as well as different scenarios of the existing building stock. The analysis is used to find the trade-off between costs and emission from a cost-optimal to a carbon-neutral energy supply.

The district Rüsdorfer Kamp that is taken as a reference in this analysis is well suited because the heat demand density of the district lies at the threshold of economic feasibility of a DHS (see Section 2.2). There are many cases in rural cities which show a sparse and moderate heat demand density similar to the Rüsdorfer Kamp, and it is questionable whether a DHS is the best option with regard to costs and emission. Also, as in many other German districts, an existing gas network supplies most of the buildings with energy for heating. Decisions on infrastructure are very long-term and involve very high investment costs. To avoid sunk costs in existing and future energy supply infrastructures, this analysis questions and reviews current heat density threshold values for the feasibility of district heating to achieve a carbon-neutral energy supply in the buildings.

Therefore, the energy systems of two reference buildings from the district Rüsdorfer Kamp are optimized for two variants: supply via DHS with a different quota of buildings connected to the DHS and individual heat supply at the building. In the context of increasing sector-coupling, the entire energy system of the buildings, including the electricity demand, is optimized with respect to costs and emissions. This analysis thereby broadens the perspective and aims for an integrated assessment, in contrast to studies that focus purely on the heat supply or purely on cost-efficiency. The optimization is performed for the different global scenarios of the upstream energy system (see Section 4.2.2) and the local scenarios that consider different potential refurbishment developments in the district (see Section 3.3.1). The time-resolved characteristics of the volatility of the renewable power generation of the electricity grid is considered by an assessment of the emissions of electricity import and export based on a dynamic emission factor as introduced in Section 2.1.

Below, firstly, existing decision criteria for the establishment of a DHS such as the heat density thresholds given in literature are reviewed. In the next section, the reference buildings that are analyzed in detail are introduced, the model for the energy supply of the buildings is explained and the technical and economic parameters of the components of the building's energy system are presented. The results are divided into two sections: The first section presents the results of the individual heat supply solutions, including the investment decisions for a cost-optimal emission reduction. This is followed by the comparison of individual heat supply versus DHS. The comparison of the analyzed scenarios is summarized by deriving heat density thresholds for each scenario, above which a DHS is favorable compared to individual heat supply to reach

Table 5.1: Heat demand density threshold in literature. Source: (Pol et al. 2016).

Heating demand density indicator	Proposed threshold value	Source
Heating power demand density	0.02–0.05 kW/m^2_{site}	Karlsson 1982 [1]
Heating energy demand density	50–70 kWh/(m^2_{site} a)	(Arbeitsgemeinschaft QM Holzheizwerke 2022)
	10 kWh/(m^2_{site} a)	(Zinko et al. 2008)
	350–400 MWh/(ha_{site} a)	(EnergieSchweiz 2017)
Linear heating energy demand density	1.2 MWh/(m a)	(ÖKL 1999)
	0.9 MWh/(m a)	Kommunalkredit 2009 [1]
	0.3 MWh/(m a)	(Zinko et al. 2008)
	0.2–0.3 MWh/(m a)	(Fröling et al. 2006)
Linear heating power demand density	1.2 kW/m	AWEL Energie 2004 [1]

[1] The references are given in (Pol et al. 2016).

a carbon-neutral building stock. Finally, a discussion of the results and a summary of the same is given.

5.1 Literature review: Heat density thresholds

Table 5.1 presents the review of heat density indicators in literature based on Pol and Schmidt (Pol et al. 2016). The aim of these threshold values is a preliminary assessment of a given area with a known heat demand regarding the economic feasibility of a district heating network (Pol et al. 2016). Thereby, two different measures are used as an indicator for the heat demand: either the heat load or the heat demand as energy per year. As a reference value for the site or district, either the total area of the site is used as the reference basis. An alternative measure is the linear heat density that relates the heat demand value to the grid length of the district heating distribution network (Dochev et al. 2018).

As Table 5.1 shows, the recommended heat density thresholds of the different literature sources reviewed by Pol and Schmidt show a significant variation, e.g. the recommendations of the linear heat density range from 0.2 to 1.2 MWh/(m a). This indicates how difficult it is to determine an absolute threshold value. Within the transformation process of the energy system, the demand-side based assessment is no longer sufficient and further energy sectors that are connected at an urban level, such as electricity and gas, need to be taken into account. (Pol et al. 2016)

There are also numerous planning guidelines that propose certain thresholds for the establishment of DHS. Thalmann et al. recommend heat densities of above 70 kWh/(m^2a) as suitable. Districts with heat density values between 50 and 70 kWh/(m^2a) could also be feasible if the

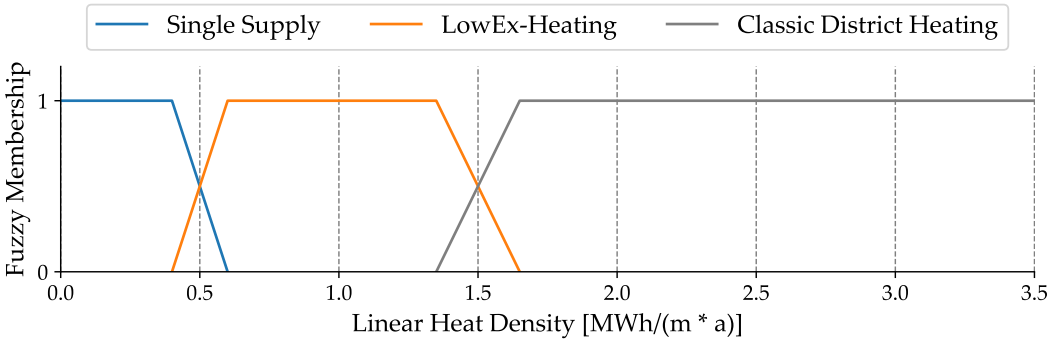

Figure 5.1: Fuzzy membership of heat supply options. LowEx: low-exergy. Reproduced figure, source: (Knies 2018).

district is characterized by certain requirements, e.g. low investment costs or low fuel costs. A district or area with a heat demand density lower than 50 kWh/(m²a) is not suitable for district heating (Thalmann et al. 2018). The recommendation is based on QM Holzheizwerke, that is also referenced by Pol and Schmidt (see Table 5.1). There are also several guidelines published by German federal states. One example is the planning guideline of the federal government of Bavaria. This guideline recommends linear heat densities of above 0.5 MWh/(m a) and area based heat densities of more than 300 MWh/(ha a), which is 30 kWh/(m²a); however, below a linear heat density value of 1.5 MWh/(m a) the thermal losses need to be kept very low (Bayerisches Landesamt für Umwelt et al. 2020).

Knies introduces the concept of suitability areas by fuzzy logic for the analysis of the heat demand and spatial mapping (Knies 2018). By using a fuzzy logic concept, the aim is to expand the threshold to a threshold range, as illustrated in Figure 5.1. Knies suggests two threshold ranges (see Knies 2018): for very high heat densities, classical district heating with supply temperatures of 70 °C in summer to 90 °C in winter is viable. At lower linear heat density values, a low-exergy DHS with a lower supply temperature that might include a seasonal operation strategy could be feasible. Below these range, low temperature DHS are no longer viable. However, the threshold ranges in the fuzzy logic should be adjusted for each region. The fuzzy logic is the basis for the identification of suitable areas by subsequent spatial analysis, including focal analysis, followed by an analysis of the local seasonal power generation and the integration of industrial excess heat (Knies 2018).

Altogether, the heat density is an important indicator for the feasibility of DHS and is often used in early project stages for identifying suitable areas for DHS. Although the threshold values or the threshold ranges differ depending on the literature source, overall, the recommendations lie within a certain range and are mostly characterized by a transition range. At the same time, many thresholds are based on older literature sources before 2010. However, in the last decade, new technologies, such as heat pumps, and a new paradigm regarding the role of the heating sector in an integrated sector-coupled energy system have arisen, as for example described in (Henrik Lund et al. 2017). At the time when most of the above-mentioned thresholds were defined, heat supply was based on burning fossil fuels like oil or gas or biomass, either at a centralized district heating facility or decentrally in the buildings. The focus was also more on economic efficiency than on the reduction of greenhouse gas emissions. Nowadays, the

perspective must be broadened, and also the development paths of the upstream infrastructures of the gas network and the power grid need to be taken into account. The heat density thresholds need to be reviewed for future scenarios. At this point, the following analysis contributes to decision-making in regard to DHS by depicting the impact of future scenarios for the transformation of the upstream infrastructures for gas and electricity on the feasibility of DHS in the trade-off between costs and emissions. The analysis therefore contemplates in detail a typical existing district with a heat density within the threshold range for the suitability of a DHS, and investigates the feasibility of a DHS based on two reference buildings in an integrated approach, taking both heat and electricity consumption into consideration.

5.2 Model and parameters

In the following section, the reference buildings analyzed, the heat and electricity supply models implemented and the technical and economic parameters at building level are introduced.

5.2.1 Selection of reference buildings

The buildings in the Rüsdorfer Kamp (introduced in Section 2.2) were clustered according to their specific heat demand, electricity demand and the usable roof area for potential solar energy appliances. For this analysis, two existing buildings, a single-family house (SFH) and a multi-family house (MFH) typical for the district were chosen for a deeper examination and to study the impact of the global scenarios on the comparison of an individual heat supply versus a DHS. There are also non-residential buildings in the district; however, the following analysis focuses on the residential building types, as the residential buildings account for more than two-thirds of the end-energy consumption in the district.

Figure 5.2 shows the specific heat demand, the electricity demand and the PV potential related to the net floor area of the buildings for the types of SFH and MFH. In this analysis, historical energy consumption data is taken as the basis for the demand values of the *Status-quo* scenario. As a reference value for the energetic key values, the net floor area of each building is used. The heat demand includes the heat demand for space heating as well as for domestic hot water. The solar potential results from a preceding calculation of the annual electricity generation if PV modules are installed on the usable roof area of each building. This means that the so-calculated PV potential already includes the orientation of the available roof areas. In total, the building stock is characterized by a high solar potential compared to the end-energy, as the building stock consists of mainly detached or semi-detached SFH and MFH with mostly not more than three stories.

For the existing building stock in question, the average specific heat demand of the SFH is slightly higher compared to MFH (see Figure 5.2). If the refurbishment level is assumed to be equal, the compactness of the building (ratio of building envelope area to volume) could be the reason for that. In contrast, the MFH are characterized by a higher specific electricity demand, as more people tend to live in MFH per floor area, and the number of people is a major driver of electricity consumption. The third key value expressing the solar potential per floor area is on average higher in the case of a SFH. This also reflects the geometry of

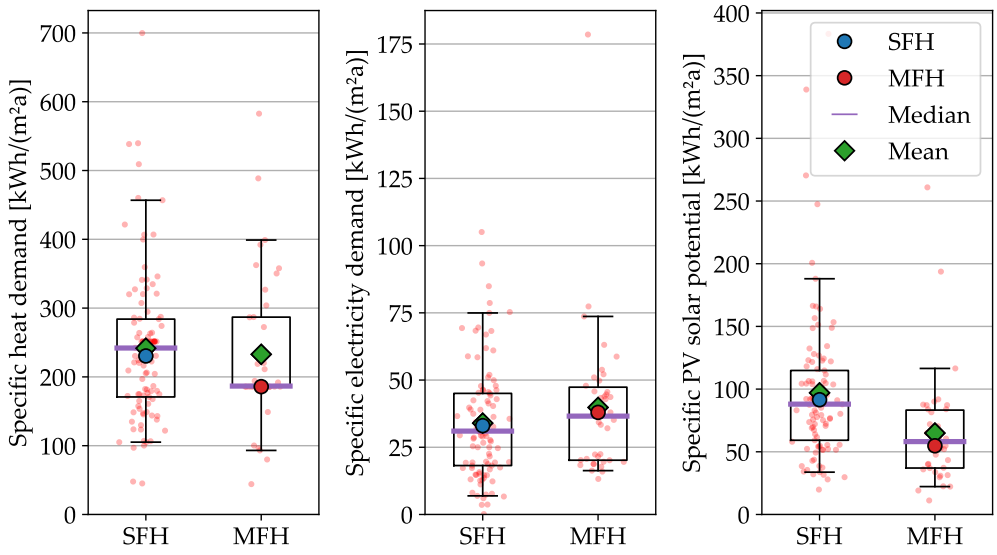

Figure 5.2: Selection and classification of the selected reference buildings of the building stock. Blue dot: selected single-family house (SFH), red dot: selected multi-family house (MFH).

the different building types in so far as larger and more compact buildings have less building envelope area and therefore also less roof area per net floor area. (see Figure 5.2)

For each of the two residential building types, a building as average as possible with respect to all three categories was selected for each of the two building types and used as a reference building in the following analysis. Table 5.2 gives an overview of the detailed energetic key values of the two reference buildings for the three refurbishment scenarios. The differences between the refurbishment scenarios are the temperature level of the heating system and the heat demand for space heating.

The SFH selected is a semi-detached house (Figure 5.3(a)). It is characterized by one and a half full floors with a total net floor area of 81 m² that is inhabited by two people. The saddle roof is oriented west-east with a usable area of 56 m² that could be utilized for solar appliances. The building itself is mainly un-refurbished and characterized by a specific heat demand of 229 kWh/(m²a), which is close to the average heat demand of all SFH in the district.

The MFH selected is inhabited by 11 people and has a total net floor area of 402 m² distributed over two and a half full floors (Figure 5.3(b)). The roof is also a saddle roof oriented north-west-south-east with a total usable area for solar appliances of 136 m². The specific heat demand is lower than the average heat demand of all MFH in the district, but about the median value. The solar potential related to the total end-energy demand is, with a value of 0.245, substantially lower compared to the SFH (0.347). Figure 5.3 illustrates the two selected building types.

As explained in Section 3.3.1, the refurbishment scenarios represent idealized extreme scenarios of the existing building stock, e.g. it is not guaranteed that this kind of supply temperature of 47 °C can be achieved in every MFH due to technical restrictions regarding the refurbishment or limitations regarding the existing heating system. Also, it might imply huge investment

Table 5.2: Overview of parameters of energetic key values and refurbishment scenarios of reference single-family house (SFH) and multi-family house (MFH).

	Scenario names	Forward / return temperature [°C]	Space heating demand [MWh/a]	Demand DHW [MWh/a]	Electricity demand [MWh/a]	Net floor area [m²]	Specific heat demand [kWh/(m²a)]	Solar potential [m²] / [kW_p]
SFH	**Status-quo**	65-80 / 50	17.1	1.5	2.7	81	229	56 / 9.8
	Refurb-1	60 / 40	12.8	1.5	2.7	81	176	56 / 9.8
	Refurb-2	47 / 32	8.6	1.5	2.7	81	124	56 / 9.8
MFH	**Status-quo**	65-80 / 50	65.5	9.3	15.3	402	186	136 / 23.8
	Refurb-1	60 / 40	49.1	9.3	15.3	402	145	136 / 23.8
	Refurb-2	47 / 32	32.8	9.3	15.3	402	105	136 / 23.8

costs in the heating systems, e.g. for replacing the radiators, exchanging the whole domestic hot water system and installing domestic hot water stations in each apartment, and so on. The focus of this analysis is to show the impact of an energy supply and infrastructure decision on achieving carbon-neutrality if this kind of deep refurbishment is achieved.

5.2.2 Energy supply model of the buildings

For each of the buildings, two energy system models shown in Figure 5.4 for the design of heat and electricity supply are developed to compare individual heat generation versus district heating: The first model Figure 5.4(a) shows the supply variant with individual heat generation. The second model illustrated in Figure 5.4(b) represents the case with district heating as the heat supply. Analogous to the energy system model of the heat supply (see Chapter 4), the models at building level are concerned with deciding on the energy converter and storage units while providing a given energy supply (here heat and electricity) based on an optimization of one year in hourly resolution. For creating the *oemof.solph* optimization models of the buildings, the package *q100opt* was developed and applied (see Röder et al. 2022a). By the application of different emission limits, the Pareto-front is calculated showing the most cost-efficient emission reduction from a cost-optimal to an emission-optimal energy supply. The detailed methodical background to the modeling approach is given in Section 2.3.

In each subfigure of Figure 5.4, the energy demands are illustrated in the form of energy sinks on the right. In both variants, the model with individual heat supply (Figure 5.4(a)) and the

(a) (b)

Figure 5.3: Illustrations of selected reference buildings. For data protection reasons, buildings very similar to the selected reference buildings are shown. (a) Single-family house (SFH); (b) multi-family house (MFH). Source and copyright: Steinbeis-Innovationszentrum energieplus (SIZ).

model with district heat supply (Figure 5.4(b)), the energy demand consists of an electricity demand and a heat demand, which is divided into the demand for space heating and domestic hot water (DHW).

In the case of individual heat supply (Figure 5.4(a)), the heat supply with DHS is not an option and is excluded from the optimization. As heat supply options, two gas-based technologies are considered: a gas boiler and a micro-CHP, both fueled with the gas-mix of the existing gas network. As electricity-based heat supply technologies, two different types of heat pumps are investigated: an air-source and a ground source heat pump. As a ground-source, geothermal probes are considered. The general technical feasibility of heat pumps in existing buildings has been shown in field tests, e.g. by (Fraunhofer ISE 2020a). The coefficient of performance (COP) of the heat pumps depends on the refurbishment scenarios that consider different forward temperatures for the heating system. The model can invest in hot water storage tanks as thermal energy storage. The roofs of the buildings can be used for solar energy appliances. Two different technologies are considered here: PV modules for the generation of electricity, and solar thermal flat plate collectors for heat generation. The periphery of the solar thermal collectors is summarized with the energy converter that considers the peripheral thermal losses as well as the additional electricity consumption for pumps. Depending on the building, several roof surfaces with different orientation and tilt angle may be available for solar energy appliances. For each of the roof areas, an additional constraint is introduced which limits the roof area used for the installation of PV and solar thermal collectors to prevent the double use of the roof area. In the model for the analysis of the individual supply options, the sectors of heat and electricity are coupled (Figure 5.4(a)).

The second configuration (Figure 5.4(b)) investigates the heat supply via DHS, which means that all heat generation options at building level, being a gas boiler, a micro-CHP, heat pumps and solar thermal collectors are excluded, that the heat must be supplied via DHS and that the construction of a substation is necessary (see Figure 5.4(b)). In this case, the heat source

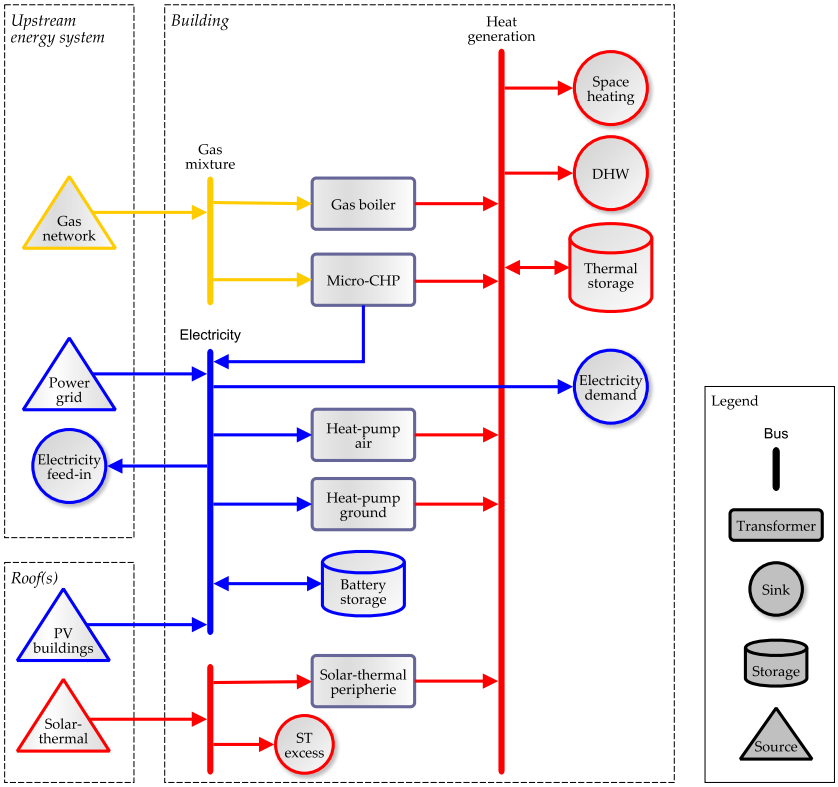

(a) Individual heat generation

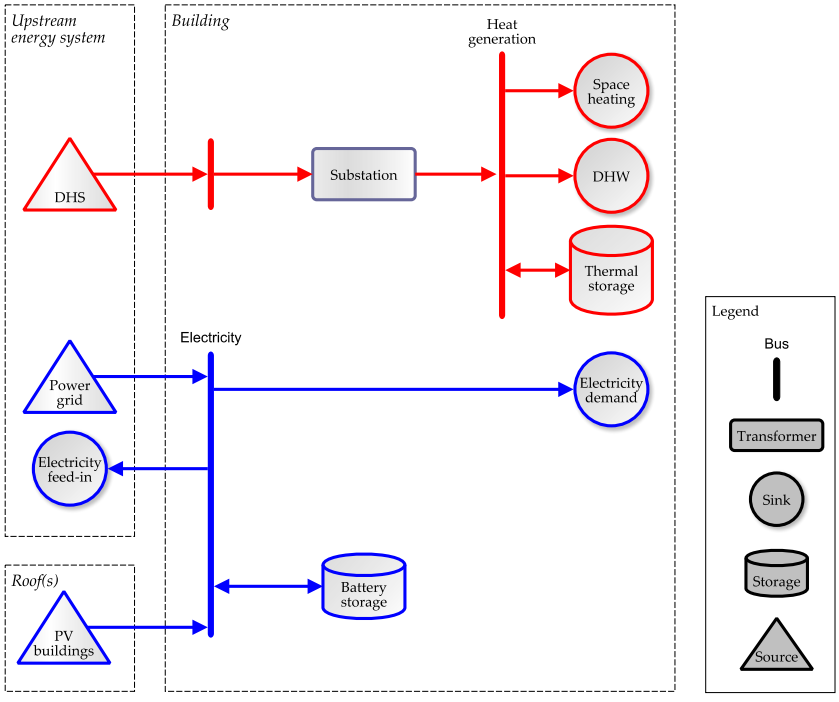

(b) Heat supply via district heating

Figure 5.4: Structure of energy supply models at building level. Blue: electricity flows; red: heat flows; yellow: gas mixtures. DHS: district heating system; DHW: domestic hot water; ST: solar thermal collectors.

of the DHS is provided by multiple commodity sources that result from the optimization of the DHS supply, presented in Section 4.3, represented by a single DHS source in Figure 5.4(b). That means that each point on the Pareto-front of the results for the district heat supply (see e.g. Figure 4.6) is implemented by an DHS commodity source. By this approach, the trade-off decision between costs and emission for the district heat supply is given with a high accuracy and can be compared with the trade-off at an individual level. In the building model with district heating as the heat source (Figure 5.4(b)), the sectors of heat and electricity are not coupled. However, to ensure a comparison between individual heat supply variant with a coupled energy system between heat and electricity at building level by the heat pumps (Figure 5.4(a)), the electricity system of the buildings is also considered in the variant with district heat supply (Figure 5.4(b)). In this way, the most cost-effective emission reduction strategies for both heat and electricity can be identified.

5.2.3 Technical and economic parameters

The modeling of the energy converter and storage units follows the same methodical approach as the technical components of the heat supply plant presented in Section 4.2.1.2.

Table 5.3 provides an overview of the technical parameters of the energy converter units and renewable energy sources applied in this model. The modeling of the heat pumps follows the same approach as in Chapter 4, considering time-resolved individual COP values depending on the temperatures of the heat source and the heating system based on a quality grade of 0.45 of the ideal Carnot-cycle. The feed-in time-series of the PV systems and solar thermal collectors are calculated individually for each roof of a building, based on the solar register (see Section 2.2.2). The feed-in time-series of PV are based on the profiles calculated as part of the QUARREE100 project (see Section 2.2.3). For the solar thermal heat generation, the library *oemof.thermal* is applied (Jnnr et al. 2020a), see Section 2.3.3. Altogether, up to three different roof areas with an individual orientation and tilt angle were considered. As most of the roof areas are tilted, no additional tilting of modules or collector is considered. The heat generation potential of the solar thermal collectors is impacted by the temperature level of the heating and domestic hot water system defined by the refurbishment scenarios. For the two building types of SFH and MFH, the maximum investment capacities are defined in such a way that they correspond to the building size (see Tables 5.3 and 5.4).

Table 5.4 presents the technical parameters of the energy storage units. The battery storage of the individual buildings is based on the same parameters as a battery storage unit at the district heat supply site, based on the currently available Lithium-Ion batteries. The thermal storage unit is assumed to be a hot water storage tank. The thermal losses of the storage are considered with two loss factors, a fixed loss factor, depending on the size of the storage, and a second factor, depending on the state of charge (see Section 2.3.2). Both factors are pre-calculated depending on the temperature level of the heating system and are given in time-resolved series for the case of a variable forward temperature. An insulation with a thermal conductivity of 0.035 W/(mK) and a thickness of 150 mm is assumed for the thermal storage at a surrounding temperature of 15 °C. The maximum storage content factor reflects the fact that a given volumetric capacity leads to different thermal storage capacities, depending on the specific temperature spread. The temperature spread is defined by the temperatures of

Table 5.3: Technical parameters of the energy converter units of the building models. SFH: single-family house; MFH: multi-family house. Own assumption based on (ASUE 2010; Danish Energy Agency 2021a).

	Thermal Efficiency	Electrical Efficiency	Maximum Full Load Hours (per year)	Maximum power	Maximum Investment Capacity (SFH)	Maximum Investment Capacity (MFH)
Symbol	$\eta_{(n,heat)}$	$\eta_{(n,elec)}$	$f_{sum,max}$	$f_{t,max}$	$P_{invest,max}$	$P_{invest,max}$
Unit	-	-	h	-	kW	kW
Gas boiler	0.94	-	-	-	50	50
Micro-CHP	0.26	0.62	-	-	15	30
Heat pump air-source	*time-series [1]	-	-	*time-series	30	60
Heat pump ground-source	*time-series [1]	-	2500	-	20	45
Solar thermal flat plate collectors	*time-series [2]	-	-	-	56 [3]	136 [3]
ST-Periphery	0.97	0.01 [4]	-	-	-	-
DHS Substation	0.98	-	-	-	50	150
PV	-	*time-series	-	-	9.8	23.8

[1] A Carnot quality grade of 0.45 is assumed for the heat pumps. The resulting efficiencies of the heat pumps depend on the refurbishment scenario and on the outside temperature in the case of air-source heat pumps.
[2] The following parameters were used for the solar thermal flat plat collector: $a_1 = 3.41$, $a_2 = 0.0161$, $\eta_0 = 0.825$ (based on Stiebel Eltron 2017). ΔT is determined by the temperature level of the buildings (see Section 3.3.1) and the ambient temperature. See also Section 2.3.3.
[3] Potential area for solar appliances in m².
[4] The value refers to the electrical energy consumption per kWh.

Table 5.4: Technical parameters of the energy storage units of the building models. SFH: single-family house; MFH: multi-family house. Own assumption based on pre-calculations and (C.A.R.M.E.N. e.V. 2021; Danish Energy Agency 2020a).

	Loss rate per energy content	Loss rate per installed capacity	Inflow efficiency	Outflow efficiency	C-rate charging	C-rate decharging	Max. capacity (SFH)	Max. capacity (MFH)
Symbol	β	γ	η_{in}	η_{out}	$f_{n,cap-in}$	$f_{n,cap-out}$	W_{max}	W_{max}
Unit	-	-	-	-	kW_{in} / $kWh_{install}$	kW_{out} / $kWh_{install}$	kWh	kWh
Battery storage	0.00001	-	0.95	0.95	0.5	0.5	30	90
Thermal storage	* time-series	* time-series	-	-	-	-	60	180

the heating system of the refurbishment scenarios. This means that a volumetric capacity of e.g. 1 m³ results in a lower thermal capacity in the refurbishment scenario *Refurb-2*, as the temperature spread decreases in this scenario, and in higher energy specific investment costs for one kilowatt-hour storage capacity. On the other hand, the thermal loss decreases in this scenario due to the lower temperature level.

Tables 5.5 and 5.6 provide the economic parameters of the energy storage options at building level. The calculation of the capital expenses per year follows the approach given in Section 2.3.3. Similar to the investment costs for the energy converter and storage units of the district heat supply, a weighted average cost of capital of 2 % per year is assumed. The yearly costs for maintenance and operation are added to the capital expenses per year and result in the specific investment costs $c_{(i,o),invest}$ and $c_{(i,o),investfix}$ (see Equation 2.3) assigned to the *oemof.solph* optimization model.

At building level, the usage of binary variables for modeling the investment decisions becomes important as many heat generation units are not available below a certain size, and the specific investment costs per kilowatt installed capacity decrease very fast due to a high share of one-time costs for installation. E.g. the specific costs per kilowatt installed capacity of a Micro-CHP are very high compared to larger CHP units (Fisch et al. 2015).

For the analysis of the heat supply options at building level, the same global scenario framework as for the district heat supply is considered (see Section 4.2.2). Therefore, the commodity prices of electricity and gas are also based on the price scenarios introduced. However, the specific energy costs of private households for one kilowatt-hour electricity or gas are higher than the prices a district heat supplier can achieve as a major customer with a high energy demand. Therefore, the historical price difference of private households and commercial customers was evaluated based on (Bundesnetzagentur 2021; BMWi 2021). For both energy commodities of

Table 5.5: Economic parameter of the energy converter units. Own assumptions based manufacturer data and (Danish Energy Agency 2021a; ASUE 2015; Prognos et al. 2020a; Fraunhofer ISE 2020c; Fisch et al. 2015).

	Variable Investment Costs	Fix Investment Costs	M/O Costs (of *capex*)	Technical Lifetime	Minimum capacity
Symbol	$capex$	$capex_{fix}$	f_m	N	$P_{invest,min}$
Unit	€/kW$_{th/el}$	€	% / a	a	kW$_{th/el}$
Gas boiler	129	4097	3.0	20	10
Micro-CHP [€/kW$_{el}$]	2470	14500	3.0	18	1
Heat pump air-source	529	6320	2.5	18	5
Heat pump ground-source	1100	17000	3.0	25	8
Solar thermal collectors [€/m²]	700	-	1.0	25	1
DHS Substation	39	4940	1.0	25	12
PV [€/kWp]	1000	-	0.5	25	-

Table 5.6: Economic parameter of the energy storage units of buildings. Own assumptions based on (Fisch et al. 2015; Fraunhofer ISE 2020c; Danish Energy Agency 2020a).

	Variable Investment Costs	Fix Investment Costs	M/O Costs (of *capex*)	Technical Lifetime
Symbol	$capex$	$capex_{fix}$	f_m	N
Unit	€/kW$_{th/el}$	€	% / a	a
Battery storage	900	-	1.0	12
Thermal storage	50	-	1.0	30

gas and electricity, the costs for procurement, distribution and margin, as well as the fees and taxes correlate with the purchase quantity. The relation of energy prices of private households to commercial and industrial customers ranges from a factor of 1.2 for small commercial customers to a factor of greater than two for large scale industrial customers (Bundesnetzagentur 2021). This factor can be observed for electricity and gas even though the absolute price level and the share of fees and taxes differs. Therefore, a factor of 1.5 is applied for the energy costs of private households compared to the district heating facility of the district analyzed. This factor corresponds well to the price assumptions for the realization of a district heat supply in the project QUARREE100 for Rüsdorfer Kamp and the net prices of private households (PHH) in 2020 (Electricity: DHS: 17–19 ct/kWh; PHH: 26–28 ct/kWh; Gas: DHS: 3–4 ct/kWh; PHH: 5–6 ct/kWh) (compare also Bundesnetzagentur 2021). It is obvious that this factor influences the feasibility of DHS versus individual heat supply, and it is also a matter of policy, as the share of fees and taxes for private households amounts to more than two-third for electricity and about half of the price for gas. Thus, this factor is kept constant throughout the analysis – also known as the *ceteris paribus* concept in economics – in order to focus on the actual subject of investigation, the impact of the global and local scenarios on the feasibility of DHS for achieving a carbon-neutral heat supply.

5.3 Results

Figure 5.5 provides an overview of the scenario combinations analyzed. For the scenarios of the upstream energy system (global scenarios), the scenario framework introduced in Section 4.2.2 is applied. The analysis is performed for three energetic refurbishment scenarios of the existing building stock that imply different heat demands and a decrease of the supply temperature in the scenarios *Refurb-1* and *Refurb-2* (see Section 3.3.1).

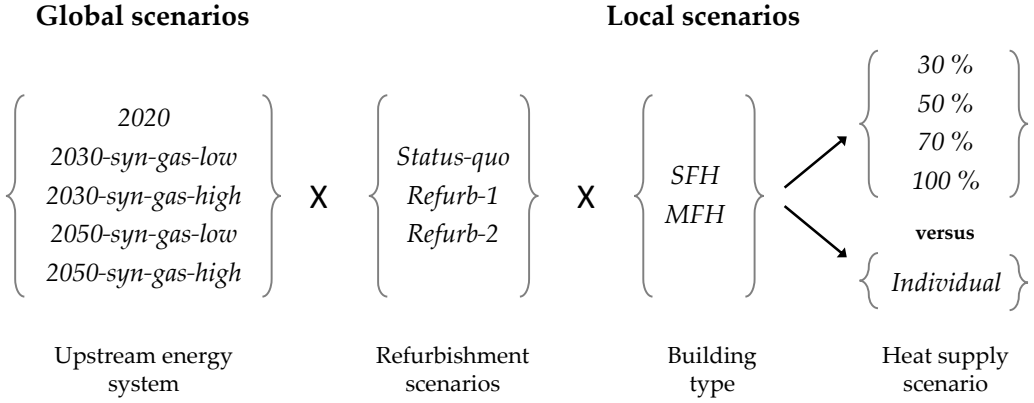

Figure 5.5: Overview of the investigated scenarios for the comparison of district heating with individual heat supply. SFH: single-family house; MFH: multi-family house.

In regard to the existing building stock, an average SFH and an average MFH introduced in Section 5.2.1 are considered. For the heat supply via DHS, different connection quota are investigated (30 % to 100 %) that are related to different heat demand densities (see Figure 3.8). In both cases, the heat supply via district heating and the individual supply, the electricity sector of the building is also considered. The corresponding energy models of both supply variants are introduced in Section 5.2.2, Figure 5.4.

5.3.1 Results of individual heat supply options

The following sections present the results of the Pareto-optimization of the individual heat and electricity supply solutions (energy model of Figure 5.4(a)). An overview of the scenarios is given in Figure 5.5. Below, the medium price paths of electricity and gas are presented for the scenarios of the upstream energy system (see Section 4.2.2.2).

5.3.1.1 Scenario Status-quo

Figure 5.6 shows the results of the Pareto optimization of costs and emission for the two exemplary buildings. The results are related to the average costs and average emission per floor area (m^2) and year (a) as in the previous chapter for a better comparison of different refurbishment scenarios. The lowest energy supply costs occur for both buildings in the cost-optimal solutions of the scenarios *2020* (points “1.00”, blue marker). With an increasing share of renewable energies in the upstream infrastructures, the absolute costs in the cost-optimal

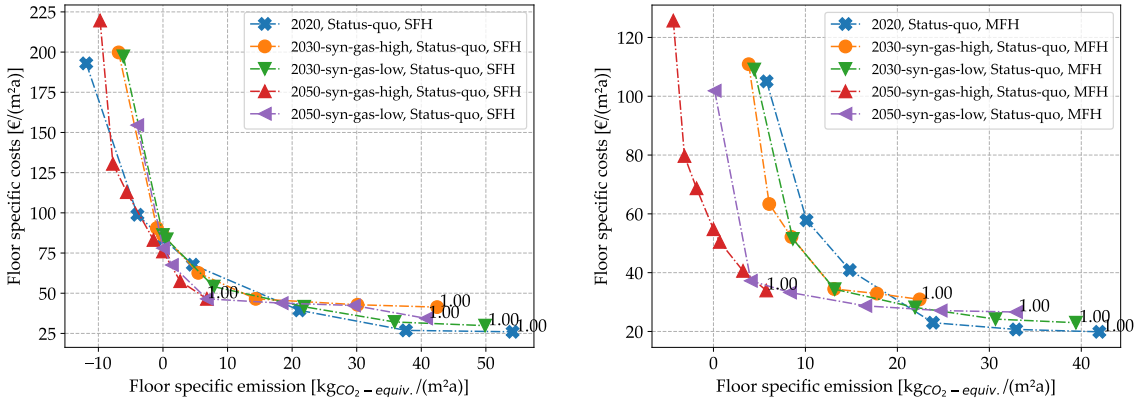

(a) Reference SFH

(b) Reference MFH

Figure 5.6: Pareto-Fronts of refurbishment scenario *Status-quo* of the (a) reference single-family house (SFH) and (b) reference multi-family house (MFH).

solutions increase and the total emissions of the energy supply decrease (Figure 5.6, points "1.00", red, purple, green and orange plots).

In the case of the SFH, carbon-neutrality can be achieved in all scenarios and the results of the carbon-neutral solution lead to about double costs compared to the most cost-efficient solution. In contrast, in the case of the MFH, carbon-neutrality is only achieved in the scenarios of 2050. As the MFH is characterized by a lower PV potential per square meter floor area and by a higher floor-specific electricity demand (see Figure 5.2), it is more difficult to achieve a carbon-neutral energy supply without relying on the high shares of renewable energies of the upstream infrastructures. Furthermore, the Pareto-fronts of the MFH show a bigger deviation for the different upstream scenarios when it comes to the low emission values. Compared to the SFH, especially the scenario of 2020 behaves differently: in the case of the SFH, this scenario performs almost as well as the scenarios with a high share of renewable energies (Figure 5.6(a), blue graph), whereas in the case of the MFH, the results of the scenario 2020 are worse than in the future energy scenarios for low emission values (Figure 5.6(b), blue graph). For the MFH, the renewable energy potential in the form of solar potential per floor area is much lower compared to the SFH. This means that the MFH needs to rely more on energy imports from the upstream energy infrastructures. In contrast, the SFH generates a surplus of renewable electricity with the PV system and feeds the electricity into power grid, which is honored by emission credits.

Figures 5.7 and 5.8 show the investment decisions for both reference buildings, depending on floor-specific emissions. For solar energy appliances, the orientation of the buildings' roofs was considered individually, based on the solar register given in Section 2.2.2, Figure 2.10(a). For the presentation of the investment decisions in Figures 5.7 and 5.8, the potential solar installations were labeled according to the main orientation of the roof. In this case, the SFH (Figure 5.7) has two roof areas usable for solar appliances facing west and east. The main direction of the roof of the MFH is south, while the north-facing roof was not taken into account (Figure 5.8).

For both buildings, gas boilers are deployed as heat generation technology in the cost-optimal solutions in all scenarios of the upstream energy system, but not in the *2050-syn-gas-high*. In this scenario, the gas price is so high that heat pump technologies are deployed for heat generation in the cost-optimal solution. In the MFH in scenario *2030-syn-gas-high*, the gas boiler is already supported by an air-source heat pump in the cost-optimal solution. Solar thermal heat generation plays in all scenarios a minor role. Only in the scenarios of 2030, a very low capacity of solar thermal flat plate collectors of about 1 m^2 is installed at the SFH. Also, in all scenarios and at both buildings, PV capacities are already installed in the cost-efficient solutions, and are rapidly extended to maximum capacity when emissions are reduced, which emphasizes that PV is a very cost-efficient technology for emission reduction.

To reduce emissions further, the next measure is to install air-source heat pumps and a thermal storage in addition to the gas boiler. An exception is the scenario *2050-syn-gas-high*. In this scenario, an air-source heat pump is already cost-optimal. A further reduction of emissions leads to a change in technology from air-source to ground-source heat pumps in the 2050 scenarios. For the SFH, this can be observed for the scenarios of 2030 and the scenario *2050-syn-gas-low*. For the MFH, the geothermal heat pump is installed additionally to the air-source heat pump in the scenarios *2050-syn-gas-low* and *2020*, and this technology shift takes also place in the scenario *2050-syn-gas-high*.

In scenarios *2020 and 2050-syn-gas-high*, a micro-CHP supports a cost-efficient emission reduction in the case of both buildings. In the scenarios *2020*, the electricity generation from the Micro-CHP profits from emission credits via feed-in to the upstream power grid. In scenario *2050-syn-gas-high*, the emission factor of the gas network is so low that a Micro-CHP and in the case of the SFH a gas boiler are an efficient emission reduction options. Lastly, the battery storage is extended and contributes to a further emission reduction by shifting electricity from times of a low emission factor to times with a high emission factor.

5.3.1.2 Refurbishment scenarios

In refurbishment scenario *Refurb-1*, carbon-neutrality can also be achieved for the MFH (see Figure 5.9(b)). In this case, the extra costs for carbon-neutrality compared to the cost-optimal case range from 50 % in the scenario *2050-syn-gas-high* to about five times the costs of the cost-optimal case in scenario *2020*. This differs in the case of the SFH (Figure 5.9(a)). Here, the additional costs for carbon-neutrality compared to the cost-efficient solutions lie between one and a half to two times more. Altogether, for both buildings, the costs for carbon-neutrality reduce drastically due the refurbishment and a carbon-neutral state can be achieved at lower cost (compare Figure 5.6).

In the refurbishment scenario *Refurb-2* (Figure 5.10), the costs for carbon-neutrality further decrease. For the SFH, carbon neutrality can be achieved in all global scenarios with almost equal costs of about 25 to 30 €/(m^2a) (equal to about 2000 to 2500 €/a given a net floor area of 81 m^2), which is slightly more than the cost-optimal solution. For the MFH, the costs amount to about twice the cost-optimal solution. Altogether, for the MFH, the three refurbishment scenarios clearly illustrate the importance of energetic refurbishment. If these types of MFH

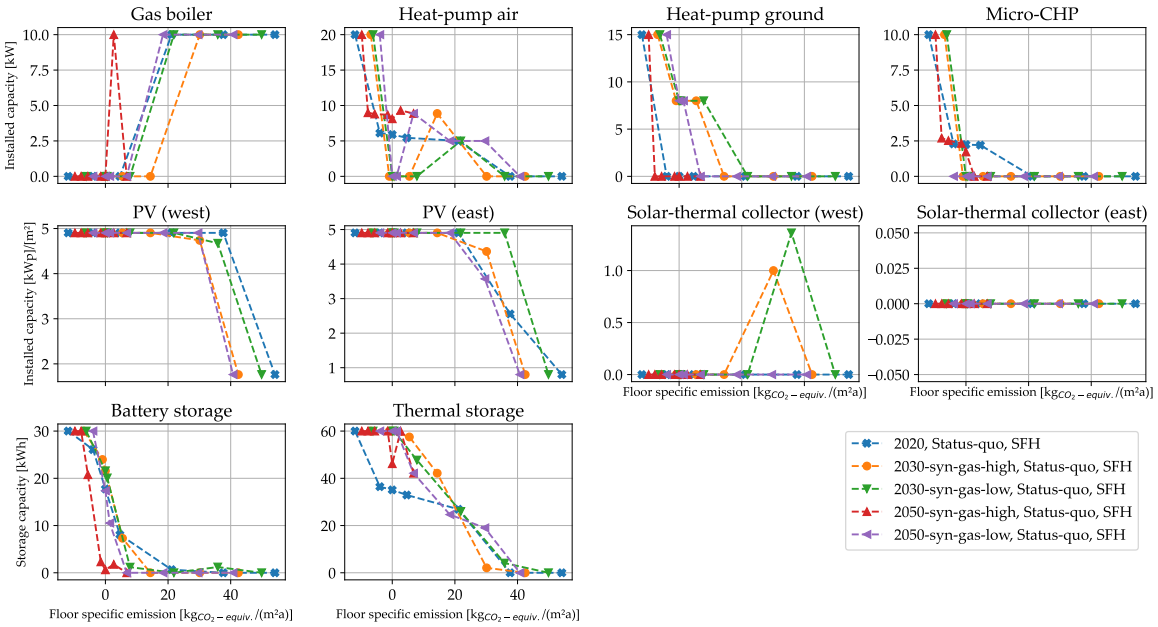

Figure 5.7: Investment decisions of refurbishment scenario *Status-quo* for the reference SFH.

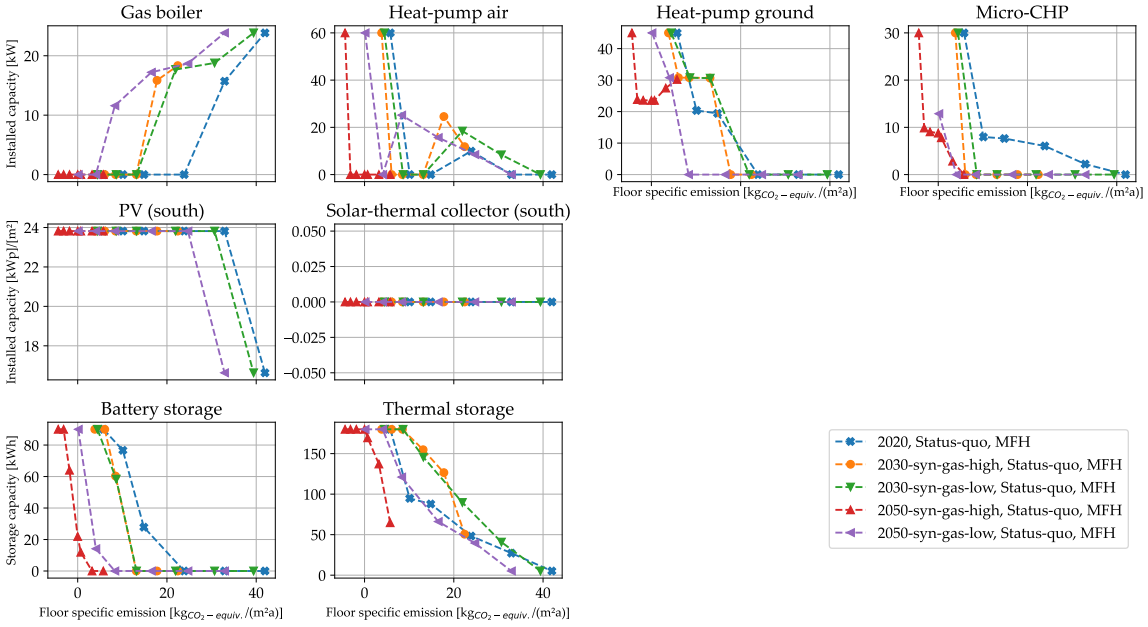

Figure 5.8: Investment decisions of refurbishment scenario *Status-quo* for the reference MFH.

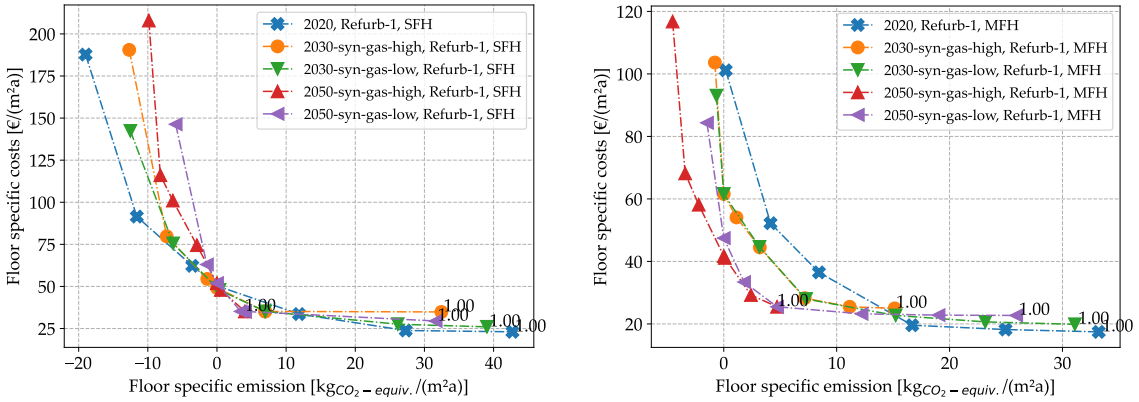

(a) Reference SFH (b) Reference MFH

Figure 5.9: Pareto-Fronts of refurbishment scenario *Refurb-1* of the (a) reference single-family house (SFH) and (b) reference multi-family house (MFH).

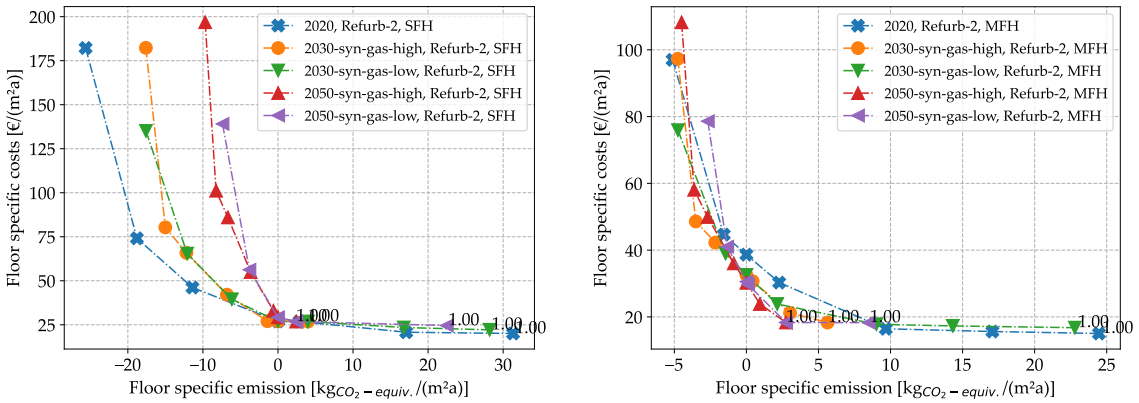

(a) Reference SFH (b) Reference MFH

Figure 5.10: Pareto-Fronts of refurbishment scenario *Refurb-2* of the (a) reference single-family house (SFH) and (b) reference multi-family house (MFH).

stay un-refurbished, carbon-neutrality can only be achieved if there is a high share of synthetic renewable gas in the gas network (in scenario *2050-syn-gas-high*).

The investment decisions for the refurbishment scenarios follow the same order as in scenario *Status-quo*. The detailed results of the investment decisions can be reviewed in Appendix B.2 in Section B.2 and are summarized within the next section.

5.3.1.3 Summary of individual heat supply solutions

The analysis of heat supply options at building level is based on an LP and MILP modeling approach. Within this modeling approach, the following conclusions can be drawn regarding the role of the different technologies at building level in the context of the scenarios investigated:

Gas boiler Gas boilers are currently the most distributed heat generation technology at building level in many districts. The analysis above confirms this choice as a gas boiler is currently the most cost-efficient heat generation technology in scenario *2020*. To reduce emissions, a gas boiler becomes less important in all scenarios investigated and is not part of any emission-optimal energy system. Even in cases with a high share of synthetic renewable gas in the gas network, a gas boiler is either not selected at all or not selected as the only heat generation technology for achieving carbon-neutrality at least cost. There are scenarios in which a bivalent system in the form of a gas boiler in combination with an air-source heat pump is selected as an emission reduction path, e.g. for the MFH in the scenarios of the *syn-gas-low* path and the scenarios of *2020*.

Heat pump For a cost-efficient emission reduction, heat pumps are the most important heat generation technology in all scenarios. Even in the case of un-refurbished buildings, heat pumps are important for an emission reduction, partly in combination with a gas boiler (see above). When emissions are reduced further, the ground-source heat pump is deployed after the air-source heat pump. The ground-source heat pump is a more expensive but also more efficient technology, which leads in many scenarios to a technology shift from an air-source to a ground-source heat pump.

Micro-CHP Compared to a gas boiler or an air-source heat pump, a Micro-CHP is a very expensive appliance at building level (compare Table 5.5). Nonetheless, this technology becomes relevant as technology at building level for the reduction of emissions in the scenarios *2020* and *2050-syn-gas-high*, especially in the case of the MFH. In the scenario *2020* representing the current state of the upstream energy system, the Micro-CHP can contribute to an emission reduction by electricity generation for the building's own consumption and for the heat pumps, and also for exporting electricity to the upstream energy system. The Micro-CHP is never deployed as the sole energy converter, and never in combination with a gas boiler.

Photovoltaic system (PV) In all scenarios, the installation of a certain capacity of PV is already part of the cost-efficient solution. The extension of PV capacities to the maximum is the cheapest emission reduction strategy for the de-carbonization of the electricity and heat demand of the buildings. The comparison of the two building types investigated shows the influence of the solar roof potential to achieve carbon-neutrality. For the SFH, it is much easier to obtain net zero emissions as the PV potential per floor area is substantially higher compared to the MFH. By feeding the PV surplus into the grid, it is further possible to contribute to the de-carbonization of the power grid.

Solar thermal collector Solar thermal heat generation via flat plate collector plays just a subordinate role in the cost-efficient emission reduction at building level in the investigated future scenario settings. Solar thermal competes with PV, which is a more flexible energy source, e.g. the electricity from PV can be used for the building's own consumption of electricity, or be fed into the power grid, or could drive heat pumps. Furthermore, as heat pumps act as the main heat generation technology and might be installed anyway, solar thermal collectors for

domestic hot water compete with a high COP of air-source heat pumps in summer. Although the specific energy yield per square meter for solar thermal collectors is higher than for PV, especially in summer, the excess heat cannot be fully utilized while the PV excess can be fed into the power grid.

Thermal storage The installation of thermal storage capacities increases in all scenarios in combination with the deployment of air-source heat pumps. To increase the COP of the air-source heat pump, the heat pump needs to be operated during the day at high outside temperatures. In the best case, there is electricity generation from the PV, or the emission factor of the electricity grid is low. To match all of this optimally with the time of actual heat demand, thermal storage capacities are absolutely necessary and an essential part of any individual supply scenario.

Battery storage The installation of a battery storage can improve the emission balance of buildings by shifting electricity from times with a high PV generation to times of actual electricity demand in the building or driving the heat pump for heat generation. Additionally, a battery storage can be used for importing electricity at times with a low emission factor of the upstream power grid (times with a high share of renewable energies in the upstream power grid) and for exporting electricity at times of a high emission factor, which means a high share of fossil electricity generation. In most of the scenarios the battery storage is installed as least option for emission reduction due to the high costs. However, if the battery capacity is expanded with the only purpose of importing electricity from and exporting electricity into the upstream power grid to contribute to a further emission reduction, this additional battery capacity does not necessarily need to be placed within the building and not even in the district, as it solely addresses shifting energy in the upstream power grid. For this purpose, the battery could be installed at critical power grid connection points on a larger scale, which also simplifies access and control if the capacity of the battery storages for many buildings can be realized via a single battery storage unit. This example also demonstrates that for deriving overall cost-efficient emission reduction strategies, an integrated cross-sectoral viewpoint needs to be taken.

Despite the existing gas network, even in the *2050-syn-gas-high* scenario with a high share of renewable synthetic gas in the gas network, simply switching the fuel of the current common gas boiler technology is not a cost-optimal supply solution for achieving a carbon-neutral building stock, independent of the refurbishment scenario. Furthermore, the analysis of individual heat supply options of two different building types reveals how difficult it can be to obtain net carbon-neutrality. Following this, the next section compares the above-described optimal emission reduction paths for the individual supply solutions with heat supply via DHS.

5.3.2 Comparison of district heating and individual heat supply

In this section, the cost-optimal emission reduction paths of the individual heat supply options from the previous section (energy model of Figure 5.4(a)) are compared with the heat supply via district heating (energy model of Figure 5.4(b)). An overview of the scenarios considered

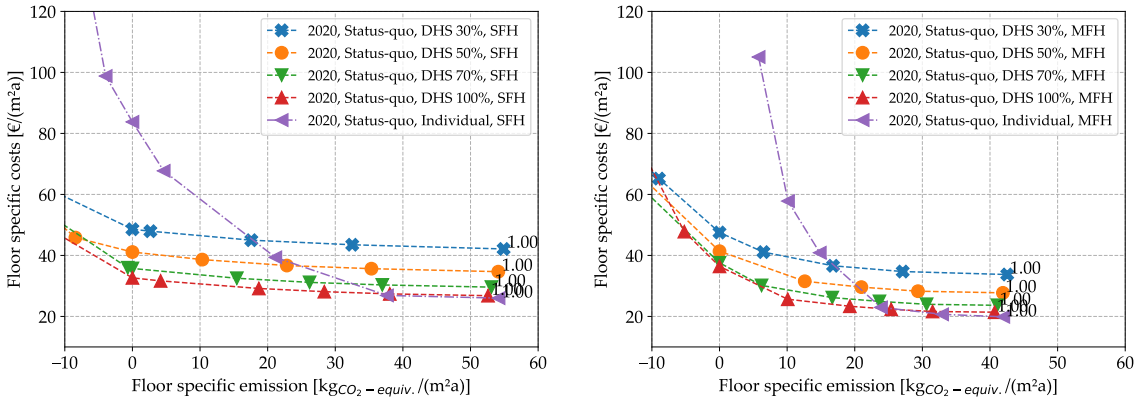

(a) SFH, *Status-quo*, *2020*

(b) MFH, *Status-quo*, *2020*

Figure 5.11: Comparison of individual heat supply versus DHS for the refurbishment scenario *Status-quo* and the global scenario *2020*. (a) Single-familiy house (SFH) and (b) multi-family house (MFH).

is given in Figure 5.5. The aim is to investigate the impact of the different global scenarios of the upstream energy infrastructure gas and electricity (see Section 4.2.2) on the economic feasibility of DHS to achieve a carbon-neutral heat and electricity supply to the buildings. Based on the corresponding heat densities of the connection scenarios, heat density thresholds for the feasibility of district heating compared to individual heat supply are determined for each scenario.

5.3.2.1 Scenario Status-quo

In the following figures, the results for the current mainly un-refurbished building stock in regard to an individual heat supply versus supply via DHS are compared. The results for the reference SFH are shown on the left and for the reference MFH on the right. In each diagram, the trade-off solutions between costs and emissions are shown for the individual heat supply options (“Individual” – purple plot) based on Section 5.3.1 and the heat supply via DHS for the different connection scenarios ranging from 30 % to 100 % of the buildings connected to a DHS. In this comparison, the costs comprise the total costs related to the net floor area of each building for supplying heat and electricity. This means that also for the cases with heat supply via DHS, a combined consideration of heat and electricity is performed as illustrated in Figure 5.4(b). The results thereby include a comparison of individual measures, e.g. the installation of PV, compared to the option of higher costs for a lower emission DHS. In each of the following figures, the focus is placed on solutions for achieving the net zero emissions, hereinafter also called “carbon-neutrality”, as the costs of further emission reductions are outside the scope of financially feasible solutions. Figure 5.11 shows the results for both reference buildings for the upstream energy system of scenario *2020*.

For both reference buildings, the cost-optimal case of the individual heat supply (purple plot at point “1.00”) is approximately equal to the DHS supply with a connection quota of 100 % of the existing building stock. This means that connecting to a DHS with a connection quota of

significantly less than 100 % would not be cost-optimal from the point of view of either reference building. Also, in both cases, the emission can be reduced at little extra cost by expanding the PV capacity (compare Figure 5.7 and Figure 5.8), where the results of the 100 % connection scenario and the individual supply are almost equal. For further emission reduction, the costs for individual heat supply increase significantly more than for heat supply with DHS. For the SFH, this is the point of the technology switch from gas boiler to heat pump (Figure 5.7). In the MFH, the gas boiler is replaced by a heat pump and a Micro-CHP (Figure 5.8). For the SFH, at the carbon-neutral point, the energy costs for the individual heat supply are well above the heat supply via DHS, also if the connection quota lies only at 30 %. In the case of the reference MFH, carbon-neutrality cannot be achieved via individual heat supply. This scenario shows an example in which the competitiveness of a DHS is strongly affected by the emission level that should be achieved: in the cost-optimal case, a connection quota of 100 % is required in order to be competitive in comparison to individual supply options, and in regard to the reduction of emissions, the required connection rate drops, which means that lower heat demand densities are sufficient for competitive DHS solutions.

In the scenarios *2030-syn-gas-low* (Figures 5.12(a) and 5.12(b)), the total costs in the cost-efficient solution are slightly above the 100 % connection scenario for both reference buildings. In case of the SFH (Figure 5.12(a)), the costs for the individual supply increase more steeply compared to the supply via DHS, as emissions are decreased. At about 35 $kg_{CO_2-equiv.}/(m^2a)$, the individual supply becomes more expensive compared to the DHS supply with a connection quota of 70 % (purple/green line). At carbon-neutrality, the individual supply is equally expensive as the DHS. In contrast, for the MFH of the scenario *2030-syn-gas-low*, the individual supply and the DHS supply with a connection quota of 100 % are equal up to an emission reduction to about 10 $kg_{CO_2-equiv.}/m^2a$. Below that, the individual supply becomes more expensive and carbon neutrality can only be achieved via DHS supply.

The results of the scenarios *2030-syn-gas-high* are shown in Figures 5.12(c) and 5.12(d). In this scenario, it is assumed that the share of renewable synthetic gas is 20 % (see Section 4.2.2). Thus, the cost-optimal solutions move to the left as the emission factor of gas is reduced, and slightly to the top as the costs for gas are increased. For the SFH, the cost-optimal solution lies between the 50 and 70 % connection scenario in regard to costs. With a reduction in emissions, the individual heat supply deteriorates relative to the DHS supply in the same way as the scenarios already presented, and leads to slightly higher costs at the carbon neutral point compared to the DHS supply with a connection quota of 30 %. Compared to scenario *2030-syn-gas-low*, the costs for carbon-neutrality are in the same range for the reference SFH. In the case of the reference MFH, the results are similar for both scenarios of the upstream energy system. At emission values above 10 $kg_{CO_2-equiv.}/(m^2a)$, the individual supply lies in the range of the 70 % to 100 % connection scenarios. For low emission values, the individual supply exceeds the costs of the lowest connection scenario, and does not achieve carbon-neutrality.

Altogether, in the scenarios of 2030, the comparison of the *syn-gas-low* and the *syn-gas-high* scenario does not impact on the decision about the economic feasibility of a DHS or increase or decrease the heat demand density thresholds.

Figure 5.13 presents the results of the scenarios with a high share of renewable energy in the upstream energy infrastructures. Thus, the emissions of the cost-optimal solutions also decrease

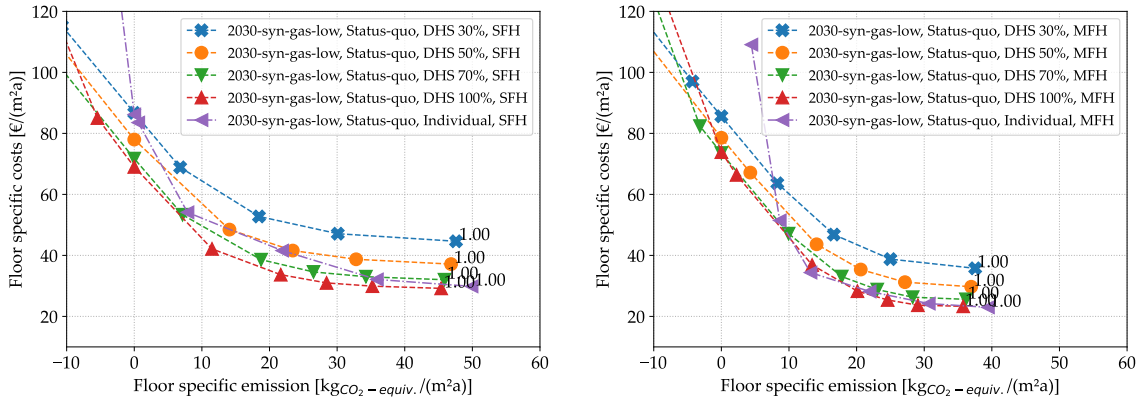

(a) SFH, *Status-quo*, *2030-syn-gas-low*

(b) MFH, *Status-quo*, *2030-syn-gas-low*

(c) SFH, *Status-quo*, *2030-syn-gas-high*

(d) MFH, *Status-quo*, *2030-syn-gas-high*

Figure 5.12: Comparison of individual heat supply versus DHS for the refurbishment scenario *Status-quo*. Scenario *2030-syn-gas-low* (top: (a) and (b)) and the Scenario *2030-syn-gas-high* (bottom: (c) and (d)). SFH (left: (a) and (c)) and MFH (right: (b) and (d)).

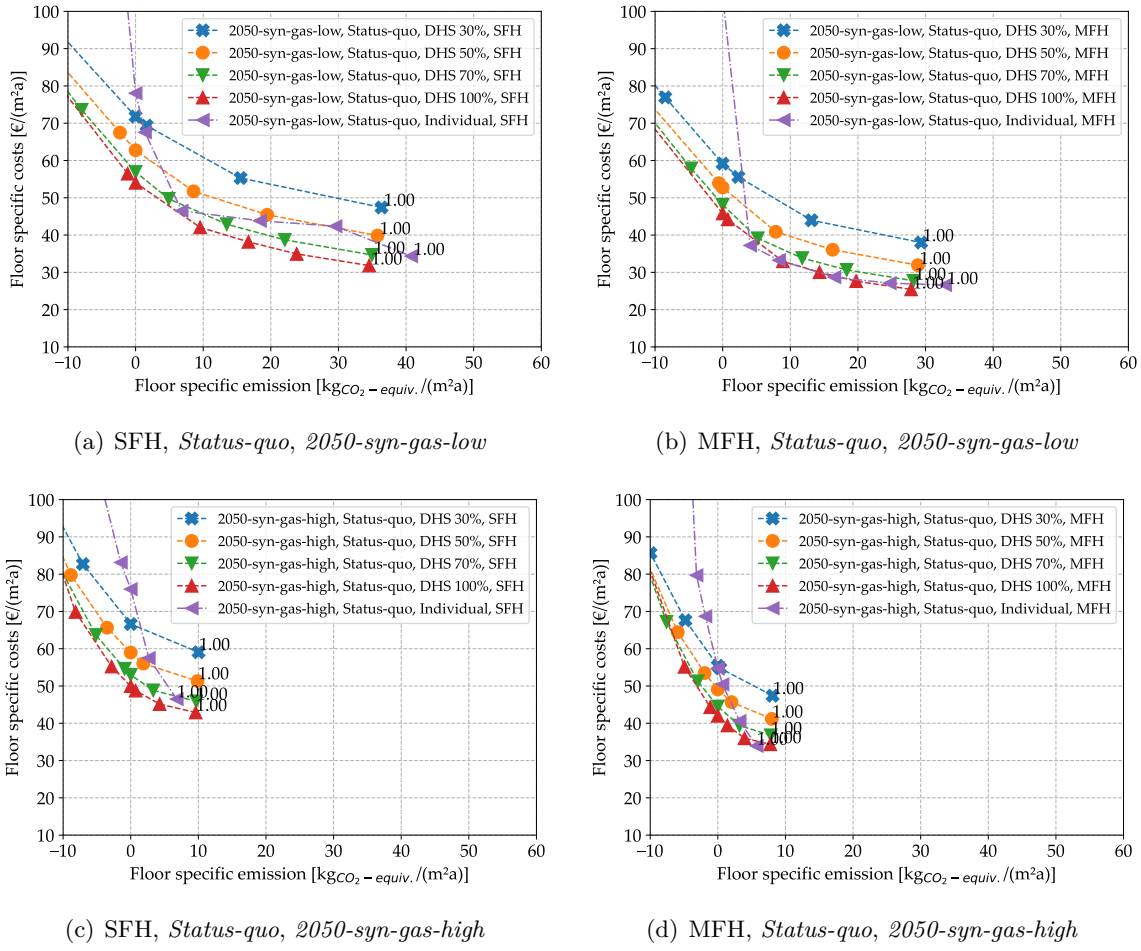

(a) SFH, *Status-quo*, *2050-syn-gas-low*

(b) MFH, *Status-quo*, *2050-syn-gas-low*

(c) SFH, *Status-quo*, *2050-syn-gas-high*

(d) MFH, *Status-quo*, *2050-syn-gas-high*

Figure 5.13: Comparison of individual heat supply versus DHS for the refurbishment scenario *Status-quo*. Scenario *2050-syn-gas-low* (top: (a) and (b)) and the Scenario *2050-syn-gas-high* (bottom: (c) and (d)). SFH (left: (a) and (c)) and MFH (right: (b) and (d)).

and the graphs move to the left of the diagram. In all cost-optimal solutions of 2050, the costs of individual heat supply scenarios lie in the range of the costs of a DHS supply with a connection quota from 70 % to 100 %.

In scenario *2050-syn-gas-low* (Figures 5.13(a) and 5.13(b)), both heat supply strategies, individually and via DHS, are characterized by a moderate increase in costs from the cost-optimal solution up to emission values of about 5 $kg_{CO_2-equiv.}/(m^2a)$. The costs of the individual heat supply for the reference SFH varies between the 50 % and 100 % connection scenario. For the MFH, the costs lie in the range of the 100 % connection scenario. Until that point, first the extension of the PV, and second, the installation of an air-source heat pump in addition to a gas boiler is a cost-efficient emission reduction strategy (see Figures 5.7 and 5.8). From that point on, a further emission reduction becomes more expensive for the individual supply by abandoning the gas boiler and installing a ground-source heat pump and a battery storage unit. Consequently, the costs of a carbon-neutral energy supply with individual heat generation are clearly higher than the 30 % connection scenario (see Figure 5.13(b) upper right: purple plot (individual heat supply) versus blue plot (30 % DHS scenario)).

In the scenario *2050-syn-gas-high* (Figures 5.13(c) and 5.13(d)), the cost-optimal solutions are already almost carbon-neutral, as both upstream infrastructures, the electricity and the gas network, are characterized by a high share of renewable energy. However, the marginal costs for emission reduction are much higher for the individual heat supply options than for the DHS scenarios. This leads to higher costs for the individual heat supply in order to achieve carbon-neutrality for both reference buildings analogous to scenario *2050-syn-gas-low*.

Altogether, the analysis of the refurbishment scenario *Status-quo* reveals that when approaching carbon-neutrality, the marginal emission abatement costs increase more for individual heat supply than for heat supply via DHS, independent of the future scenarios considered for the upstream energy infrastructures. In the cost-optimal cases, high connection quota of 70 % or 100 % are required to compete with individual heat generation via gas boilers and the existing gas network. To obtain a carbon-neutral energy supply, the heat supply via DHS outperforms the individual heat supply due to the higher marginal emission abatement costs, especially towards carbon-neutrality. For the reference MFH, carbon-neutrality via individual heat supply can only be achieved in the scenarios of 2050. For the reference SFH, the individual heat supply scenario only competes in the scenarios of 2030 at very high costs in the low connection scenarios.

A comparison of the *syn-gas-low* and the *syn-gas-high* scenarios reveals that the higher availability of renewable gas in the *syn-gas-high* scenarios does not unambiguously shift the heat demand density threshold for the economic feasibility of district heating compared to individual heat supply for achieving carbon-neutrality. Despite the fact that the gas network exists and no extra costs for the gas network are involved, for the SFH, the costs of energy for individual heat generation are higher than the lowest connection scenario for both *syn-gas-high* scenarios of 2030 and 2050 (see Figures 5.12(c) and 5.13(c), carbon-neutral solutions). For the MFH, the only case in which the heat density threshold increases for achieving carbon-neutrality is in scenario *2050-syn-gas-high* compared to scenario *2050-syn-gas-low* (compare Figures 5.13(b) and 5.13(d), carbon-neutral solutions). Here, in the scenario *2050-syn-gas-high*, the individual heat supply is competitive with the lowest connection scenario if only 30 % of the buildings

were supplied via district heating, which means that district heating is still favorable in any scenario with a higher connection quota.

In contrast, the difference between the two reference buildings has a greater impact on the economic advantage of a DHS. For example, if the aim of the MFH was to achieve carbon-neutrality within the global energy scenarios of 2030, the MFH needs to connect to the DHS. Contrary to this, the individual heat supply is already competitive with the DHS at a low connection quota of 30 % in the scenarios of 2030 (Figure 5.12). The SFH has a higher potential of renewable energy sources in the form of solar applications per kilowatt-hour end-energy (see Table 5.2). This integrated analysis of sector-coupled energy systems at building level illustrates that the economic feasibility becomes increasingly complex in the upcoming years during the transition of the energy system. In the cost-optimal cases, as the system is mainly based on natural gas, the heat density threshold for the feasibility of a DHS lies in the same range: for the two reference buildings, a connection quota of 70 % and 100 % is required in order to compete with the individual heat supply options. In the emission-optimal cases, the required connection scenarios for the feasibility of a DHS deviate. This underlines the importance of an integrated assessment, including the renewable energy potentials of each building as well as the electricity demand. An assessment which solely compares different individual heat supply options with a heat supply via district heating is no longer an option. This also implies that in future, the availability of battery electric vehicles could also influence the decision about the economic feasibility of district heating as they come with an additional electrical load at building level and could also contribute as electric storage for the building's energy system.

5.3.2.2 Refurbishment scenarios

After contemplating the un-refurbished existing building stock, this section analyses potential future refurbishment scenarios. In the refurbishment scenarios, a moderately refurbished (scenario *Refurb-1*) and very ambitiously refurbished building stock (scenario *Refurb-2*) are considered. The refurbishment scenarios lead to a reduction of space heating demand and a decrease in the supply temperature of the building's heating system. As before, the comparison is made on the basis of the reference SFH and the reference MFH, introduced in Section 5.2.1.

Figure 5.14 presents the results for the global scenario of the current upstream energy infrastructure (scenario *2020*). In both refurbishment scenarios and for both buildings (scenario *Refurb-1* Figures 5.14(a) and 5.14(b), scenario *Refurb-2* Figures 5.14(c) and 5.14(d)), the cost-optimal solutions for individual heat supply turn out to be more favorable than the 100 % connection scenario. However, despite the substantial reduction of heat demand due to the refurbishment, which implies a reduction of the heat demand density in the district, the individual heat supply scenarios do not stand out clearly below the 100 % connection scenario in comparison to Scenario *Status-quo* (see previous section Figure 5.11). The marginal costs for emission reduction are low, moving from the cost-optimal point to the left, as already observed in scenario *Status-quo*, and increase significantly for the individual heat supply scenarios when approaching carbon-neutrality. For the SFH, carbon-neutrality can be achieved at costs of about 50 €/(m²a) for the *Refurb-1* scenario, which is higher than the 30 % connection scenario (Figure 5.14(a)). In scenario *Refurb-2*, the costs for carbon-neutrality amount to 27 €/(m²a), which is almost equal to the 70 % connection scenario (Figure 5.14(c)). This means that in

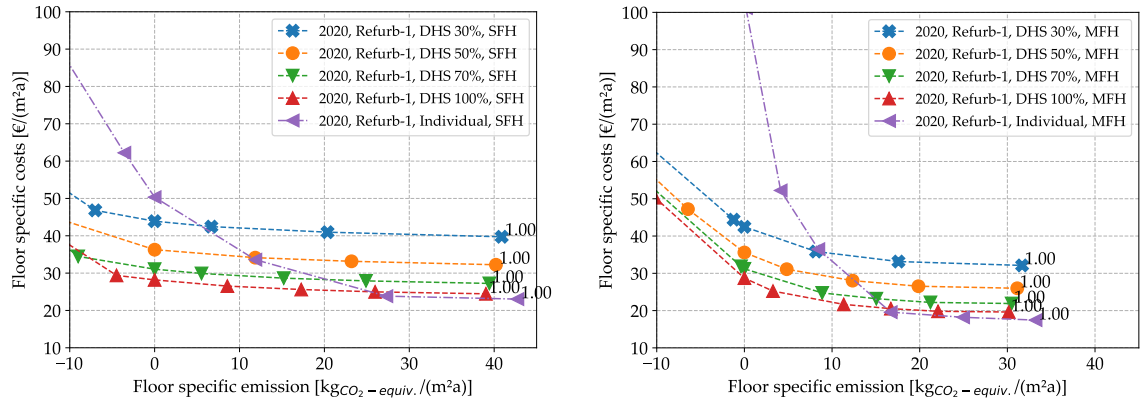

(a) SFH, *Refurb-1*, *2020*

(b) MFH, *Refurb-1*, *2020*

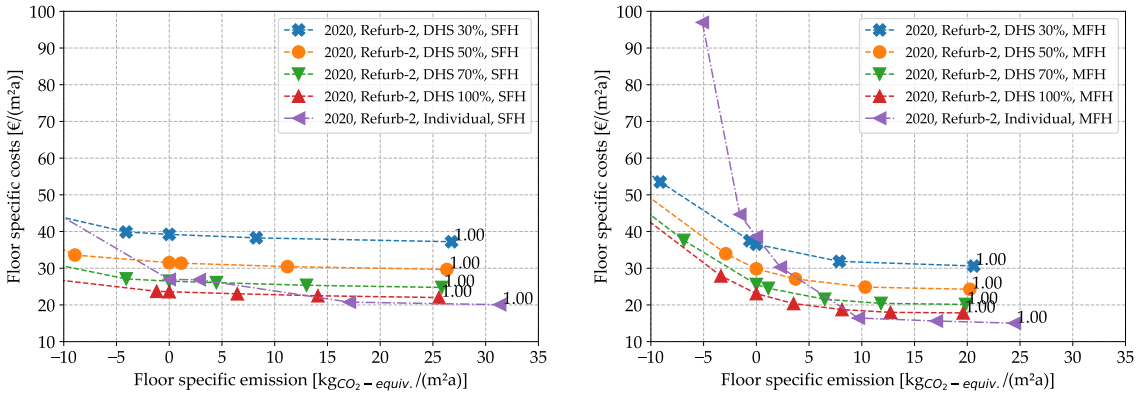

(c) SFH, *Refurb-2*, *2020*

(d) MFH, *Refurb-2*, *2020*

Figure 5.14: Results of individual heat supply versus DHS for the global scenarios *2020*. Refurbishment scenarios *Refurb-1*: (a) and (b) (top); *Refurb-2*: (c) and (d) (bottom). SFH: (a) and (c) (left); MFH: (b) and (d) (right).

absolute terms the costs per square meter considerably decrease, as already illustrated in the analysis of the design of the DHS supply in Section 4.3 and the individual supply options in Section 5.3.1.2. Also relatively, with respect to the individual versus the DHS supply, the breakeven point moves towards higher connection quota in the scenario *Refurb-2*. The same can be observed at the reference MFH. However, the threshold values for a DHS becoming favorable lie at lower heat densities from the perspective of the MFH. In the scenario *Refurb-1*, the costs of carbon-neutrality for the individual heat supply are distinctly higher than the costs of the DHS with at a connection quota of 30 % (Figure 5.14(b)), and in scenario *Refurb-2*, the individual heat supply becomes competitive with the DHS with a connection quota of 30 % (Figure 5.14(d)).

Figure 5.15 illustrates the results for the global scenario framework of 2030. With respect to cost-optimality, the individual supply scenarios lie in the range of the 100 % connection scenario for most of the refurbishment scenarios of 2030. In scenario *Refurb-2*, the costs for the individual heat supply are below the 100 % connection scenario for the MFH.

The marginal costs for emission abatement increase in the individual scenarios and DHS scenarios in the same manner. In the scenarios of 2030, the costs of district heating for achieving carbon-neutrality are higher compared to the scenarios 2020 and 2050 (compare Section 4.3, e.g. Figure 4.6). For the carbon-neutral solutions of the SFH (Figures 5.15(a), 5.15(c), 5.15(e) and 5.15(g)), the individual supply is competitive at a connection quota of almost 70 % for scenario *Refurb-1*. In scenario *Refurb-2*, the individual heat supply is less expensive than the DHS, even where the connection quota is 100 %. For achieving a carbon-neutral supply at the MFH, the thresholds for scenario *Refurb-1* lie at 30 to 50 % connected buildings, and for scenario *Refurb-2* the individual heat supply is less expensive than a DHS (Figures 5.15(b), 5.15(d), 5.15(f) and 5.15(h)).

The comparison of the *syn-gas-low* and *syn-gas-high* scenarios of 2030 shows only marginal differences for the carbon-neutral solutions as the heat generation is based mainly on heat pumps. For the cost-optimal solutions of 2030, a greater deviation can be observed: As gas-based heating is still the cost-optimal choice in both scenarios of 2030, the higher costs of gas in scenario *2030-syn-gas-high* due to a share of renewable gas of 20 % lead to higher overall costs for both the individual heat supply and DHS.

Figure 5.16 shows the results of the comparison of the individual heat supply and the DHS for the scenarios of 2050. These scenarios are characterized by a very high share of renewable energy in the upstream electricity and gas network. The cost-optimal solutions of the individual heat supply and the 100 % DHS scenario lie in a cost range similar to the scenarios of 2030. Only for the MFH, the individual cost-optimal solutions are clearly below the 100 % DHS scenario for both refurbishment scenarios in scenario *2050-syn-gas-high* (Figure 5.16(h)). In refurbishment scenario *Refurb-2* (Figures 5.16(e), 5.16(f), 5.16(g) and 5.16(h)), the costs lie generally at a lower level and the cost difference between the different connection scenarios becomes lower compared to the scenario *Refurb-1*.

Further, it turns out that energetic refurbishment leads to a shift to a higher connection quota with a cost advantage for district heating at carbon-neutrality. For the SFH, the thresholds for the DHS heat supply, that are more economic than the individual supply, move from a required connection quota of 50 % in the scenarios *Refurb-1* (Figures 5.16(a) and 5.16(c)), position of

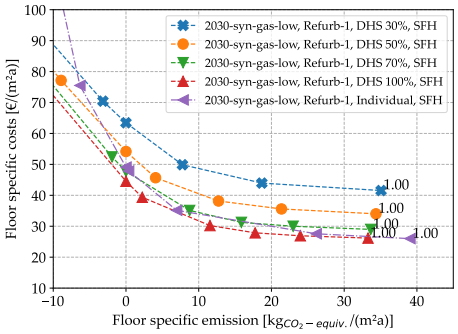

(a) SFH, *Refurb-1*, *2030-syn-gas-low*

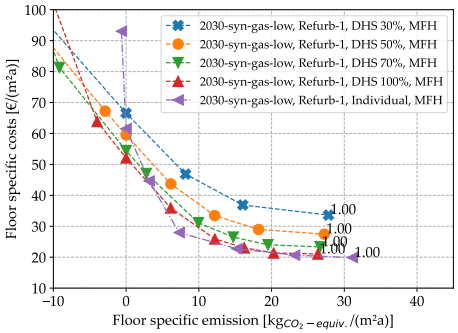

(b) MFH, *Refurb-1*, *2030-syn-gas-low*

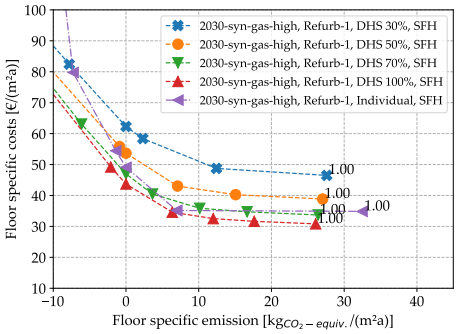

(c) SFH, *Refurb-1*, *2030-syn-gas-high*

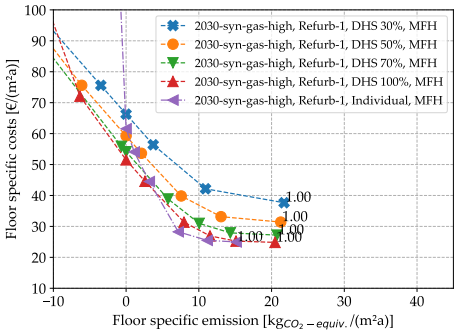

(d) MFH, *Refurb-1*, *2030-syn-gas-high*

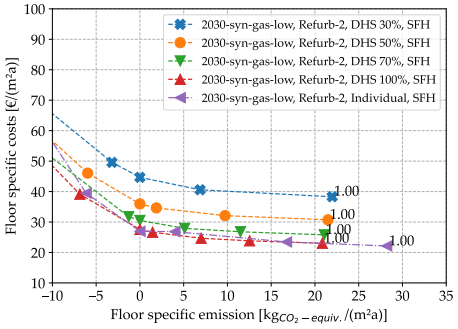

(e) SFH, *Refurb-2*, *2030-syn-gas-low*

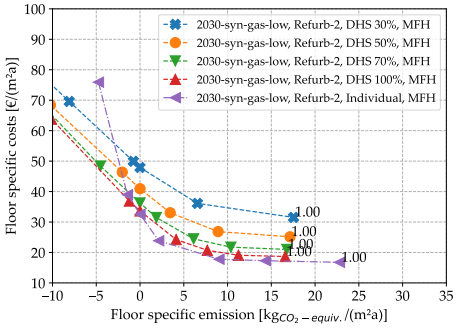

(f) MFH, *Refurb-2*, *2030-syn-gas-low*

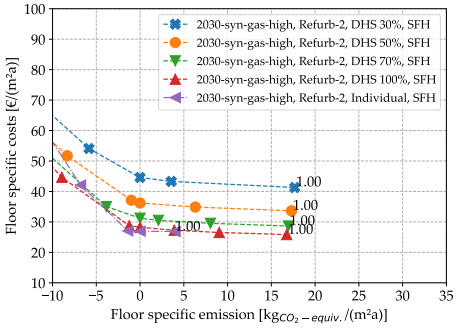

(g) SFH, *Refurb-2*, *2030-syn-gas-high*

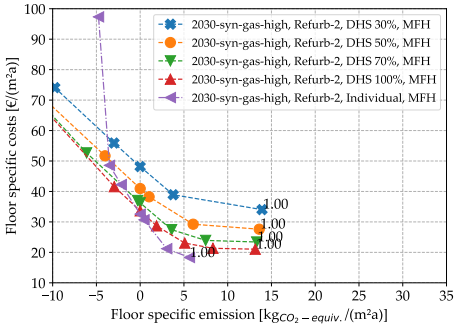

(h) MFH, *Refurb-2*, *2030-syn-gas-high*

Figure 5.15: Results of individual heat supply versus DHS for the global scenarios of 2030. Refurbishment scenario *Refurb-1*: (a)–(d). Refurbishment scenario *Refurb-2*: (e)–(h). SFH: (a), (c), (e) and (g) (left). MFH: (b), (d), (f) and (h) (right).

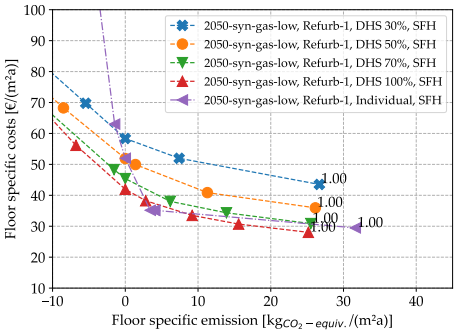

(a) SFH, *Refurb-1*, *2050-syn-gas-low*

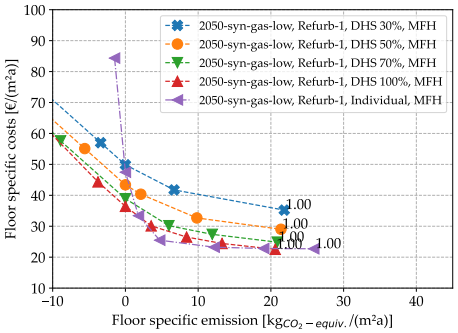

(b) MFH, *Refurb-1*, *2050-syn-gas-low*

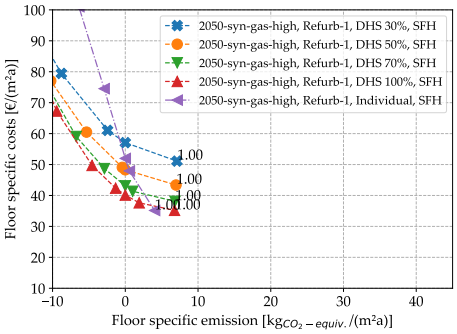

(c) SFH, *Refurb-1*, *2050-syn-gas-high*

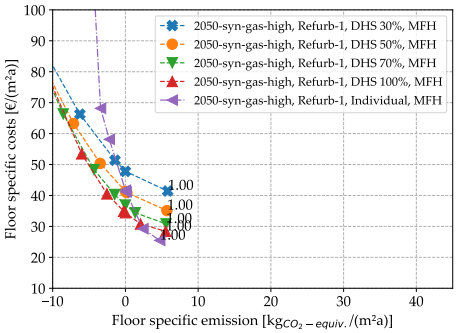

(d) MFH, *Refurb-1*, *2050-syn-gas-high*

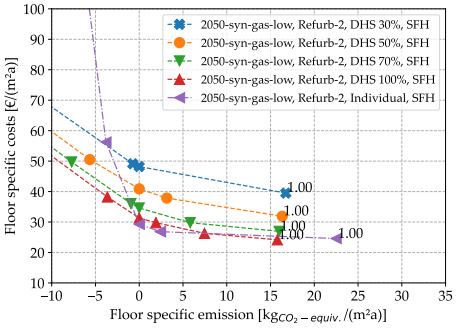

(e) SFH, *Refurb-2*, *2050-syn-gas-low*

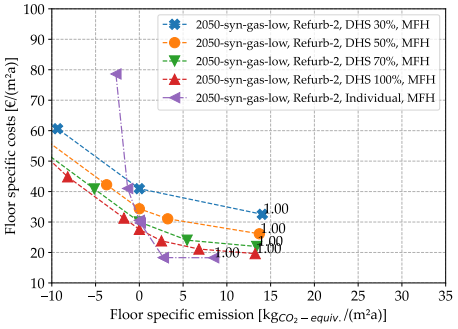

(f) MFH, *Refurb-2*, *2050-syn-gas-low*

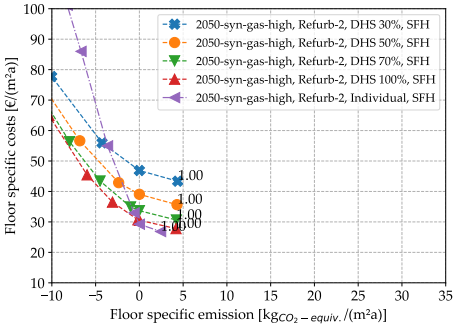

(g) SFH, *Refurb-2*, *2050-syn-gas-high*

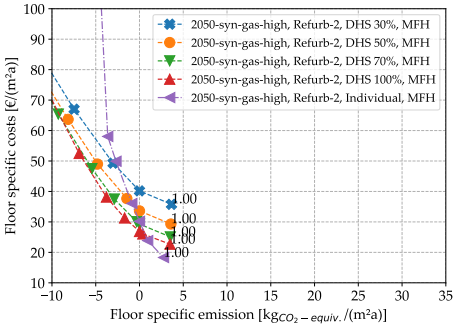

(h) MFH, *Refurb-2*, *2050-syn-gas-high*

Figure 5.16: Results of individual heat supply versus DHS for the global scenarios of 2050. Refurbishment scenario *Refurb-1*: (a)–(d). Refurbishment scenario *Refurb-2*: (e)–(h). SFH: (a), (c), (e) and (g) (left). MFH: (b), (d), (f) and (h) (right).

purple point relative to the results of the DHS solutions at zero floor-specific emissions) to 100 % (Figures 5.16(f) and 5.16(g)). However, if emissions are reduced further below carbon-neutrality by exporting electricity, the individual solutions result in higher costs than the DHS supply, also in scenario *Refurb-2*. For the reference MFH, this trend can also be observed, but is less severe. In scenario *Refurb-1* (Figures 5.16(b) and 5.16(d)), the costs for individual heat supply lie in the range of the DHS scenarios with a connection quota from 30 % to 50 %. In scenario *Refurb-2* (Figures 5.16(f) and 5.16(h)), the costs of the individual supply variants for reaching carbon-neutrality are comparable to a DHS with a connection quota of 70 %.

The two transformations paths for the upstream gas infrastructure (*syn-gas-low*, *syn-gas-high*) have a low impact on the results of the individual supply options compared to district heating. The individual supply scenarios achieve slightly lower costs for both building types in scenario *2050-syn-gas-high* for the cost-optimal solution compared to the DHS. This is illustrated by Figure 5.16(b) versus Figure 5.16(d): The points "1.00" of the 100 % DHS variant (red) and the point "1.00" of the individual variant (purple) are even in scenario *2050-syn-gas-low*, and in scenario *2050-syn-gas-high*; the purple point "1.00" lies below the 100 % DHS variant (red). When emissions are reduced, the individual supply becomes more expensive than the DHS (crossing of the purple lines and the DHS results). In order to reach a carbon-neutral energy supply – results at floor-specific emissions equal zero – the costs for the individual heat supply lie in the range of a DHS with a connection quota of 30 % to 50 % for the refurbishment scenario *Refurb-1*, for both reference buildings independent of the gas scenario (see Figures 5.16(a), 5.16(b), 5.16(c) and 5.16(d)). For scenario *Refurb-2*, the costs of individual heat supply lie below the costs of the 100 % connection scenario for the SFH for both gas scenarios. Also for the MFH, the costs for carbon-neutrality of the individual supply are almost even with the DHS at a connection quota of 70 % for both scenarios without a clear deviation between the synthetic gas scenarios.

5.3.2.3 Derivation of heat density thresholds

Figure 5.17 summarizes the comparison for the carbon-neutral and cost-optimal results from the previous section. These results form the basis for deriving the heat density thresholds for the feasibility of a DHS compared to individual heat supply for the scenarios examined.

As illustrated in the previous section in detail, the comparison of the *syn-gas-low* and *syn-gas-high* scenarios of 2030 and 2050 shows only marginal deviations regarding the feasibility of a DHS to achieve a carbon-neutral heat and electricity supply (see Figure 5.17). Where deviations occur, no clear trend can be observed. Gas-based heating plays a subordinate role for a carbon-neutral energy supply with individual heat generation (see Section 5.3.1). Also in the case of a district heat supply, the scenarios with a high share of synthetic gas do not lead to a significant cost benefit in carbon neutral heat generation (see Section 4.3). Consequently, the share of renewable synthetic gas in the gas network does not clearly shift the connection quota threshold at which a DHS is economically favorable in one direction or another.

Based on the results of Figure 5.17, the heat density thresholds are estimated for the different connection and refurbishment scenarios to review the existing heat density thresholds in literature. Each connection and refurbishment scenario corresponds to an average heat line

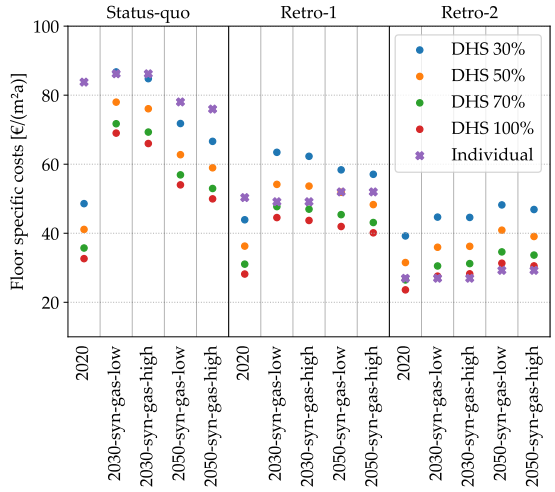

(a) Carbon-neutral solutions (SFH)

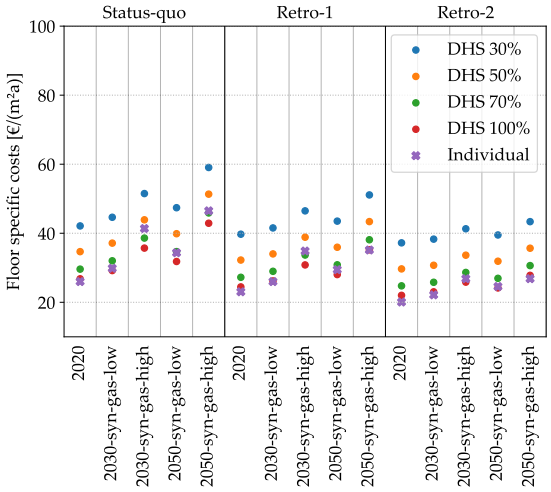

(b) Cost-optimal solutions (SFH)

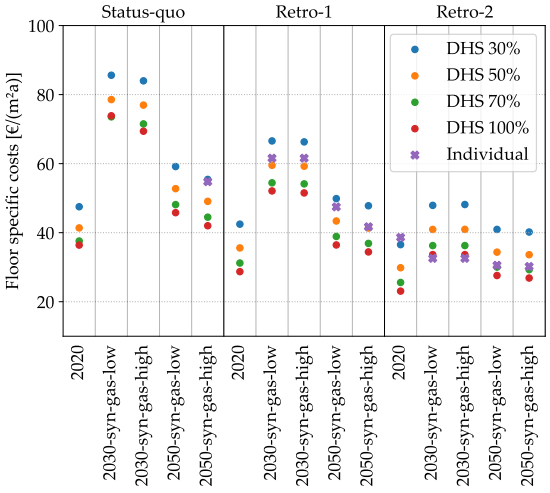

(c) Carbon-neutral solutions (MFH)

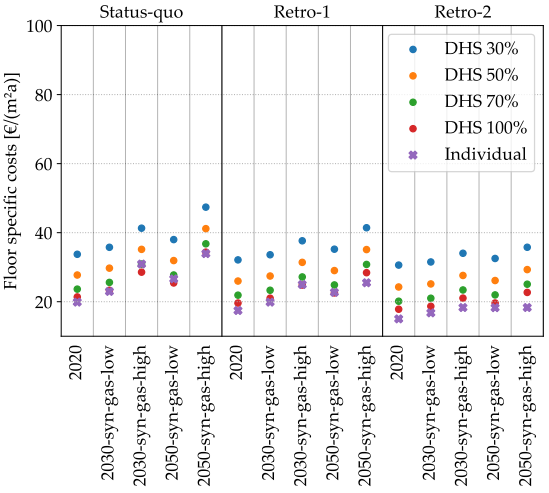

(d) Cost-optimal solutions (MFH)

Figure 5.17: Summary of results of carbon-neutral (left figures (a) and (c)) and cost-optimal solutions (right figures (b) and (d)); SFH: (a) and (b); MFH: (c) and (d).

density related to the aggregated street length and a heat density related to the total area of the district (see Figure 3.8). By linearly interpolating the results of the DHS solutions proportional to the costs given in Figure 5.17, heat density thresholds are estimated for each scenario. However, the results should be interpreted with caution since the linear interpolation leads to inaccuracies and the actual intermediate results are not known. Nevertheless, the interpolated results show a tendency for the heat density threshold when comparing the different scenarios.

Figure 5.18 shows the outcome of the estimated heat density thresholds for the carbon-neutral and cost-optimal solutions. If the costs for the individual results lie below the DHS scenario with the highest connection quota (purple marker below 100 % DHS scenario in Figure 5.17), or if the individual costs lie above the lowest connection scenario (purple marker above 30 % DHS scenario in Figure 5.17), no distinct heat demand density threshold value can be calculated and the hatched areas indicate the uncertainty range, where the heat density threshold must lie. The resulting heat density threshold values are shown depending on the linear heat density (kWh/(m a), left y-axis) and for the corresponding area specific heat density (kWh/(m²a), right y-axis).

For both reference buildings, the required heat density for a DHS shifts to lower values in the case of carbon-neutrality (Figures 5.18(a) and 5.18(c)) compared to cost-optimality (Figures 5.18(b) and 5.18(d)). To achieve carbon-neutrality, the costs for both, the individual heat supply and the DHS, increase compared to the cost-optimal supply strategies (compare Figures 5.18(a) and 5.18(c) with Figures 5.18(b) and 5.18(d)). In future sector-coupled and flexible systems, a DHS is more suitable and cost-efficient for the deployment of multiple different energy converter technologies such as heat pumps, CHP and thermal storage, to react flexibly to different emission intensities of the power grid. At building level, such concepts would be difficult to implement and disproportionately expensive. The decrease of the heat density threshold from cost-optimality to carbon-neutrality becomes especially evident in the refurbishment scenarios *Status-quo* and *Refurb-1* and is more apparent for the MFH (Figure 5.18). In scenario *Refurb-2*, the heat density thresholds of the cost-optimal and carbon-neutral solutions do not show a clear trend for all scenarios. Only in the case of the current upstream infrastructures represented by scenario *2020* do the heat density thresholds drop for both reference buildings when carbon-neutrality is achieved. For the MFH, this is also the case in the scenarios of 2050.

This outcome questions whether lower supply temperatures – as is the case in the refurbishment scenarios, e.g. in scenario *Refurb-2* with a forward temperature of 50 °C – lead to lower heat density threshold values for the economic feasibility of district heating compared to individual heat supply as proposed in literature (see Figure 5.1). For the SFH (Figure 5.18(a)), the heat density threshold values increase in all scenarios for the upstream energy infrastructures from the scenario *Status-quo* to *Refurb-2* for the carbon-neutral solutions. In this case, it does not matter that the threshold values of scenario *Refurb-2* are not known for all scenarios as the threshold ranges, where the values must be located, lie above the threshold values of the scenarios *Status-quo* and *Refurb-1*. For the MFH, a similar trend is observed. Refurbishment measures that include a lower temperature level assumed in these scenarios lead to higher heat density threshold values for all upstream scenarios (Figure 5.18(c)).

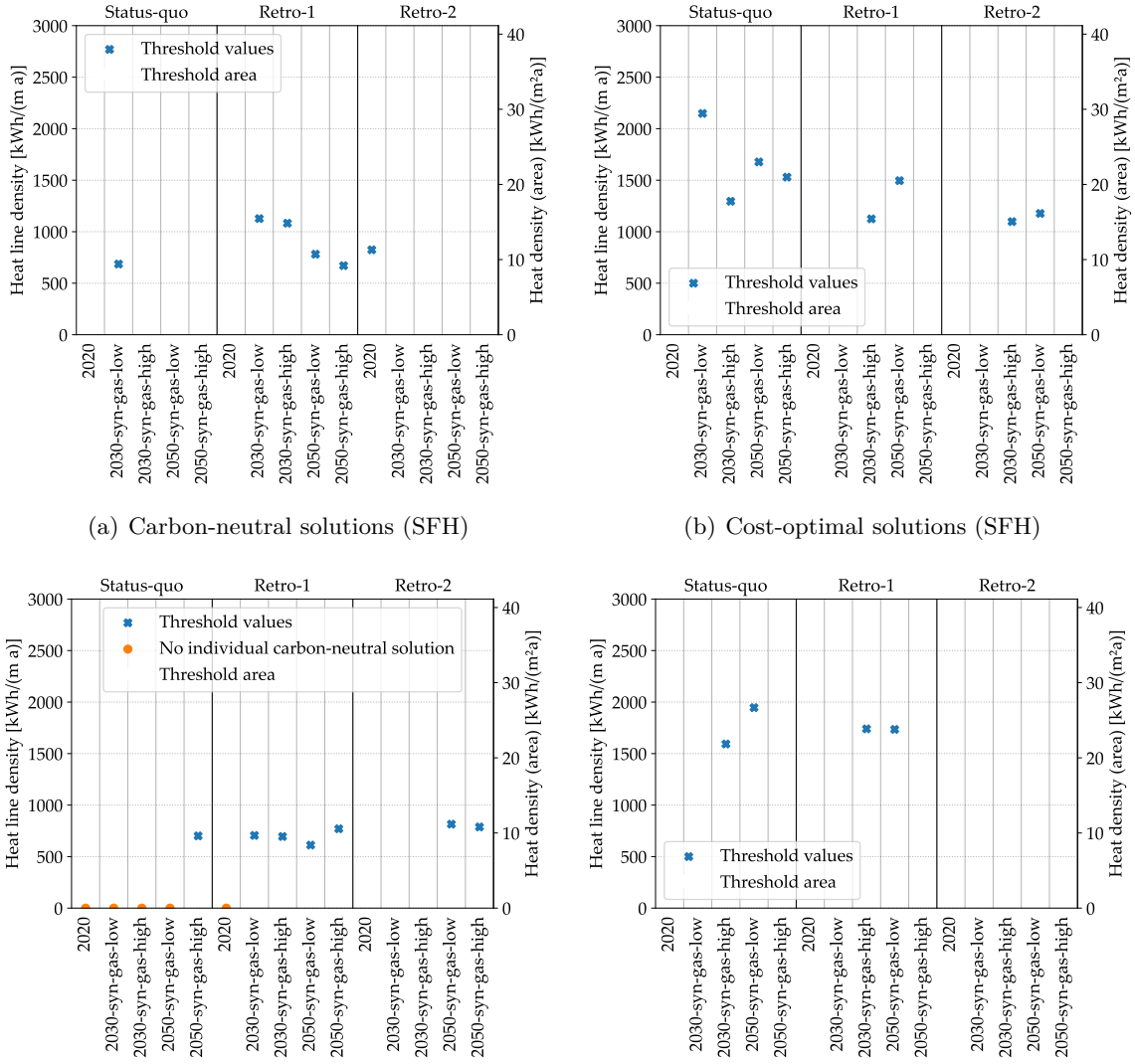

(a) Carbon-neutral solutions (SFH)

(b) Cost-optimal solutions (SFH)

(c) Carbon-neutral solutions (MFH)

(d) Cost-optimal solutions (MFH)

Figure 5.18: Heat density threshold of carbon-neutral solutions (left figures (a) and (c)) and cost-optimal solutions (right figures (b) and (d)); SFH: (a) and (b); MFH: (c) and (d). Left y-axis: linear heat density; right y-axis: area specific heat density. Hatched areas indicate the uncertainty range if no heat density threshold could be estimated (if the costs of individual supply lie below the 100 % connection scenarios or above the 30 % scenarios).

The results in regard to the two reference buildings demonstrate that the heat density threshold depends strongly on the individual characteristics of the buildings and thereby on the individual marginal costs for emission reduction in order to achieve the goal of a carbon-neutral energy supply. In case of the cost-optimal solutions, the minimum threshold for the DHS being economically favorable for the SFH lies above 1090 kWh/(m a) (in the case of the district investigated equal to an area specific heat demand density of 15 kWh/(m²a)) for all scenarios (Figure 5.18(b)), and in the case of the MFH, above about 1230 kWh/(m a) (16.9 kWh/(m²a), Figure 5.18(d)). In contrast, to reach carbon-neutrality, lower heat density thresholds are observed. For the SFH, the maximum heat density threshold results in 1027 kWh/(m a) (15.4 kWh/(m²a), *2030-syn-gas-low*) for the refurbishment scenarios *Status-quo* and *Refurb-1* in the case of carbon-neutrality (Figure 5.18(a)). For the scenario *Refurb-2*, no upper boundary of the heat density threshold can be given, as the costs for individual heat supply lie below the costs of district heating with 100 % of buildings connected to the DHS. In case of the MFH, the required heat density threshold values are even lower, as the renewable potentials of especially the reference MFH are limited. For the refurbishment scenarios *Status-quo* and *Refurb-1*, the maximum heat density threshold value lies at 770 kWh/(m a) (10.6 kWh/(m²a)) in scenario *2050-syn-gas-high* (Figure 5.18(c)). By designing a flexible DHS supply combining different types of heat generation units that can support the upstream energy infrastructures and improve the emission balance, carbon neutrality can still be obtained. The results show that the overall tendency for transforming the existing building stock goes towards lower heat demand density thresholds for the feasibility of DHS, especially if the building stock remains un-refurbished or only moderate energetic refurbishment measures are undertaken.

Altogether, the analysis performed in this thesis indicates lower required heat densities for the feasibility of district heating compared to the recommendations given by Thalmann et al. that suggest district heating is favorable above heat density values of 50 to 70 kWh/(m²a) (Thalmann et al. 2018) (see Section 5.1). However, the results are in line with the recommendations of Möller et al. and Persson et al., according to which heat density values of 20 to 50 TJ/(km²a), which corresponds to 5.5 kWh/(m²a) to 13.8 kWh/(m²a), are feasible for district heating under good conditions (Möller et al. 2019; Persson et al. 2019). The threshold ranges of Knies are also confirmed with values from 0.5 MWh/(m a) to 1.5 MWh/(m a) (Knies 2018), even though a trend towards lower heat density threshold values in the case of lower supply temperatures, as indicated by Knies (see Figure 5.1), is not observed.

5.3.2.4 Sensitivity analysis of commodity prices

Different price ranges were defined for the energy prices of the upstream infrastructures of gas and electricity (see Section 4.2.2.2). To evaluate the effect of the different energy prices on the heat density thresholds, a sensitivity analysis of the previous scenario analysis was performed for various combinations of the maximum and minimum values of the price ranges defined in Section 4.2.2.2, Figure 4.4. The results of this analysis are shown in Figure 5.19.

The blue markers show the results of the medium price path of electricity and gas, that correspond to the results presented in the previous section (Figure 5.18). In addition, Figure 5.19 illustrates cases of a high electricity price once in combination with a high gas price (Elec. price high, Gas price high – orange markers) and once with a low gas price (Elec. price high,

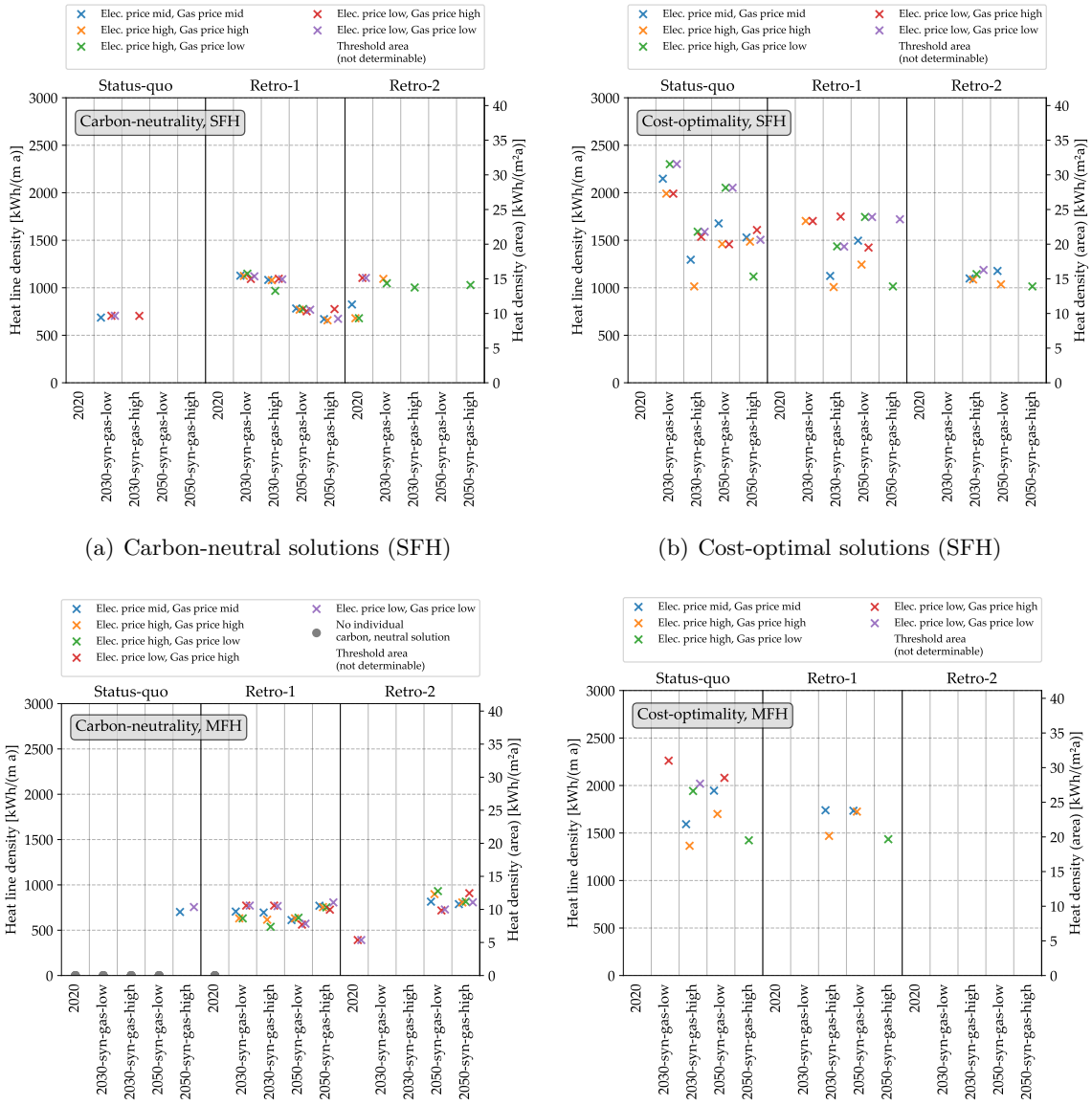

(a) Carbon-neutral solutions (SFH)

(b) Cost-optimal solutions (SFH)

(c) Carbon-neutral solutions (MFH)

(d) Cost-optimal solutions (MFH)

Figure 5.19: Sensitivity analysis of energy commodity prices on the heat density threshold values. Heat density threshold for carbon-neutral results (Figures (a) and (c)) and cost-optimal results (Figures (a) and (c)). (a) and (b) Reference single-family house (SFH); (c) and (d) Reference multi-family house (MFH). Hatched area indicate the uncertainty range of the heat density threshold if no heat density threshold could be estimated.

Gas price high – green markers). And analogously, the combination of a low electricity price with a high gas price (Elec. price low, Gas price high – red markers), and with a high gas price (Elec. price low, Gas price low – purple markers). For the different scenario years 2020, 2030 and 2050, the electricity price range analyzed is equal for each of the scenario years (see Figure 4.4(b)). The price range of the gas mix depends on the share of renewable synthetic gas, which implies a price decrease in the scenario years 2030 and 2050. This results in individual gas price ranges for each scenario (see Figure 4.4(a)). The relation of the energy prices for the individual households and for the district heating facility is kept constant with a factor of 1.5, as described in Section 5.2.3. As this is an obvious factor which impacts on the economic feasibility of DHS compared to individual heat supply, the impact of this factor is not analyzed within this thesis.

The results of the sensitivity analysis show that the variation of energy prices has a stronger impact on the cost-optimal solutions compared to the carbon-neutral solutions (Figure 5.19). For the reference SFH, the deviations between the different price scenarios amount to up to heat density values of 500 kWh/(m a) and more, which can be seen in the scenarios of 2030 and 2050 for the refurbishment scenario *Status-quo* (Figure 5.19(b)), and in scenarios *2030-syn-gas-high* and *2050-syn-gas-low* of *Refurb-2*. For the reference MFH, such a wide spread of heat density thresholds can be observed in the scenarios *2030-syn-gas-high* and in both scenarios of 2050 of the *Status-quo* scenario (Figure 5.19(d)). For the scenario *Refurb-2* of both reference buildings, the informative value of the results are limited, as in most of the solutions the costs of the individual heat supply scenario lie below the costs of the DHS supply with a connection quota of 100 %.

In contrast, the resulting heat density threshold values lie closer together for the carbon-neutral solutions. This is particularly evident for both reference buildings in the *Refurb-1* scenarios, and in the scenarios of 2050 for the MFH in the case of a very ambitious refurbished building stock (*Refurb-2*) (Figure 5.19(c)). However, also in the carbon-neutral cases, there are a couple of scenarios where the absolute deviations of the price sensitivities are not completely assessable, as the heat density threshold cannot be determined in cases of higher costs of the individual heat supply than the 30 % DHS (*Status-quo* scenarios of the SFH), or where the individual solutions are cheaper than the 100 % DHS variant (*Refurb-2* scenarios of the SFH). The different impact of the price sensitivities on the heat demand density thresholds in the case of the cost-optimal solutions can be explained by a high deployment of gas-based technology in these scenarios, which, however, are already competing strongly with electricity-based technologies in scenarios with a higher share of renewable energy in the upstream gas and electricity grids (see also Sections 4.3.1, 4.3.4 and 5.3.1). In the case of a carbon-neutral energy supply, electricity-based heating dominates. This means that relative price changes of electricity to gas have less impact. If electricity becomes more expensive, this affects both a potential district heating facility and private households. As long as the ratio between these two remains the same, the effect on the required heat density for the economic feasibility of district heating is small.

The sensitivity analysis further shows that the overall tendencies observed above are not significantly affected by the variation of the commodity prices. The required heat density for the economic feasibility of district heating moves to lower values if the emissions are reduced and a carbon-neutral energy supply is realized, which becomes clearly evident in the

refurbishment scenarios *Status-quo* and *Refurb-1* for both reference buildings. In scenario *Refurb-2*, no statement can be made on all scenarios. Furthermore, for the realization of a carbon-neutral energy supply, the impact of the share of gas in the gas network is low. Also the differences between the two reference buildings become clear in each of the price variations for the carbon-neutral solutions, which are evident in the *Status-quo* scenarios, in the scenarios of 2030 for the refurbishment scenarios *Refurb-1* and in the scenarios of 2050 of *Refurb-2*.

5.4 Discussion

Besides the individual prerequisites of the buildings, the individual conditions of the district are also crucial for the feasibility of a DHS. This implies available free areas for geothermal applications, the availability of other renewable resources in the district or available space for thermal storage capacities. In this analysis, for example, no waste heat potentials were taken into account to enable transferability to a greater number of existing districts. The focus of the analysis was on a typical existing district with an existing gas infrastructure and with few special features regarding energetic potentials. The district analyzed lies in a low to medium heat density range, where it is yet undecided whether a grid-connected or individual heat supply is favorable. This aspect makes it interesting to investigate the impact of the scenarios presented above on the feasibility of a DHS.

Furthermore, the absolute costs, e.g. for the civil engineering of the district heating network or the costs for planning and construction of the district heating plant, are based on the price level of 2020 for the district analyzed. This also applies to the costs of the energy converter and storage units. However, these costs might vary, depending on the district, and might change over time. The absolute heat density thresholds need therefore to be interpreted carefully, and only apply to the contemplated district under the assumptions made. However, the relative trends of the heat density threshold values observed by the investigation of the different scenarios for the upstream energy system, the connection and the refurbishment scenarios stay the same, if e.g. the absolute planning costs for the district heating supply increase. This aspect also applies to the difference in commodity prices of the district heating operator and the commodity prices of the households. Of importance is the relation of the prices. For example, if the prices for electricity and gas for energy-intensive customers, such as the district heating operator, decrease more than those for private households, the threshold of the heat demand density shifts to a lower connection quota. The same applies to technology costs. However, if prices for individual households change in the same proportion as for the district heating utility, only a small impact on the heat demand density thresholds is expected. Altogether, this also implies that the legislator impacts on the feasibility of DHS by imposing or alleviating taxes or fees for certain customer groups, or by a selective funding of investment costs, such as heat pumps, for certain customer groups. These taxes or subsidies could lead to sub-optimal infrastructure design in the long term.

In the analysis, a sector-coupled approach is pursued that considers the heat and electricity demand of the buildings to determine the best solutions for the de-carbonization of both. At the infrastructure level, however, only the district heating network is considered in detail. The electricity and gas networks were not examined in regard to restrictions or capacity limits. With

regard to the gas network, no additional investment costs were taken into account, for example, if the high share of renewable synthetic gas, as is assumed in scenario *2050-syn-gas-high*, requires a strengthening of the existing gas infrastructure in order to cope with possibly higher shares of hydrogen. Also, the electricity grid within the district might face capacity limits if the electricity demand of the buildings is increased by the additional load of the heat pumps. The elimination of both simplifications could favor the variants with DHS, the individual heat generation might also require additional infrastructure costs either for adaptions of the gas network or for a reinforcement of the power grid at district level to deal with an increased electricity demand. Especially in the case of a decommissioning of an existing gas infrastructure, the electricity grid would remain as the only energy distribution infrastructure at district level. In this case, DHS could also contribute to a diversified energy infrastructure. As the results of the future scenarios show, the tendency towards renewable heat generation clearly shifts towards electricity-based heating. In the case of a DHS, no additional load is generated in the electricity distribution network by electricity-based heating, as the heating energy is transported to the households via hot water. The reinforcement of the upstream electricity grid – if necessary – would occur in both heat supply variants. The same applies to the gas network. If reinforcements or upgrades in the context of an increased share of renewable synthetic gas need to be undertaken, the gas network within the district is not affected if a DHS is economically favorable and the gas network can be shut down. This reinforcement or upgrade would only be necessary from the supra-regional transmission network to the heat supply plant of the district.

Within the refurbishment scenarios, it is assumed that all buildings have a certain state of refurbishment that implies a certain temperature level and a certain heat demand. Of course, in reality, the refurbishment of the buildings is a gradual process that lasts for decades. Therefore, the scenarios must be interpreted as idealized states that allow a better comparison. For the planning and development of DHS, this temporal aspect of a subsequent refurbishment makes it additionally complex. Especially, due to the temperature dependency within a DHS, in which the customer with the highest temperature demand determines the forward temperature for all, a large number of further scenarios would be conceivable. An investigation of all sub-variants is beyond the scope of this thesis. The focus here is to showcase the different extreme states of possible refurbishment scenarios.

The last aspect worth mentioning is the feasibility of realizing the control of the energy converter and storage units. In both supply strategies, the individual heat supply and the supply via DHS, the operation routines become more complex and a forecast-based unit commitment is required that anticipates e.g. heat and electricity demand as well as electricity generation via solar panels. However, when it comes to monitoring and plant optimization, it might be more cost-efficient to perform this plant optimization task at an aggregated level compared to individual households. Also from the perspective of the upstream infrastructures, a DHS would reduce the number of agents, including sensors and actors that have to communicate with upstream energy infrastructures. These aspects also point in favor of district heating networks.

5.5 Conclusion

Below, based on the results presented, suggestions and recommendations for the development of a future-proof district energy supply for existing districts are made to achieve a carbon-neutral energy system. Firstly, the conclusions in regard to the research objective RO 3 concerning the analysis of the impact of future developments on the required heat density threshold for the economic feasibility of district heating are summarized. Then, conclusions for the development of renewable heat supply concepts and infrastructures with regard to energetic refurbishment and the electricity and gas networks at district level are drawn.

District heating networks The level of emission reduction that is aimed to be achieved in a district strongly influences the economic feasibility of district heating compared to individual heat generation. As the analysis of this chapter shows, the heat density thresholds for a DHS that are economically feasible decrease if the emissions of heat supply are reduced from a cost-optimal to a carbon-neutral energy supply of the buildings. In contrast, the impact of the two transformation paths *syn-gas-low* and *syn-gas-high* for the upstream energy system on the heat density threshold values is low. Even if the share of renewable synthetic gas in the gas network is very high and the prices of synthetic renewable gas drastically decreases by 2050 (see assumption in Figure 4.4), individual heat generation via gas boilers is not the most economical solution for achieving carbon-neutrality despite the existing gas infrastructure. Also in this extreme scenario, the impact on the heat density threshold is low, and the trend is going in the opposite direction in some scenarios. This means that renewable synthetic gas, if available in large quantities, can be used more efficiently at aggregated level in a district heating facility by an efficient and system-supportive operated CHP. In contrast to the scenarios of the upstream gas network, the refurbishment scenarios have a stronger influence on the heat demand density, and especially the individual results of the two reference buildings differ clearly. The individual marginal costs for emission reduction and for achieving carbon-neutrality strongly vary between the analyzed SFH and MFH. The low impact of the transformation paths *syn-gas-low* and *syn-gas-high* on the heat density threshold is a very important finding because it means that the heat demand density can continue to be focused on as the most important parameter in determining the feasibility of a DHS. The development and transformation of gas infrastructure has a low impact on the urban heat planning and on the heat demand density threshold that is required for district heating. But, in addition to the heat density, the individual sector-coupled aspects of the individual buildings, such as usable roof area for PV, electricity demand, e-mobility, geothermal or other heat potentials and also space for the installation of thermal storage capacities, must be given greater consideration in future. These factors also influence the possibilities to become carbon-neutral at building level and to react to the volatile characteristic of renewable energy generation in the power grid.

Energetic refurbishment There is no doubt that energetic building refurbishment is an important pillar in order to achieve climate targets (Arning et al. 2020). By decreasing the total heat demand and the forward temperature, costs and emissions can be reduced drastically. Especially the reduction of the temperature level plays a crucial role, as electricity-based heating via heat pumps is in all scenarios a dominant technology on the way to carbon-neutrality. The

analysis further demonstrates that energetic refurbishments pay off much faster in future while the total costs for energy increase if a carbon-neutral energy supply is realized. Or vice versa, if no energetic refurbishment is performed, the costs for achieving a carbon-neutral building stock are much higher, and also more "primary" renewable energy sources, like wind or solar farms are required to supply the renewable electricity or to supply the increasing amount of renewable synthetic gas. The latter implies the installation of even more renewable energy sources as wind or solar parks due to the conversion losses for the synthetization of synthetic gas from electricity. This aspect could intensify the urgency for energy efficiency refurbishments as the rate of refurbishment is at a low level in Germany (Arning et al. 2020). With respect to the development of district heating systems, the impact of refurbishment measures on the feasibility of district heating is obvious as energetic refurbishment measures reduce the heat demand density of a district at the same connection quota. However, also in regard to the absolute heat density threshold values calculated, an impact is observed. For the moderate and ambitious refurbishment scenarios, competitive district heating systems demand for higher heat densities when carbon-neutrality should be achieved. Altogether, this means that potential developments of the existing building stock need to be projected very well in order obtain a reliable basis for the urban heat planning which includes a detailed analysis of possible energetic refurbishment measures of the existing buildings and a projection of a potential densification of the existing building stock by new buildings.

Electricity grid At infrastructure level, the low-voltage distribution network needs also to be taken into account in future as the total electricity demand of districts might increase due to heat pumps and electric vehicles. If an evaluation of the feasibility of a DHS comes to the conclusion that individual heat supply via heat pumps is the more economical option, then, additionally, the power grid must be taken into account. Instead of investments in the enforcement of the power network, a DHS could support the reduction of the electrical load of the decentral heat pumps in the buildings. This means that in order to determine whether a DHS is a viable option for the individual district, the low-voltage distribution network needs also be considered more thoroughly in the urban heat planning.

Gas infrastructure In this analysis, districts with an existing gas infrastructure, as it is the case in the analyzed district, are addressed. Below, the consequences for low pressure distribution gas network at district level are described, depending on the economic feasibility of district heating.

If the above-described projection and evaluation of a specific district concludes that individual heat generation is favorable to reach carbon-neutrality, the existing gas infrastructure should be kept only as long as the transition takes place with a decreasing throughput. The installation of heat pumps successively reduces the demand for gas, and by a flexible commitment of the heat pumps, depending on the share of renewable energies in the electricity grid, emissions can be reduced rapidly in the next years. Also, in un-refurbished buildings with a high forward temperature, the installation of heat pumps and thermal storage units additional to the gas boiler mostly existing can contribute to an efficient emission reduction and to a system-supportive heat supply. In this bivalent system, the gas boiler can be used on cold winter

days when the buildings demand very high forward temperatures, or if the share of renewable energies in the electricity system are low or if the power grid is facing capacity limits. For the rest of the year, especially in summer and in transitional seasons, the heat pumps contribute to a fast reduction of emissions. Also here, the thermal storage is of crucial importance for the flexibility of the system. As soon as the building undergoes refurbishment and the temperature level of the space heating can be decreased, the gas boiler can be abandoned and the heat pump could take over the total heat generation.

If a DHS is favorable for reaching carbon-neutrality of the building stock of a certain district, the low-pressure gas distribution network at district level should be shut down and a DHS should be rolled out. The upstream gas network to which the district heat supply is connected should be kept up. The share of renewable synthetic gas in the gas network does not largely impact on the heat density threshold in favor of individual gas-based heat supply. That means that simply feeding renewable gas into the gas network and keeping up the individual heat generation is not a cost-efficient emission reduction strategy in district with a sufficient heat demand density. If the heat demand density is sufficient for a DHS, the gas – whether fossil or synthetic renewable gas – can be more efficiently used within the district heating plant in large scale CHPs instead of decentral units within the buildings. At the DHS supply site, it is easier to install a CHP in combination with heat pumps and large thermal storage capacities. At building level, the installation of multiple technologies is disproportionately costly and complex. In such a district with a sufficiently high heat demand density, there is no reason to keep up the lowest distribution level of the gas network for the purpose of heating. From an overall economic perspective, it makes no sense to maintain a redundant infrastructure that cannot prospectively contribute to a cost-efficient emission reduction in any of the contemplated scenarios, especially as the economic viability of an infrastructure such as district heating networks essentially depends on its utilization rate in the form of a high connection quota. Often, it is argued that the gas infrastructure and district heating networks must be in competition with each other for the benefit of the customers. However, in future, the competition should only be between DHS and individual solutions at building level in the objective of becoming carbon-neutral. And this competition needs to be based on an integrated sector-coupled contemplation, taking into account the volatility of the upstream electricity grid as well as the heat and electricity system at building level, as pursued in this thesis. As the results of this thesis demonstrate, the costs of energy for reaching carbon neutrality will increase compared to the past decades where fossil gas was available at low cost (compare e.g. Figure 5.17). There is no room for additional burdens by maintaining redundant infrastructures at district level.

6 Conclusions and outlook

The objective of this thesis is to develop future-proof renewable and system-supportive heat supply concepts and district heating infrastructures for existing districts. This includes the development of methods and software tools for achieving this purpose and the in-depth scenario analysis of a typical existing district with a sparse to medium heat density to analyze the role of district heating systems (DHS) for the transformation of similar districts. The research objective is divided into three parts: the development of tools and methods (RO 1), the development of future-proof DHS, including the heat supply and the district heating network (RO 2), and the analysis of the impact of future developments on the heat density threshold for the economic feasibility of district heating compared to individual heat supply (RO 3). The contributions and main findings of this thesis are highlighted below, and an outlook for future research is given.

6.1 Conclusions

This section is divided into two parts: in the first section, the methodical contributions of this thesis that concern the development of tools and methods for the design of renewable and system-supportive DHS are summarized (RO 1). The second section compiles the results of the research objectives RO 2 and RO 3, which address the application and scenario analysis for the design of future-proof district heat supply concepts and infrastructures.

6.1.1 Methodical contributions

The following contributions to the fields of modeling and the analysis of urban energy systems and the development of future-proof DHS were made by this thesis. These aspects refer to the research objective RO 1 that addresses the development of tools and methods. Below, the single aspects are explained in detail:

- The development and demonstration of an overall model-chain based on open source tools to develop future-proof heat supply concepts and to compare district heating versus individual heat supply at building level in the trade-off between costs and emission.
- The development, evaluation and application of a methodical approach for the design of renewable and system-supportive district energy systems by using time-resolved emission factors for the electricity exchange of the district with the upstream electricity network.
- The development and application of an open source software tool for optimizing district heating networks in an open library.

This thesis develops and demonstrates an overall approach and model chain based on open source tools for the development of district heat supply concepts that follows a three step modeling approach which includes the design of a district heating network (Chapter 3), the selection and dimensioning of the energy converter and storage units of the heat supply site (Chapter 4) and a comparison of a centralized heat supply via district heating with decentral individual heat

supply options at building level (Chapter 5). The methodical approach developed is successfully demonstrated based on the existing district Rüsdorfer Kamp. It has succeeded in designing renewable and system-supportive heat supply concepts in a sector-coupled environment for future scenarios of the upstream energy system and the existing building stock. The underlying modeling approach is based on mixed-integer linear programming (MILP), and the open source library *oemof.solph* is used as a modeling basis. With this library, optimization models for the district heating network, the heat supply site of the DHS and the energy system at building level are developed.

To design system-supportive district energy systems, an appropriate methodical approach is developed. The dynamic emission factor is identified and used as a grid-based reference quantity for the assessment of electricity imported into the district and exported into the electricity grid. Based on an analysis of historical data, it is shown that the emission factor increasingly correlates to other grid-based reference quantities such as the day-ahead price and the residual load. Furthermore, it is shown that historically low values of the emission factor and the occurrence of feed-in management measures coincide (see Section 2.1). Thus, the emission factor is selected as a grid-based reference quantity that achieves both the attainment of a renewable and system-supportive district energy system. The application of the dynamic emission factor within the Pareto-optimization with costs and emissions as objectives demonstrates that a system-supportive unit commitment is achieved while at the same time evaluating the actual emission (in CO_2-equivalents) compared to other energy commodity sources such as fossil gas. The emission factor is a suitable grid-based reference quantity for the prospective design of renewable and system-supportive district energy systems (see Chapter 4). Especially in the medium term, the emission factor provides a suitable alternative to other flexibility signals or incentives, like the market clearing price, that may be more difficult to estimate and depend on the future market design. However, the emission factor also faces limitations. Firstly, it is not possible to determine absolute levels of emission reduction or grid-supportiveness that should be achieved. Instead, the assessment method enables a comparison of different alternatives and the evaluation of the marginal emission reduction costs. Secondly, the approach is limited when it comes to 100 percent renewable electricity systems, where also in times without wind and solar power generation, renewable synthetic gas fueled power plants are operated. In this case, the emission factor would converge to a constant value of zero and would no longer provide sufficient incentive for a grid-supportive plant design (see Section 4.4). Thus, the emission factor is a suitable concept during the energy transition as long as there are still fossil power plants in the system. For a 100 percent renewable power grid, the methodical approach needs to be developed further (see also in the outlook Section 6.2).

Within planning DHS, the design of district heating networks is an essential task in the overall modeling approach and is required for the development of DHS. For this purpose, a novel optimization tool was developed within this work (see Chapter 3) and published as open source tool in the package *DHNx* on the platform GitHub (oemof developer group 2022b). The tool can be used and further developed by other scientists and is already integrated in other projects, for example in the tool SESMG (Klemm et al. 2022). This drives the scientific progress and avoids duplicated work in science. The optimization tool allows the fast design of district heating networks that includes the routing of the distribution lines based on open-street-maps data and the dimensioning of the district heating pipelines. Thus, the tool enables a fast

estimation of the investment costs and thermal losses of potential district heating networks. The tool is flexible in its usage and allows the application of more complex design tasks such as the consideration of redundancy or additional energy converter and storage units such as distributed thermal energy storages. Furthermore, a novel method to consider the simultaneity in the district heating network design process has been introduced within this thesis. The tool has been applied to the Rüsdorfer Kamp for different connection and refurbishment scenarios of the existing building stock. A relation between the heat density of different connection scenarios and the district heating network costs is thereby derived that matches well with existing empirical formulas given in literature (see Persson et al. 2019). The routing and dimensioning tool developed does not replace a detailed thermo-hydraulic simulation in the detailed planning stage of district heating networks, but provides the basis for all subsequent planning steps in early planning stages.

6.1.2 Application and scenarios analysis

The research objectives RO 2 and RO 3 are answered based on an in-depth scenario analysis of a typical existing district. The Rüsdorfer Kamp is therefore used throughout the thesis as a reference district with a typical existing building stock. The relevant energetic key values of the district correspond well to the existing buildings in Germany. The Rüsdorfer Kamp is well suited for the investigation of heat density thresholds required for DHS, as the heat density in the district lies in the range of currently recommended threshold values. The scenario framework includes different transformation paths for the upstream electricity and gas infrastructures until 2050 (see Section 4.2.2). For the gas infrastructure, a scenario with a low and a high share of renewable gas is projected. The expansion of renewable energies in the upstream electricity grid is represented by a scenario with a medium share of renewable energies in 2030 and a scenario with a high share of renewable energies in 2050. In addition to the global scenarios, the analysis was carried out for different scenarios at the district level (local scenarios) that take three differently ambitious refurbishment scenarios with varying heat demand and temperature level into account (see Section 3.3.1).

The results of the optimization of the heat supply site (Chapter 4, RO 2) show that heat pump capacities in combination with a thermal storage are of great importance in all scenarios for a future carbon-neutral heat supply. The thermal storage, as the cheapest storage option for energy, enables electricity to be sourced from the power grid flexibly when the emission factor is low. Additionally, a gas-based combined heat and power plant helps to reduce emissions in the short term by the efficient generation of heat and power at times of a high emission factor of the electricity mix – times with low electricity generation from wind and solar power plants in the upstream electricity grid. However, only if the gas network has a high share of renewable energies this technology will compete with electricity-based heating via heat pumps to achieve a carbon-neutral heat supply. In the future, heat pumps could take over most of the heat generation, and, depending on the emission factor of the gas network, the CHP could support the power grid at times of low renewable energy generation from wind and solar power plants. Thus, the CHP should be equipped to be fueled by a flexible share of hydrogen so that it can deal with any gas mix of the gas network, also in the case of an increased share of hydrogen. The results show that electrolysis is not, at least in the short term, a viable option

for designing a cost-efficient carbon-neutral district heat supply. Only if the share of renewable gas in the gas network is low, an electrolysis improves the emission balance of the district energy system by feeding hydrogen into the gas network. Using hydrogen that is produced by electrolysis within the district energy system for heating purposes is not a cost-efficient or emission-efficient option in any of the scenarios.

In Chapter 5, the results of Chapter 4 for heat supply by DHS are compared to individual heat supply options in a sector-coupled approach at building level to evaluate the role of DHS for the emission reduction and to estimate heat density threshold values for the feasibility of district heating under different scenarios (RO 3). By the use of different connection quota of buildings connected to the DHS, it was possible to derive heat density thresholds for the feasibility of district heating for future scenarios and thereby to analyze the impacting factors on the heat density threshold. The calculated heat density threshold values are in accordance with the recommendations of Knies (2018), Persson et al. (2019), and Möller et al. (2019) but contradict the recommendations given in Thalmann et al. (2018) and suggest lower required heat demand densities for the feasibility of district heating. Overall, the results of this thesis thereby indicate a higher district heating potential than the trend outlined by HIC et al. (2021) based on current studies for Germany, which suggest a share of district heating of 20 % to 25 %.

The comparison of DHS and individual heat generation shows that in all scenarios the heat density thresholds for an economically feasible DHS decrease if the emissions are reduced towards a carbon-neutral supply. The impact of the scenarios of the upstream gas network considering a low and a high share of renewable synthetic gas on the heat density threshold is low. Even if the share of renewable synthetic gas in the gas network is very high (scenario *2050-syn-gas-high*), individual heat generation via gas boilers is not the most economical solution for achieving carbon-neutrality, despite the existing gas infrastructure. Also in this extreme scenario, district heating is not less important; in fact, the opposite is true in some scenarios. In the case of a high share of synthetic renewable gas, the gas can be more efficiently used at the DHS supply site by coupling combined heat and power units with heat pumps and large scale thermal storage. At an aggregated level, this combination is more efficient and leads to lower costs compared to the building level. Consequently, the heat demand density continues to be the most important parameter in determining the feasibility of a DHS. No additional dependency as the availability and share of renewable gas must be considered in the urban heat planning when deciding on district heating networks.

In contrast to the scenarios for the upstream gas infrastructure, the connection and refurbishment scenarios have a stronger influence on the heat density threshold. And, especially the individual building's point of view differs clearly. This means that besides the heat density, the prerequisites of the individual building play a stronger role in future scenarios, as is shown by the comparison of a reference SFH and a reference MFH. This means that individual factors, such as usable roof area for PV, electricity demand, electric vehicles, geothermal or other heat potentials and also space for the installation of thermal storage capacities become more important in a future, strongly sector-coupled energy system, regarding the feasibility of DHS. These factors influence the possibilities to become carbon-neutral at building level and to react to the volatile characteristics of renewable energy generation in the upstream power grid.

The analysis of different refurbishment scenarios, including a reduction in the space heating demand and different temperature levels, clearly shows the benefits of refurbishment to obtain carbon-neutrality. Especially the reduction of the temperature level plays a crucial role, as electricity-based heating via heat pumps is a dominant technology in reaching carbon-neutrality in all scenarios. Consequently, energetic refurbishment will pay off much faster in future as the total costs for energy increase on the way to a carbon-neutral energy supply. With respect to the heat density threshold, no a clear shift towards lower heat densities is observed with increasing refurbishment measures and lower supply temperatures for achieving carbon-neutrality. This stands in contrast to literature sources that indicate that low temperature DHS are feasible at lower heat densities (e.g. Knies 2018).

Altogether, with the analysis carried out in this thesis, it was possible to investigate the impact of different scenarios on the heat density threshold for the economic feasibility of district heating compared to individual heat supply. However, it was not possible to identify heat density thresholds for all scenarios, e.g. if the costs for individual heat supply exceed the costs of district heat supply with a connection quota of 30 %, or if the costs of individual heat supply lie below the 100 % connection scenario. This aspect could be addressed by investigating further types and scales of districts in subsequent research projects (see also the following section).

6.2 Outlook

In the analysis carried out in this thesis, it becomes clear that infrastructure decisions for future (district) heating systems are increasingly complex, and not only the upstream energy infrastructures but also the individual options at building level must be considered more deeply to achieve a carbon-neutral heat supply. The tools that support the planning and optimization of DHS therefore need to be continuously enhanced. For doing this, the open source tools developed in this thesis provide a good starting point. For example, the models could be extended with a cross-sectoral infrastructure planning by a combined investigation of heat, electricity and gas networks and the consideration of electric vehicles at building or district level. However, this leads to more comprehensive and complex models if the same level of detail, such as the consideration of the time-resolved characteristic of the upstream electricity grid, is maintained. Thus, modeling strategies and tools that are capable of considering these additional aspects are needed to keep the models with their spatial and temporal resolution feasible.

As shown in the review of existing assessment parameters for the electricity exchange with the upstream power grid, the current regulations do not provide any incentive for the design of system-supportive DHS. However, the approach of this thesis, that uses a time-resolved emission factor as a grid-based reference quantity, also faces limits with respect to the design of system-supportive district energy systems when it comes to a 100 % renewable upstream electricity system. If, in times of a low generation of volatile renewable energy sources, renewable hydrogen and renewable synthetic gas is used for electricity generation, the emission factor converges towards a constant value of zero. In fact, the emission factor still provides an assessment basis for the emissions; however, it does not deliver a distinctive time-resolved signal for a system-supportive unit and storage commitment anymore. The methodical approach

of this thesis therefore needs to be developed further for such scenarios. One possible way is to introduce a new definition for primary energy and a new primary energy factor analogous to the one for fossil fuels. This new primary energy factor describes the amount of volatile renewable energy from wind and solar plants that is required for a certain energy application. For example, the primary energy factor of the direct use of volatile renewable electricity could be set to one, while the new primary energy factor of renewable hydrogen needs to include the conversion factor and losses for converting volatile renewable energies into hydrogen, which might lead to a factor of about two. This new primary energy factor could be used in analogy to the dynamic emission factor as a signal of scarcity for electricity imports and exports in order to design system-supportive district energy systems. Nonetheless, the assessment approach of this thesis with dynamic emission factors is still required for the transition phase. As long as fossil fuels are in the system, the emission factor is a useful instrument to derive the most cost-efficient emission reduction strategies and to obtain a system-supportive design.

Besides the development of tools and methods, further research could address the application of the proposed methodical approach to additional types and scales of districts and to other scenarios. This thesis analyses a specific type of district where DHS lie at the thresholds of feasibility for a wide range of potential scenarios. The critical review of the existing recommendations for heat density thresholds carried out in this thesis can be used as a reference and starting point for the analysis of other types of districts. It might also be worth evaluating districts with even higher and lower heat demand densities and a different building structure. This thesis demonstrated that it is difficult to determine a single heat density threshold value in order to achieve a carbon-neutral energy supply. It also showed that the individual options at building level significantly impact on the heat density threshold. The investigation of further examples and building types could confirm the observations of this thesis and might also reveal new dependencies for the feasibility of DHS. In addition, a review and adaption of the overall scenario framework will be essential after a couple of years, so that new developments and technologies that evolve in the ongoing energy transition are considered.

The research on the best techno-economic and ecological options for the transformation of district energy systems is crucial for a successful energy transition. The techno-economic facts form the basis and represent an important input for subsequent social and political negotiation, participation and decision-making processes. Especially with respect to DHS, the individual perspective versus a communal supply strategy that might imply additional dependencies and be impacted by collective behavior must be evaluated from a neutral point of view to which this thesis hopes to contribute.

Bibliography

AGFW (2021a). *AGFW - Hauptbericht 2020*. Ed. by AGFW | Der Energieeffizienzverband für Wärme, Kälte und KWK e. V. Frankfurt am Main, 2021. URL: https://www.agfw.de/zahlen-und-statistiken/agfw-hauptbericht/ (visited on June 10, 2022).

AGFW (2021b). *Arbeitsblatt AGFW FW 309 Teil 1: Energetische Bewertung von Fernwärme und Fernkälte*. Ed. by AGFW | Der Energieeffizienzverband für Wärme, Kälte und KWK e. V. 2021.

Agora Energiewende (2020). *Agorameter*. Ed. by Agora Energiewende. 2020. URL: https://www.agora-energiewende.de/service/agorameter/ (visited on June 10, 2022).

Agora Verkehrswende and Agora Energiewende (2018). *Die zukünftigen Kosten strombasierter synthetischer Brennstoffe*. 2018. URL: https://www.agora-verkehrswende.de/fileadmin/Projekte/2017/Die_Kosten_synthetischer_Brenn-_und_Kraftstoffe_bis_2050/Agora_SynCost-Studie_WEB.pdf (visited on Feb. 16, 2022).

Amanpour, Saman, Daniel Huck, Mark Kuprat, and Harald Schwarz (2018). "Integrated energy in Germany–A critical look at the development and state of integrated energies in Germany". In: *Frontiers in Energy* 12.4 (2018), pp. 493–500. DOI: 10.1007/s11708-018-0570-2.

Arbeitsgemeinschaft QM Holzheizwerke (2022). *Planungshandbuch: Schriftenreihe QM Holzheizwerke Band 4: Erarbeitet von der Arbeitsgemeinschaft QM Holzheizwerke*. 3., komplett überarbeitete Auflage. Vol. 4. Schriftenreihe QM Holzheizwerke. 2022. ISBN: 978-3-937441-96-2. URL: https://www.qmholzheizwerke.ch/fileadmin/sites/qm/files/00_3_Publikationen/QMH_Planungshandbuch_2022_3.Auflage.pdf (visited on May 1, 2022).

Arning, Katrin, Elisabeth Dütschke, Joachim Globisch, and Barbara Zaunbrecher (2020). "The challenge of improving energy efficiency in the building sector: Taking an in-depth look at decision-making on investments in energy-efficient refurbishments". In: *Energy and Behaviour*. Elsevier, 2020, pp. 129–151. ISBN: 9780128185674. DOI: 10.1016/B978-0-12-818567-4.00002-8.

ASUE (2010). *BHKW-Grundlagen*. Ed. by ASUE Arbeitsgemeinschaft für sparsamen und umweltfreundlichen Energieverbrauch e.V. Berlin, 2010.

ASUE (2015). *BHKW-Kenndaten 2014/15*. 2015.

Aunedi, Marko, Antonio Marco Pantaleo, Kamal Kuriyan, Goran Strbac, and Nilay Shah (2020). "Modelling of national and local interactions between heat and electricity networks in low-carbon energy systems". In: *Applied Energy* 276 (2020), p. 115522. DOI: 10.1016/j.apenergy.2020.115522.

Barthelemy, H., M. Weber, and F. Barbier (2017). "Hydrogen storage: Recent improvements and industrial perspectives". In: *International Journal of Hydrogen Energy* 42.11 (2017), pp. 7254–7262. DOI: 10.1016/j.ijhydene.2016.03.178.

Bayerisches Landesamt für Umwelt and Bayerisches Staatsministerium für Wirtschaft, Landesentwicklung und Energie (2020). *Wärmenetze in Kommunen – Leitfaden: In zehn Schritten zum Wärmenetz*. München/Augsburg, 2020. URL: http://www.bestellen.bayern.de/shoplink/lfu_klima_00152.htm (visited on June 10, 2022).

BDEW (2017a). *Positionspapier—10 Thesen zur Sektorkopplung*. 2017. URL: https://www.bdew.de/media/documents/Stn_20170427_Thesen-Sektorkopplung.pdf (visited on June 10, 2022).

BDEW (2017b). *Strategiepapier "Zukunft Wärmenetzsysteme"*. 2017. URL: https://www.bdew.de/media/documents/Stn_20170615_Strategiepapier-Zukunft-Waermenetzsysteme.pdf (visited on June 10, 2022).

Best, Isabelle, Janybek Orozaliev, and Klaus Vajen (2018). "Impact of Different Design Guidelines on the Total Distribution Costs of 4th Generation District Heating Networks". In: *Energy Procedia* 149 (2018), pp. 151–160. DOI: 10.1016/j.egypro.2018.08.179.

Biegler, Lorenz T. and Ignacio E. Grossmann (2004). "Retrospective on optimization". In: *Computers & Chemical Engineering* 28.8 (2004), pp. 1169–1192. DOI: 10.1016/j.compchemeng.2003.11.003.

BMU (2019). *Klimaschutz in Zahlen: Fakten, Trends und Impulse deutscher Klimapolitik Ausgabe 2019*. Ed. by Bundesministerium für Umwelt, Naturschutz und nukleare Sicherheit. 2019.

BMU (2020). *Klimaschutz in Zahlen: Fakten, Trends und Impulse deutscher Klimapolitik Ausgabe 2020*. Ed. by Bundesministerium für Umwelt, Naturschutz und nukleare Sicherheit. 2020.

BMU (2021). *Klimaschutz in Zahlen: Fakten, Trends und Impulse deutscher Klimapolitik Ausgabe 2021*. Ed. by Bundesministerium für Umwelt, Naturschutz und nukleare Sicherheit. 2021. URL: https://www.bmu.de/fileadmin/Daten_BMU/Pools/Broschueren/klimaschutz_zahlen_2021_bf.pdf (visited on June 10, 2022).

BMWi (2021). *Gesamtausgabe der Energiedaten: Letzte Aktualisierung: 27.09.2021*. 2021. URL: https://www.bmwi.de/Redaktion/DE/Binaer/Energiedaten/energiedaten-gesamt-xls.html (visited on June 10, 2022).

Boeing, Geoff (2017). "OSMnx: New methods for acquiring, constructing, analyzing, and visualizing complex street networks". In: *Computers, Environment and Urban Systems* 65 (2017), pp. 126–139. DOI: 10.1016/j.compenvurbsys.2017.05.004.

Böing, Felix and Anika Regett (2019). "Hourly CO2 Emission Factors and Marginal Costs of Energy Carriers in Future Multi-Energy Systems". In: *Energies* 12.12 (2019), p. 2260. DOI: 10.3390/en12122260.

Bordin, Chiara, Angelo Gordini, and Daniele Vigo (2016). "An optimization approach for district heating strategic network design". In: *European Journal of Operational Research* 252.1 (2016), pp. 296–307. DOI: 10.1016/j.ejor.2015.12.049.

Böswirth, Leopold and Sabine Bschorer (2014). *Technische Strömungslehre*. Wiesbaden: Springer Fachmedien Wiesbaden, 2014. ISBN: 978-3-658-05667-4. DOI: 10.1007/978-3-658-05668-1.

Bundesministerium für Wirtschaft und Klimaschutz (2021). *Zeitreihen zur Entwicklung der erneuerbaren Energien in Deutschland: unter Verwendung von Daten der Arbeitsgruppe Erneuerbare Energien-Statistik (AGEE-Stat) (Stand: September 2021)*. 2021. URL: https://www.erneuerbare-energien.de/EE/Redaktion/DE/Downloads/zeitreihen-zur-entwicklung-der-erneuerbaren-energien-in-deutschland-1990-2021.pdf (visited on June 10, 2022).

Bundesnetzagentur (2014). *Monitoringbericht 2014*. Ed. by Bundesnetzagentur für Elektrizität, Gas, Telekommunikation, Post und Eisenbahnen and Bundeskartellamt. Bonn, 2014. URL: https://www.bundesnetzagentur.de/SharedDocs/Downloads/DE/Allgemeines/Bundesnetzagentur/Publikationen/Berichte/2014/Monitoringbericht_2014_BF.pdf?__blob=publicationFile&v=4 (visited on June 1, 2022).

Bundesnetzagentur (2020a). *Monitoringbericht 2019*. Ed. by Bundesnetzagentur für Elektrizität, Gas, Telekommunikation, Post und Eisenbahnen and Bundeskartellamt. Bonn, 2020. URL: https://www.bundesnetzagentur.de/SharedDocs/Mediathek/Monitoringberichte/Monitoringbericht_Energie2019.pdf?__blob=publicationFile&v=6 (visited on June 1, 2022).

Bundesnetzagentur (2020b). *Regulierung von Wasserstoffnetzen: Bestandsaufnahme*. Ed. by Bundesnetzagentur für Elektrizität, Gas, Telekommunikation, Post und Eisenbahnen. Bonn, 2020. URL: https://www.bundesnetzagentur.de/SharedDocs/Downloads/DE/Sachgebiete/Energie/Unternehmen_Institutionen/NetzentwicklungUndSmartGrid/Wasserstoff/Wasserstoffpapier.pdf?__blob=publicationFile&v=2 (visited on June 1, 2022).

Bundesnetzagentur (2021). *Monitoringbericht 2020*. 2021. URL: https://www.bundesnetzagentur.de/SharedDocs/Mediathek/Monitoringberichte/Monitoringbericht_Energie2020.html (visited on June 10, 2022).

Bundesnetzagentur (2022). *Monitoringbericht 2021*. Ed. by Bundesnetzagentur für Elektrizität, Gas, Telekommunikation, Post und Eisenbahnen and Bundeskartellamt. Bonn, 2022. URL: https://www.bundesnetzagentur.de/SharedDocs/Mediathek/Monitoringberichte/Monitoringbericht_Energie2021.pdf?__blob=publicationFile&v=7 (visited on June 10, 2022).

Bürger, Veit, Tilman Hesse, Andreas Palzer, Benjamin Köhler, Sebastian Herkel, and Peter Engelmann (2017). *Klimaneutraler Gebäudebestand 2050: Energieeffizienzpotentiale und die Auswirkungen des Klimawandels auf den Gebäudebestand*. Ed. by Umweltbundesamt. 2017. URL: https://www.umweltbundesamt.de/sites/default/files/medien/1410/publikationen/2017-11-06_climate-change_26-2017_klimaneutraler-gebaeudebestand-ii.pdf (visited on June 10, 2022).

C.A.R.M.E.N. e.V. (2021). *Marktübersicht Batteriespeicher 2021*. Ed. by C.A.R.M.E.N. e.V. 2021. URL: https://www.carmen-ev.de/service/marktueberblick/marktuebersicht-batteriespeicher/ (visited on Sept. 20, 2021).

Cischinsky, Holger and Nikolaus Diefenbach (2018). *Datenerhebung Wohngebäudebestand 2016: Datenerhebung zu den energetischen Merkmalen und Modernisierungsraten im deutschen und hessischen Wohngebäudebestand*. Ed. by Institut Wohnen und Umwelt. 2018. URL: http://wohngebaeudedaten2016.iwu.de/dl/Endbericht%20Datenerhebung%20Wohngeb%C3%A4udebestand%202016.pdf (visited on June 10, 2022).

co2online (2022). *Energiedaten von Wohngebäuden in Deutschland*. 2022. URL: https://www.wohngebaeude.info/ (visited on June 10, 2022).

Connolly, D., H. Lund, B. V. Mathiesen, S. Werner, B. Möller, U. Persson, T. Boermans, D. Trier, P. A. Østergaard, and S. Nielsen (2014). "Heat Roadmap Europe: Combining district heating with heat savings to decarbonise the EU energy system". In: *Energy Policy* 65 (2014), pp. 475–489. DOI: 10.1016/j.enpol.2013.10.035.

Connolly, David, Henrik Lund, Brian Vad Mathiesen, Poul Alberg Østergaard, Bernd Möller, Steffen Nielsen, Iva Ridjan, Frede Hvelplund, Karl Sperling, Peter Karnøe, Anna M. Carlson, Pil Seok Kwon, Sean Michael Bryant, and Peter Sorknæs (2013). *Smart Energy Systems: Holistic and Integrated Energy Systems for the era of 100% Renewable Energy*. Ed. by Aalborg University. 2013. URL: https://vbn.aau.dk/ws/files/78422810/Smart_Energy_Systems_Aalborg_University.pdf (visited on Feb. 16, 2022).

Cordroch, Luisa, Simon Hilpert, and Frauke Wiese (2022). "Why renewables and energy efficiency are not enough - the relevance of sufficiency in the heating sector for limiting global warming to 1.5 °C". In: *Technological Forecasting and Social Change* 175 (2022), p. 121313. DOI: 10.1016/j.techfore.2021.121313.

Danish Energy Agency (2019). *Technology Data: Generation of Electricity and District heating*. Ed. by Danish Energy Agency. 2019. URL: https://ens.dk/sites/ens.dk/files/Analyser/technology_data_catalogue_for_el_and_dh.pdf (visited on June 10, 2022).

Danish Energy Agency (2020a). *Technology Data: Energy Storage*. Ed. by Danish Energy Agency. 2020. URL: https://ens.dk/sites/ens.dk/files/Analyser/technology_data_catalogue_for_energy_storage.pdf (visited on June 10, 2022).

Danish Energy Agency (2020b). *Technology Data: Generation of Electricity and District heating*. Ed. by Danish Energy Agency. 2020. URL: https://ens.dk/sites/ens.dk/files/Statistik/technology_data_catalogue_for_el_and_dh_-_0009.pdf (visited on June 10, 2022).

Danish Energy Agency (2021a). *Technology Data for heating installations*. Ed. by Danish Energy Agency. 2021. URL: https://ens.dk/en/our-services/projections-and-models/technology-data/technology-data-individual-heating-plants (visited on June 10, 2022).

Danish Energy Agency (2021b). *Technology Data: Renewable fuels*. Ed. by Danish Energy Agency. 2021. URL: https://ens.dk/sites/ens.dk/files/Analyser/technology_data_for_renewable_fuels.pdf (visited on June 10, 2022).

Dau-Schmidt, Wulf (2018). *Stadt Heide Rüsdorfer Kamp – Städtebauliches Quartiersemtwicklungskonzept*. Heide, 2018.

dena (2016). *dena Gebäudereport: Statistiken und Analysen zur Energieeffizienz im Gebäudebestand*. Ed. by Deutsche Energie-Agentur GmbH. 2016. URL: https://www.dena.de/fileadmin/user_upload/8162_dena-Gebaeudereport.pdf (visited on June 10, 2022).

dena (2018). *dena-Leitstudie Integrierte Energiewende: Impulse für die Gestaltung des Energiesystems bis 2050*. Ed. by Deutsche Energie-Agentur GmbH. Berlin, 2018. URL: https://www.dena.de/fileadmin/dena/Dokumente/Pdf/9261_dena-Leitstudie_Integrierte_Energiewende_lang.pdf (visited on June 10, 2022).

Dochev, Ivan, Irene Peters, Hannes Seller, and Georg K. Schuchardt (2018). "Analysing district heating potential with linear heat density. A case study from Hamburg". In: *Energy Procedia* 149 (2018), pp. 410–419. DOI: 10.1016/j.egypro.2018.08.205.

Dorfner, Johannes (2016). "Open Source Modelling and Optimisation of Energy Infrastructure at Urban Scale". Dissertation. München: Technische Universität München, 2016. URL: https://mediatum.ub.tum.de/doc/1285570/document.pdf (visited on June 10, 2022).

Dorfner, Johannes and Thomas Hamacher (2014). "Large-Scale District Heating Network Optimization". In: *IEEE Transactions on Smart Grid* 5.4 (2014), pp. 1884–1891. DOI: 10.1109/TSG.2013.2295856.

Dorotić, Hrvoje, Tomislav Pukšec, and Neven Duić (2019). "Economical, environmental and exergetic multi-objective optimization of district heating systems on hourly level for a whole year". In: *Applied Energy* 251 (2019), p. 113394. DOI: 10.1016/j.apenergy.2019.113394.

Dunkelberg, Elisa, Alexander Deisböck, Benjamin Herrmann, Bernd Hirschl, Tino Mitzinger, Johannes Röder, Steven Salecki, Pablo Thier, and Timo Wassermann (2020). *Fernwärme klimaneutral transformieren. Eine Bewertung der Handlungsoptionen am Beispiel von Berlin Nord-Neukölln*. Ed. by Institut für ökologische Wirtschaftsforschung. Berlin, 2020. URL: https://www.ioew.de/fileadmin/user_upload/BILDER_und_Downloaddateien/Publikationen/Schriftenreihen/IOeW_SR_218_Fernwaerme_klimaneutral_transformieren.pdf (visited on June 10, 2022).

EnergieSchweiz (2017). *Räumliche Energieplanung: Werkzeuge für eine zukunftstaugliche Wärme- und Kälteversorgung: Information für kommunale Behörden und Fachpersonen*. Ed. by EnergieSchweiz für Gemeinden. 2017. URL: https://www.local-energy.swiss/dam/jcr:f43a8c6a-9db4-4c8c-9295-00c86f5c264d/Werkzeugkoffer_Energieplanung_Modul6_DE.pdf (visited on June 10, 2022).

ENERPIPE GmbH (2022). *Caldo PEX von ENERPIPE: Mit Sicherheit, mehr Wärme*. URL: https://www.enerpipe.de/produkte/pdl/?file=CaldoPEX_6S_ENERPE_06_2015_DE.pdf (visited on June 10, 2022).

European Comission (2019). *The European Green Deal*. Brussels, 2019. URL: https://eur-lex.europa.eu/legal-content/EN/TXT/?uri=CELEX:52019DC0640 (visited on June 10, 2022).

F. Holmgren, William, Clifford W. Hansen, and Mark A. Mikofski (2018). “pvlib python: a python package for modeling solar energy systems”. In: *Journal of Open Source Software* 3.29 (2018), p. 884. DOI: 10.21105/joss.00884.

Fekete, Patrick (2021). *Redispatch in Deutschland: Auswertung der Transparenzdaten April 2013 bis einschließlich Dezember 2020*. Ed. by BDEW - Bundesverband der Energie- und Wasserwirtschaft e.V. Berlin, 2021. URL: https://www.bdew.de/media/documents/2021_Q2_Bericht_Redispatch.pdf (visited on June 10, 2022).

FfE (2020). *Curtailment (German Districts)*. Ed. by Forschungsstelle für Energiewirtschaft e. V. München, 2020. URL: http://opendata.ffe.de/dataset/curtailment-german-districts/ (visited on June 10, 2022).

Fisch, Norbert, Mathias Schlosser, Sven Reiser, Peter Ruschin, Thomas Wilken, and Robert Kellner (2015). *future:solar: Systemanalyse zur solaren Energieversorgung: Forschungsbericht*. Ed. by Technische Universität Braunschweig. 2015. URL: https://www.tu-braunschweig.de/index.php?eID=dumpFile&t=f&f=75024&token=07b2e695b15593eff6604c2c1bfab8bd4365b7d8 (visited on June 10, 2022).

Forschungsgesellschaft für Energiewirtschaft mbH (2007). *Ganzheitliche dynamische Bewertung der KWK mit Brennstoffzellentechnologie - Forschungsvorhaben im Forschungsverbund EduaR&D*. München, 2007. DOI: 10.2314/GBV:559930046.

Fraunhofer IEE, Fraunhofer ISE, and Becker Büttner Held Rechtsanwälte Wirtschaftsprüfer Steuerberater PartGmbB (2021). *Neues Strommarktdesign für die Integration fluktuierender Erneuerbarer Energien*. Ed. by Bundesverband Erneuerbare Energie e.V. Kassel, Freiburg, and Berlin, 2021. URL: http://klimaneutrales-stromsystem.de/pdf/Strommarktdesignstudie_BEE_final_Stand_14_12_2021.pdf (visited on June 10, 2022).

Fraunhofer ISE (2020a). *Wärmepumpen in Bestandsgebäuden: Ergebnisse aus dem Forschungsprojekt "WPsmart im Bestand": Abschlussbericht*. 2020. URL: https://www.ise.fraunhofer.de/content/dam/ise/de/downloads/pdf/Forschungsprojekte/BMWi-03ET1272A-WPsmart_im_Bestand-Schlussbericht.pdf (visited on June 10, 2022).

Fraunhofer ISE (2020b). *WEGE ZU EINEM KLIMANEUTRALEN ENERGIESYSTEM: Die deutsche Energiewende im Kontext gesellschaftlicher Verhaltensweisen*. Ed. by Fraunhofer-Institut für Solare Energiesysteme ISE. 2020. URL: https://www.ise.fraunhofer.de/content/dam/ise/de/documents/publications/studies/Fraunhofer-ISE-Studie-Wege-zu-einem-klimaneutralen-Energiesystem.pdf (visited on June 10, 2022).

Fraunhofer ISE (2020c). *WEGE ZU EINEM KLIMANEUTRALEN ENERGIESYSTEM: Die deutsche Energiewende im Kontext gesellschaftlicher Verhaltensweisen: Anhang zur Studie*. Ed. by Fraunhofer ISE. 2020. URL: https://www.ise.fraunhofer.de/content/dam/ise/de/documents/publications/studies/Anhang-Studie-Wege-zu-einem-klimaneutralen-Energiesystem.pdf (visited on June 10, 2022).

Fraunhofer ISE (2020d). *WEGE ZU EINEM KLIMANEUTRALEN ENERGIESYSTEM: Die deutsche Energiewende im Kontext gesellschaftlicher Verhaltensweisen: Update unter einer Zielvorgabe von 65% CO2-Reduktion in 2030 und 100% in 2050*. Ed. by Fraunhofer-Institut

für Solare Energiesysteme ISE. 2020. URL: https://www.ise.fraunhofer.de/content/dam/ise/de/documents/publications/studies/Fraunhofer-ISE-Studie-Wege-zu-einem-klimaneutralen-Energiesystem-Update-Zielverschaerfung.pdf (visited on June 10, 2022).

Fraunhofer IWES and Fraunhofer IBP (2017). *Wärmewende 2030: Schlüsseltechnologien zur Erreichung der mittel- und langfristigen Klimaschutzziele im Gebäudesektor: Studie im Auftrag von Agora*. Ed. by Agora Energiewende. Kassel, 2017. URL: https://static.agora-energiewende.de/fileadmin/Projekte/2016/Sektoruebergreifende_EW/Waermewende-2030_WEB.pdf (visited on June 10, 2022).

Fröling, Morgan, Hans Bengtsson, and Olle Ramnäs (2006). "Environmental performance of district heating in suburban areas compared with heat pump and pellets furnace". In: *10th International Symposium on District Heating and Cooling*. 2006. URL: http://www.lsta.lt/files/events/12_froeling.pdf (visited on June 10, 2022).

Frontier Economics, IAEW, 4Management, and EMCEL (2017). *Der Wert der Gasinfrastruktur für die Energiewende in Deutschland: Eine modellbasierte Analyse*. Ed. by Vereinigung der Fernleitungsnetzbetreiber. 2017. URL: https://fnb-gas.de/wp-content/uploads/2021/09/fnb_gas-wert_von_gasinfrastruktur-endbericht.pdf (visited on June 10, 2022).

Gabrielli, Paolo, Florian Fürer, Georgios Mavromatidis, and Marco Mazzotti (2019). "Robust and optimal design of multi-energy systems with seasonal storage through uncertainty analysis". In: *Applied Energy* 238 (2019), pp. 1192–1210. DOI: 10.1016/j.apenergy.2019.01.064.

Gatzen, Christoph and Ann-Katrin Lenz (2021). *Wasserstoff zur Dekarbonisierung des Wärmesektors*. Ed. by DVGW Deutscher Verein des Gas- und Wasserfaches e. V. 2021. URL: https://www.dvgw.de/medien/dvgw/forschung/berichte/g202101-h2-waermemarkt-abschlussbericht.pdf (visited on June 10, 2022).

GEG (2020). *Gesetz zur Einsparung von Energie und zur Nutzung erneuerbarer Energien zur Wärme- und Kälteerzeugung in Gebäuden* (Gebäudeenergiegesetz - GEG) § 22 Primärenergiefaktoren, Anhang 4: GEG*. 2020. URL: https://www.gesetze-im-internet.de/geg/GEG.pdf (visited on June 10, 2022).

GeoPandas community (2022). *GeoPandas documentation*. 2022. URL: https://geopandas.org/en/stable/index.html (visited on June 10, 2022).

GitHub, Inc. (2022). *GitHub*. 2022. URL: https://github.com/ (visited on June 10, 2022).

Gudmundsson, Oddgeir, Jan Eric Thorsen, and Marek Brand (2018). "The role of district heating in coupling of the future renewable energy sectors". In: *Energy Procedia* 149 (2018), pp. 445–454. DOI: 10.1016/j.egypro.2018.08.209.

Gurobi Optimization LLC (2022). *Gurobi Optimizer Reference Manual*. 2022. URL: http://www.gurobi.com (visited on June 10, 2022).

Hamels, Sam, Eline Himpe, Jelle Laverge, Marc Delghust, Kjartan van den Brande, Arnold Janssens, and Johan Albrecht (2021). "The use of primary energy factors and CO2 intensities for electricity in the European context - A systematic methodological review and critical evaluation of the contemporary literature". In: *Renewable and Sustainable Energy Reviews* 146 (2021), p. 111182. DOI: 10.1016/j.rser.2021.111182.

Hampp, Johannes, Michael Düren, and Tom Brown (2021). *Import options for chemical energy carriers from renewable sources to Germany*. 2021. DOI: 10.48550/arXiv.2107.01092.

Hank, Christoph, André Sternberg, Nikolas Köppel, Marius Holst, Tom Smolinka, Achim Schaadt, Christopher Hebling, and Hans-Martin Henning (2020). "Energy efficiency and economic assessment of imported energy carriers based on renewable electricity". In: *Sustainable Energy & Fuels* 4.5 (2020), pp. 2256–2273. DOI: 10.1039/D0SE00067A.

Hart, William E., Carl D. Laird, Jean-Paul. Watson, David L. Woodruff, Gabriel A. Hackebeil, Bethany L. Nicholson, and John D. Siirola (2017). *Pyomo – Optimization Modeling in Python*. 2nd ed. 2017. Vol. 67. Springer Optimization and Its Applications. Cham: Springer International Publishing and Imprint: Springer, 2017. ISBN: 978-3-319-58821-6.

Heilmann, Erik, Nikolai Klempp, and Heike Wetzel (2020). "Design of regional flexibility markets for electricity: A product classification framework for and application to German pilot projects". In: *Utilities Policy* 67 (2020), p. 101133. DOI: 10.1016/j.jup.2020.101133.

Hesaraki, Arefeh, Adnan Ploskic, and Sture Holmberg (2015). "Integrating Low-temperature Heating Systems into Energy Efficient Buildings". In: *Energy Procedia* 78 (2015), pp. 3043–3048. DOI: 10.1016/j.egypro.2015.11.720.

HIC and FfE (2021). *Grüne Fernwärme für Deutschland – Potenziale, Kosten, Umsetzung: Kurzstudie*. Ed. by BDEW - Bundesverband der Energie- und Wasserwirtschaft e.V. Hamburg and München, 2021. URL: https://www.bdew.de/media/documents/2021-04-06_Bericht_Kurzstudie_gr%C3%BCne_Fernw%C3%A4rme_Finalfassung.pdf (visited on June 10, 2022).

Hilpert, S., C. Kaldemeyer, U. Krien, S. Günther, C. Wingenbach, and G. Plessmann (2018). "The Open Energy Modelling Framework (oemof) - A new approach to facilitate open science in energy system modelling". In: *Energy Strategy Reviews* 22 (2018), pp. 16–25. DOI: 10.1016/j.esr.2018.07.001.

Hinton, Tom, Mark Gibbons, Neil Justice, and jthu (2022). *Thermos UI*. https://api.github.com/repos/cse-bristol/110-thermos-ui. 2022. URL: https://github.com/cse-bristol/110-thermos-ui (visited on June 3, 2022).

IWU (2015). *Deutsche Wohngebäudetypologie: Beispielhafte Maßnahmen zur Verbesserung der Energieeffizienz von typischen Wohngebäuden*. Ed. by Institut Wohnen und Umwelt. Darmstadt, 2015. URL: https://episcope.eu/fileadmin/tabula/public/docs/brochure/DE_TABULA_TypologyBrochure_IWU.pdf (visited on June 10, 2022).

Jnnr, Caroline Möller, FranziPl, MaGering, jakob-wo, Patrik Schönfeldt, felixj9, Uwe Krien, Sabine Haas, Cord Kaldemeyer, and Stephan Günther (2020a). *oemof/oemof-thermal: Virtuous Validation*. 2020. DOI: 10.5281/zenodo.4087977.

Jnnr, Johannes Röder, MaGering, Joris Zimmermann, Uwe Krien, and — (2021). *oemof/DHNx: Geo Processing*. 2021. DOI: 10.5281/zenodo.5084392.

Jnnr, Johannes Röder, MaGering, Okan Akca, and Joris Zimmermann (2020b). *oemof/DHNx: Gorgeous Grids*. 2020. DOI: 10.5281/zenodo.4147049.

Johnjforrest, Stefan Vigerske, Haroldo Gambini Santos, Ted Ralphs, Lou Hafer, Bjarni Kristjansson, Jpfasano, EdwinStraver, Miles Lubin, Rlougee, Jpgoncal1, H-I-Gassmann, and Matthew Saltzman (2020). *coin-or/Cbc: Version 2.10.5*. 2020. DOI: 10.5281/ZENODO.3700700.

Jonas, Hans (1979). *Das Prinzip Verantwortung: Versuch einer Ethik für die technologische Zivilisation*. Frankfurt am Main, 1979.

Jonas, Hans and David Herr (1985). *The Imperative of Responsibility: In Search of an Ethics for the Technological Age*. University of Chicago Press, 1985. ISBN: 9780226405971.

Juhrich, Kristina (2016). *CO2-Emissionsfaktoren für fossile Brennstoffe*. Ed. by Umweltbundesamt. 2016. URL: https://www.umweltbundesamt.de/sites/default/files/medien/1968/publikationen/co2-emissionsfaktoren_fur_fossile_brennstoffe_korrektur.pdf (visited on June 10, 2022).

Kersten, Mathias, Max Bachmann, Tong Guo, and Martin Kriegel (2021). "Methodology to design district heating systems with respect to local energy potentials, CO2-emission restrictions, and federal subsidies using oemof: 39-58 Pages / International Journal of Sustainable Energy Planning and Management, Vol. 31 (2021)". In: (2021). DOI: 10.5278/IJSEPM.6323.

KfW (2022). *Die Effizienzhaus-Stufen für bestehende Immobilien und Baudenkmale*. 2022. URL: https://www.kfw.de/inlandsfoerderung/Privatpersonen/Bestehende-Immobilie/Energieeffizient-sanieren/Das-Effizienzhaus/ (visited on June 10, 2022).

Klein, Konstantin, Doreen Kalz, and Sebastian Herkel (2014). "Netzdienlicher Betrieb von Gebäuden: Analyse und Vergleich netzbasierter Referenzgrößen und Definition einer Bewertungskennzahl". In: *Bauphysik* 36.2 (2014), pp. 49–58. DOI: 10.1002/bapi.201410019.

Klein, Konstantin, Robert Langner, Doreen Kalz, Sebastian Herkel, and Hans-Martin Henning (2016). "Grid support coefficients for electricity-based heating and cooling and field data analysis of present-day installations in Germany". In: *Applied Energy* 162 (2016), pp. 853–867. DOI: 10.1016/j.apenergy.2015.10.107.

Klemm, Christian, Gregor Becker, Janik Budde, Yannik Wittor, Pascal Kerkeling, jan-frank, Philipp Sommer, and Vinxenx (2022). *SESMG: Spreadsheet Energy System Model Generator*. 2022. URL: https://github.com/chrklemm/SESMG (visited on June 1, 2022).

Klemm, Christian and Peter Vennemann (2021). "Modeling and optimization of multi-energy systems in mixed-use districts: A review of existing methods and approaches". In: *Renewable and Sustainable Energy Reviews* 135 (2021), p. 110206. DOI: 10.1016/j.rser.2020.110206.

Knies, Jürgen (2018). "A spatial approach for future-oriented heat planning in urban areas". In: *International Journal of Sustainable Energy Planning and Management* 16 (2018), pp. 3–30. DOI: 10.5278/IJSEPM.2018.16.2. (Visited on June 10, 2022).

Köppl, Simon, Adrian Ostermann, and S. Fattler (2020). "Congestion management and its interdependency with the energy system in Germany – an empirical analysis". In: *19th International Workshop on Large-Scale Integration of Wind Power into Power Systems as well as on Transmission Networks for Offshore Wind Plants* (2020). URL: https://windintegrationworkshop.org/virtual2020/ (visited on June 10, 2022).

Krien, Uwe (2019). "Erweiterung der Bewertungskriterien von regionalen Strom-Wärme-Modellen durch die Kopplung mit einem überregionalen Modell". Dissertation. Berlin: Technischen Universität Berlin, 2019. URL: https://www.reiner-lemoine-stiftung.de/pdf/dissertationen/Dissertation-Uwe_Krien.pdf (visited on June 10, 2022).

Krien, Uwe, Patrik Schönfeldt, Jann Launer, Simon Hilpert, Cord Kaldemeyer, and Guido Pleßmann (2020). "oemof.solph—A model generator for linear and mixed-integer linear optimisation of energy systems: Software Impacts, 100028". In: (2020). DOI: 10.1016/J.SIMPA.2020.100028.

KSG (2021). *Bundes-Klimaschutzgesetz (KSG)*. 2021. URL: https://www.gesetze-im-internet.de/ksg/index.html (visited on Mar. 9, 2022).

Kuhn, Philipp (2011). "Iteratives Modell zur Optimierung von Speicherausbau und -betrieb in einem Stromsystem mit zunehmend fluktuierender Erzeugung". Dissertation. München: Technischen Universität München, 2011. URL: https://mediatum.ub.tum.de/doc/1271192/1271192.pdf (visited on June 10, 2022).

Kuriyan, Kamal and Nilay Shah (2019). "A combined spatial and technological model for the planning of district energy systems". In: *International Journal of Sustainable Energy Planning and Management* 21 (2019), pp. 111–131. DOI: 10.5278/ijsepm.2019.21.8.

Lambert, Romain Stephane Claude, Sebastian Maier, Nilay Shah, and John W. Polak (2016). "Optimal phasing of district heating network investments using multi-stage stochastic programming: International Journal of Sustainable Energy Planning and Management". In: 9 (2016), pp. 57–74. DOI: 10.5278/IJSEPM.2016.9.5.

Le Truong, Nguyen, Ambrose Dodoo, and Leif Gustavsson (2015). "Renewable-based heat supply of multi-apartment buildings with varied heat demands". In: *Energy* 93 (2015), pp. 1053–1062. DOI: 10.1016/j.energy.2015.09.087.

Li, Hongwei and Svend Svendsen (2013). "District Heating Network Design and Configuration Optimization with Genetic Algorithm". In: *Journal of Sustainable Development of Energy, Water and Environment Systems* 1.4 (2013), pp. 291–303. DOI: 10.13044/j.sdewes.2013.01.0022.

Lund, H., B. Möller, B. V. Mathiesen, and A. Dyrelund (2010). "The role of district heating in future renewable energy systems". In: *Energy* 35 (2010), pp. 1381–1390. DOI: 10.1016/j.energy.2009.11.023.

Lund, Henrik (2014). *Renewable energy systems: A smart energy systems approach to the choice and modeling of 100% renewable solutions*. 2nd edition. Amsterdam et al.: Elsevier Academic Press, 2014. ISBN: 978-0-12-410423-5.

Lund, Henrik, Poul Alberg Østergaard, David Connolly, and Brian Vad Mathiesen (2017). "Smart energy and smart energy systems". In: *Energy* 137 (2017), pp. 556–565. DOI: 10.1016/j.energy.2017.05.123.

Lund, Henrik, Poul Alberg Østergaard, David Connolly, Iva Ridjan, Brian Vad Mathiesen, Frede Hvelplund, Jakob Zinck Thellufsen, and Peter Sorknæs (2016). "Energy Storage and Smart Energy Systems". In: *International Journal of Sustainable Energy Planning and Management* 11 (2016), pp. 3–14. DOI: 10.5278/IJSEPM.2016.11.2.

Lund, Henrik, Sven Werner, Robin Wiltshire, Svend Svendsen, Jan Eric Thorsen, Frede Hvelplund, and Brian Vad Mathiesen (2014). "4th Generation District Heating (4GDH)". In: *Energy* 68 (2014), pp. 1–11. DOI: 10.1016/j.energy.2014.02.089.

Mancarella, Pierluigi (2014). "MES (multi-energy systems): An overview of concepts and evaluation models". In: *Energy* 65 (2014), pp. 1–17. DOI: 10.1016/j.energy.2013.10.041.

Maurer, Christoph, Christian Zimmer, and Lion Hirth (2018). *Nodale und zonale Strompreissysteme im Vergleich: Abschlussbericht*. 2018. URL: https://www.bmwk.de/Redaktion/DE/Publikationen/Studien/nodale-und-zonale-strompreissysteme-im-vergleich.html (visited on June 10, 2022).

Meier, Hermann, Christian Fünfgeld, Thomas Adam, and Bernd Schieferdecker (1999). *Repräsentative VDEW-Lastprofile*. Ed. by Brandenburgische Technische Universität Cottbus. Frankfurt (Main), 1999. URL: https://www.bdew.de/media/documents/1999_Repraesentative-VDEW-Lastprofile.pdf (visited on June 10, 2022).

Merten, Frank, Alexander Scholz, Christine Krüger, Simon Heck, Yann Girard, Marc Mecke, and Marius George (2020). *Bewertung der Vor- und Nachteile von Wasserstoffimporten im Vergleich zur heimischen Erzeugung*. Ed. by Wuppertal Institut für Klima, Umwelt, Energie gGmbH and DIW Econ GmbH. 2020. URL: https://wupperinst.org/fa/redaktion/downloads/projects/LEE-H2-Studie.pdf (visited on June 10, 2022).

Metzger, Sebastian, Katy Jahnke, Nadine Walikewitz, Markus Otto, Andreas Grondey, and Sara Fritz (2019). *Wohnen und Sanieren: Empirische Wohngebäudedaten seit 2002*. Ed. by Umweltbundesamt. Dessau-Roßlau, 2019. URL: https://www.umweltbundesamt.de/publikationen/hintergrundbericht-wohnen-sanieren (visited on June 10, 2022).

Möller, Bernd and Steffen Nielsen (2014). "High resolution heat atlases for demand and supply mapping: 41-58 Pages / International Journal of Sustainable Energy Planning and Management, Vol 1 (2014)". In: (2014). DOI: 10.5278/IJSEPM.2014.1.4.

Möller, Bernd and Sven Werner (2016). *Quantifying the Potential for District Heating and Cooling in EU Member States: Work Package 2 Background Report 6*. 2016. URL: https://heatroadmap.eu/wp-content/uploads/2018/09/STRATEGO-WP2-Background-Report-6-Mapping-Potenital-for-DHC.pdf (visited on June 10, 2022).

Möller, Bernd, Eva Wiechers, Urban Persson, Lars Grundahl, Rasmus Søgaard Lund, and Brian Vad Mathiesen (2019). "Heat Roadmap Europe: Towards EU-Wide, local heat supply strategies". In: *Energy* 177 (2019), pp. 554–564. DOI: 10.1016/j.energy.2019.04.098.

Moradi, Ramin and Katrina M. Groth (2019). "Hydrogen storage and delivery: Review of the state of the art technologies and risk and reliability analysis". In: *International Journal of Hydrogen Energy* 44.23 (2019), pp. 12254–12269. DOI: 10.1016/j.ijhydene.2019.03.041.

Müller-Syring, Gert, Marco Henel, Marek Poltrum, Anja Wehling, Elias Dannenberg, Josephine Gladien, Hartmut Krause, Fabian Möhrke, Markus Zdrallek, and Felix Ortloff (2018). *Transformationspfade zur Treibhausgasneutralität der Gasnetze und Gasspeicher nach COP 21*. Ed. by DVGW Deutscher Verein des Gas- und Wasserfaches e. V. 2018. URL: https://www.dvgw.de/medien/dvgw/forschung/berichte/transformationspfade-treibhausgasneutralitaet-1810mueller.pdf (visited on June 10, 2022).

Nastasi, Benedetto and Gianluigi Lo Basso (2016). "Hydrogen to link heat and electricity in the transition towards future Smart Energy Systems". In: *Energy* 110 (2016), pp. 5–22. DOI: 10.1016/j.energy.2016.03.097.

NREL (2022). *EnergyPlus*. Ed. by National Renewable Energy Laboratory. 2022. URL: https://github.com/NREL/EnergyPlus.

Nussbaumer, T. and S. Thalmann (2016). "Influence of system design on heat distribution costs in district heating". In: *Energy* 101 (2016), pp. 496–505. DOI: 10.1016/j.energy.2016.02.062.

oemof developer group (2020a). *oemof-solph - a model generator for energy systems - v0.4.1*. 2020. DOI: 10.5281/ZENODO.3906081. URL: https://github.com/oemof/oemof-solph (visited on July 20, 2020).

oemof developer group (2020b). *oemof.solph documentation: v0.4.1*. 2020. URL: https://oemof-solph.readthedocs.io/en/v0.4.1/ (visited on June 10, 2022).

oemof developer group (2020c). *oemof.tools - documentation*. 2020. URL: https://oemof-tools.readthedocs.io/en/latest/reference/oemof_tools.html (visited on June 10, 2022).

oemof developer group (2022a). *DHNx documentation*. 2022. URL: https://dhnx.readthedocs.io/en/latest/index.html (visited on June 10, 2022).

oemof developer group (2022b). *DHNx: District heating system optimisation and simulation models*. 2022. URL: https://github.com/oemof/DHNx (visited on June 10, 2022).

ÖKL (1999). *Technischwirtschaftliche Standards für Biomasse-Fernheizwerke: 1. Auflage*. Ed. by Bund-Länder-Arbeitsgruppe Ökoenergiefonds. 1999.

openmod contributors (2021). *Open Models*. 2021. URL: https://wiki.openmod-initiative.org/wiki/Open_Models (visited on June 10, 2022).

OpenStreetMap contributors (2022). *Planet dump retrieved from https://planet.osm.org.* URL: https://www.openstreetmap.org (visited on June 10, 2022).

Pacific Northwest National Laboratory (2014). *ANSI/ASHRAE/IES Standard 90.1 Prototype Building Model Package.* 2014. URL: https://www.energycodes.gov/development/commercial/prototype_models (visited on June 10, 2022).

Pehnt, Martin, Peter Mellwig, Sebastian Blömer, Hans Hertle, Michael Nast, Amany von Oehsen, Julia Lempik, Nora Langreder, Nils Thamling, Andreas Hermelink, Markus Offermann, Peter Pannier, and Michael Müller (2018). *Untersuchung zu Primärenergiefaktoren: Endbericht: Auftraggeber BMWi, Abt. II, Ref. C2.* Heidelberg, 2018. URL: https://www.gih.de/wp-content/uploads/2019/05/Untersuchung-zu-Prim%C3%A4renergiefaktoren.pdf (visited on June 10, 2022).

Persson, Urban and Sven Werner (2011). "Heat distribution and the future competitiveness of district heating". In: *Applied Energy* 88.3 (2011), pp. 568–576. DOI: 10.1016/j.apenergy.2010.09.020.

Persson, Urban, Eva Wiechers, Bernd Möller, and Sven Werner (2019). "Heat Roadmap Europe: Heat distribution costs". In: *Energy* 176 (2019), pp. 604–622. DOI: 10.1016/j.energy.2019.03.189.

Pinel, Dimitri, Magnus Korpås, and Karen B. Lindberg (2021). "Impact of the CO2 factor of electricity and the external CO2 compensation price on zero emission neighborhoods' energy system design". In: *Building and Environment* 187 (2021), p. 107418. DOI: 10.1016/j.buildenv.2020.107418.

Pol, O. and R.-R. Schmidt (2016). *Development of district heating and cooling in the urban planning context.* 2016. DOI: 10.1016/b978-1-78242-374-4.00015-x.

Prina, Matteo Giacomo, Giampaolo Manzolini, David Moser, Benedetto Nastasi, and Wolfram Sparber (2020). "Classification and challenges of bottom-up energy system models - A review". In: *Renewable and Sustainable Energy Reviews* 129 (2020), p. 109917. DOI: 10.1016/j.rser.2020.109917.

Prognos, Öko-Institut, and Wuppertal-Institut (2020a). *Klimaneutrales Deutschland: Datenanhang: Studie im Auftrag von Agora Energiewende, Agora Verkehrswende und Stiftung Klimaneutralität.* Ed. by Agora Energiewende, Agora Verkehrswende, and Stiftung Klimaneutralität. 2020. URL: https://www.agora-energiewende.de/veroeffentlichungen/klimaneutrales-deutschland-datenanhang/ (visited on June 10, 2022).

Prognos, Öko-Institut, and Wuppertal-Institut (2020b). *Klimaneutrales Deutschland: Studie im Auftrag von Agora Energiewende, Agora Verkehrswende und Stiftung Klimaneutralität.* Ed. by Agora Energiewende, Agora Verkehrswende, and Stiftung Klimaneutralität. 2020. URL: https://www.agora-energiewende.de/veroeffentlichungen/klimaneutrales-deutschland/ (visited on June 10, 2022).

Razani, Amru Rizal and Ingo Weidlich (2016). "A genetic algorithm technique to optimize the configuration of heat storage in DH networks". In: *International Journal of Sustainable Energy Planning and Management* 10 (2016), pp. 21–32. DOI: 10.5278/IJSEPM.2016.10.3.

Regett, Anika, Felix Boing, Joehen Conrad, Steffen Fattler, and Constanze Kranner (2018). "Emission Assessment of Electricity: Mix vs. Marginal Power Plant Method". In: *2018 15th International Conference on the European Energy Market (EEM)*. IEEE, 2018, pp. 1–5. ISBN: 978-1-5386-1488-4. DOI: 10.1109/EEM.2018.8469940.

Renz, Ina and Ulrike Hacke (2016). *Einflussfaktoren auf die Sanierung im deutschen Wohngebäudebestand: Ergebnisse einer qualitativen Studie zu Sanierungsanreizen und -hemmnissen privater und institutioneller Eigentümer*. Ed. by Institut Wohnen und Umwelt. Darmstadt, 2016. URL: https://www.iwu.de/fileadmin/publikationen/wohnen/prj/IWU_2016_6363_1603_KfW_Einflussfaktoren_Sanierung_Abschlussbericht.pdf (visited on June 10, 2022).

Reuß, M., T. Grube, M. Robinius, P. Preuster, P. Wasserscheid, and D. Stolten (2017). "Seasonal storage and alternative carriers: A flexible hydrogen supply chain model". In: *Applied Energy* 200 (2017), pp. 290–302. DOI: 10.1016/j.apenergy.2017.05.050.

Rezaie, Behnaz and Marc A. Rosen (2012). "District heating and cooling: Review of technology and potential enhancements". In: *Applied Energy* 93 (2012), pp. 2–10. DOI: 10.1016/j.apenergy.2011.04.020.

Risse, Oliver, Cyril Stephanos, and Berit Erlach, eds. (2020). *Netzengpässe als Herausforderung für das Stromversorgungssystem: Optionen zur Weiterentwicklung des Marktdesigns*. Stellungnahme / Deutsche Akademie der Naturforscher Leopoldina. Halle (Saale), Mainz, and München: Deutsche Akademie der Naturforscher Leopoldina e.V. - Nationale Akademie der Wissenschaften, Union der deutschen Akademien der Wissenschaften e. V, and acatech - Deutsche Akademie der Technikwissenschaften e. V, 2020. ISBN: 978-3-8047-4116-4. URL: http://nbn-resolving.org/urn:nbn:de:gbv:3:2-126924 (visited on June 10, 2022).

Robinius, Martin, Alexander Otto, Philipp Heuser, Lara Welder, Konstantinos Syranidis, David Ryberg, Thomas Grube, Peter Markewitz, Ralf Peters, and Detlef Stolten (2017). "Linking the Power and Transport Sectors—Part 1: The Principle of Sector Coupling". In: *Energies* 10.7 (2017), p. 956. DOI: 10.3390/en10070956.

Röder, Johannes, David Beier, Benedikt Meyer, Joris Nettelstroth, Torben Stührmann, and Edwin Zondervan (2020). "Design of Renewable and System-Beneficial District Heating Systems Using a Dynamic Emission Factor for Grid-Sourced Electricity". In: *Energies* 13.3 (2020), p. 619. DOI: 10.3390/en13030619.

Röder, Johannes and Uwe Krien (2022a). *q100opt: Model builder for oemof-solph optimisation models with focus on district energy systems*. 2022. URL: https://github.com/quarree100/q100opt (visited on June 10, 2022).

Röder, Johannes, Benedikt Meyer, Uwe Krien, Joris Zimmermann, Torben Stührmann, and Edwin Zondervan (2021). "Optimal Design of District Heating Networks with Distributed Thermal Energy Storages – Method and Case Study: 5-22 Pages / International Journal of

Sustainable Energy Planning and Management, Vol. 31 (2021)". In: (2021). DOI: 10.5278/ijsepm.6248.

Röder, Johannes and Edwin Zondervan (2022b). "Development of future-proof supply concepts for sector-coupled district heating systems based on scenario-analysis". In: *Physical Sciences Reviews* 0.0 (2022). DOI: 10.1515/psr-2020-0053.

Saletti, Costanza, Mirko Morini, and Agostino Gambarotta (2020). "The Status of Research and Innovation on Heating and Cooling Networks as Smart Energy Systems within Horizon 2020". In: *Energies* 13.11 (2020), p. 2835. DOI: 10.3390/en13112835.

Schleswig-Holstein Ministerium für Energiewende, Landwirtschaft, Umwelt, Natur und Digitalisierung (2022). *Bericht zum Engpassmanagement in Schleswig-Holstein: Einspeisemanagement in den Jahren 2010 - 2018 und Redispatch in den Jahren 2016 - 2018*. Ed. by Schleswig-Holstein Ministerium für Energiewende, Landwirtschaft, Umwelt, Natur und Digitalisierung, Schleswig-Holstein Netz AG, and TenneT TSO GmbH. URL: https://www.schleswig-holstein.de/DE/Fachinhalte/E/erneuerbareenergien/Bericht_Einspeisemanagement.pdf;jsessionid=07892D42FC5731581126920DCCD8CA4C.delivery2-replication?__blob=publicationFile&v=1 (visited on June 10, 2022).

Schleswig-Holstein Netz AG (2022). *Abgeschlossene Maßnahmen Einspeisemanagement*. URL: https://www.sh-netz.com/de/energie-einspeisen/einspeisemanagement/veroeffentlichungen/abgeschlossene-massnahmen.html (visited on June 10, 2022).

Schmeling, Lucas, Patrik Schönfeldt, Peter Klement, Steffen Wehkamp, Benedikt Hanke, and Carsten Agert (2020). "Development of a Decision-Making Framework for Distributed Energy Systems in a German District". In: *Energies* 13.3 (2020), p. 552. DOI: 10.3390/en13030552.

Schüwer, Dietmar, Thomas Hanke, and Hans-Jochen Luhmann (2015). *Konsistenz und Aussagefähigkeit der Primärenergie-Faktoren für Endenergieträger im Rahmen der EnEV : Diskussionspapier*. Wuppertal, 2015. URL: http://nbn-resolving.de/urn:nbn:de:bsz:wup4-opus-62673 (visited on June 10, 2022).

Shashi Menon, E. (2015). "Fluid Flow in Pipes". In: *Transmission Pipeline Calculations and Simulations Manual*. Elsevier, 2015, pp. 149–234. ISBN: 9781856178303. DOI: 10.1016/B978-1-85617-830-3.00005-5.

Singhal, Puja and Jan Stede (2019). *Wärmemonitor 2018: Steigender Heizenergiebedarf, Sanierungsrate sollte höher sein*. Ed. by DIW - Deutsches Institut für Wirtschaftsforschung. 2019. URL: https://www.diw.de/documents/publikationen/73/diw_01.c.676231.de/19-36-1.pdf (visited on June 10, 2022).

Sneum, Daniel Møller (2020). "Flexibility in the interface between district energy and the electricity system". PhD thesis. Technical University of Denmark, 2020. URL: https://orbit.dtu.dk/files/216181703/2020_DMS_Flexibility_in_the_interface_between_district_energy_and_the_electricity_system.pdf (visited on June 10, 2022).

Sneum, Daniel Møller and Eli Sandberg (2018). "Economic incentives for flexible district heating in the Nordic countries". In: *International Journal of Sustainable Energy Planning*

and Management 16 (2018), pp. 27–44. DOI: 10.5278/IJSEPM.2018.16.3. URL: https://journals.aau.dk/index.php/sepm/article/view/2018.

Stiebel Eltron (2017). *Planung und Installation Solar*. Ed. by STIEBEL ELTRON GmbH & Co. KG. 2017. URL: https://www.stiebel-eltron.de/content/dam/ste/de/de/products/downloads/Planungsunterlagen/Planungshandbuch/Planungshandbuch_EE_Solar.pdf (visited on June 10, 2022).

Talebi, Behrang, Parham A. Mirzaei, Arash Bastani, and Fariborz Haghighat (2016). "A Review of District Heating Systems: Modeling and Optimization". In: *Frontiers in Built Environment* 2.16 (2016), p. 7839. DOI: 10.3389/fbuil.2016.00022.

TenneT TSO GmbH (2022). *Eisman-Einsatzberichte*. URL: https://www.tennet.eu/de/strommarkt/transparenz/transparenz-deutschland/berichte-marktrelevante-informationen/einspeisemanagement-einsaetze-nach-14-eeg/eisman-einsatzberichte/ (visited on June 10, 2022).

Thalmann, S., T. Nussbaumer, A. Jenni, and J. Ködel (2018). *Planungshandbuch Fernwärme*. Bern, 2018. URL: http://www.verenum.ch/Dokumente/PLH-FW_V1.2.pdf (visited on June 10, 2022).

The pandas development team (2021). *pandas-dev/pandas: Pandas 1.3.5*. 2021. DOI: 10.5281/zenodo.5774815.

The Python Community (2022). *Python*. 2022. URL: https://www.python.org/ (visited on June 10, 2022).

Thermal Energy System Specialists (2022). *TRNSYS: Transient System Simulation Tool*. URL: http://trnsys.com/ (visited on June 10, 2022).

THERMOS project (2020). *THERMOS Tool*. 2020. URL: https://www.thermos-project.eu/tool-resources/thermos-tool/ (visited on June 10, 2022).

Ueckerdt, Falko, Christian Bauer, Alois Dirnaichner, Jordan Everall, Romain Sacchi, and Gunnar Luderer (2021). "Potential and risks of hydrogen-based e-fuels in climate change mitigation". In: *Nature Climate Change* 11.5 (2021), pp. 384–393. DOI: 10.1038/s41558-021-01032-7.

Umweltbundesamt (2008). *Kipp-Punkte im Klimasystem: Welche Gefahren drohen?* Ed. by Umweltbundesamt. 2008. URL: https://www.umweltbundesamt.de/sites/default/files/medien/publikation/long/3283.pdf (visited on June 10, 2022).

Umweltbundesamt (2022a). *Nationale Trendtabellen in der Abgrenzung der Sektoren des Klimaschutzgesetzes (KSG)*. Dessau, 2022. URL: https://www.umweltbundesamt.de/sites/default/files/medien/361/dokumente/2021-01-12_em_entwicklung_in_d_thg_sektoren_v1.0_0.xlsx (visited on June 10, 2022).

Umweltbundesamt (2022b). *Treibhausgas-Emissionen in Deutschland*. 2022. URL: https://www.umweltbundesamt.de/daten/klima/treibhausgas-emissionen-in-deutschland#emissionsentwicklung (visited on June 10, 2022).

UNFCCC (2015). *Paris agreement*. 2015. URL: http://unfccc.int/files/essential_background/convention/application/pdf/english_paris_agreement.pdf (visited on June 10, 2022).

VDI - The Association of German Engineers (2008). *VDI 4655: Reference load profiles of single-family and multi-family houses for the use of CHP systems*. 2008.

VDI Technologiezentrum (2019). *Quartiere und Städte setzen auf Wasserstoff*. Ed. by Bundesministerium für Bildung und Forschung. 2019. URL: https://www.fona.de/de/aktuelles/nachrichten/2019/staedte-und-quartiere-setzen-auf-wasserstoff.php (visited on June 10, 2022).

Verband kommunaler Unternehmen e.V. (2017). *Erdgasinfrastruktur in der Zukunft: Darauf können wir aufbauen*. Ed. by Verband kommunaler Unternehmen e.V. 2017. URL: https://www.vku.de/fileadmin/user_upload/Verbandsseite/Sparten/Energiewirtschaft/Gasthemen/VKU_Broschuere-Erdgas_2050.pdf (visited on June 10, 2022).

Vismann, Ulrich (2021). *Wendehorst Bautechnische Zahlentafeln*. Wiesbaden: Springer Fachmedien Wiesbaden, 2021. ISBN: 978-3-658-32217-5. DOI: 10.1007/978-3-658-32218-2.

Weinand, Jann Michael, Max Kleinebrahm, Russell McKenna, Kai Mainzer, and Wolf Fichtner (2019). "Developing a combinatorial optimisation approach to design district heating networks based on deep geothermal energy". In: *Applied Energy* 251 (2019), p. 113367. DOI: 10.1016/j.apenergy.2019.113367.

Weyer, Hartmut and Felix Müsgens (2020). *Netzengpässe als Herausforderung für das Stromversorgungssystem: Regelungsfelder, Status quo und Handlungsoptionen*. Ed. by acatech – Deutsche Akademie der Technikwissenschaften e. V. 2020. URL: https://energiesysteme-zukunft.de/publikationen/analyse/analyse-netzengpaesse (visited on June 10, 2022).

Winter, W., T. Haslauer, and I. Obernberger (2001). "Simultaneity surveys in district heating networks - results and project experience; Untersuchungen zur Gleichzeitigkeit in Nahwaermenetzen. Ergebnisse und Projekterfahrungen". In: *Euroheat and Power* 30.10 (2001), pp. 42–47. URL: https://www.osti.gov/etdeweb/biblio/20210986 (visited on June 10, 2022).

Zinko, Heimo, Ulrika Ottosson, Benny Boehm, Kari Sipilae, Miika Raemae, and Halldor Kristjansson (2008). "District Heating Distribution in Areas with Low Heat Demand Density". In: *11. international symposium on district heating and cooling, Reykjavik (IS), 08/31/2008* (2008). URL: http://www.dhc2008.hi.is/session/greinar/p55_Zinko.pdf (visited on June 10, 2022).

A Student contributions

The presented work contains results that were obtained in the course of supervising the following student project:

- Tobias Fortmann, Entwicklung eines Optimierungsmodells zur erneuerbaren Versorgung und energieeffizienten Gestaltung von Bestandswohngebäuden, Master thesis, 2020

B Supplementary

B.1 Appendix to Chapter 4: Supplementary analysis of the heat and electricity energy flows

The following sections provide an supplementary analysis to the results given in Section 4.3.2 to illustrate the heat generation and commitment of the thermal storage. Therefore, the hourly time-resolved results of one year of the unit commitment given e.g. in Figure 4.9 were grouped with respect to the outside temperature and the emission factor. This process is performed for the heat generation and storage units and the electricity bus (see also Figure 4.1). The results of the refurbishment scenario *Refurb-1* are shown according to the results given in Section 4.3.2 for the following scenarios:

- Scenario *2020*
- Scenario *2030-syn-gas-low*
- Scenario *2030-syn-gas-high*
- Scenario *2050-syn-gas-low*
- Scenario *2050-syn-gas-high*

Scenario 2020

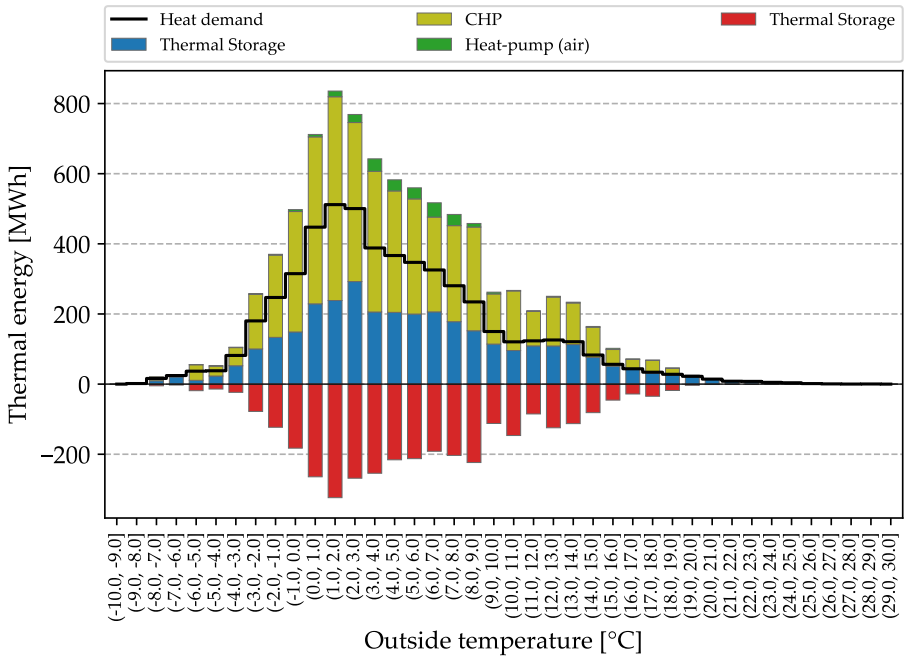

Figure B.1: Unit commitment of heat generation and storage units dependent on the outside temperature of the carbon-neutral solution of scenario *2020*.

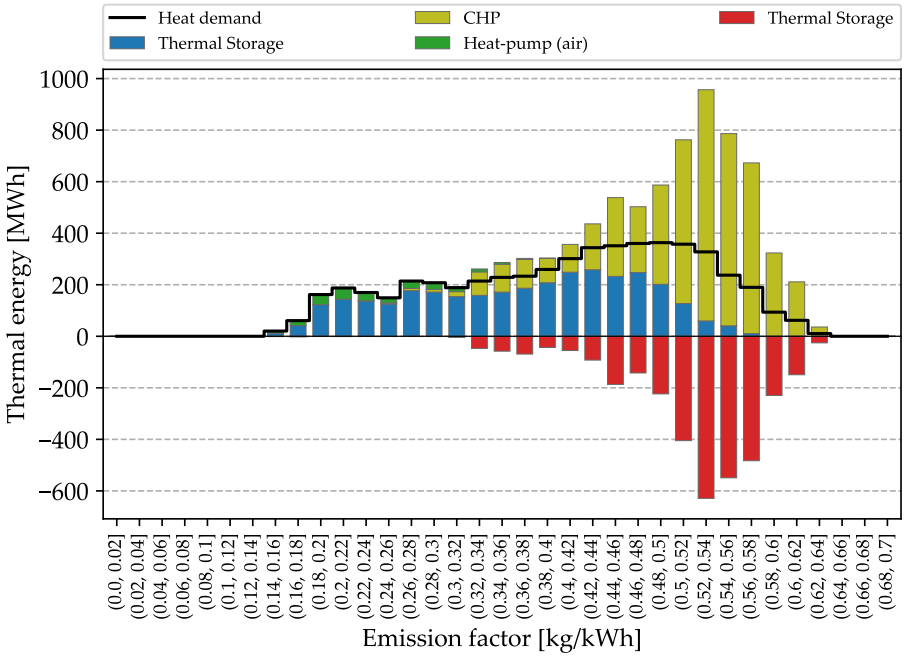

Figure B.2: Unit commitment of heat generation and storage units dependent on the emission factor of the upstream electricity grid of the carbon-neutral solution of scenario *2020*.

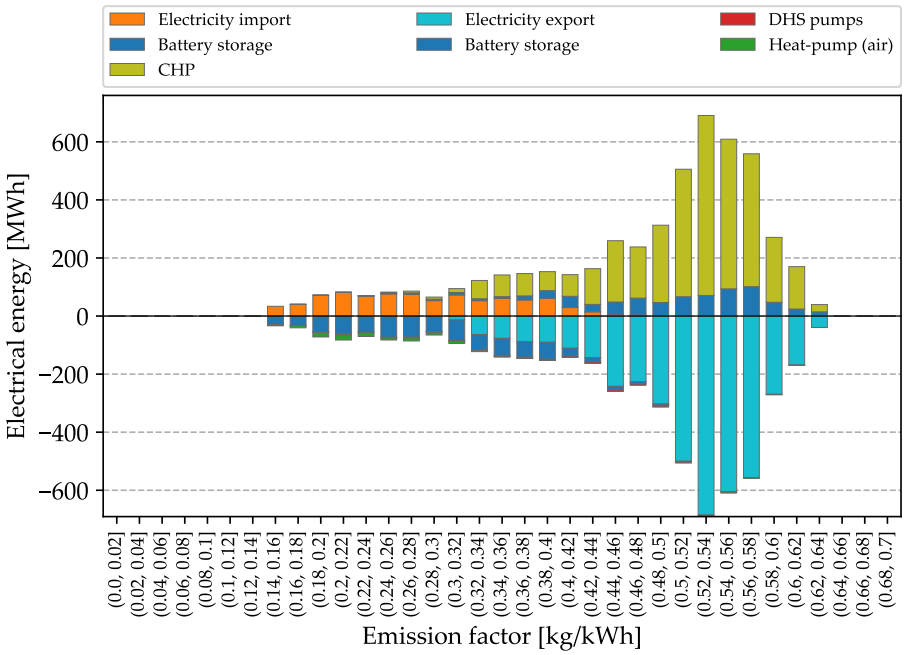

Figure B.3: Electricity consumption and electricity exchange with the upstream power grid dependent on the emission factor for the carbon-neutral solution of scenario *2020*.

Scenario *2030-syn-gas-low*

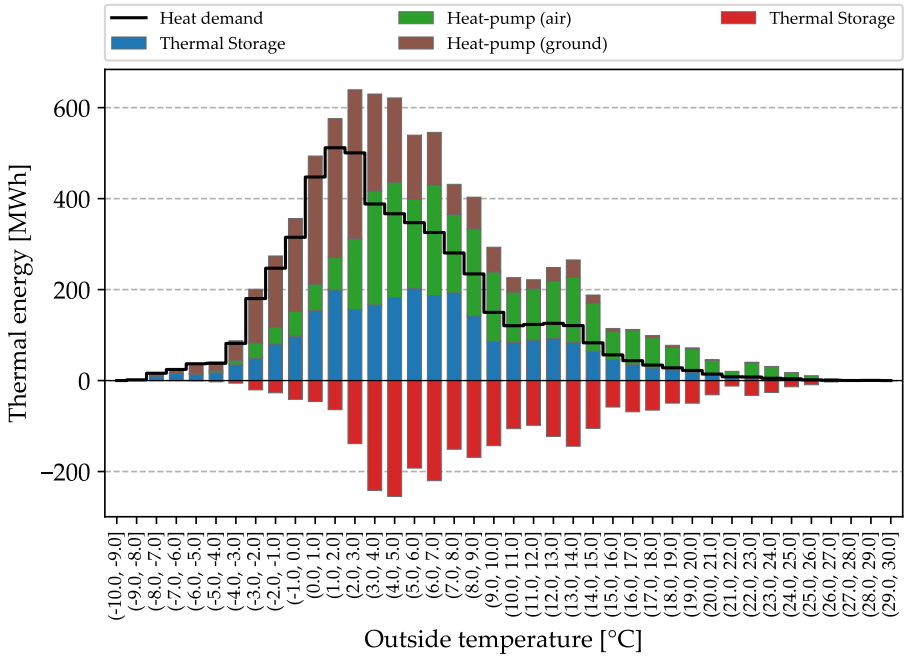

Figure B.4: Unit commitment of heat generation and storage units dependent on the outside temperature of the carbon-neutral solution of scenario *2030-syn-gas-low*.

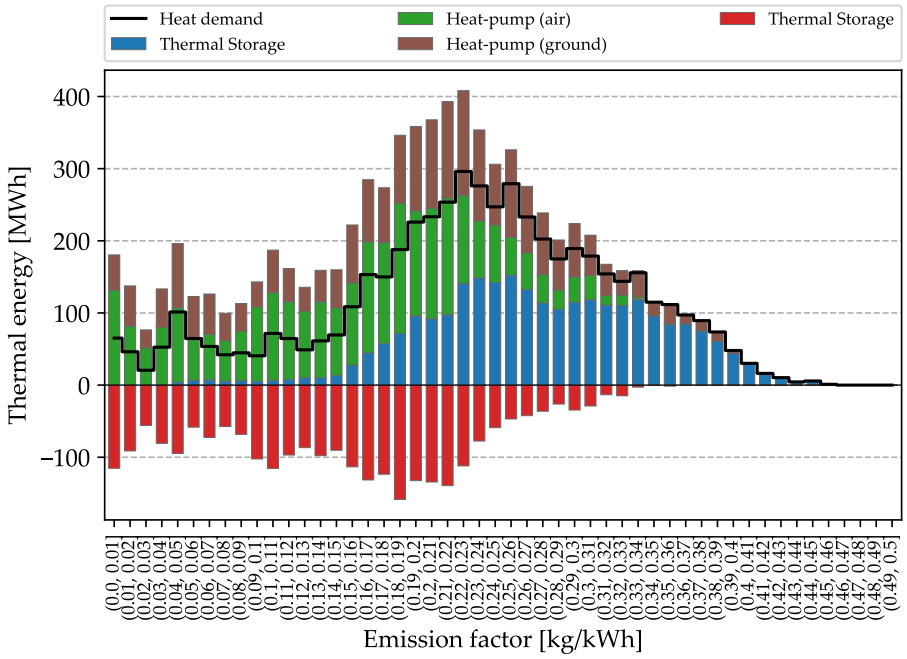

Figure B.5: Unit commitment of heat generation and storage units dependent on the emission factor of the upstream electricity grid of the carbon-neutral solution of scenario *2030-syn-gas-low*.

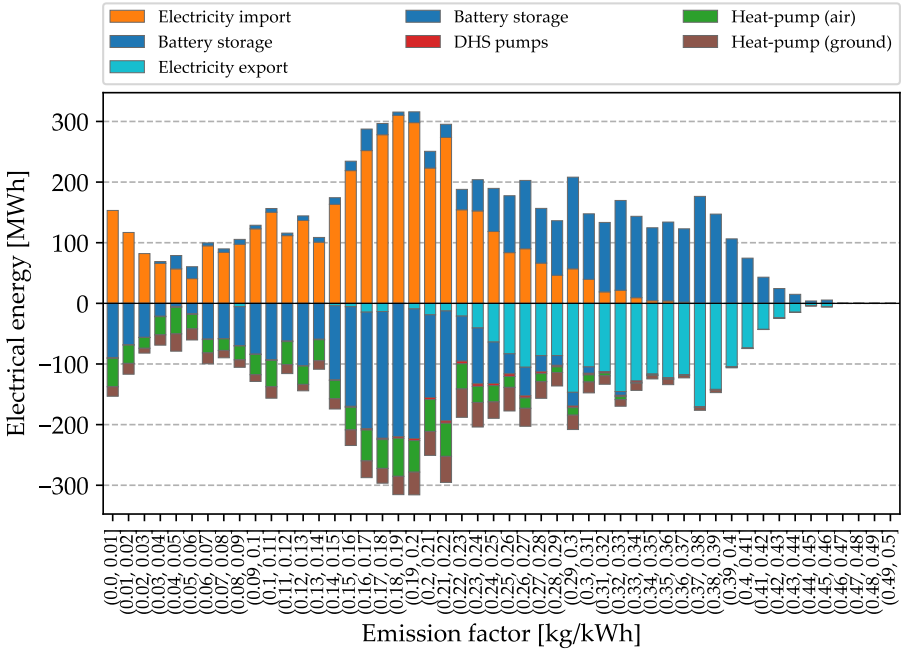

Figure B.6: Electricity consumption and electricity exchange with the upstream power grid dependent on the emission factor for the carbon-neutral solution of scenario *2030-syn-gas-low*.

Scenario *2030-syn-gas-high*

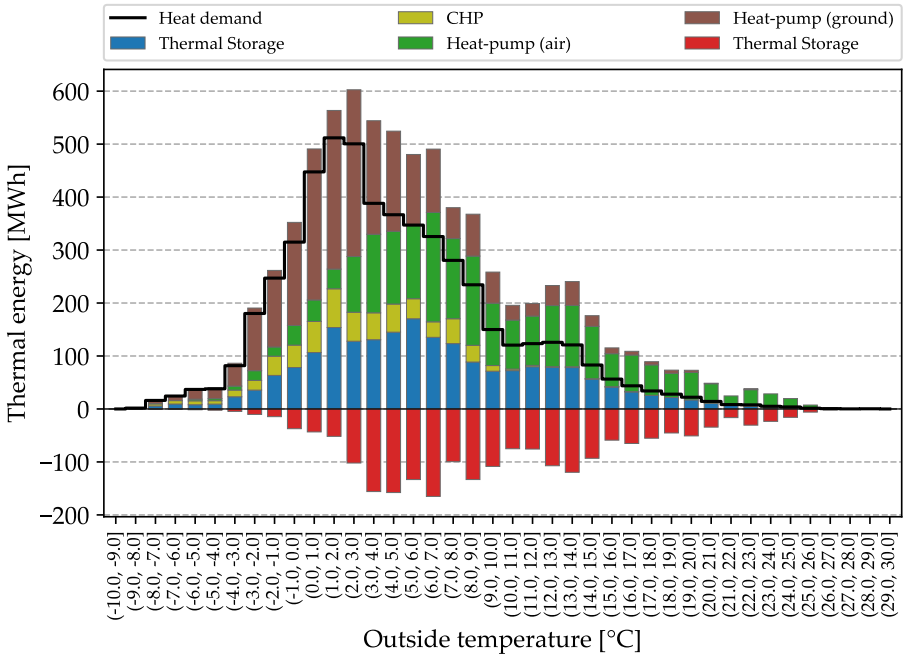

Figure B.7: Unit commitment of heat generation and storage units dependent on the outside temperature of the carbon-neutral solution of scenario *2030-syn-gas-high*.

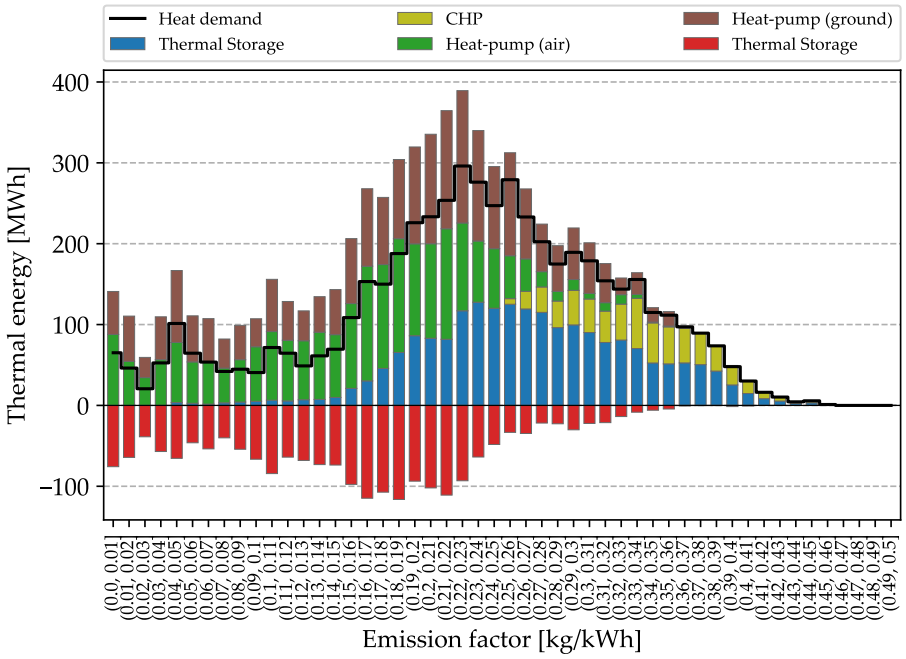

Figure B.8: Unit commitment of heat generation and storage units dependent on the emission factor of the upstream electricity grid of the carbon-neutral solution of scenario *2030-syn-gas-high*.

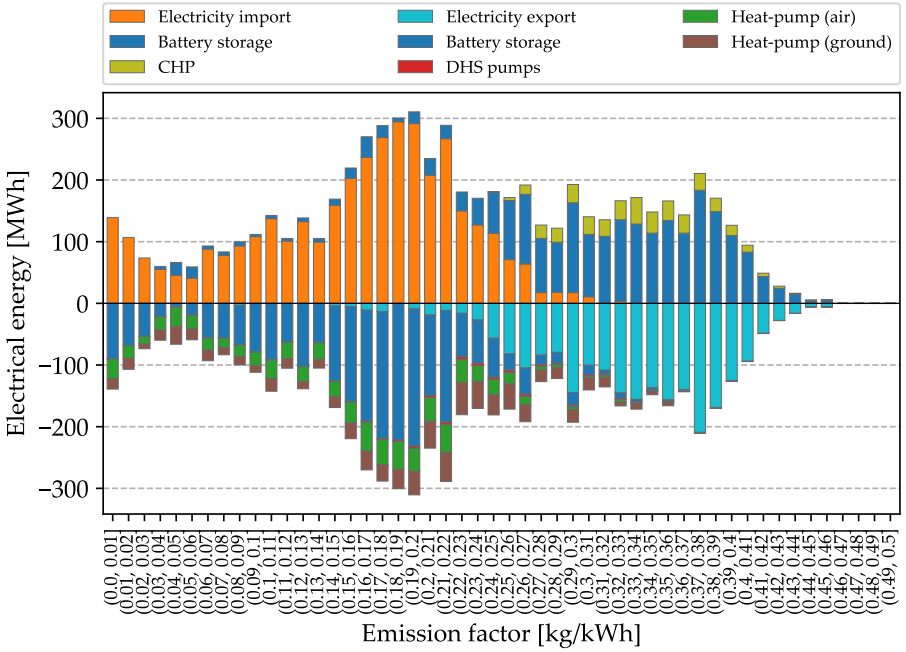

Figure B.9: Electricity consumption and electricity exchange with the upstream power grid dependent on the emission factor for the carbon-neutral solution of scenario *2030-syn-gas-high*.

Scenario *2050-syn-gas-low*

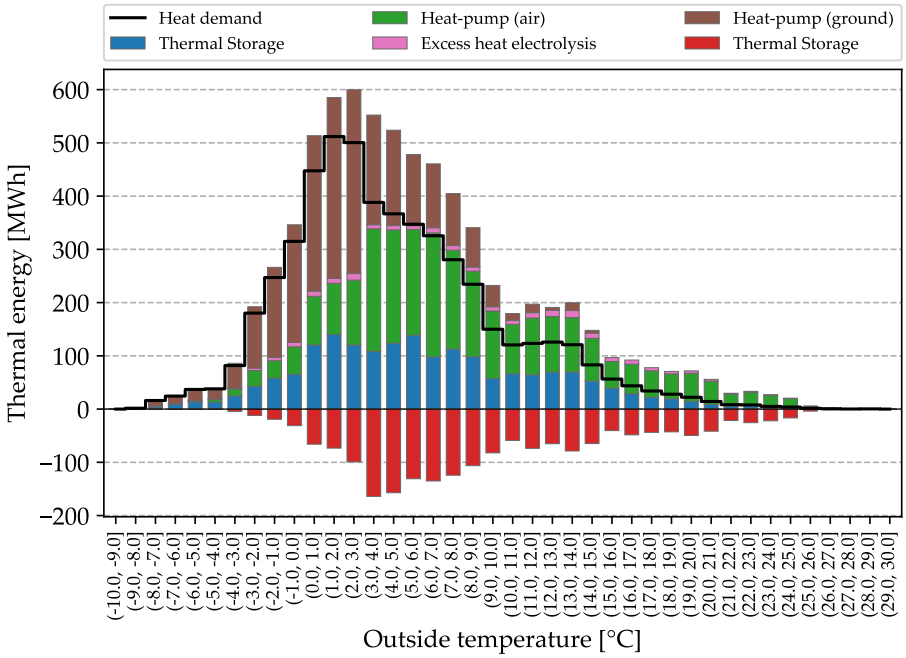

Figure B.10: Unit commitment of heat generation and storage units dependent on the outside temperature of the carbon-neutral solution of scenario *2050-syn-gas-low*.

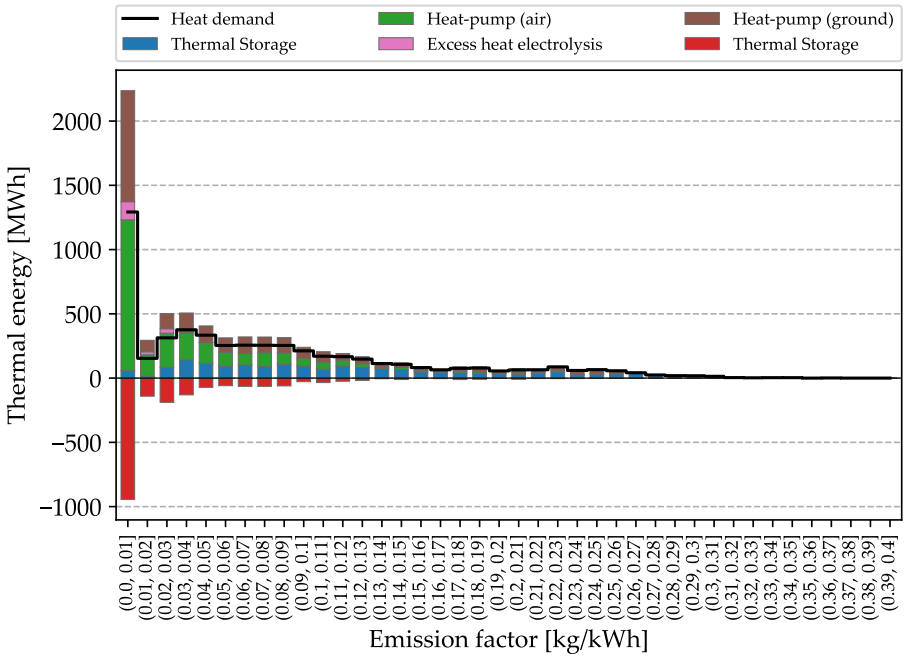

Figure B.11: Unit commitment of heat generation and storage units dependent on the emission factor of the upstream electricity grid of the carbon-neutral solution of scenario *2050-syn-gas-low*.

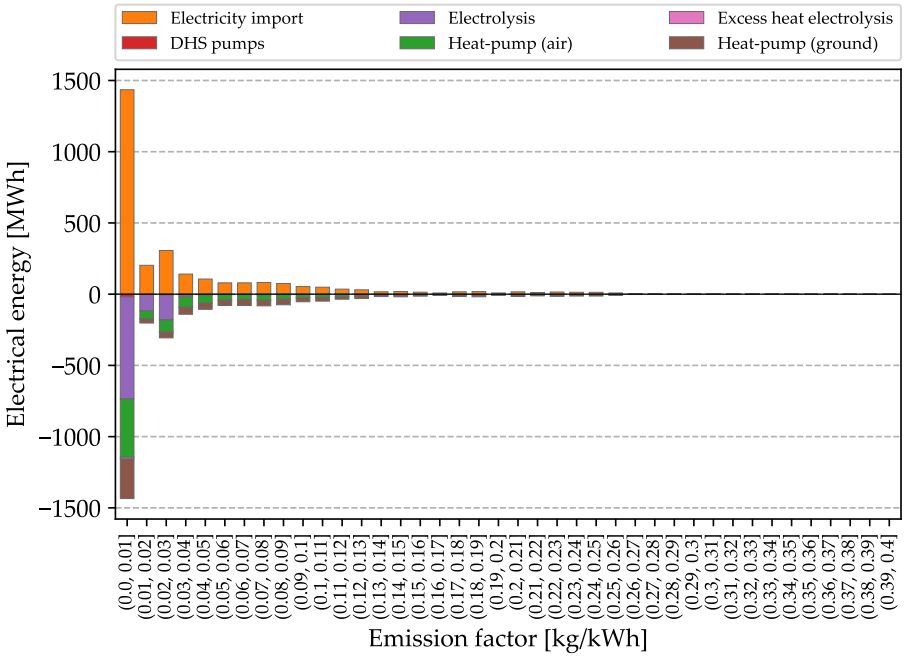

Figure B.12: Electricity consumption and electricity exchange with the upstream power grid dependent on the emission factor for the carbon-neutral solution of scenario *2050-syn-gas-low*.

Scenario *2050-syn-gas-high*

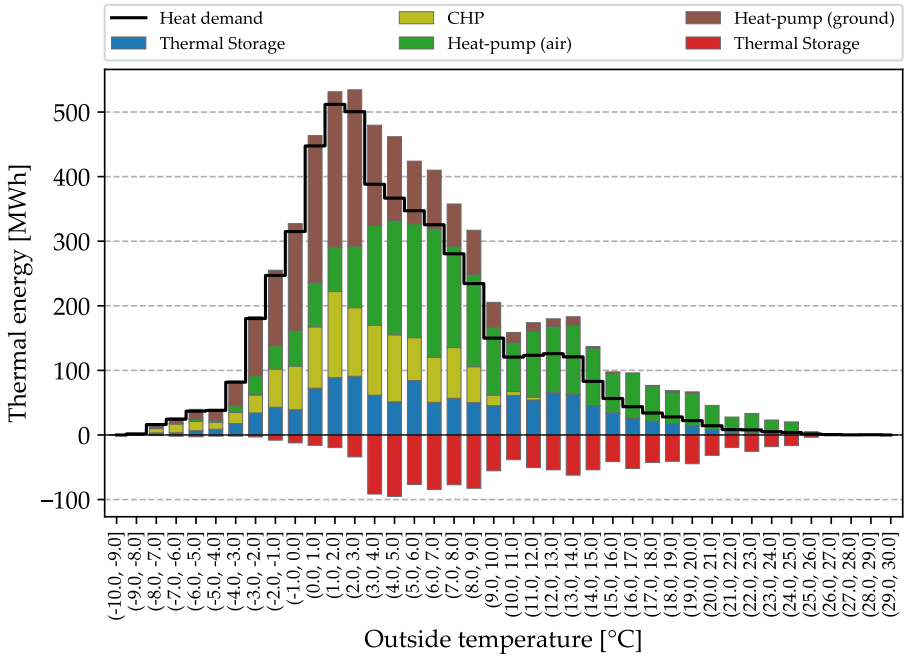

Figure B.13: Unit commitment of heat generation and storage units dependent on the outside temperature of the carbon-neutral solution of scenario *2050-syn-gas-high*.

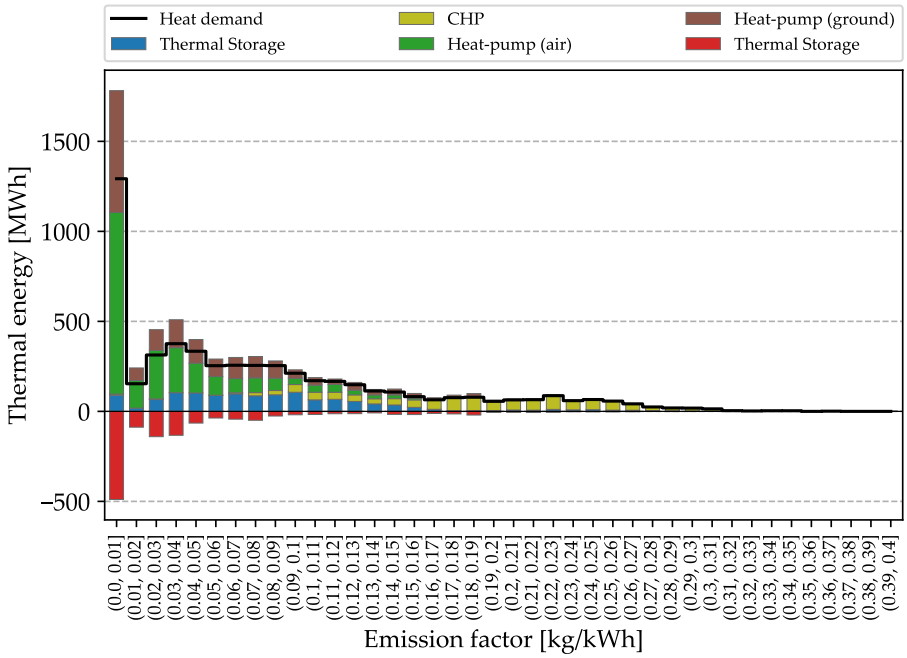

Figure B.14: Unit commitment of heat generation and storage units dependent on the emission factor of the upstream electricity grid of the carbon-neutral solution of scenario *2050-syn-gas-high*.

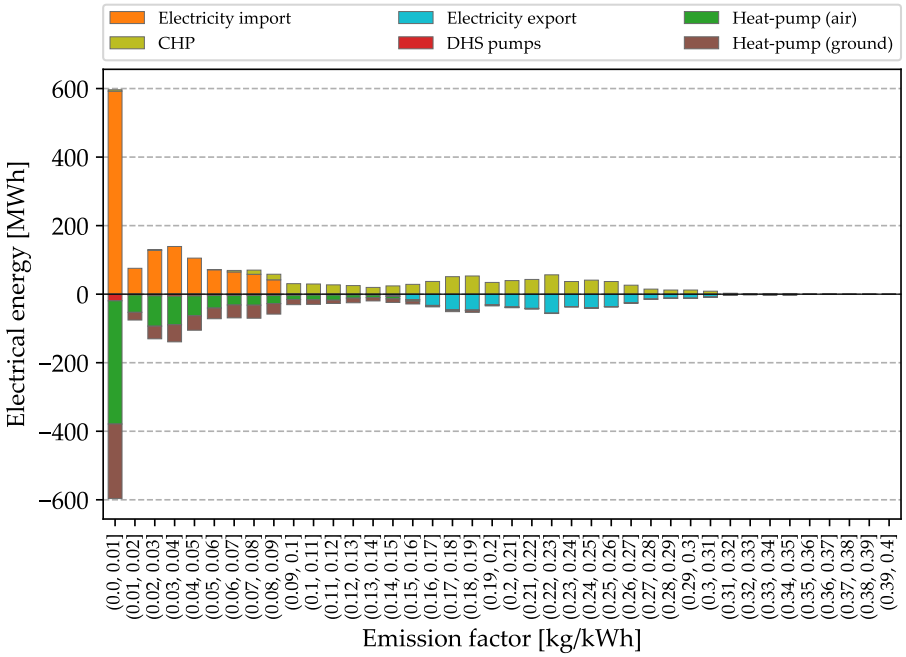

Figure B.15: Electricity consumption and electricity exchange with the upstream power grid dependent on the emission factor for the carbon-neutral solution of scenario *2050-syn-gas-high*.

B.2 Appendix to Chapter 5: Investment decisions of refurbishment scenarios for individual heat supply

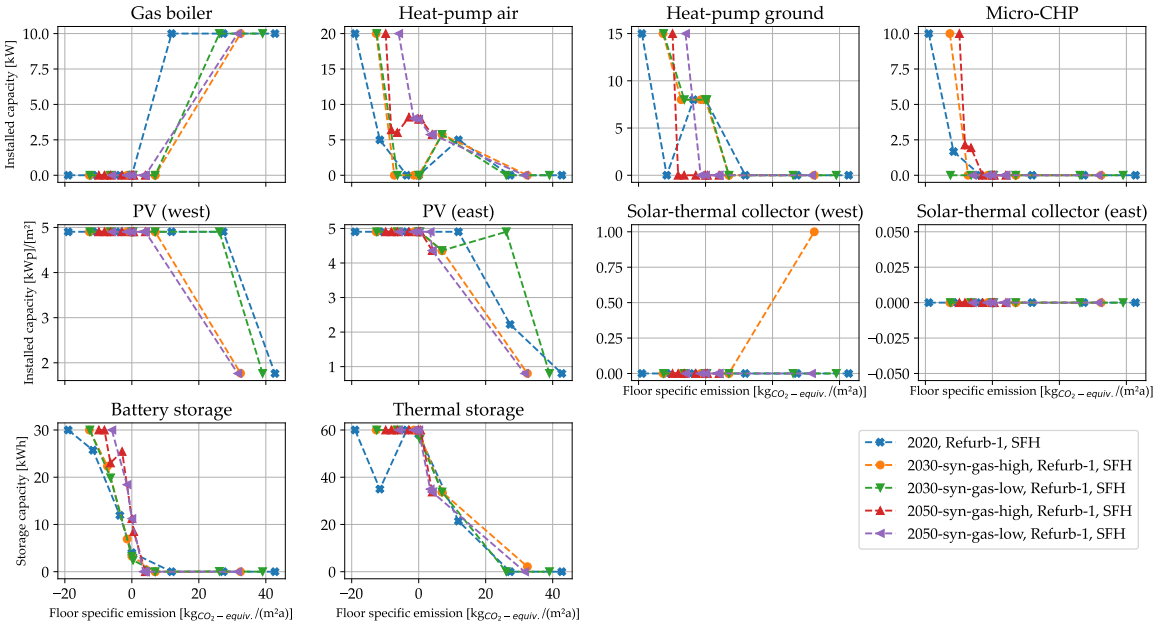

Figure B.16: Investment decisions of refurbishment scenario *Refurb-1* of the reference SFH.

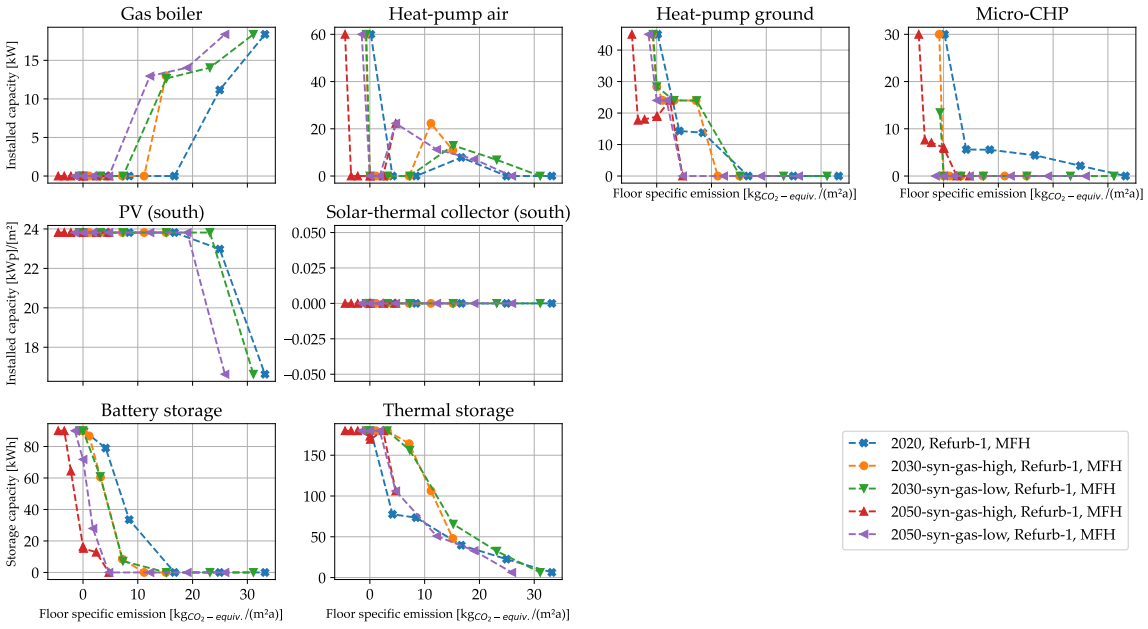

Figure B.17: Investment decisions of refurbishment scenario *Refurb-1* of the reference MFH.

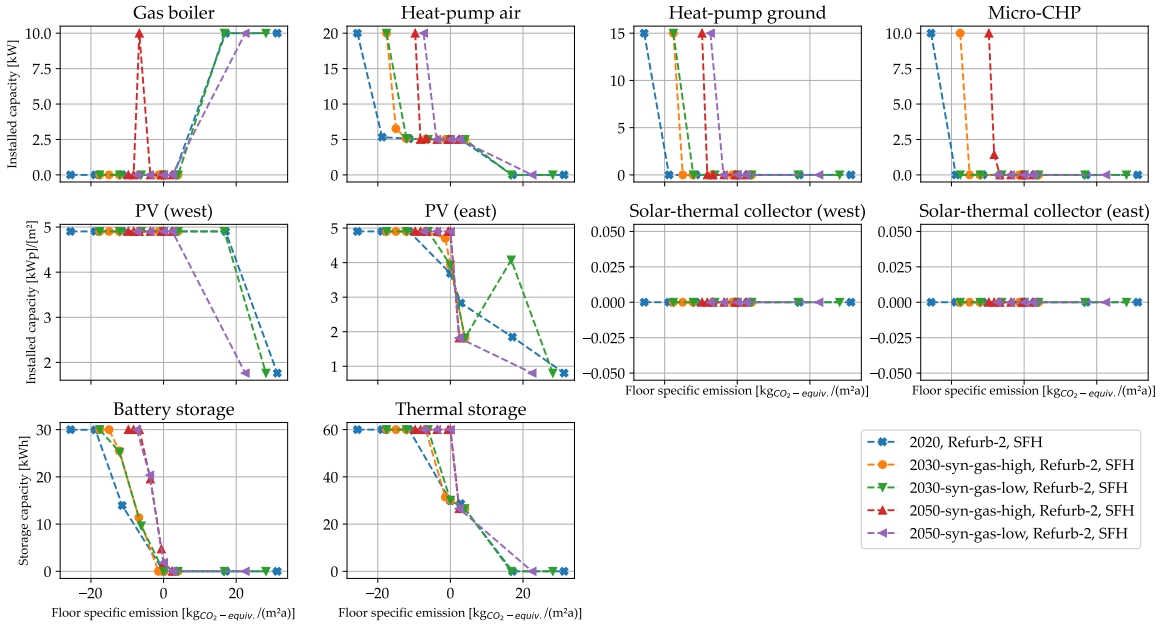

Figure B.18: Investment decisions of refurbishment scenario *Refurb-2* of the reference SFH.

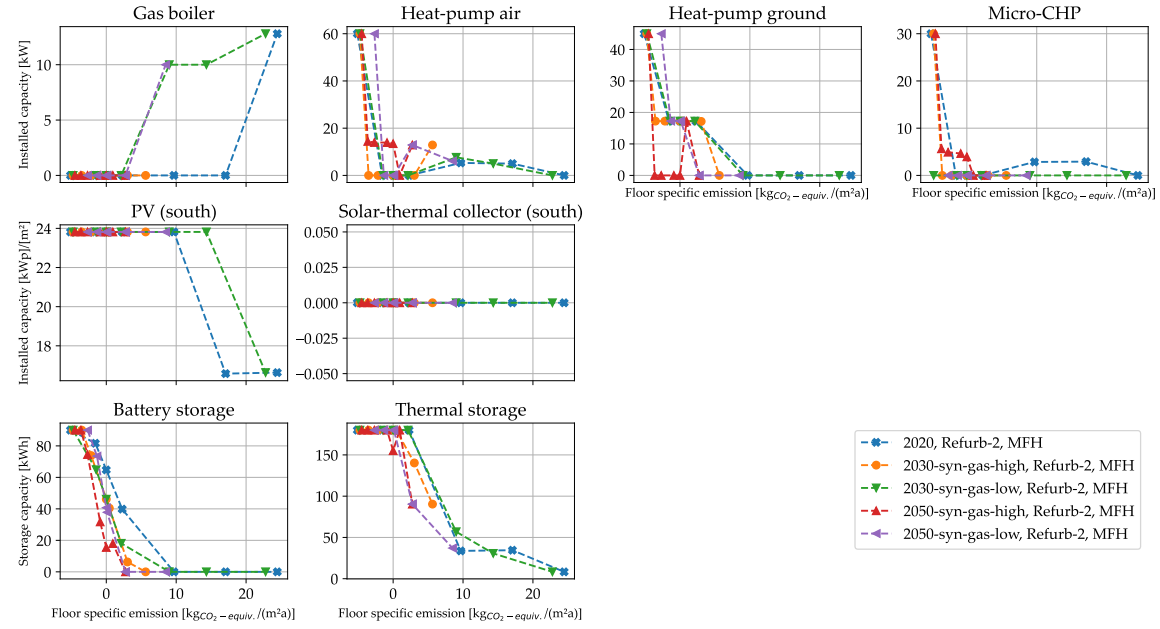

Figure B.19: Investment decisions of refurbishment scenario *Refurb-2* of the reference MFH.